Regulation of Post-Transcriptional Gene Expression in Human Mitochondria

Agata Rozanska
M.Sc.

Thesis submitted to Newcastle University in candidature for
the degree of Doctor of Philosophy

Newcastle University
Faculty of Medical Sciences
Wellcome Trust Centre for Mitochondrial Research
Institute for Ageing and Health
July 2014

Abstract

Mitochondria are cellular organelles that have evolved from the eubacterial ancestor into highly specialized compartment of the eukaryotic cell. They are unique among animal cells in that they retain a level of autonomy through the genetic information in their genome. Human mtDNA is built of ~16.5 kbp encoding 13 polypeptides, which are synthesised by mitoribosomes. The latter consist of two RNA species also transcribed from mtDNA and approximately 80 proteins originating from the nucleus. All 13 products of intramitochondrial translation are incorporated into the inner mitochondrial membrane where they co-build the oxidative phosphorylation (OXPHOS) system. OXPHOS is a multicomplex machinery, the final product of which is adenosine triphosphate, ATP, a carrier of energy that is necessary to sustain cell homeostasis and growth.

The malfunctions of mitochondria have a severe impact on the 'host' organism and are the causative factor in many human diseases. Pathological changes of mitochondrial function can be triggered by mutations in the mitochondrial genome and/or defects in nuclear genes involved in mitochondrial activity. The mitochondrial gene expression pathway has been increasingly investigated during last twenty years and combines both types of factors, those translated in the cytosol and those synthesised in the mitochondrial matrix. A functional mitochondrion requires over 1500 proteins to be imported from the cytosol, a significant subset of these are devoted to the maintenance, replication, transcription and subsequently for translation of the minimal mitochondrial genome fostered within. In the course of my PhD study three of these nuclear encoded but mitochondrially destined proteins were investigated.

The first of these proteins that I contributed to investigating was SLIRP. As the specificity of this RNA binding protein had not been established I performed CLIP (cross-linking immunoprecipitation) assay in order to assess the ability of SLIRP to bind RNA. The data generated from this analysis directly showed that SLIRP can interact with all mt-mRNAs apart from *MTND6*. This work confirmed that SLIRP participates in the stability of mt-mRNA species, as has now been subsequently published by other research groups.

A main part of my PhD studies centred on characterisation of MRPL12. This protein belongs to the pool of conserved mitochondrial proteins having the bacterial orthologue

called L7/L12. One of the unique features of these proteins is their dynamic character and ability to exchange location between ribosomal LSU and the free pool. This has been postulated to be a regulatory mechanism of translation process in response to fluctuations in cell metabolism. To test this hypothesis I characterised immortalised fibroblasts obtained from a patient with a homozygous mutation in MRPL12 caused by c.542C to T transition in exon 5. This cell line allowed me to study the consequence of this defect on the regulation of translation in human mitochondria. I could conclude that a reduced number of MRPL12 molecules per mt-LSU in subject fibroblasts did not affect overall mitoribosome assembly, but a visible decline in mitochondrial translation was detected although the reduction in translational efficiency for different mitochondrially encoded subunits varied.

The third protein that I characterised was mitochondrial RBFA. This protein was identified in my host laboratory and preliminary characterisation performed prior to my involvement. My studies included the CLIP assay that showed direct interaction of this protein with a 3' terminal stem loop of helix 45 of the 12S mt-rRNA. The methylation status of two conserved neighbouring adenines located in helix 45 was altered by changes in steady state level of RBFA. Moreover, the CLIP data identified a second rRNA species associated with RBFA. This was an unexpected RNA species in the form of 5S rRNA. The data regarding the mitochondrial localisation and specifically any submitochondrial location has been controversial. Intriguingly my data identified a number of chimeric CLIP sequences containing both 5S and 12S rRNA fragments, strongly suggesting that within the mitochondrial matrix RBFA interacts simultaneously with both RNA species. Similarity between the 5S rRNA secondary structure and snoRNA, which guides modifications on cytosolic rRNA, led to the hypothesis proposing a novel function for 5S rRNA guiding methylation at helix 45 of the 12S mt-rRNA. My data therefore assign RBFA as a new member of the group of maturation factors of the mammalian mt-SSU.

Acknowledgment

First of all, I would like to express my gratitude to my supervisors, Prof. Zofia Chrzanowska-Lightowlers and Prof. Robert Lightowlers for giving me the opportunity to undertake this PhD in their laboratory. I am enormously grateful for all their help, guidance, encouragement and understanding during the course of study. I can not thank enough for teaching me to be more independent as a researcher, involved in planning of the experiments, thinking of new approaches to arising questions. I have been privileged to have so wonderful supervisors, who have so much passion for science and enormous knowledge which they so freely share.

I thank all the members of the lab, for being great colleagues, always ready to help and share their knowledge and skills. Being part of this team has been wonderful experience. Entering the lab in the morning has been always joyful no matter how much rain was pouring outside. I am proud and grateful to work alongside people, who not only share passion for science but also can brighten the darkest day.
I would like to thank dr. Francesco Bruni for all the help with *in vivo* ^{35}S-metabolic labelling assay. Casey Wilson for helping me with sequencing gels. Ola Pajak for sharing her knowledge about northern blot and sucrose gradient techniques and all scientific discussions.

I would like to write special thanks for Karolina Rygiel and Ola Pajak for all their support and friendship. It is a privilege to have real friends in the workplace, who are always ready to listen, share a laugh and help.

I would like also thank my mum for all the encouragement and never fading believes in me.

At last but not least, I would like to thank my little son Damian for being there for me in the moments of despair, when I was completely stuck on some impossibly to start or finish sentence, staring at the structures of mitoribosome or some complex patterns of mitochondrial genes expression. Somehow, my son's unscientific descriptions of those very scientific figures with giraffes and zebras on the train, allowed me to write all of them. I will always cherish in my memory those imaginary and so joyful explanations.

Author's declaration

I declare that the data presented in this thesis is based solely on work carried out by the author, unless stated otherwise. Moreover, neither this thesis nor any of the data within has been submitted before for any other degree or award. The contributions by others have been acknowledged, where appropriate,

Agata Rozanska

Table of Contents

List of Figures

List of Tables

Abbreviations

aa - tRNA - aminoacyl-tRNA

ADP - adenosine diphosphate

Amp - ampicillin

APS - ammonium-persulphate

A-site - aminoacyl-tRNA site within the ribosome

ATP - adenosine triphosphate

B - beads before elution

BN - Blue Native

bp - base pair(s)

BSA - bovine serum albumin

cyt c - cytochrome *c*

CBB - Coomassie Brilliant Blue

CL - cell lysate

CLIP - Crosslinking immunoprecipitation

COX - Cytochrome *c* oxidase

CoQ - Coenzyme Q

cpm - counts per minute

CTDs - C-terminal domains

cyt - cytochrome

DEPC - diethyl pyrocarbonate

dH_2O - distilled water

D-loop - displacement loop

DMEM - Dulbecco's modified Eagle's medium

DMSO - dimethyl-sulphoxide

DNA - deoxyribonucleic acid

dNTP - deoxynucleotide triphosphate

DTT - dithiothreitol

E. coli - Escherichia coli

EDTA - ethylene diamine tetra-acetic acid

EF(-G/-Ts/-Tu) - elongation factor (-G/-Ts/-Tu)

EGTA - ethylene glycol tetra-acetic acid

EM - electron microscopy

E-site - exit site within the ribosome

EtOH - ethanol

FAD - flavin-adenine dinucleotide

FADH2 - reduced flavin-adenine dinucleotide

FBS - foetal bovine serum

Fe-S - iron-sulphur

Met - methionine

fMet - formyl-methionine

FRT - Flp-recombination-target

GDP - guanine diphosphate

GTP - guanine triphosphate

g - relative centrifugal force

hr - hour(s)

H - heavy strand

HEK293T - human embryonic kidney cells

HeLa - human cervical cancer carcinoma cells from Henrietta Lacks

hmtPAP - human mitochondrial poly(A) polymerase

IAA - isoamylalcohol

IF - initiation factor

IgG - immunoglobulin type G

IM - inner mitochondrial membrane

IMS - intermembrane space

IP - immunoprecipitation

IPTG - Isopropyl β-D-1-thiogalactopyranoside

kDa - kilo-Dalton

kb - kilo-base(pairs)

KCl - potassium chloride

L- light strand

LB - Luria-Bertani

LRPPRC - leucine-rich pentatricopeptide-repeat containing protein

LSU - large subunit of the ribosome

min - minute(s)

MOPS - morpholinopropanesulfonic acid

mRNA - messenger RNA

MRP(L/S) - mitochondrial ribosomal protein (of the LSU/ SSU)

mt - mitochondrial

mtDNA - mitochondrial genome

N - amino-terminus

NAD - nicotinamide-adenine dinucleotide

$NADH_2$ - reduced nicotinamide-adenine dinucleotide

nDNA - nuclear DNA

NOA1 - nitric oxide-associated-1

NP-40 - Nonidet P-40, octyl phenoxy-polyethoxy-ethanol

nt - nucleotide(s)

NTDs - N-terminal domains

OD - optical density

OM - outer mitochondrial membrane

ORF - open reading frame

OXPHOS - oxidative phosphorylation

PAGE - polyacrylamide gel electrophoresis

PAS - polypeptide accessible site

PBS - phosphate buffered saline

PES - polypeptide exit site

PCR - polymerase chain reaction

PMSF - phenylmethylsulphonyl fluoride

POLRMT - mitochondrial RNA polymerase

PPR - putative pentatricopeptide repeat

P-site - peptidyl-tRNA site within the ribosome

PVDF - polyvinylidine fluoride

RBP - RNA binding protein

RF - release factor

RNA - ribonucleic acid

ROS - reactive oxygen species

rpm - revolutions per minute

RRF - ribosome recycling factor

rRNA - ribosomal RNA

s – seconds

SAM - S-adenosyl-L-methionine

SDS - sodium-dodecyl-sulphate

siRNA - silencing RNA, small interfering RNA

SLIRP - stem-loop interacting RNA binding protein

SSU - small subunit of the ribosome

TAE - Tris-acetate EDTA

Taq - DNA polymerase from *Thermus aquaticus*

TBS - Tris buffered saline

TBS-T Tris buffered saline, containing Tween-20 (0.1%)

TEMED - N, N, N', N'-tetramethylethylene-diamine

TFAM - transcription factor A

TFB1M and TFB2M - mitochondrial transcription factor B1 or 2 (synonym mtTFB1/2)

TIM - translocase of the inner mitochondrial membrane

TOM - translocase of the outer mitochondrial membrane

tRNA - transfer RNA

Tris - 2-Amino-2-hydroxymethyl-propane-1,3-diol

Triton X-100 - polyethylene glycol p-(1,1,3,3-tetramethylbutyl)-phenyl ether

T. thermophilus - Thermus thermophilus

Tween-20 - polyoxyethylene sorbitanmonolaurate

U - unit (enzyme activity; 1U = 1μmol/ min)

UV - ultra-violet

vol - volume

v/v - volume/ volume

WT – wild type

w/v - weight/ volume

Chapter 1

Introduction

1. Chapter 1: Introduction

1.1 General overview of the mitochondrion.

1.1.1 Origin of mitochondria.

The human mitochondrial network is a multifunctional organelle, the origin of which has been widely discussed and analysed. One of the most accepted theories combines a rise of eukaryotic cells and mitochondria in one event, in a symbiotic association of an anaerobic archaebacterium (the host) with aerobic eubacterium (the symbiont) (Martin and Müller, 1998, Rivera and Lake, 2004, Cox et al., 2008, Yutin et al., 2008, Williams et al., 2013). Mitochondria are the only organelle in non-plant eukaryotic cells, outside the nucleus, containing their own DNA. Variations in the size of mitochondrial genetic information, physical form and content of coding and noncoding fragments raised the question of possible multisymbiotic events occurring during cellular evolution. The size of mammalian mtDNA oscillates around 16 kb and investigation in non-animal species revealed much smaller genomes of just ~6 kbp genome of *Plasmodium falciparum* (human malaria parasite) and related apicomplexans (Feagin, 2000). In contrast the mitochondrial genome of land plants hugely expanded in size to 570 kbp in corn or even larger than 2000 kbp in some cucurbit plants (Bullerwell and Gray, 2004). The largest known by far is mtDNA of *Silene conica* (~11000 kb) with a massive proliferation of noncoding content that exceeds the size of even some nuclear genomes (Sloan et al., 2012). Despite these genetic variations, data obtained from gene sequencing strongly suggest that the mitochondrial genome is monophyletic (Gray et al., 1999, Bullerwell and Gray, 2004). Although the mitochondrial network has retained its autonomy in the cell, its genome has become hugely reduced during the course of evolutionary changes. The number of encoded proteins has dropped in some cases from 67 to 3, and from a maximum of 27 mt-tRNAs to none (Adams and Palmer, 2003). Indeed some non-respiring microbial eukaryotes such as parasitic trichomonads lack mtDNA completely but still contain derived mitochondria called hydrogenosomes producing ATP anaerobically (Embley et al., 2003). Other eukaryote species that for many years were believed to lack mitochondria, such as *Trachipleistophora,* contain reduced mitochondrial structures termed mitosomes (Roger and Silberman, 2002). This mitochondrion-related organelle also lacks mtDNA but in contrast to hydrogenosomes is unable to generate ATP (Gray, 2012). Extremely reduced metabolic capacity of mitosomes manifests in Fe-S cluster formation (Regoes et al., 2005). Overall, it seems that evolutionary changes in some unicellular organisms where the need for aerobic

respiratory function of mitochondria was no longer required caused the reduction or remodelling of the organelle. Nevertheless mitochondria are highly organised and complex structures, requiring many hundreds of proteins (over 1500 in mammals) to maintain their functions (Bar-Yaacov et al., 2012).

Interestingly mitochondria in four major lineages of aerobic eukaryotes; animals, most fungi, apicomplexans and chlamydomonad green algae have lost the coding capacity for all of the ribosomal proteins but retained at least 3 respiratory chain proteins with *cyt c* and *cox1* considered as universal (Adams and Palmer, 2003). Many mitochondria have also retained two genes encoding the small and large ribosomal RNA species, which exhibit a striking spectrum in size, in contrast to those of their eubacterial and chloroplast orthologues. Moreover, some of mitochondrial rRNA are highly fragmented and dispersed throughout the mitochondrial genome, examples include *Plasmodium falciparum* and *Chlamydomonas reinhardtii* (Adams and Palmer, 2003). Most of mitochondrial genomes have lost the gene encoding 5S rRNA. The reported absence of it, in many of the organisms analysed may be due to a failure in experimental and /or bioinformatic approaches (Adams and Palmer, 2003) or can be the result of an evolutionary driven substitution by a cytosolic orthologue (Entelis et al., 2001). Furthermore, there is a specific hierarchy in the gene loss, with some genes lost more readily than others (Lang et al., 1999). However, certain genes have been retained in the mtDNA and these require the involvement of hundreds of proteins imported from cytosol for their maintenance, replication, repair, and all the steps of their expression and regulation. The reasons for this energetically demanding service are not clear. One of the hypotheses addressing this issue, points out the hydrophobic nature of OXPHOS subunits, which make them very difficult to transport across the mitochondrial membranes and sort to a precise location (Claros et al., 1995). Another explanation proposes potential toxicity of the gene products if they were present in cytosol, but which remain 'safe' when enclosed in the mitochondrion (Adams and Palmer, 2003). A further hypothesis suggests that the non-standard genetic code applied in the mitochondrion of many eukaryotes, including animals, would act as a block to further gene transfer to the nucleus. The rapid development of bioinformatic tools as well as progressing research in biology of mitochondria should soon clarify the biogenesis and mutual dependence between the eukaryotic cell and one of the mysteries of its organelles.

1.1.2 The dynamic complexity of mitochondrial structure.

Although the basics about structure of mitochondria have been known for many years, the advanced microscopy developed more recently has been used to investigate its morphology to generate a more accurate and complex picture (Ernster and Schatz, 1981, Frey et al., 2002). Mitochondrial shapes vary widely between different cell types from long filaments in fibroblasts to spheres in hepatocytes (Youle and Van der Bliek, 2012). Moreover, morphologies of mitochondria are far from static, continuously changing via the combined processes of fission, fusion and motility.

Mitochondria consist of two membranes: outer (OM) and inner (IM) that create 5 compartments, which provide specific environments for many metabolic and regulatory processes (Figure 1.1). In addition to the OM and IM, the cavity between these is the intermembrane space (IMS), the invaginations of the IM create the cristae and the innermost compartment is the matrix harbouring the mtDNA, mt-RNA and the soluble proteins responsible for their expression.

matrix   cristae   IM   intermembrane   OM
                                 space
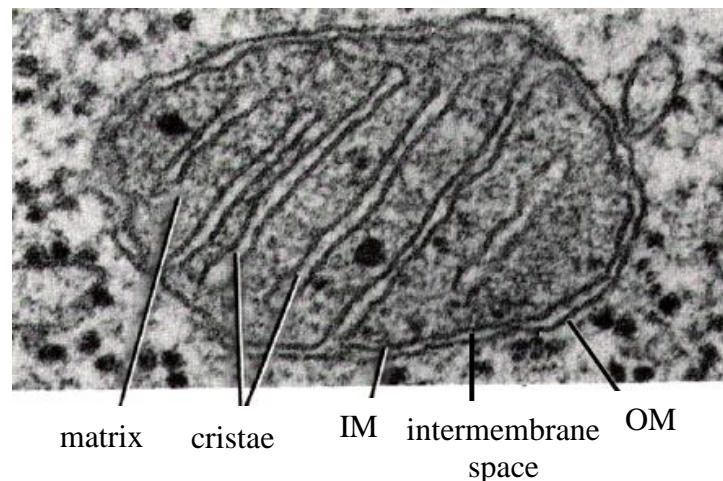
Figure 1.1 Structure of the mitochondrion. A transmission electron micrograph showing a section through a mitochondrion that illustrates the 5 different compartments. Description of each compartment is given in the text. IM, inner membrane; OM, outer membrane.
Image adapted from http://academic.brooklyn.cuny.edu/biology/bio4fv/page/mito.htm

The OM is the first barrier separating the mitochondrion from the cytosol. It stops the entrance of macromolecules but allows smaller particles, up to a few kDa, free passage due to its porous structure. The inner membrane is a very complex and dynamic compartment, which is still intensively investigated. It seals the matrix and strictly regulates the movement of particles even as small as ions. This protein rich membrane

is subdivided into two domains. First, named the inner boundary membrane (IBM) is in very close proximity to OM with the intermembrane space dividing them. The second domain consists of cristae invaginations, in which two leaflets of inner membrane are juxtaposed to each other creating range of structures from tubules to complex, interconnected plates. The more energy demanding the cell, the more of the IM is reportedly structured into cristae (Vogel et al., 2006). The IBM is connected with its invaginations by narrow, tubular structures termed cristae junctions (CJs) of around 28 nm diameter. There are a few theoretical models explaining formation and maintenance of cristae but none fully explain this complex process (Zick et al., 2009). It has been proposed that F_1F_0-ATP synthase supercomplexes are involved in maintaining cristae structure and they could possibly influence the membrane curvature that locally increases the pH gradient and in the result optimize the synthase performance.
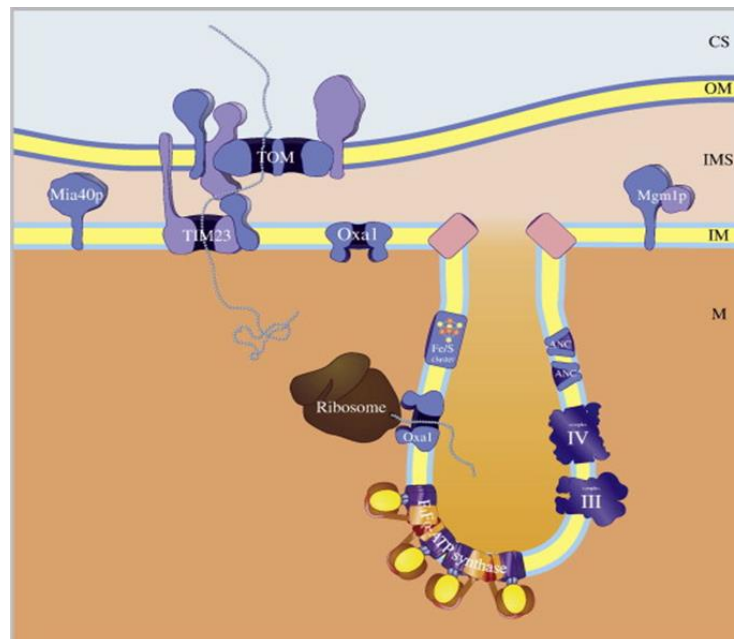
Figure 1.2. Schematic representation of the mitochondrial IM subcompartmentalisation. Location of proteins is based on research in *S. cerevisiae*. Mia40p; facilitates the oxidative biogenesis of intermembrane space proteins, Tim23; translocase of the inner mitochondrial membrane, Mgm1p; mitochondrial fusion, are enriched in the inner boundary membrane. ANC, CIII, CIV and F_1F_0-ATP synthase dominate in cristae membrane. CS, cytosol; OM, outer membrane; IMS, intermembrane space; IM, inner membrane; M, matrix. Image taken from Zick et al., 2009.

Recently performed research on yeast shows subcompartmental localization of protein complexes in the inner mitochondrial membrane (Vogel et al., 2006), with those engaged in either the fusion process (Mgm1) or nuclear-encoded protein translocation (Mia40p, TIM23) being preferentially placed in IBM. In contrast, proteins of the

OXPHOS system, iron-sulphur cluster biogenesis, as well as proteins involved in mitochondrial translation and transport of mtDNA-encoded polypeptides are in higher density located in the cristae membrane (Figure 1.2). However, the distribution of these proteins between the two compartments undergoes dynamic changes triggered by the physiological state of the cell.

Nevertheless, it is accepted that the structure of the inner membrane is very dynamic, going through processes of fusion and fission during mitochondrial network reshaping, remodelling in response to the cellular conditions (Benard and Karbowski, 2009). The structure and swift remodelling of mitochondrial compartments is of great importance for cellular homeostasis, and perturbations in morphology are seen in numerous human diseases including Alzheimer's and Parkinson's disease (Trimmer et al., 2000). Mitochondrial fission is crucial for growing and dividing cells to supply them with sufficient population of mitochondria (Youle and Van der Bliek, 2012). Moreover, fission allows segregation of damaged beyond repair mitochondria from the mitochondrial network in order to be degraded (mitophagy). In contrast, fusion is driven by energy demand in the face of stress; it allows mitochondria to exchange proteins, lipids, RNA, in order to compensate for one another's defects and maintain energy output.

1.1.2.1 Mitochondrial remodelling in cell death.

Alterations in the morphology of mitochondria are also reported in apoptosis and necrosis, manifesting in the fragmentation of mitochondrial tubules and the reshaping of inner-membrane cristae (Itoh et al., 2013). Apoptosis is a programmed cell death that is, for example, responsible for separation of fingers and toes in a developing human embryo. Whereas necrotic cell death is distinct from the apoptotic signal transduction pathway, caused by factors external to the cell or tissue, such as extreme temperature changes or infections (Vanlangenakker et al., 2008). Mitochondria play an important role in the regulation of apoptosis via caspase-dependent or caspase-independent death pathways in response to diverse signals. Caspases are cysteinyl aspartate –directed proteases cleaving a broad range of cellular proteins (Kurokawa and Kornbluth, 2009). The caspases 9 and 3 cascade is activated by the release of cytochrome *c* from permeabilised mitochondria into the cytosol (Jiang and Wang, 2004, Frey and Sun, 2008). Increased accessibility of cytochrome *c,* which is stored in the intracristal space, has been shown to occur upon extensive remodelling of the mitochondrial inner membrane (Zick et al., 2009). In the caspase-independent cascade an apoptosis-inducing

factor (AIF) is relocated to the nucleus from the IM (Dawson and Dawson, 2004). AIF is required for the maintenance of normal cristae structure (Cheung et al., 2006). The loss of AIF from mitochondria was proposed to cause disintegration of the IM topology (Zick et al., 2009).

1.1.3. Functions of mitochondria.

As already mentioned, a broad range of metabolic and bioenergetic pathways is located in mitochondria. These pathways include oxidative phosphorylation (OXPHOS), Krebs cycle, β-oxidation of fatty acids, iron-sulphur clusters biogenesis (Lill and Mühlenhoff, 2006), certain amino acid metabolism as well as regulatory pathways, such the above mentioned programmed cell death or Ca^{2+} buffering and signalling (Glancy and Balaban, 2012). The long list of functions also needs tightly regulated transport machinery embedded in both of the mitochondrial membranes (Neupert and Herrmann, 2007).

Energy transduction is one of the most studied functions of mitochondria, as it is essential for cell survival and functionality. In order to sustain its homeostasis cells require a constant source of ATP, which is a carrier of energy locked in phosphate bonds (Koopman et al., 2012). There are two sources of adenosine triphosphate, first in cytosol through a purely anaerobic process called glycolysis, which produces two particles of ATP, NADH and pyruvate. The latter is then transported to the mitochondrial matrix, converted to acetyl coenzyme A and processed by Krebs cycle to yield NADH and $FADH_2$ molecules that feed electrons into the oxidative phosphorylation pathway. Five protein complexes located in mitochondrial inner membrane take part in generating ~32 ATP molecules from one event of a glucose full oxidation to CO_2 and H_2O.

1.1.3.1. OXPHOS system.

Respiratory complexes I, II, III and IV transfer electrons from donors (NADH and $FADH_2$) to an acceptor (O_2), which releases energy used in transport of H^+ protons from the mitochondrial matrix to the intermembrane space in order to create a pH gradient and electrical potential across the IM. The fifth complex, the FoF1- ATP synthase couples the flow of protons back to the matrix and converts this chemiosmotic energy into phosphate bonds, generating ATP from ADP (Mitchell, 2011). The OXPHOS machinery is a very complex and dynamic structure, consisting of ~ 92 subunits. Although mostly encoded by nuclear genes, genetic information for 13 of these

polypeptides (embedded in complex I, III, IV and V) is held in the mtDNA genome and the proteins are produced in the mitochondrial matrix. This is in contrast to complex II, which consists of polypeptides entirely encoded by the nDNA. Correct biogenesis of respiratory complexes also requires assembly factors, of which 35 are currently described (Koopman et al., 2012). It has been also proposed that complexes can create higher molecular structures named 'respirasomes' supporting their dynamic stability. The present view is that such supercomplexes are composed of CI, CIII and CIV. The newest publications in *Science* proposes a further two supercomplexes to be embedded in IM, the first composed of CI and CIII and second built of CIII and CIV (Lapuente-Brun et al., 2013).
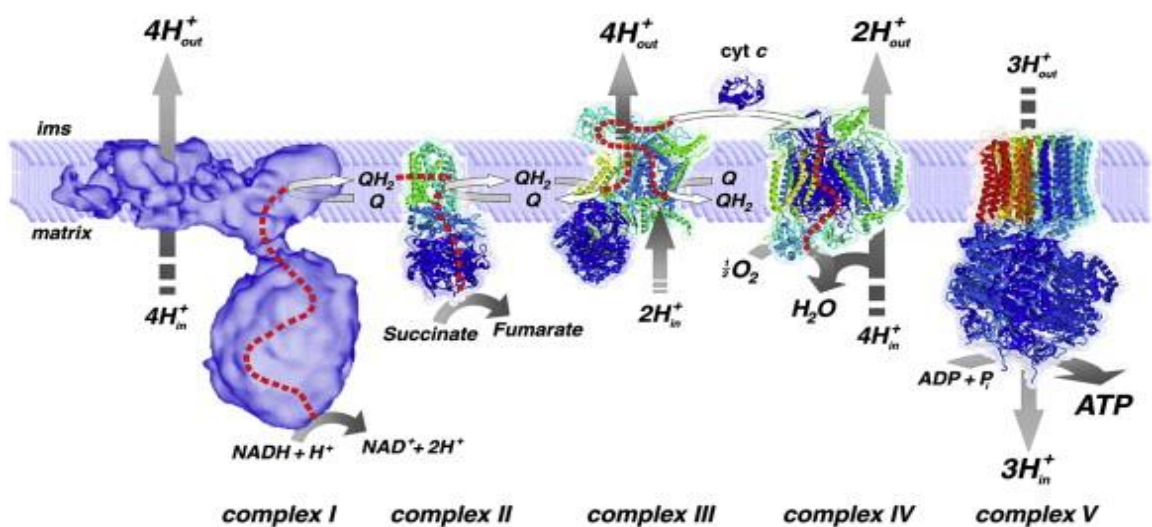
Figure 1.3. **Schematic representation of OXPHOS system embedded in the mitochondrial inner membrane.** This illustrates the established electron movement in complexes I, II, III and IV of the OXPHOS system, which transduces energy, transformed by complex V into phosphate bonds of ATP molecules. Electrons extracted from NADH and $FADH_2$ are passed to CI and CII respectively, and are transported by a chain of Fe-S clusters to CoQ_{10}, which carriers them to CIII. Cytochrome *c* (cyt *c*) passes electrons to CIV. At CV, the chemiosmotic energy created by CI, III and IV by pumping H^+ protons across the inner membrane from mitochondrial matrix to intermembrane space is released by controlled backflow and coupled to the formation of ATP from ADP and phosphate (P_i), (taken from Yu-Wai-Man et al., 2011).

Different types of cells, their physiological demands and environmental conditions influence the balance between glycolytic and mitochondrial ATP production. Some, such as mature erythrocytes that lack nuclei and mitochondria depend completely on cytosolic ATP synthesis. Other cell types mostly rely on the complete oxidation of glucose (brain cells) or fatty acids (liver cells). Skeletal muscle cells switch from fatty acids to glucose oxidation during high activity events that provide them with the biggest ATP supply. Because of these differences in energy demand and its sources, cells and

tissues can be more or less severely affected by malfunction of the OXPHOS system (Smeitink et al., 2006).

Nevertheless, as a major supplier of ATP produced from energy-rich molecules, influencing many other metabolic and signaling pathways, dysfunctions of OXPHOS machinery can cause many disorders, some of which are lethal in an early onset (Chan, 2006, Nunnari and Suomalainen, 2012). Mitochondrial disorders can be caused by single deficiency of a specific complex, due to a defect in one of the subunits or assembly factor failure (Sugiana et al., 2008). In contrast, multiple deficiencies, affecting more than one of the complexes are often induced by mutations in mtDNA, or nuclear factors maintaining its expression (Shutt and Shadel, 2010, Rötig, 2011, Nicholls et al., 2013, Schon et al., 2012). Clinical presentation of OXPHOS impairment can include developmental regression, dystonia (neurological movement disorder), failure to thrive, ataxia and nystagmus (involuntary eye movement) (Koopman et al., 2012) and commonly display neuromuscular defects.

1.2   Mitochondrial DNA expression.
1.2.1 The human mitochondrial genome.

The 16.6 kilobase mitochondrial genome of humans encodes 13 subunits of the OXPHOS system, as well as 22 mitochondrial tRNAs and 2 mt-rRNAs that are crucial in translation mt-mRNA (Anderson et al., 1981). It lacks introns and the only long non-coding region of the genome (1.1 kilobase), the D-loop, contains the majority of the control elements of transcription and replication (Taanman, 1999).
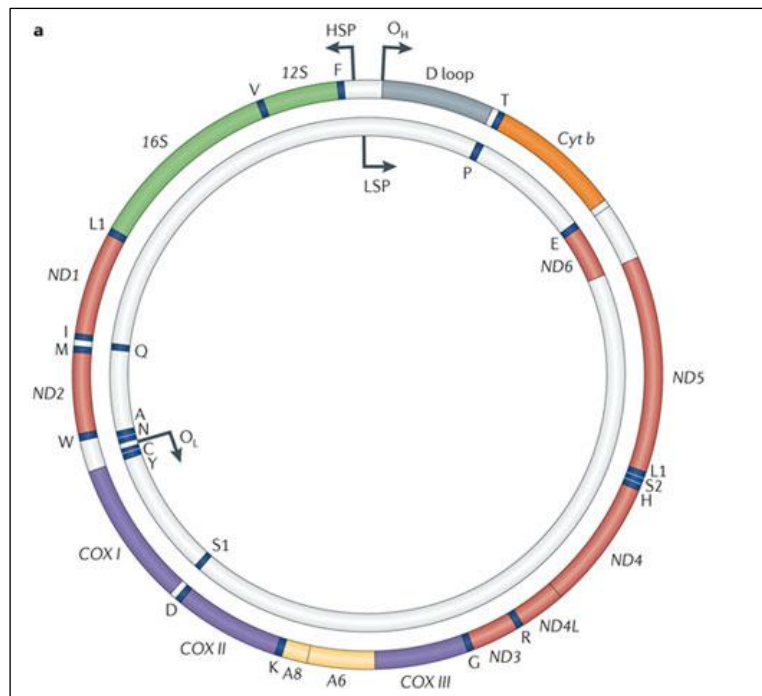
Figure 1.4. Human mitochondrial DNA map.
The map depicts the positions of the 37 mitochondrial genes; 13 of which encodes polypeptide subunits of Complex I (red; *ND1*, *ND2*, *ND3*, *ND4*, *ND4L*, *ND5*, *ND6*), Complex III (orange; Cyt *b*), Complex IV (purple; *COXI*, *COXII*, *COXIII*) and Complex V (yellow; *ATP6*, *ATP8*) located on heavy DNA strand apart from ND6 based on light strand. 2 mt-rRNA (12S and 16S) species and 22 mt-tRNAs. O_L and O_H are the origins of heavy and light strand replication, respectively. HSP and LSP are the promoters of transcription for heavy and light chain DNA. Non-coding regions are indicated in grey, mt-tRNAs in dark blue. (Taken from Schon et al., 2012).

The mtDNA can be easily described as compact as it does not contain introns but harbours several overlapping genes and incomplete termination codons. Moreover, the mtDNA is not a diploid like nuclear DNA but a multicopy genome. Most human mitochondria accommodate approximately ten copies of maternally inherited mtDNA (Phillips et al., 2014), although the copy number depends on the cell type and demand for energy (Schon et al., 2012). A cell contains hundreds of mitochondria and depending on the tissue 500-10,000 mtDNA molecules. An exception is mature oocytes that have between 100,000 to 600,000 mtDNA copies. As mtDNA resides in the mitochondrial matrix in close proximity to the high concentration of reactive oxygen species (ROS) it is prone to damage-induced mutations that can remain and potentially propagate (Phillips et al., 2014). Since cells contain multiple mitochondrial genomes, if a mutation is present, it is possible to have a heterogeneous set of mtDNA in a cell, tissue or even organelle, a condition named heteroplasmy. The opposite is homoplasmy, where all mtDNA molecules are identical.

Heteroplasmy can be inherited by the fetus from a heteroplasmic mother, but the mutation load passed to the offspring depends on the mitochondrial bottleneck (Smeets, 2013). The latter depends on clonal proliferation of mtDNA in the developing oocyte and mtDNA segregation among the cells of blastocyst (Poulton et al., 2010). Heteroplasmy can also be a result of somatic mutations contributing to the ageing process and degenerative diseases of ageing such as cancer (Ames et al., 1993, Lee et al., 2010).

1.2.1.1. Replication of mtDNA.

Mitochondrial DNA is organized in protein-rich structures called nucleoids that have been shown to be sites of replication (Spelbrink, 2009, Gilkerson et al., 2013). Strikingly, it has been reported recently that mitochondria in a single cell are organized in populations that differ in DNA processing activities like initiation of replication or the relative amount of transcripts expression (Chatre and Ricchetti, 2013). Current knowledge of the mitochondrial replication system is still incomplete and needs far more investigation in order to draw clear mechanistic schemes of this process. There are at least two major patterns of replication proposed (reviewed in Stumpf and Copeland, 2011). First, the asynchronous strand displacement model, proposes that replication at Ori_H is initiated by transcription at the light strand promoter (LSP) producing a processed RNA primer, which is extended by mitochondrial DNA polymerase γ (*POLG)*. When approximately two thirds of H strand replication is complete, the replication forks triggers synthesis of L-strand from O_L in the opposite direction, by unfolding it to the single-stranded form (Xu and Clayton, 1996, Lee and Clayton, 1996). Second, the coupled replication model based on analysis of partially nuclease digested mtDNA by 2D gel electrophoresis, proposes the ribosubstitution pattern in coupled leading and lagging strand replication (Holt et al., 2000, Yang et al., 2002). In this model nascent L chains of mtDNA contain ribonucleotides patches, removed during the maturation step and converted to DNA. In contrast, the H strand contain only scattered ribonucleotides (Yang et al., 2002). The same research group in their next publication postulates also, that replication originates from multiple sites located in *MTCYB*, *MTND5* and *MTND6* genes. The replication fork arrests near the O_H, and restricts replication to one direction only (Bowmaker et al., 2003). Recently, the strand-displacement model has been supported with new evidence obtained by *in vivo* saturation mutagenesis indicating that O_L is indispensable for mtDNA replication in the

mouse (Wanrooij et al., 2012). Moreover the biochemical and bioinformatic data presented in the report show that O_L is conserved in vertebrates.

Despite the lack of a final picture of how mitochondrial DNA replication proceeds, a few of the proteins taking part in this process have been identified and probably a lot more awaits description. Mitochondrial transcription factor (TFAM), mitochondrial single-stranded DNA binding protein (mtSSB), Twinkle helicase and POLG have been shown to colocalize in nucleoids (Garrido et al., 2003). Very recently it has been published that Twinkle helicase is firmly associated with IM, where it transiently interacts with mtDNA to facilitate replication and that nucleoids have dynamic composition and activity (Rajala et al., 2013).

TFAM is a multifunctional protein taking part in the transcription initiation (Asin-Cayuela and Gustafsson, 2007), packaging of mtDNA (Alam et al., 2003) and regulation of mtDNA copy number (Ekstrand et al., 2004). Overexpression of human TFAM in mice showed a slight increase in the steady state level of mtDNA, so it has been proposed as a main component of nucleoids wrapping and bending nucleotides chains; influencing the rate of replication (Ekstrand et al., 2004). Indeed, high-resolution assessment with Chip-seq technique in HeLa cells revealed that TFAM binds to the whole mitochondrial genome (Wang et al., 2013), which confirms the recent super-resolution microscopy analysis of mitochondrial nucleoids (Kukat et al., 2011). Phosphorylation of TFAM within high-mobility-group box 1 (L-shaped three-helix domain that binds DNA in the minor groove) impairs its ability to bind mtDNA and triggers degradation by the Lon protease (Lu et al., 2012). Phosphorylation and proteolysis has been proposed to be a regulatory mechanism of TFAM function and abundance in mitochondria, which are essential in mtDNA maintenance and expression. Furthermore, TFAM dimerization increases mtDNA compaction by stimulating looping of the DNA (Ngo et al., 2014).

POLG enzyme is a heterotrimer built of a 140 kDa catalytic subunit and two copies of a 55 kDa accessory subunit, which increases processivity. It has been reported, that *POLG* together with mtSSB and Twinkle proteins, are able to synthesise ssDNA of more than 15000 nt *in vitro* (Korhonen et al., 2004). Mutations in the POLG gene inhibiting its function have been identified in a subset of mitochondrial diseases (Stumpf et al., 2013).

1.2.2. Transcription of the mitochondrial genome.

Maintenance and replication of mtDNA is of great importance for cell homeostasis. Mutations in *POLG* enzyme can cause many mitochondrially linked diseases (Milone and Massie, 2010, Cohen and Naviaux, 2010). The next step for the correct function of mitochondria is the expression of information coded in its genome. Transcription, delivers 11 mRNA species (as 2 are present as bicistronic RNA units: *ATPase 8/6* and *ND4L/ND4*) to the mitoribosomes that contain two mt-rRNA molecules also transcribed from mtDNA, as are the tRNA species that are required for translation. The correct decoding of information prescribed by mtDNA and the processing of the resultant mtRNA is one of the main points of regulation in correct mitochondrial function (Mercer et al., 2011).

Ten out of eleven mRNA containing transcripts and both rRNAs are transcribed from H strand DNA. Only *MTND6* is decoded from the L strand. In contrast, tRNAs are quite evenly spread between both strands (Bonawitz et al., 2006). Promoters for heavy strand, HSP1 (H1) and HSP2 (H2) are located in close proximity, near the 5'end of 12S rRNA (Figure 1.4), but are differently regulated (Montoya et al., 1982). H2 promotes synthesis of a polycistronic molecule that covers almost the total H strand. Whereas, transcription initiated from H1 generates transcription units that harbour only two rRNAs and stops at a specific site in the tRNA^{LEU} (Asin-Cayuela and Gustafsson, 2007). The existence of this mt-rRNA specific promoter has been much debated as has the termination function of mTERF. The generally accepted definitions are given here. This early termination of transcription from H1 is determined by a 34 kDa protein, mTERF1, binding to promoter-independent bidirectional termination site. The single promoter for the L strand is located in 7S DNA. Transcripts originating from HSP2 and LSP are transcribed in a polycistronic manner. These RNA transcription units are precursors that are processed to individual species where the extraction of tRNAs that flank most of the ORFs plays a major role (Ojala et al., 1981). This process takes place in the recently identified mitochondrial RNA granules (Jourdain et al., 2013).

The final mechanism of transcription initiation is still not fully clarified. Recently published data, which will be addressed further in this subsection, suggest that the main proteins taking part in initiation are mitochondrial RNA polymerase (POLRMT), TFB2M and TFAM.

Human POLRMT is a single subunit, phage-derived, 140 kDa enzyme, sharing common features with the bacteriophage T3, T7 and SP6 family of RNA polymerases.

It consists of two functional domains. The C-terminal region in eukaryotic and prokaryotic organisms retains high levels of conservation with the bacteriophage homologue, and it is the domain responsible for catalytic activity (Tiranti, 1997). The N-terminal domain, presenting lower similarity to bacteriophage RNA polymerases, is also less conserved in eukaryotes. In mammals it accommodates a PPR motif (Asin-Cayuela and Gustafsson, 2007, (Ringel et al., 2011). This motif was originally identified in the plant kingdom, where it is a common motif in proteins that take part in RNA processing, editing and translation (Small and Peeters, 2000).

In contrast to the yeast homologue, human POLRMT requires additional proteins in order to initiate the transcription process (Asin-Cayuela and Gustafsson, 2007). The first of these is already mentioned TFAM, a high mobility group (HMG) family protein, which contains a 25 amino acid C-terminal tail crucial for DNA recognition (Dairaghi et al., 1995a). Removal of this tail does not affect unspecific binding ability to DNA. Its definite interaction upstream of transcription promoters is essential in the initiation stage (Dairaghi et al., 1995b). It has been proposed that TFAM can influence the structure of the promoter, which facilitates sequence-specific binding of the POLRMT/TFB2M complex at a start site for transcription (Gaspari et al., 2004).

Mitochondrial TFB1 and TFB2 are the methyltransferase-related transcription factors (Falkenberg et al., 2002) that contain specific binding sites for S-adenosyl-L-methionine, SAM, which acts as the methyl donor (McCulloch et al., 2002). These two proteins are homologues of the eubacterial RNA adenine dimethytransferase KsgA (Shutt, 2006, Cotney and Shadel, 2006), which introduces methyl groups in neighbouring adenine residues in the terminal stem-loop of 16S rRNA (helix 45). Although this modification is highly conserved in most metazoa, it is not significant for bacteria. The lack of methylation in *E. coli* 16S rRNA gives resistance to kasugamycin (Helser et al., 1971). Interestingly, this modification does not occur in mt-SSU rRNA of yeast, *S. cerevisiae* (Klootwijk et al., 1975) but it is present in human 12S mt-rRNA.

Human mitochondrial TFB1 and 2 have both retained predicted methyltransferase ability (Cotney and Shadel, 2006), moreover it has been shown that both can bind POLRMT and activate transcription initiation *in vitro* (Cotney et al., 2007). Further investigations of their functions in mitochondria clearly show that the first, TFB1M, is the primary methyltransferase influencing mitochondrial translation, metabolism and cell growth (Cotney et al., 2009, Metodiev et al., 2009), whereas TFB2M is a main primary transcription factor (Shutt et al., 2010).

It is important to mention that all of the experimental approaches in investigating the initiation step of mitochondrial transcription, performed *in vitro*, failed to obtain RNA derived from the speculated HSP2 promoter, which might be due to additional involvement of as yet not described factors, or mismapped initiation start sites through methods that have now been refined and superseded. The HSP1 and 2 promoter sites will be discussed again later in the text.

Experimental data published during the last few years concerning the process of transcription initiation, have presented so many opposing claims, that it is quite difficult to draw from these findings some consistent, even if not complete, picture. Shadel and colleagues showed stimulatory involvement of MRPL12 protein in LSP and HSP1 transcription *in vitro* and an increase in the steady state levels of mitochondrial mRNAs; based on *MTND2* and *MTND6* in HeLa cells overexpressing FLAG-tagged MRPL12 (Wang et al., 2007). In a later publication the same research group dismisses the necessity of any TFAM interaction with mtDNA in the process of promoter-dependent initiation from LSP and HSP1 and proposes instead the role of the activator for this protein (Shutt et al., 2010). In this study they use "a faithful, fully recombinant human mitochondrial transcription system with all proteins purified from *E. coli*", in which the template for transcription is a linear DNA.
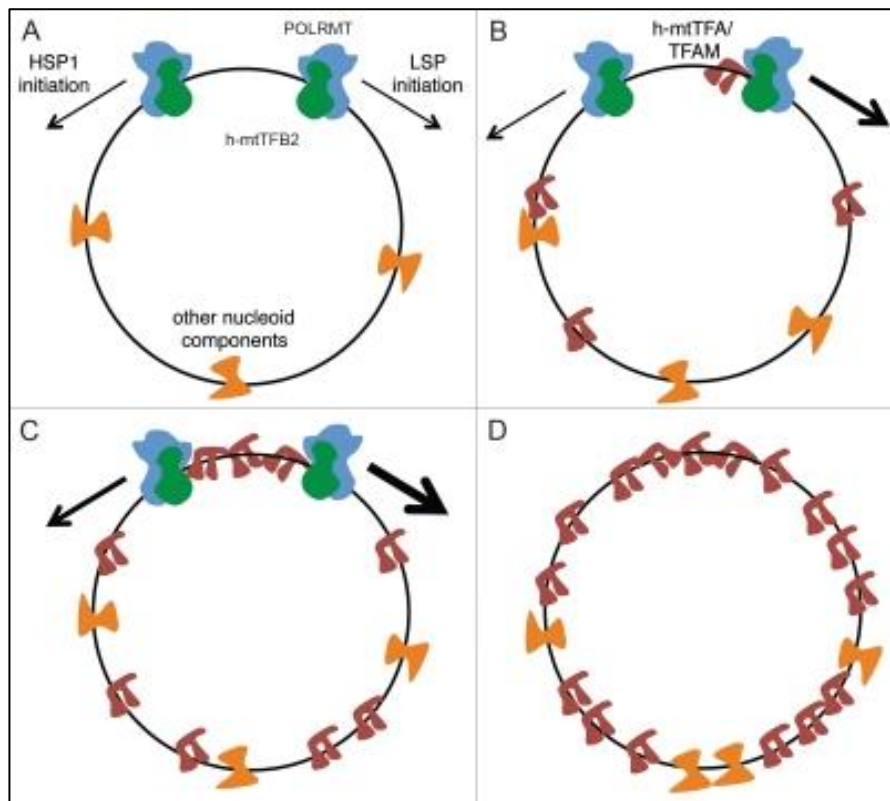
Figure 1.5. **Representation of theoretical states of transcription initiation governed by the amount of mammalian TFAM interacting with mtDNA molecule.**
A. mtDNA associated with minimal amount of mtTFA (brown particle), demonstrates a basal level of transcription (indicated with arrows) from both promoters; HSP1 and LSP. **B.** Depicts mtTFA bound at the high-affinity LSP site where it preferentially stimulates transcription (thickness of the arrows refers to the level of transcription initiation). **C.** Higher amounts of mtTFA associated with mtDNA activate both promoters. **D.** Very high level of TFAM inhibits transcription. Image taken from Shutt et al., 2011.

Interestingly, another research group published results presenting the ability of POLRMT to synthesize RNA in a promoter-independent manner on supercoiled circular double stranded DNA as a template in complex with TFB2M. The same capability was observed for transcription initiated from LSP promoter. Strikingly, in both cases TFAM presence was not required to obtain a strong signal from synthesised RNA in the *in vitro* reactions (Fukuoh et al., 2009). In the light of these findings Shadel and colleagues proposed a new model of transcription initiation, the schematic representation of which is shown in Figure 1.5, (Shutt et al., 2011).

The dispute continued with the report from Temiakov and Gustafsson research group, which insists on a three factor (POLRMT, TFB2M and TFAM) dependent initiation of transcription *in vitro*, dismissing also stimulation of LSP transcription by MRPL12 and pointing out that TFB2M acts as an exclusive transcription stimulator *in vitro* (Litonin et al., 2010). Previous results showed this activity for both TFB1M and

TFB2M, although the latter had far greater activity (Falkenberg et al., 2002). In the next publication, Shadel and colleagues, present data that reinforces their previous publication, reporting a stimulatory effect of MRPL12 protein on promoter dependent and independent transcription *in vitro* (Surovtseva et al., 2011). Furthermore, they specify a pool of MRPL12 that is free and not bound to the mt-ribosome, as directly binding with POLRMT and distinct from complexes of the RNA polymerase/TFB2M. Interestingly, they also report that depletion of MRPL12 in HeLa cells causes a decrease in the steady state level of mitochondrial transcripts *MTND1, MTND6, MTCO2, 12S* and *16S*. It is tempting to address the last finding and point out that northern blot analysis of mRNAs of *MTND1* and *MTCOI* in immortalised, patient derived fibroblast with point mutation in MRPL12 gene, where free pool of this protein is undetectable in sucrose gradient fractions, did not show the same pattern. Indeed, in this report only 16S rRNA was modestly decreased to 68%, with 12S rRNA affected to a lesser extent (79.2%) (this thesis; Serre et al., 2013). The next publication regarding mitochondrial transcription machinery again addresses the requirement of TFAM in the initiation step, demonstrating its absolute necessity (Shi et al., 2012). The authors argue that the observations excluding TFAM from a core component of transcription initiation (Shutt et al., 2010) are due to incorrect experimental conditions, which allows DNA 'breathing', such as low salt concentrations.

The publications described above, although they do not draw the final mechanism of the transcription initiation step, definitely give an insight into the complicated mechanism of the human mitochondrial gene expression pathway. Clearly, the proteins described here, are only a few of those already reported, with many more still not identified. For example; recently TEFM protein, encoded by the C17orf42 gene was proposed as a significant factor in transcription elongation (Minczuk et al., 2011).

1.2.3. Processing and maturation of mitochondrial RNA.

Following completion of transcription, the three polycistronic primary transcripts (Montoya et al., 1983) are mostly processed into individual species by endonucleolytic cleavage of mt-tRNAs at their 5' and 3'ends (Ojala et al., 1981) performed by RNase P (Holzmann et al., 2008) and RNase Z (ELAC2) (Brzezniak et al., 2011), respectively. Still, three of the mtORF junctions (*MTND6-ncRNA, MTND5-MTCYB* and *RNA14-MTCO3*) that lack mt-tRNAs are not cleaved by RNase P/ Z (Brzezniak et al., 2011). Pentatricopeptide (PPR) RNA-binding protein, PTCD2 has been shown to take part in processing of *MTND5-MTCYB* (Xu et al., 2008). PPR motifs have been well

characterised in plants and take part in processing, editing and stability of transcripts in chloroplasts and mitochondria (Small and Peeters, 2000, Nakamura et al., 2012). Currently, six other mammalian mitochondrial PPR proteins have been characterised (reviewed in Lightowlers and Chrzanowska-Lightowlers, 2013).

Recently, GRSF1 protein (first identified as cytosolic RNA binding protein with high affinity for G-rich sequences: Qian and Wilusz, 1994) has been reported to be required for the processing of *MTND6-ncRNA* and *RNA14-MTCO3* precursors (Jourdain et al., 2013, Antonicka et al., 2013).

Once mt-RNAs are processed to individual species they undergo posttranscriptional maturation and modification. The latter are important in their stability and function (Borowski et al., 2010). Free 3' ends of mt-mRNAs, are polyadenylated by mitochondrial poly(A) polymerase, hmtPAP (Tomecki et al., 2004). The polyadenylation is necessary in seven transcripts to complete the UAA stop codon in the open reading frame by the addition of either one or two A residues. Further, a poly(A) extension of 50-60 nucleotides has been shown to influence stability of mt-mRNAs (Nagaike et al., 2005, Wydro et al., 2010, Rorbach et al., 2011).

A distinct difference between human mitochondrial mRNAs and those from the eukaryotic cytosol is that they are not 5'-capped and have no introns. In contrast to eubacterial mRNAs, mitochondrial RNA species lack Shine-Dalgarno sequences. Only, a limited 3' oligoadenylation to mt-rRNAs and CCA addition to all 3'ends of mt-tRNAs has been reported (Gagliardi et al., 2004). Both RNA components of mitoribosome as well as tRNAs species require a number of base modifications (reviewed in Rorbach and Minczuk, 2012).

1.2.4. Turnover of mitochondrial RNA.

The mechanism of mRNA degradation is still not well explored. Suv3 helicase has been reported as a decay regulator of correctly formed, mature mRNAs, aberrant transcripts and noncoding processing intermediates mostly originating from the L-strand transcripts (Szczesny et al., 2010). Another enzyme, polynucleotide phosphorylase (PNPase), which has both PAP and 3' to 5' phosphorolytic activities (uses phosphorolysis to degrade RNA), was suggested to take part in poly(A) tail removal and RNA turnover (Piwowarski et al., 2003). Curiously, subsequent studies of this protein showed its intermembrane space localisation (Chen et al., 2006) and a role in RNA transport into mitochondria has been postulated (Wang et al., 2010). The most recent publication, however, shows a subset of PNPase and Suv3 helicase in one complex, referred to by

the authors as a degradosome, which is co-localised in specific foci with RNA and nucleoids in the mitochondrial matrix (Borowski et al., 2013). Another protein, PDE12, was recently described as a 3' to 5' exoribonuclease. PDE12 (2'-phosphodiesterase) is located in the mitochondrial matrix and removes poly(A) tails from mRNA species *in vitro* and *in vivo* (Rorbach et al., 2011). Its overexpression depletes the poly(A) status of mt-mRNA, and has a transcript specific effect on stability. Finally, the first mitochondrial oligonuclease REXO2, capable of degrading short RNA species has been identified (Bruni et al., 2013). Intriguingly, it has dual localisation in mitochondria; it is found both in the intermembrane space and the matrix (Bruni et al., 2013).

Disturbance of mt-RNA turnover deregulates mitochondrial functions as the above mentioned publications describe. Mitochondrial homeostasis strongly depends on balance between synthesis and stability/ degradation of RNA species. The keepers of this order are just emerging from the pool of more than 1000 proteins (Pagliarini et al., 2008) involved in mitochondrial maintenance. Importantly, although originating from a common polycistronic RNA source, mitochondrial transcripts abundance varies significantly, which suggests involvement of complex posttranscriptional regulatory mechanisms (Mercer et al., 2011). On one pole can be placed proteins involved in the decay of RNA, on the other, protectors that guard these molecules from too early deterioration.

1.2.5. Mitochondrial RNA binding proteins regulating mitochondrial RNA stability.

Ten years ago, a number of unidentified proteins binding mitochondrial RNA were reported, ranging in molecular mass from 15 to 120 kDa, (Koc and Spremulli, 2003). Recently, a few of them have been described as factors playing significant roles in stability of mt-mRNAs and rRNAs. The first one, SLIRP (SRA – stem loop interacting RNA – binding protein) was characterised as crucial for OXPHOS function (Baughman et al., 2009). SLIRP is ~12 kDa protein containing one RNA recognition motif (RRM), and it is localized to mitochondria (Hatchell et al., 2006). Its depletion in immortalized human fibroblasts caused a global decrease in mt-mRNAs steady state levels, with the most affected being the bicistronic ND4/ND4L transcript, and mt-mRNAs encoding all three complex IV proteins. SLIRP has been reported to interact in high-molecular-weight complexes with another RNA binding protein, LRPPRC (leucine-rich pentatricopeptide repeat motif containing protein) (Sasarman et al., 2010). The latter has 16 PPR motifs and as the already mentioned PTCD2 (subsection 1.2.3.) belongs to the

family of mitochondrial PPR proteins (Sterky et al., 2010). Mutations in LRPPRC cause the French Canadian variant of Leigh syndrome (LSFC), which is usually fatal in an early onset neurodegenerative disease (Mootha et al., 2003). The majority of patients are homozygous for a single missense mutation changing A_{354} to V, leading to tissue-specific decline in cytochrome *c* oxidase activity, which mostly affects brain and liver (Sasarman et al., 2010). Studies in fibroblasts, derived from the LSFC patients, show a decreased level of mutated LRPPRC that correlates with reduction in the levels of most mt-mRNAs, whilst rRNAs and tRNAs remain unchanged. This phenotype was reproduced in control cells depleted of LRPPRC with siRNA (Sasarman et al., 2010). Interestingly, maturation of primary transcripts was not affected, indicating involvement of this protein in the stability of processed mRNAs. Translation deficiency was most severe for mitochondrially encoded COX subunits, but further depletion of LRPPRC caused the global effect of deregulated assembly in all OXPHOS complexes containing polypeptide subunits produced in mitochondria, with all mRNAs severely decreased (Sasarman et al., 2010). Furthermore, the same research group confirmed co-immunoprecipitation of LRPPRC with SLIRP and reported a decrease of the latter in LSFC patient fibroblasts. Cells that do not contain mtDNA, 143B rho^{0}, and thus no mt-mRNAs, show reduced level of both proteins but these are still able to remain in a complex (Sasarman et al., 2010). This last observation was challenged by another research group, which investigated further the functions of LRPPRC in a mouse model (Ruzzenente et al., 2011), proposing an RNA-dependent complex formation of both proteins. They propose that LRPPRC aggregates in the absence of RNA or interacts with another protein complex. Interestingly, they also show, using FLAG-tagged LRPPRC in complex with SLIRP, the presence of a wide spectrum of mt-mRNAs species in the immmnuoprecipitated complexes. This is in contrast with the narrow substrate specificity described for plant PPR motifs (Nakamura et al., 2012). Furthermore, they also report an effect on polyadenylation, with only oligoadenylated mt-mRNAs present in its absence and a deregulation of translation. Studies in HeLa cells, also report a role for LRPPRC in mtPAP-catalyzed polyadenylation *in vitro* as well as providing a protective role for mt-mRNAs against PNPase mediated degradation when complexed with SLIRP (Chujo et al., 2012).

A protein from the pool of mitochondrial RBPs that was reported to have RNA protective function is ERAL1. It is found in association with the small ribosomal subunit mt-SSU (Dennerlein et al., 2010). Crosslinking Immunoprecipitation (CLIP)

assay via the FLAG moiety was used to determine the ERAL1 binding on 12S-rRNA *in vivo*. CLIP analysis revealed that ERAL1 bound to defined region (Dennerlein et al., 2010). The sequence mapped to 33 nucleotides that form part of helix 45, which is a stem-loop at the 3' terminus. The loop accommodates two dimethylated adenine residues (Seidel-Rogol et al., 2002). Hypermethylation of these residues was reported in patients with maternally inherited deafness (Cotney et al., 2009). Involvement of enhanced 12S rRNA methylation in loss of hearing was also investigated in a mouse model overexpressing TFB1M (Raimundo et al., 2012). This augmented modification was reported to cause ROS-dependent activation of AMP kinase and proapoptotic E2F1, nuclear transcription factor in patient-derived A1555G cells (Raimundo et al., 2012).

Depletion of ERAL1 in HEK293 cells caused severe decline in the nascent 12S rRNA steady state level (Dennerlein et al., 2010, Uchiumi et al., 2010). Interestingly, *de novo* translation appeared unaffected and steady state level of mt-mRNAs increased, although these observations are in contrast with another publication (Uchiumi et al., 2010). Silencing of this protein caused growth arrest and induction of apoptosis (30% *cf* 3% in controls) in cell population in a ROS-independent manner (Dennerlein et al., 2010).

This specific checkpoint in human mitoribosome biogenesis seems to play significant role in cell functionality, which is able to trigger programed death through two opposite pathways; ROS-dependent and independent. These recent findings show how complicated is the dependence between the cell and mitochondrion. Although this organelle contains a very minimalistic genome, somehow this limited information and its expression pathway is able to influence the host cell to a great extent.

1.2.6. The mitoribosome – a tool for translation.
1.2.6.1. Structure of mammalian mitoribosome.

The final stage of decoding mitochondrial genes and translating them from mt-mRNA ribonucleotides to polypeptides chains requires purpose-build machinery in the form of the mitoribosome. Through the evolutionary pathway, this highly organised structure has developed differently in different organisms. Here I describe the mammalian machinery that has unique features by which it differs from cytosolic ribosomes and although it shares some similarities of prokaryotic origin, the mammalian mitoribosome has its own exclusive structural and functional character.

The presence of mitoribosomes was first reported in rat liver (McLean et al., 1958) but mammalian mitoribosomal particles were only isolated 10 years later (O'Brien and Kalf, 1967). The characterisation of mitoribosomes from different organisms showed their divergent structure and size, with sedimentation values ranging from 55S to 80S (Kitakawa and Isono, 1991). The mammalian ribosome (55S) is composed of two subunits; small 28S (mt-SSU) and large 39S (mt-LSU) (Figure 1.6).
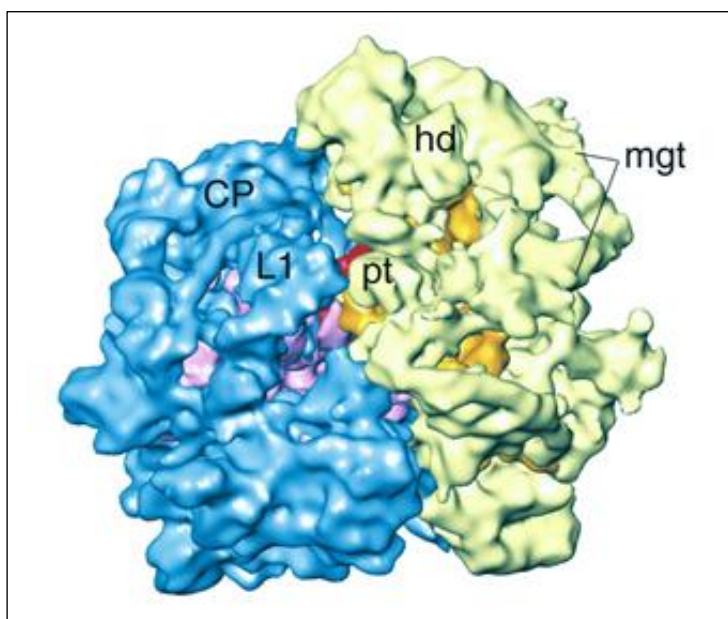
Figure 1.6. Cryo-EM structure of the bovine mitoribosome (55S) obtained at 13.5 Å resolution. Various features are indicated as follows, 12S rRNA is indicated in orange, 16S rRNA in purple, proteins in the SSU in yellow, LSU in blue. CP, central protuberance; L1, L1 protein side of LSU; hd, head of the SSU; p, platform side of the SSU; mgt, mRNA-entry gate. The image was taken from Sharma et al., 2003.

Each subunit includes an rRNA particle of mitochondrial origin and a set of proteins coded by the nuclear genome, produced in cytosol and imported to the mitochondrial matrix. The unique aspect of the mammalian mitoribosome starts with its weight ratio of RNA to protein content which is ~30%: 70%. This is in striking contrast to their eukaryotic cytosolic counterparts, which are built of ~60% RNA and eubacterial ribosomes, which contain 67% RNA (Mears et al., 2006, Koc et al., 2010). The small and large subunits of the mammalian mitoribosome are connected by 15 bridges. Nine of these contacts are distinct to the mitoribosome and the interactions are believed to be mainly via protein: protein or protein: RNA. Bacterial 70S particles by contrast are all RNA-RNA bridges (Koc et al., 2010).

Mammalian 12S (950 nt) and 16S (1560 nt) rRNA of the small and large subunit respectively are dramatically shortened in comparison with the eubacterial 16S (1542

nt) and 23S (2904 nt) rRNAs. Alignment of the secondary structure of mammalian rRNAs with the bacterial counterparts shows precise deletion of specific helices and shortening of others, with the anti-Shine-Dalgarno sequence completely absent from the 12S particle (Sharma et al., 2003). These reduced rRNA species influence the structure of the 55S, with it appearing to be highly porous in comparison with *E. coli* 70S. Interestingly, although the number of mitochondrial ribosomal proteins (MRPs) is increased and some that have eubacterial homologues are enlarged, many of them occupy new spatial positions in the mitoribosomes. These positions may potentially be compensating for missing rRNA segments, however they only occupy around 20% of space that is created by the relative loss of rRNA. In comparison, the subsequently obtained cryo-EM map of the protista (*Leishmania tarantolae*) mitoribosome shows more than 50% compensation by proteins (Sharma et al., 2009).

A 13.5 Å resolution structure of highly purified bovine 55S mitoribosome obtained by cryoelectron microscopy revealed positions of many mitoribosomal proteins, coating almost entirely the rRNA molecules, possibly creating a shield against reactive oxygen species (Sharma et al., 2003).

Twenty nine MRPs are located in the SSU of which 14 are homologues of eubacterial ribosomal proteins and 15 are 'new' specific mitoribosomal proteins. The small ribosomal subunit has a characteristic structure divided into three distinct parts named the body, head and platform. The mt-SSU accommodates the mRNA entry site, which in the mammalian ribosome has a distinctive triangular, possibly highly dynamic gate-like structure, built entirely of MRPs. These proteins cover part of the gate and may play a role in recruitment of the leaderless mRNAs to the mt-SSU (Agrawal and Sharma, 2012). A face of the small ribosomal subunit of the 55S also contains the A-site. This decoding site of the mitoribosome accommodates conserved residues on the 12S rRNA interacting with incoming tRNA species. These A-site retained contacts manifest similarities with the prokaryotic ribosome in the selection process of the tRNAs (Mears et al., 2006). The same conservation of rRNA segments was reported for peptide-bond formation (P) site on the 39S subunit. Interestingly, the interaction between tRNAs located in the P-site and the mitoribosome is strong enough to withhold several purification steps through sucrose gradients, as deacylated mt-tRNA still occupies the P site following purification. The most mysterious aspect of the mitoribosomal structure is the E-site, which in its eubacterial counterparts binds a de-aminoacylated tRNA before it exits the ribosome. The mammalian 55S has lost 14 of the 38 potential sites of contact with tRNA that are present in prokaryotic 70S (Mears et

al., 2006). This finding together with inability to detect E-site-bound tRNA on the mammalian ribosome indicates its probable absence or significant alteration (Koc et al., 2010).

The LSU accommodates at least 50 proteins; 28 of them are characterised as eubacterial homologues (Koc et al., 2001) and 22 are specific to the mammalian mitoribosome. Only five or six of the eubacterial ribosomal proteins do not have equivalents in the mammalian 55S. Two of these, L5 and L25 are positioned in the central protuberance (CP) of the bacterial LSU and interact with 5S rRNA (Figure 1.7), which is considered as absent from mammalian mitoribosome. Depletion of L5 protein in *E. coli* causes accumulation of a 45S ribosomal LSU, which lacks the majority of the CP elements (5S rRNA and proteins L5, L16, L18, L25, L27, L31, L33 and L35) (Korepanov et al., 2012) and is unable to associate with SSU. Both L5 and 5S rRNA are proposed to play a role in the inter-subunit bridges between the 30S and the 50S central protuberance (Zhang et al., 2011). L5 protein is conserved in eubacteria, archaea and eukaryote ribosomes (Wool et al., 1995) and it has been shown to be crucial for the survival of *E. coli* (Korepanov et al., 2007). Bacterial L5 protein and 5S rRNA interacts with S13, also absent in mammalian mt-SSU. Another protein, L31 located in close proximity to 5S rRNA in bacteria also lacks a homologue in mammalian mt-LSU.
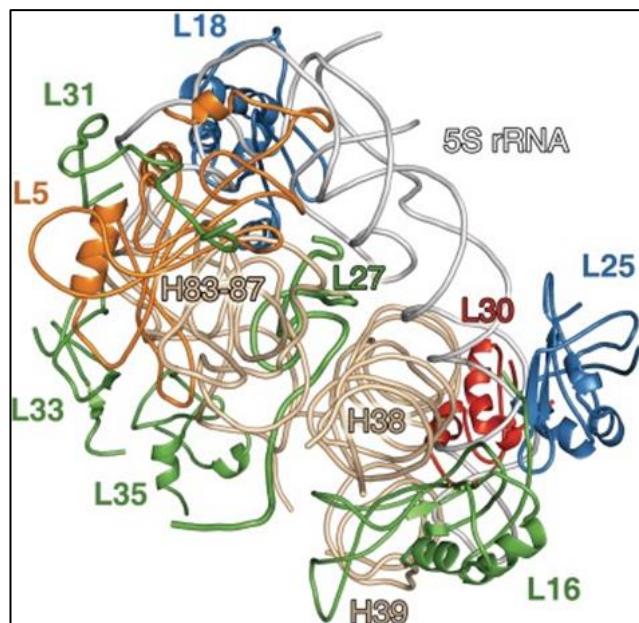
Figure 1.7. Structural model of *E. coli* central protuberance (CP). Bacterial ribosomal proteins (L5, L16, L18, L25, L27, L30, L33, L35), 5S rRNA and helices of 23S rRNA (H38, H39, H83-87) are demonstrated. Image taken from Korepanov et al., 2012.

Although cryo-EM structure of the bovine mitochondrial LSU is lacking a 5S rRNA particle, the central protuberance itself, which in bacteria contains the 5S rRNA,

is ~2-fold larger in the mitoribosome (Mears et al., 2006). Interestingly, it is partially replaced by MRPs. Moreover, a handle-like structure is noticeable in the cryo-EM model, connecting the central protuberance to the body of the LSU, possibly taking over some of the 5S rRNA role, present in cytosolic and prokaryote ribosomes.

Whilst compiling this introduction, a new high resolution structure of the porcine mitoribosomal LSU was reported (Greber et al., 2013). This three-dimensional structure of the mt-LSU of the porcine mitoribosome determined by cryoelectron microscopy at 4.9 Å resolution reveals an additional RNA density at the central protuberance (CP), which resembles domain β of the eubacterial 5S rRNA (Greber et al., 2013). Still, the observed RNA density does not account for the full length 5S rRNA and does not reach to the main body of the 39S subunit. Instead a long α-helical protein density corresponding to mitoribosome specific MRPL52 protein connects the mitoribosomal central protuberance to the subunit body (Figure 1.8). It is important to mention another very recent publication presenting the structure of yeast mitochondrial large subunit obtained by single-particle cryo-electron microscopy at 3.2 Å resolution (Amunts et al., 2014). The CP of yeast 54S lacks 5S rRNA, is extensively remodelled with mitochondria specific proteins, the extensions of the five bacterial homologues, and RNA expansion clusters. Overall, in spite of the 5S rRNA absence, the yeast CP tripled the volume of the bacterial one.
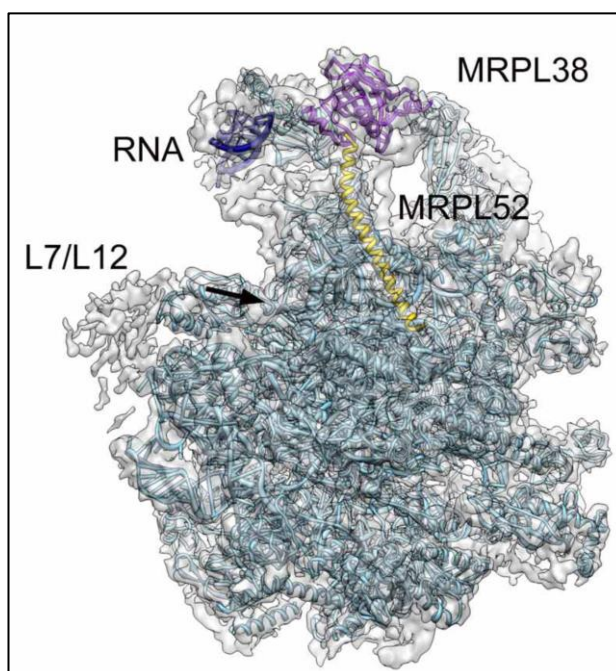
Figure 1.8. Structure of 39S mitoribosomal subunit with positioned unidentified second rRNA molecule and MRPL52 protein. Unidentified RNA (dark blue), MRPL38 protein (purple) positioned at the central protuberance, MRPL52 (gold) connecting central protuberance with the body of mt-LSU. Image taken from Greber et al., 2013.

The large subunit of bovine mitoribosome has three distinct structural units extending from the body; L1 stalk, L7/L12 stalk and the above mentioned central protuberance, which all are larger than their eubacterial homologues (Mears et al., 2006, Greber et al., 2013) (Figure 1.9). Most of the outer surface of bovine mt-LSU is covered with mitochondria specific MRPs.
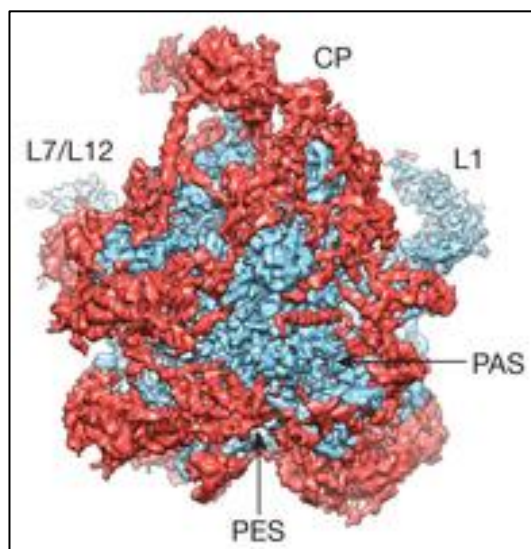
Figure 1.9. Cryo-EM structure of the porcine 39S mitoribosomal subunit obtained in a 4.9 Å resolution. Conserved elements of 39S are presented in blue, mitoribosome-specific in red. L7/L12, L7/L12 stalk base; ; L1, L1 stalk; CP, central protuberance; PAS, polypeptide accessible site; PES, polypeptide exit site. Image taken from Greber et al., 2013.

Their main mass is located in the central protuberance, mostly on the solvent side and in the lower portion of the body (Mears et al., 2006, Greber et al., 2013) (Figure 1.9). The cryo-EM map of 39S was updated with identified positions of mitoribosome-specific proteins MRPL38, mentioned already MRPL52, MRPL49 and ICT1 located at the CP (Greber et al., 2013).

The most distinctive characteristic of mitochondrial LSU is the polypeptide exit tunnel. It has two openings on the solvent side. The first is similar to the conventional polypeptide exit site (PES) (Nissen et al., 2000). The second, around 25 Å ahead of the PES, has been called the polypeptide-accessible site (PAS). It arose from the loss of significant portion of domains I and III in the mt-LSU rRNA. It has been postulated that both of these exits can be functional and some of the nascent polypeptide chains emerge from the PAS opening. In general the presence of two exit sites is seen as an element of the ribosome that possibly allows monitoring of translation and inserting nascent polypeptides to specific locations in the IM (Koc et al., 2010). Moreover, hypothetical models have been proposed of the mammalian mitoribosome interplaying with the mitochondrial inner membrane based on the newest findings (Agrawal and Sharma, 2012). Recently, a few proteins have been found to take part in coupling mitochondrial

translation with assembly of respiratory complexes. Oxa1L was characterised as an integral inner membrane protein, in human mitochondria (Stiburek et al., 2007). Its depletion in HEK293 cells caused deregulation of F_1F_o-ATP synthase and NADH: ubiquinone oxidoreductase biogenesis. The C-terminal ~100-amino acid tail of Oxa1L, which is exposed to the mitochondrial matrix was cross-linked with several proteins of the mitochondrial LSU (Haque et al., 2010). Intriguingly, none of these proteins belong to the conserved components of the conventional PES. In yeasts another inner membrane protein, Mba1, was defined as a ribosome receptor collaborating with the C-terminal Oxa1 (yeast homologue of mammalian Oxa1L) tail in coordinating the insertion of nascent polypeptide species to the IM (Ott et al., 2006). Recently, new data were published concerning the role of two proteins, ObgH1 and Mtg1 in human mitochondria. Both were postulated to bind the mitochondrial inner membrane and associate with the mt-LSU and possibly play a role in correct insertion of mitochondrial subunits into OXPHOS complexes (Kotani et al., 2013). The most recent cryo-EM map of 39S again reveals more information about the structure of the PES, presenting new layer of proteins MRPL39, MRPL44, MRPL45 positioned on top of the conserved proteins surrounding the conventional polypeptide exit site (Greber et al., 2013). MRPL45 has been also proposed to take part in the interaction of mitoribosomes with the mitochondrial inner membrane.

Features of the mammalian mitoribosome described above clearly show its divergence in comparison with cytosolic or eubacterial ribosomes. The unique aspect of the 55S complex manifests in a reversed RNA: protein ratio, a porous structure, enriched with new protein masses and specific appearance of an mRNA entry site and polypeptide exit tunnel. All of these characteristics evolved in order to create a highly specialised machinery, producing exclusively hydrophobic membrane proteins, responding to energy demands from the cell but also sensitive to intraorganellar homeostasis requirements. It can be easily hypothesised that the process of ribosome assembly must be complex and tightly regulated, considering the dual source of molecules that build it.

1.2.6.2. Biogenesis of mitoribosome.

Unfortunately, current knowledge about the assembly of the mitochondrial ribosome is poor. In yeast there are three G-proteins identified; two of them, Mtg1 (Barrientos et al., 2003) and Mtg2 (Datta et al., 2005) are implicated in assembly of the LSU. One, Mtg3 takes part in assembly of the SSU (Paul et al., 2012).

Also, in human, only a few proteins have been reported to take part in biogenesis of the mitoribosome. C7orf30 was described as an mt-LSU protein, as its depletion causes an impairment of mitochondrial translation (Wanschers et al., 2012), and abnormal assembly of mt-LSU, which leads to a decrease in monosome formation (Rorbach et al., 2012). Another protein C4orf14 (or NOA1), containing a highly conserved GTPase domain, has been reported to take part in assembly of the mt-SSU and was found associated with mitochondrial nucleoids (He et al., 2012). It has been proposed to participate in maturation of the small subunit and maintenance of mtDNA. Intriguingly, C4orf14 apart from interacting with proteins of mt-SSU and mtDNA binding proteins, also associates with MRPL12, which independently from being part of mt-LSU and fully assembled monosome, interacts with POLRMT, influencing the rate of transcription (Wang et al., 2007).

ERAL1 is a protein that belongs to the family of GTP-binding proteins and has been reported to be an RNA chaperone as it directly binds with 12S rRNA (Dennerlein et al., 2010) and hence associates transiently with the mt-SSU. As already mentioned, the interaction site with 12S rRNA includes two dimethylated adenines. This post-transcriptional modification is believed to be introduced into the 12S rRNA by TFB1M, which in organ specific depletion in mice has been shown to lead to impaired assembly of the monosome (Metodiev et al., 2009).

Recently, a new publication has arisen, proposing a transcription-independent function of POLRMT in complex with TFB1M (Surovtseva and Shadel, 2013). The authors, using HeLa cells expressing hemagglutinin-tagged (HA) mitochondrial RNA polymerase, show an independent interaction of this enzyme with TFB1M and TFB2. Moreover, co-association of POLRMT and TFB1M with the small ribosomal subunit even in the absence of transcription apparently causes a minor increase in 12S rRNA methylation at the 3'end stem-loop. On the basis of this finding, the group led by Shadel propose a new function for POLRMT, co-operating with TFB1M, as a guard of SSU maturation and assembly into mitochondrial ribosome (Surovtseva and Shadel, 2013). Finally, it has been published that a non-ribosomal protein hMTERF4 (belonging to the mitochondrial termination factor (MTERF) family) complexes with ribosomal RNA methyltransferase NSUN4, recruits it to the LSU and thus influences mitochondrial ribosomal assembly and translation (Cámara et al., 2011). A following publication presents that MTERF4 strongly stimulates the specificity of NSUN4 in *in vitro* methylation experiment (Yakubovskaya et al., 2012).

Apart from all the factors described here, which play a role in the biogenesis of the mammalian mitoribosome as well as many more still awaiting identification, it has become clear that post-translational modifications of MRPs including phosphorylation and acetylation are of significant importance for translational regulation (Miller et al., 2009, Koc and Koc, 2012). The modifications of ribosomal proteins in mitochondria and eubacteria are very well conserved and located in the regions essential for ribosome function, like L1 and L7/L12 stalks or near the sarcin-ricin loop (SRL) in the ribosomal RNAs. These alterations are thought to modulate various steps of protein synthesis, by affecting mt-mRNA interactions with mt-tRNA and translation factors binding to the mitochondrial ribosome. For example, phosphorylation of mitochondrial ribosomal proteins was proposed to inhibit the synthesis of the 13 mitochondrial subunits of OXPHOS system (Miller et al., 2009). The same was reported for NAD^+ dependent deacetylation of translational machinery components (Koc and Koc, 2012).

1.2.6.3. Translation process in mitochondria.

Although, research of the last 10 years has given an insight into the mitochondrial translation machinery, this system is still far from being well described and understood. Despite some striking similarities with bacterial counterparts, mammalian mitoribosomes have developed a range of unique features driven by evolutionary adaptations to cope with high demand for energy provision requiring precise regulation. Unfortunately, the mitochondrial research field still lacks techniques that allow the genetic manipulation of the mitochondrial genome and there is no *in vitro* system capable of synthesizing mitochondrial polypeptides, so the basic model of this process is copied from studies in bacteria supported with some mitochondria-specific observations. The translation process is divided into four major steps; initiation, elongation, termination and recycling. The first requires two mitochondrial initiation factors *in vitro*; $IF2_{mt}$ (Liao and Spremulli, 1990) and $IF3_{mt}$ (Koc and Spremulli, 2002). These proteins are essential in the initiation complex assembly, consisting of the 55S ribosome with fMet-tRNA^{met} located at the AUG start codon of mt-mRNA in the mitoribosomal P-site (Christian and Spremulli, 2010). It is important to mention that both of these factors are orthologous to bacterial IF2 and IF3 but there is no identified mitochondrial orthologue of prokaryotic IF1 (Spremulli et al., 2004). In the proposed model of initiation, IF3 assures that the mt-SSU and mt-LSU remains dissociated, preventing 55S formation. IF2-GTP stimulates binding of fMet-tRNA^{met} to the SSU followed by sequence - independent complex formation between 28S and a mt-mRNA

(Liao and Spremulli, 1989). Interestingly, the interaction between mt-SSU and mRNA does not require any additional factors, unlike the prokaryotic and cytosolic systems (Smits et al., 2010). Moreover, the leaderless nature of mt-mRNAs is essential in initiation complex formation, suggesting that processing of the polycistronic mitochondrial transcripts has to occur before translation can initiate (Christian and Spremulli, 2010).

The polypeptide chain elongation step in mammalian mitochondria has more conserved features than either the initiation or termination stages in comparison to prokaryotes (Agirrezabala and Frank, 2009, Woriax et al., 1997). It requires the 55S complex to be associated with mt-mRNA and an fMet-tRNA^{met} located in the P site. Then GTP-bound elongation factor Tu (EF-Tu$_{mt}$) associates with aminoacyl-tRNA. This enters the A-site of mitoribosome. Positive recognition of a correct codon-anticodon match by the ribosome triggers hydrolysis of GTP, which frees EF-Tu. Elongation factor Ts (EF-Ts$_{mt}$) reactivates EF-Tu-GDP by promoting the exchange of GDP to GTP. Peptide bond formation is catalysed by the mitoribosome itself, leaving a deacylated tRNA in the P-site and a peptidyl-tRNA enriched by one amino acid in the A-site. Next, mitochondrial elongation factor G1 (EF-G1$_{mt}$) catalyses the removal of the deacylated tRNA from the P-site and the relocation of the peptidyl-tRNA from the A-site to the P-site. As mentioned before, there is apparently no E-site identified in the cryo-EM structure of the bovine mitochondrial ribosome, so the exact mechanism of how the deacylated tRNA leaves the 55S complex is unknown (Sharma et al., 2003).

The next step of translation, termination, starts when a stop codon either UAA or UAG is detected in the A-site (Christian and Spremulli, 2012). In human mitochondria two reading frames are followed by either an AGA or AGG triplet, each of which would code for arginine in the standard genetic code. In the mitochondrion, however, there are no tRNAs or proteins that recognise these triplets and so they remain unassigned. A -1 frameshift is promoted, in part by the 3' structure of the bound mt-mRNA, which creates a classical UAG in the A-site (Temperley et al., 2010a). Both the UAA and UAG stop codons are recognized by the release factor mtRF1a (Soleimanpour-Lichaei et al., 2007), which binds in the A-site of the mitoribosome and through the GGQ motif, causes hydrolysis of the ester bond between the nascent polypeptide chain and the mt-tRNA (Lightowlers and Chrzanowska-Lightowlers, 2010). Three other proteins (mtRF1, C12orf65, ICT1) that contain GGQ motifs have been identified, and are classified as mitochondrial release factor family members and have been shown by my host lab to be localized to mitochondria (Antonicka et al., 2010, Richter et al., 2010b). The function of

mtRF1 is still unknown. Interestingly, the other two mt-RF family members lack the regions involved in codon recognition (Richter et al., 2010a). ICT1 in contrast to other family members is an integral member of the mitoribosome in the LSU (Richter et al., 2010b). It has been proposed that it is a ribosome-dependent, codon-independent, peptidyl-tRNA hydrolase with activity that can play a role in rescuing stalled ribosomes. A quality control rescue function was also suggested for C12orf65 protein by other groups (Antonicka et al., 2010, Kogure et al., 2012).

After departure of synthesized proteins from the mitoribosome, two recycling factors RRF1 (Rorbach et al., 2008) and RRF2 (Tsuboi et al., 2009, Christian et al., 2009) bind to the A-site and induce mitoribosome subunit dissociation and release of the tRNA and the mRNA. The hydrolysis of GTP is not required for dissociation of subunits but is necessary for the release of recycling factors from the LSU.

1.2.7. Significance of ribosomal 5S in human mitochondria.

The reviews concerning one of the most sophisticated machineries found in all types of cells, the ribosome, usually starts with the basic description of it addressing the heterogeneity in its composition and asymmetry in the structure. The sentence that always is present in summaries of established knowledge confirmed through analysis of the crystal structures of LSUs and complete ribosomes from different organisms inform that a 5S rRNA is present in virtually all ribosomes except mitoribosomes of some fungi, mammals and most protists (Barciszewska et al., 2001, Szymański et al., 2003). Interestingly, the function of eubacterial and eukaryotic cytosolic 5S rRNA despite years of research remains unclear. Published results on studies in bacteria localise 5S rRNA in the central protuberance of LSU, where it interacts with three proteins L5, L18 (the bacterial homologue of eukaryotic L5) and L25. However, in eukaryota this interaction is limited only to L5 protein. Structural analyses of ribosomes from many species, positions 5S rRNA in the junction between small and large subunit, which allows it a broad interaction with many centres crucial for translation (Kiparisov et al., 2005, Kouvela et al., 2007). Indeed, its absence causes a decline in protein synthesis in both bacterial and eukaryotic cells (Ciganda and Williams, 2011). Furthermore, the most recent publication, presenting cryo-EM structures of the final-stage assembly precursors of the bacterial LSU shows involvement of 5S rRNA in the maturation process of 50S (Li et al., 2013). In addition, data on silencing of TFIIIA in human U2OS cells reports an inhibition of 5S rRNA transcription and impairment of ribosome biogenesis (Donati et al., 2013).

The 5S rRNA is the smallest ribosomal RNA molecule, built of 120 nt (40 kDa), with a secondary (Figure 1.10) and tertiary structures largely preserved across phylogeny (Ciganda and Williams, 2011, Cheng et al., 2012).
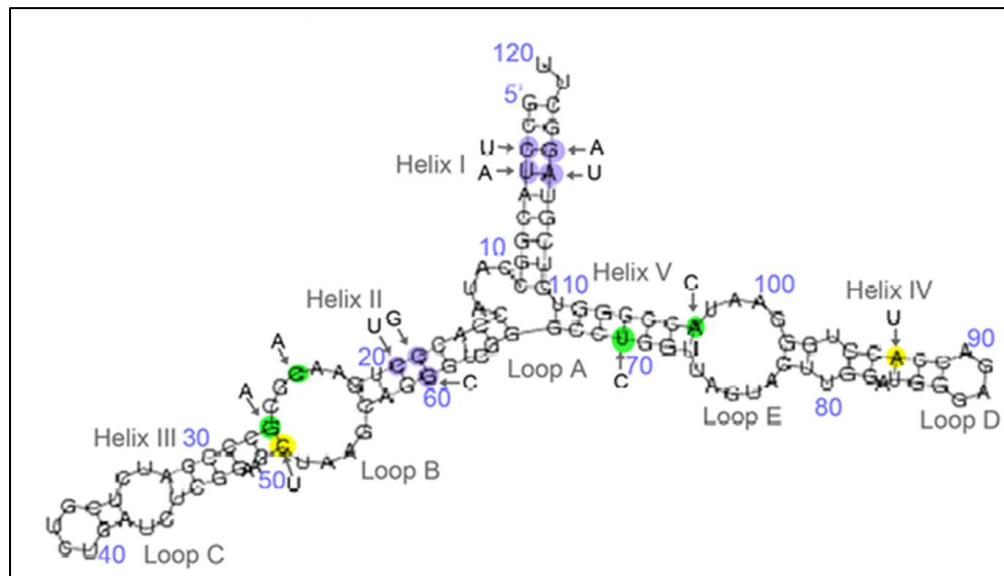
Figure 1.10. Secondary structure of human 5S rRNA. Evolutionary changes in the sequence of the 5S rRNA are indicated with yellow, green and purple. Image taken from Cheng et al., 2012.

Intriguingly, the 5S gene is present in a different number of tandem or multiple repeats spread throughout the genome. Recently, it has been shown that each mammalian species has a greatly conserved 5S rRNA type and many variable ones (Vierna et al., 2013). In eukaryotic cells, 5S rRNA is synthesized by RNA polymerase III, is transported from the nucleus to the cytosol in a complex with TFIIIA (transcription factor), and then re-enters the nucleus in the complex with protein L5. It is the only reported RNA species that creates complexes with ribosomal proteins before incorporation into the ribosomes in prokaryotes and eukaryotes (Szymański et al., 2003). Furthermore, it has been already reported that 5S rRNA plays roles outside the ribosome. The most recent publication, shows this small RNA particle in a complex with L5 and L11 protein implicated in p53 level regulation (Donati et al., 2013). This pre-ribosomal complex is redirected from assembly into nascent 60S ribosomes to Hdm2 inhibition, which activates p53, as a result of defective ribosome biogenesis. These intriguing data implicate 5S rRNA in very complicated and still elusive processes of carcinogenesis, as p53 is known as a tumour suppressor, which is lost or mutated in over 50% of all human tumours (Cairns and White, 1998). The role, if any, of 5S rRNA in mitoribosomes is even more mysterious. There are very limited data available

concerning the function of this molecule in mammalian mitochondria. As already mentioned it was not detected in a 13.5 Å resolution structure of bovine 55S obtained by cryoelectron microscopy (Sharma et al., 2003). However, this observation was challenged in a recent publication, showing its presence in mitoribosomes immunoprecipitated via either overexpressed FLAG tagged ICT1 or MRPS27 (Smirnov et al., 2011). The ratio of mitoribosomes to bound 5S rRNAs was reported as 1:1. This astonishing result needs further investigation as it is the first reported finding, standing against very strongly established dogma in mitochondrial research. There are no more publications supporting it directly, but there are at least a few that strongly suggest the presence of 5S rRNA in mammalian mitochondria. Two of the first reports shows the presence of this particle in stringently purified mitochondria and mitoplasts of bovine, chicken, rabbit, rat and human cells (Yoshionari et al., 1994, Magalhães et al., 1998). However, since the cytosolic ribosomes co-purify with mitochondria it is very difficult to eliminate contamination. It is important to underline, that the new mammalian 39S structure has an RNA fragment present that is not the 16S but has not been identified (Greber et al., 2013).

Structural analysis of 5S rRNA suggests two distinct regions, α- and γ- domains as critical for its mitochondrial targeting *in vitro*, confirmed by decline of import *in vivo* (Smirnov et al., 2008). The same research group, point out two proteins, mitochondrial enzyme rhodanese and MRPL18, as involved in 5S rRNA transport into mammalian mitochondria (Smirnov et al., 2010, Smirnov et al., 2011). There are also two independent publications showing involvement of PNPase (polyribonucleotide nucleotidyltransferase) in mitochondrial RNA import. This protein has a 3' to 5' exoribonuclease and poly(A) polymerase activity. As mentioned before it has a dual location in mitochondria; inner membrane and matrix. PNPase has also been shown to enhance transport of RNase P RNA, 5S rRNA and MRP RNAs into the mammalian mitochondrial matrix (Wang et al., 2010). These results were reinforced with a recent report, describing two patients with homozygous missense mutation in the PNPase gene who presented with severe encephalomyopathy, choreoathetotic movements (irregular involuntary movements that may involve the face, neck, trunk, limbs or respiratory muscles) and respiratory chain deficiencies (Vedrenne et al., 2012). The analysis of patient 1 fibroblasts showed a reduction in 5S rRNA and MRP RNA import into mitochondria, and a decrease in translation. Overexpression of the wild type PNPase

cDNA enhanced 5S rRNA transfer to mitochondria and rescued the translation deficiency.

Overall, the significance and functions of 5S rRNA in human cells is far from defined. Presented in this subsection publications clearly show how incomplete is our knowledge about this 120 nt RNA species especially in regard to its mitochondrial appearance. Although, few published findings suggest that 5S rRNA is a part of mitochondrial ribosome in human cells with the most recent cryo-EM structure of the porcine 39S at 4.9 Å resolution presenting additional density of unidentified short RNA fragment positioned in the CP, the only strong conclusion which can be made at this stage is that the 5S rRNA is present in human mitochondria. Beyond this conclusion there is not enough experimental evidence deciphering its exact location or functions.

1.3 Aims of this study.

As can be seen from the introduction, many of the processes regulating post transcriptional gene expression are still poorly characterised. My PhD project is focused on three proteins SLIRP, MRPL12 and RBFA to identify if they are involved, and if so what is their role, in different aspects of this regulation. During the course of my study I have undertaken numerous experimental approaches to investigate and define the precise functions of these proteins in mitochondrial gene expression.

Regarding SLIRP, my project aimed to:
  ➢ assess the ability of this protein to bind the mitochondrial RNA *in vivo*
  ➢ identify interacting RNA species and
  ➢ specify the location of binding.

Further investigation was not undertaken due to publications that arose during my studies, describing SLIRP function in mt-mRNAs maintenance and turnover.

The second part of my project was focused on one of the mitoribosomal proteins of the LSU, MRPL12. This protein is highly conserved throughout phylogeny, however, the role of MRPL12 in mitochondrial gene expression is still enigmatic. Available data suggest involvement of MRPL12 protein not only in the mitochondrial translation but also in modulation of the transcription process.

Immortalised fibroblasts from a patient harbouring a mutated form of MRPL12 caused by homozygous c.542C to T transition in exon 5 changing a highly conserved alanine into a valine were obtained from a collaborating laboratory and allowed me to study its function in human mitochondria.

My experimental investigation aimed to establish:
> the role of MRPL12 protein in mt-LSU and mitoribosome assembly
> the influence of MRPL12 on the steady state level of mt-RNA species
> the impact of MRPL12 on mitochondrial translation.

The third part of my study was concentrated on RBFA. Preliminary data gathered in my host laboratory by Joanna Rorbach and Ricarda Richter identified RBFA as a mitochondrial protein interacting with the small subunit of the mitoribosome. The eubacterial orthologue of this protein also named RbfA is a cold shock protein, taking part in the maturation of the 5' end of pre-16S rRNA. When associated with the bacterial small ribosomal subunit it interacts directly with numerous sections of 16S. Moreover some of these sections are binding sites of another protein Era, participating in maturation of the 3'end of pre-16S rRNA. Interestingly, bacterial cells lacking RbfA protein can be partially rescued by overexpression of Era. As I already mentioned in the introduction, the mitochondrial counterpart of Era; ERAL1 was investigated in my host laboratory. The CLIP assay analysis for ERAL1 protein that I performed clearly showed direct interaction with the 12S mt-rRNA 3'end.

The experiments with RBFA that I have undertaken were designed to answer:
> whether RBFA interacts directly with 12S mt-rRNA of SSU and if so what is the location of binding?
> Can RBFA and ERAL1 reciprocally compensate for each other's function following siRNA silencing in human cells?
> what is the role of RBFA in the maturation and/ or assembly of mt-SSU and formation of the mitoribosomes?

Each of the results chapters that follows reports the progress I made with respect to each of these sets of aims.

Chapter 2

Materials and Methods

2. Chapter 2: Materials and Methods.

2.1 Cell culture.

2.1.1 Human cell lines used in the project:

- ✓ HEK293T FLP-IN TRex (Invitrogen)
- ✓ HEK293T inducibly expressing FLAG tagged SLIRP
- ✓ HEK293T inducibly expressing FLAG tagged RBFA
- ✓ HEK293T inducibly expressing FLAG tagged ERAL1
- ✓ Immortalised Control skin fibroblasts
- ✓ Immortalised Patient skin fibroblasts with point mutation in MRPL12 gene changing A181 to V in polypeptide chain.

2.1.2 Cell culture maintenance.

HEK293T cells and HEK293T expressing C-terminal FLAG tagged versions of SLIRP, RBFA and ERAL1 protein were grown in DMEM medium (Sigma D6429, 4500 mg/L glucose, 1 mM sodium pyruvate, 2.5 mM L-glutamine) supplemented with 10% FCS, non-essential amino acids (1x) and uridine (50 µg/ml). During every third passage cells were treated with Blasticidin^S (10 µg/ml final concentration) to retain the tetracycline repressor, and Hygromycin^B (100 µg/ml final concentration) to avoid growth of construct-free cells. Immortalised fibroblasts were grown in DMEM medium (Sigma, 4500 mg/L glucose) supplemented with 10% FCS, 100IU Penicillin, 100 µg Streptomycin, non-essential amino acids (1x), 1 mM sodium pyruvate, 0.2 mM uridine. Cells were kept in a humidified Sanyo Incubator, at 37°C with 5% CO_2 and passaged twice per week at ~80% confluency. In order to remove cells from the surface of the flask HEK293T were incubated in 1mM EDTA/PBS for ~2 - 3 min at 37 °C. Fibroblasts were harvested with 1x Trypsin (Sigma) in 1mM EDTA/PBS. After pelleting at 230 g (bench centrifuge) for 4 minutes, cells were resuspended in fresh media and for general maintenance 1/10 of HEK293T cells were transferred to a new flask containing 15ml of fresh media. Fibroblasts were split 1:6.

2.1.3 Cells storage.

Cells of ~ 80% confluence, grown in 75 cm^2 flasks were stripped, pelleted and resuspended in ice-cold FCS. Equal volume of 20% DMSO in FCS was added drop-wise to the cells suspension. Cells in 10% DMSO were kept on ice for ~5 min. Next

transferred to pre-cooled cryopreservation tubes. Placed in polystyrene container, overnight at -80°C, and afterwards transferred to liquid nitrogen.

2.1.4 Mycoplasma detection.

Cells were kindly tested for Mycoplasma infection every 3 months by Mrs Debra Jones. MycoAlert® Mycoplasma Detection Kit (Lonza) was used following the manufacturer's instruction. In case of an infection, cells were discarded or treated with Plasmocin following the manufacturer's instruction.

2.1.5 Cells counting.

Cells counting were performed with haemocytometer; Hawksley, depth 0.1 mm, $1/400mm^2$. Directly before pipetting cells suspension to microscope counting chamber, Trypan Blue (0.4% solution, Sigma) was added in ratio 1:1, in order to distinguish dead cells and eliminate them from counting pool. In order to estimate the number of cells in 1 ml of medium, the average counted in 4 large squares was multiplied by 10^4.

2.1.6 Transfection of HEK293T cell lines using siRNA.

HEK293T cell lines seeded in 6-well plates, 25 cm^2 or 75 cm^2 flasks (Corning) were reverse transfected with a final concentration of 33.3 nM siRNA, apart from RbfA siRNA for which 50 nM concentration was applied, using Lipofectamine RNAiMAX (Invitrogen). Lipofectamine (2 µl/ well, 4 µl/ 25 cm^2, 12 µl/ 75 cm^2 flasks) was mixed with siRNA in Opti-MEM® I+Glutatmax™I (Gibco) (250 µl/ well, 500 µl/ 25 cm^2 flask, 1.5 ml/ 75 cm^2 flasks) and incubated for 10-20 min at RT. Next it was added to the cells suspended in growing medium (1.25 ml/ well, 2.5 ml/ 25 cm^2, 7.5ml/ 75 cm^2 flasks), described in 2.1.2. Cells were grown in the presence of siRNA for 72 hr and if required re-transfected with the same amount of siRNA and kept in the culture for additional 48-72. All siRNAs were custom synthesised by Eurogentec and stored as 20 µM or 100 µM stocks in RNase free water at -20°C/-80˚C.

Table 2.1.**Sequences of siRNA used in transient transfections of HEK293T cell lines.**

Name of the siRNA	Sequence (sense strand)
si-RBFA-ORF A (481)	5' GGA GCU GUA UGA CCU UAA C dTdT 3'
si-ERAL1-ORF1	5' GUG UCC UGG UCA UGA ACA A dTdT 3'
si-non-targetting control (NT)	siRNA negative control duplex OR-0030-NEG05

2.1.7 Stable Transfection of control and patient immortalized fibroblasts.

Fibroblasts (20 000 per well) of 6-well plate were transfected with 2 µg of pcDNA3.1 plasmid containing MRPL12 open reading frame, linearized with BsmI restriction enzyme (NEB), re-suspended in TE buffer. Transfection was performed using SuperFect® Transfection Reagent (Qiagen) according to the manufacturer protocol. The selection of cells was started after 72 hr with Geneticin G-418 Sulphate (400 µg/ml final concentration). During second attempt, transfection was repeated twice with a 4 hr interval.

2.2 Bacterial culture and manipulations.

2.2.1 Bacterial strains and plasmids.

Bacterial strains used in this study are:

- for CLIP method, TOP10 Chemically Competent cells transfected with pCR®4-TOPO® (Invitrogen)
- for generation of MRPL12 protein (antibody purification) *E. coli* expression strain Rosetta (DE3 cells, Novagen)
- for amplification of pcDNA3.1 plasmid containing MRPL12 gene used in stable transfection of patient and control fibroblasts, bronze α-select chemically competent cells (Bioline).

2.2.2 Transformation.

Transformations of chemically competent bacterial cells were performed according to manufacturers' protocols.

2.2.3 Isolation of plasmid DNA and insert screening.

Following transformation, Bioline α-select bacterial cells were seeded on selective agar plates (containing ampicillin 100µg/ml, LB with 2% agar) and grown overnight at 37°C. Single colonies were moved to 5 ml of LB medium (1% Bacto-tryptone, 0.5% yeast extract, 1% NaCl) with antibiotics and again grown overnight in the incubator at 37°C, 200 rpm. Afterwards bacteria were harvested and plasmids were extracted with GeneJET™ Plasmid Miniprep Kit (Fermentas).

In each case 5 colonies transformed with pcDNA3.1 were sequenced as described in subsection 2.3.5. CLIP tags were analysed as described in 2.6.1.

2.3 DNA manipulation.

2.3.1 DNA electrophoresis.

DNA samples were mixed with loading dye (bromophenol blue, xylene cyanol FF, 3% (v/v) glycerol) and separated on agarose gels in 1x TAE buffer (40mM Tris acetate, 1mM EDTA pH 8.0). Solution of ethidium bromide (0.5µg/ml final concentration) was added to dissolved agarose in 1xTAE buffer in order to visualise DNA with UV light, before casting the gel and electrophoresis in the 1xTAE running buffer.

2.3.2 Measurement of nucleic acid concentration.

The concentration of samples diluted in ddH$_2$O or TE buffer was measured with Nano-drop Spectrophotometer ND-1000, using a millimolar extinction coefficient of 33 for single stranded DNA and 50 for double stranded DNA and 40 for RNA.

2.3.3 Polymerase Chain Reaction (PCR).

All PCRs were performed with *Taq* DNA Polymerase (Thermo Scientific), *Taq* Polymerase (Fermentas) or KOD hotstart polymerase (Novagen). The latter was used as a proofreading polymerase where amplification of fragments for cloning was required. Reactions were performed in 25 to 50 µl volumes according to suppliers' protocols unless otherwise specified in the subsections.

2.3.4 PCR product purification.

PCR products were purified either directly from PCR reaction (if there was single DNA product of the correct size when analysed by agarose gel electrophoresis) with QIAquick PCR Purification Kit (QIAGEN) or excised from 4% low melting agarose gels and extracted with phenol-chloroform, followed by ethanol precipitation (used in CLIP method; 2.6.1).

2.3.5 DNA Sequencing.

The MRPL12 gene sequence in pcDNA3.1 plasmid was determined with CMV Forward (5'CGC AAA TGG GCG GTA GGC GTG3') and BGH Reverse (5'TAG AAG GCA CAG TCG AGG3') primers, which have sites in the recipient vector. The detailed protocol of sample preparation for sequencing with Genetic Analyzer 3130xI (Applied Biosystems) is given in CLIP method subsection.

2.3.6 Restriction digest.

Restriction enzymes used in this study are; EcoRI, Xho1 and BsmI (NEB). Digestion reactions were carried in 10 or 50 µl volumes and 1 or 10 µg of DNA respectively according to the suppliers' protocols.

2.4 RNA manipulations.

2.4.1 Trizol extraction.

Total RNA extractions from cell pellets were carried with TRIzol Reagent (Invitrogen) according to supplier protocol. TRIzol LS Reagent (Ambion) was used to extract RNA from sucrose gradient fractions.

2.4.2 Northern blot.

RNA samples (2-8 µg) extracted from cells or sucrose gradient fractions were prepared in total volume of 20 µl containing 1x MOPS, 35 % (v/v) formamide and 5.5 % (v/v) formaldehyde. Samples were incubated for 15 min at 55°C. Ethidium bromide (0.1 µg/µl final concentration) and RNA loading buffer (to 1x final; 10% (v/v) glycerol, 0.01% (w/v) bromophenol blue, 0.01% (w/v) xylene cyanol FF) were added before loading the samples on the 1.2% (w/v) denaturing agarose gel containing 1x MOPS and 0.9% formaldehyde. RNA was separated through the gel at 80 Volts (in 1x MOPS). After ~3 hr electrophoresis, the separation was assessed by exposure to UV light, if separation was sufficient the gel was rinsed 3x in DEPC dH$_2$O. The RNA was transferred to GeneScreen Plus membrane by capillary transfer overnight in 10x SSPE buffer and the efficiency of transfer assessed with the UV light. The membrane was rinsed in 2x SSPE and vacuum baked at 80°C for 2h followed by prehybridisation in 10ml of 50 % (v/v) formamide, 5x SSPE, 1% (w/v) SDS and 5x Denhardt's solution for minimum 2 h at 42°C.

The radiolabeled probes were prepared with specific DNA fragments (50-100 ng) in total volume of 9 µl in DEPC ddH$_2$O, denatured at 95°C, 4 min. After cooling on ice, DNA was mixed with random hexamers (3µl/sample; mix also contained 5x buffer, dATP, dGTP, dTTP), 2.5U Klenow DNA polymerase I (Promega) and 2 µl of ^{32}P dCTP (~10-20 µCi, PerkinElmer NEG513H). After 1 hr incubation at 37°C, the probe was purified to remove free nucleotides on a NICK^{TM} Column, Sephadex^{TM} G50, DNA Grade (GE Healthcare). The activity of the probe in 400 µl of DEPC ddH$_2$O was measured by a Cerenkov counter and minimum of 500,000 cps were added to 10 ml of hybridisation buffer. The incubation with the membrane was carried over-night at 42°C.

The membrane was washed twice with 20 ml of 2x SSPE in DEPC dH$_2$O for 15 min at RT and once with 2x SSPE/2% SDS at 65°C. Next it was placed in SARAN Wrap and exposed to a screen in Phosphor-Imager cassette. Detection of signal was performed with a Storm PhosphorImager and analysed with Image-Quant software (Molecular Dynamics, GE Healthcare). If the membrane had to be re-probed, the signal was stripped by 3x washes in boiling 0.1x SSC for 15 min and once with 0.1x SSC/0.1% (w/v) SDS. New hybridisation buffer would be applied for at least 2 hr and required probe added.

2.4.3 Reverse transcription.

RNA obtained from TRIzol extractions was reverse transcribed to cDNA with Super Script VILO ^{TM} Mastermix (Invitrogen) according to the supplier's protocol. Random hexamers were used in the 20 μl RT reactions, containing 100 ng of RNA.

2.4.4 Real time PCR.

1:100 or 1:1000 dilutions of cDNA were used in real time PCRs. Fast start DNA Master SYBR Green I - kit (Roche) and the Roche Lightcycler (capillary system) were used. All reactions were made up in 20 μl volume with the following components: 2 μl of the template (cDNA), ddH$_2$O, forward and reverse primer (concentration given in Table 2.2), MgCl$_2$ (concentration dependent on pair of primers used, given in Table 2.2) and 1μl of SYBR green mix (Roche).

Table 2.2. **Sequences of primers used in Real Time PCRs.**

Primer	Sequence from 5' to 3'	[MgCl$_2$]	T$_a$	[Primer]
12S forward	ACA CTA CGA GCC ACA G	3 mM	59°C	1 μM
12S reverse	ACC TTG ACC TAA CGT C			
16S forward	CCA ATT AAG AAA GCG TTC AAG	4 mM	57°C	0.5 μM
16S reverse	CAT GCC TGT GTT GGG TTG ACA			
5S forward	GTC TAC GGC CAT ACC ACC CTG	3 mM	59°C	1 μM
5S reverse	AAA GCC TAC AGC ACC CGG TAT			
28S forward	TCA TCA GAC CCC AGA AAA GG	3 mM	60°C	1 μM
28S reverse	GAT TCG GCA GGT GAC TTG TT			

2.5 Protein manipulation.

2.5.1 Isolation of mitochondria from human cell lines.

Cells grown in 75 or 300 cm^2 flasks were harvested at ~80% confluence, if required the cell lines with FLAG-tagged proteins were induced as indicated with either 1 μg/ml tetracycline (SLIRP and ERAL1) or 1 ng/ml doxycycline (RbfA) for 2-3 days. Pelleted cells were washed once with ice-cold Dulbecco's PBS and re-suspended in homogenisation buffer (0.6 M Mannitol, 10 mM Tris; pH 7.4, 1 mM EGTA) adjusted with 1mM PMSF and 0.1% BSA. The homogenisation step was repeated three times, each time followed by centrifugation at 400g, 10 min, 4°C in order to separate mitochondria from unbroken cells. Obtained supernatants containing mitochondria were centrifuged at 11000g, 10 min, 4°C. Pelleted mitochondria were washed in 1 ml of homogenisation buffer (lacking BSA) and lysed (Sigma lysis buffer, FLAG-IP kit with EDTA-free Roche Protease Inhibitor Cocktail, and 1 mM PMSF, 10 mM MgCl$_2$ and RNase inhibitor if required).

For the Real Time PCR assessment of monosomes immunoprecipitated from cells that over-expressed FLAG-ICT1, a further treatment to more stringently purify mitochondria was applied. Around 100 μl of mitochondrial pellet (~2.5 mg proteins) was incubated in 1 ml of 1x homogenisation buffer supplemented with 10 mM MgCl$_2$, 1mM CaCl$_2$ and 1.2 μl DNase I for 15 min on ice. After washing with 10 mM Tris-HCl; pH 7.4 mitoplasts were obtained by 30 min incubation (Thermomixer; 16°C, 1000 rpm every 3 min for 15 sec) in 500 μl 10 mM Tris-HCl pH 7.4, adjusted with 10 mM MgCl$_2$, 1mM CaCl$_2$ and Proteinase K; Invitrogen (5 μg/1 mg of proteins). Proteinase K was inactivated by addition of 1mM PMSF, mitoplasts were washed twice with 5 mM Tris-HCl; pH 7.4 containing PMSF. Next, the pellet was re-suspended in 500 μl of homogenisation buffer (with 10 mM MgCl$_2$, 1mM CaCl$_2$) and treated with RNase A (5 μl of 10 mg/ml stock) for 20 min in Thermomixer (the same program as described above). Afterwards, mitoplasts were washed once with 1 ml of 10 mM Tris-HCl; pH 7.4 containing 10 mM EDTA, 1 mM PMSF and 5 μl SUPERase In and once with Tris without EDTA. Each incubation or wash was followed by centrifugation at 6000g, 4 min, 4°C.

2.5.2 Preparation of cell and mitochondrial lysates.

Harvested cells were pelleted and rinsed once with ice-cold PBS (tissue culture grade; Dulbecco's A lacking Mg^{2+} and Ca^{2+}). Cell and mitochondrial (obtained as described in

the subsection 2.5.1) pellets were re-suspended in lysis buffer from the FLAG Immunoprecipitation Kit (Sigma), adjusted according to requirements of a technique used and analysis performed, which are specified in subsections of methods. Cells or mitochondria were incubated in the buffer for 30 min, at 4°C, on a rotating wheel. Obtained lysates were centrifuged for 10 min at 12000g, 4°C (unless stated otherwise). Supernatants were used for further analysis.

2.5.3 Protein concentration - Bradford Assay.

Protein concentration was measured by Bradford Assay. 1µl of cell or mitochondrial lysate was added to 799 µl of ddH$_2$O. Dilutions of BSA ranging from 0, 2, 5, 10, 15 to 20 mg/ml were prepared in the same volume. 200 µl of Bradford Reagent (BioRad) was added to each sample and mixed. BSA standard samples were loaded in duplicate, the lysates four times in 200 µl aliquots onto 96 well-plate to be measured in Microplate Reader (Elx800) at the absorbance of 595 nm.

2.5.4 SDS-PAGE.

Proteins from mitochondria and cell lysates as well as fractions from sucrose gradient fractionation (as described) were mixed with loading buffer (1x final concentration: 62.5 mM Tris-HCl pH 6.8, 2% SDS, 10% Glycerol, 0.01% Bromophenol Blue and 50 mM DTT) incubated at 95°C, 3 min and separated on 10%, 12%, or 14% Tris-glycine SDS/PAGE, alongside Spectra Multicolour Broad Range Protein Ladder (Thermo Scientific).

If required for western blot analysis the proteins were transferred on to PVDF membranes (Millipore, activated with 100 % methanol) by wet transfer where the gel and membrane were assembled between Whatman paper and sponges in a cassette that was then placed in the TE22 Apparatus from Hoefer. The transfer was performed for 2 h in case of one gel or 2.5 hr (two gels) at constant 100 Volt, at 4˚C, with agitation of the buffer.

2.5.5 Staining of polyacrylamide gels.

Gels for Coomassie Brilliant Blue (CBB) staining were incubated for 15 min in CBB solution (45% (v/v) methanol, 10% (v/v) glacial acetic acid and 0.2% (w/v) Coomassie Blue R) then destained for 2x 10 min in the CBB destaining solution (45% (v/v) methanol and 10% (v/v) acetic Acid).

2.5.6 Immunodetection of proteins.

Proteins of interest were visualized by membrane incubation with primary antibody **(Table 2.3)**, followed by appropriate secondary antibody conjugated to horseradish-peroxidase (Dako), and using ECL Plus reagent (GE Healthcare) and Storm 860 (GE Healthcare) PhosphorImager or by standard autoradiography. For the detection of signal with ChemiDoc MP Imaging System (BioRad), ECL Prime Reagent (GE Healthcare) was used.

Table 2.3. **Description and details of primary antibodies used.**

Protein	Size (kDa)	Antibody information
COXII	~20	Molecular Probes (A6404), mouse, 1:1000
Cyt c	~11.5	MitoSciences, mouse (MSA06), 1:2000
DAP3	~46	Abcam (ab11928), mouse, 1:1000
ERAL1	~48	Protein Tech Group (11478-1-AP), rabbit, 1:1000
FLAG	-	Sigma (F1804), mouse, 1:1000
ICT1	~20	Protein Tech Group (10403-1-AP) rabbit, 1:750
MRPL3	~35	Abcam (ab39268), goat, 1:2000
MRPL12	~19	Custom made Affinity purified, rabbit, 1:1000
MRPS18B	~29	Protein Tech Group (16139-1-AP), rabbit, 1:4000
NDUFB8	~20	MitoSciences (MS105), mouse, 1:1000
RbfA	~42	Custom made Affinity purified, rabbit, 1:800
POLRMT	~140	Abcam, rabbit (ab32988), 1:300
Porin	~39	Molecular probes (A31855), mouse, 1:10000

2.5.7 ^{35}S metabolic labelling of mitochondrially encoded proteins.

Control and patient fibroblasts were grown in 25 cm^2 flasks to ~70% confluence. Cells were then incubated twice with methionine/cysteine free DMEM supplemented with L-glutamine, 1 mM sodium pyruvate, 0.2 mM uridine for 10 min, 37˚C. This was followed by 10 min incubation in 1.5 ml of the same medium containing 10% dialysed FCS and emetine dihydrochloride (100 µg/ml final). Next, 0.5 ml of medium was removed from each flask and 20 µl of ^{35}S- methionine/cysteine mix (PerkinElmer; 125 µCi/ml EasyTag^{TM} express ^{35}S protein labelling mix NEG-772, 73% L-met, 22% L-cys) was added. After 1hr incubation, the medium was removed, cells were washed twice with standard growth medium (subsection 2.1.2) without antibiotics but supplemented with additional 7.5 µg/ml of cold methionine. Cells were harvested in 1mM EDTA/PBS and centrifuged at 250g, 4 min. Pellets were washed 3x with ice-cold PBS and re-suspended in ice-cold PBS containing EDTA-free, Protease Inhibitor Cocktail (Roche) and 1mM PMSF. Cell pellets were snap frozen and stored at -80°C. When required aliquots were thawed on ice, protein concentration estimated and equal protein amounts

(50 µg) were mixed with 2x dissociation buffer (20% glycerol, 4% SDS, 250 mM Tris-HCl pH 6.8, 100 mM DTT). Samples were incubated 1 hr at RT with 12 U Benzonase® nuclease (Novagen) and electrophoresed in 15% (w/v) SDS-PAGE.

Gels were fixed over-night (fixer: 3% (v/v) glycerol, 10% (v/v) glacial acetic acid, 30% (v/v) methanol) after which they were vacuum dried at 60 °C, 2 hr. Nascent proteins were visualized with PhosphorImager and analysed using Image-Quant software (Molecular Dynamics, GE Healthcare).

2.5.8 Isokinetic sucrose gradient.

Linear sucrose gradient was prepared in Centrifuge Tube (11 x 34 mm; Beckman 343778) as follows:

- ✓ 10% and 30% sucrose solutions in gradient buffer (0.05 M Tris, pH 7.2, 0.01 M MgOAc, 0.4 M NH_4Cl, 1 M KCl, 1 mM PMSF, 50 µg/ml chloramphenicol, 0.5µl RNase inhibitors/1 ml were prepared
- ✓ 0.5 ml of 30% sucrose solution was injected under 0.5 ml of 10% sucrose solution and mixed by Gradient Master$_{ip}$ 107 (BIOCOMP) for 55 seconds using programme for TL55, 10-30% S1/1 0:55/85.0/22 and incubated for ~1 hr at 4°C in the Ultra Clear plastic tube (for 1ml volume with an open top, Beckman).
- ✓ Cell (700 µg) or mitochondrial (300 µg) lysate (max 100 µl volume) was pipetted on top of the gradient, directly before centrifugation.

The lysates were prepared with Sigma lysis buffer adjusted with Protease Inhibitor Cocktail, EDTA-free (Roche), 1 mM PMSF, 10 mM $MgCl_2$ and 3 µl of SUPERase In™ RNase Inhibitor (Ambion)/500 µl of buffer.
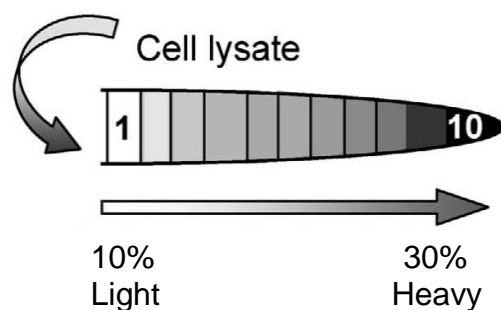
Figure 2.1. Schematic illustration of cell lysate fractionation in the sucrose gradient.
The percentage of sucrose is indicated showing where light and heavy particles would be expected, and the positions of the fractions (numbers within tube).

Cell or mitochondrial lysates were loaded on to a linear sucrose gradient (1ml, 10-30% [v/v]), and fractionated by centrifugation in Beckman OptimaTLX ultracentrifuge, TLS55 rotor at 39000 rpm/min for 135 min at 4°C. (acceleration and deceleration rate settings were 1 and 4 respectively). Fractions (100 µl) were collected and analysed by western blot or treated with TRIzol LS Reagent (Ambion) in order to extract RNA for northern blot.

2.5.9 Affinity purification of antibody.

I. Expression and purification of MRPL12 protein.

One litre of LB medium (supplemented with 100µg/ml ampicillin) was inoculated with two 5 ml cultures of Rosetta cells transformed with the plasmid (pTYBII) containing sequence of self-cleavable intein fusion with the chitin binding domain and ORF MRPL12 protein. Cells were grown at 37°C, 200 rpm in a floor standing orbital shaker until the culture reached OD_{600} 0.6. Next, flasks with liquid culture were transferred to 16°C and after 30 min, production of MRPL12 protein was induced with IPTG (1.0 mM final concentration) for 18 hr. Bacteria were centrifuged at 5000 rpm (Sorvall GSA centrifuge, rotor code 10) for 15 min at 4°C and the pellet was frozen at -80°C. Next, cells were thawed on ice, and resuspended in 20 ml of 1x **I**ntein **B**uffer (**IB**: 20 mM Tris-HCl; pH 7.9, 500 mM NaCl, 1mM EDTA) containing Protease Inhibitor Cocktail, EDTA-free (Roche), 1 mM PMSF, 2 µl Benzonase® nuclease (Novagen) and sonicated for 20 min (30 seconds on; 18 microns amplitude, 30 seconds off; Soniprep 150; (SANYO)). Afterwards this was centrifuged at 15000*g*, 20 mins, at 4°C. The supernatant was loaded onto equilibrated chitin beads (2 ml of slurry was twice washed in 50 ml of **IB** and centrifuged at 2000*g,* 2 min) and incubated 1 hr on a rotary shaker. Next, the supernatant was discarded and beads were washed twice with 50 ml of **IB** (containing Protease inhibitor Cocktail, EDTA-free (Roche), 1 mM PMSF) supplemented with 1 M NaCl for 40 min, at 4°C, on the rotary shaker. The beads, re-suspended in 10 ml of IB were moved to an empty Sephadex® G25 column. The flowthrough was discarded, and beads were washed 3x with 10 mls IB and further 3x with IB containing 50 mM β-Mercaptoethanol. During the last wash the flow was stopped and beads were incubated for 24 hr in remaining 4 ml of IB with 50 mM β-Mercaptoethanol. The target protein was eluted by continuing the column flow. The eluate was dialysed twice overnight, at 4°C against 1 L of 50 mM NaCl and 10 mM β-Mercaptoethanol. The eluate (20 µl) before and after concentration (with Aquacide II,

Calbiochem), alongside sample obtained by boiling a small amount of chitin beads in 20 µl elution buffer with loading dye, were separated by 12% SDS-PAGE and stained with CBB (as described in subsection 2.5.4 and 2.5.5) in order to determine the cleavage efficiency.

II. Antibody purification using NHS- activated Sepharose^{TM} 4 Fast Flow, (GE Healthcare).

An aliquot of packed beads (0.6 ml volume) was added to 10 ml BioRad column and washed 3x with cold 1 mM HCl followed by overnight incubation with 1 mg of purified MRPL12 protein. After removing the flowthrough, beads were blocked with 0.1 M Tris-HCl, pH 7.4, over-night at 4°C. Next, the beads were washed 5x with PBS and incubated over-night with 7 ml of filtered (0.45 µm filter) serum from the immunized animal [sample identification number: ZGB08099, R0906, SAB: 26/11/08, Eurogentec (6)] and 3 ml PBS on the rocker, at 4°C. The flowthrough was saved and beads were washed 2x with PBS, 1x with Tris-buffer, pH 8.0 (50 mM Tris-HCl pH 8.0, 0.1% Triton X-100, 0.5 M NaCl), 1x with Tris-buffer, pH 9.0 (50 mM Tris-HCl pH 9.0, 0.1% Triton X-100, 0.5 M NaCl), 1x with Na-phosphate buffer, pH 6.3 (50 mM Na-phosphate pH 6.3, 0.1% Triton X-100, 0.5 M NaCl). Two types of elution buffers were applied. First, an acid elution with 5 ml Glycine-buffer, pH 2.5 (50 mM Glycine pH 2.5, 0.1% Triton X-100, 0.15 M NaCl). Each 850 µl of eluate were collected in 1.5 ml eppendorfs containing 150 µl Tris-HCl pH 9.0. Afterwards 1 ml of Tris-HCl pH 9.0 was added to the beads and the flowthrough was collected. The protein concentration in each fraction was assessed with Bradford Reagent (BioRad). Positive antibody fractions were dialyzed against 1L of PBS, with stirring, at 4°C, over-night, at least twice. The volume of dialyzed IgG was reduced to 1 ml with Aquacide II, Calbiochem.

To store antibody long term, glycerol (10% final volume), BSA (2% final volume) and sodium azide (0.02% final volume) were added. Aliquots were frozen in -20°C.

2.5.10 Immunoprecipitation of endogenous proteins.

Immunoprecipitation of MRPL12 protein was performed with affinity purified antibody (technique described above, subsection 2.5.9), coated on magnetic Dynabeads® Protein G (Invitrogen). 20 µl of beads were washed 3x with 0.1M Na-phosphate, pH 8.1, and resuspended in 60 µl of 0.1M Na-phosphate pH 8.1 and 20 µl of antibody added, followed by incubation on a rotating wheel at RT for 45 min. After the incubation,

beads were pelleted and washed 3x with lysis buffer (Immunoprecipation Kit, Sigma adjusted with EDTA-free Protease Inhibitor Cocktail (Roche), 1 mM PMSF, 10 mM $MgCl_2$, 3 µl of SUPERase In™ RNase Inhibitor (Ambion)/500 µl of buffer). Mitochondria were isolated (according to protocol described in 2.5.2) from immortalised control and patient fibroblasts grown to ~80% in 300 cm^2 flasks. These were then lysed in the buffer described above, according to the subsection 2.5.2. Control and patient fibroblast lysates, of equal protein amount (830 µg) were incubated with beads for 1 hr on the rotating wheel, at 4°C. Removal of supernatant was followed by three washes with lysis buffer. The pull-down was eluted from beads with 25 µl of 1x sample buffer (described in 2.5.4) diluted in lysis buffer during 3 min incubation at 95°C, 1000 rpm in Thermomixer. Supernatants were analysed by western blot.

2.5.11 Immunoprecipitation of FLAG tagged proteins.

Immunoprecipitation of FLAG tagged ICT1 and MRPS27 were performed with FLAG® Tagged Proteins Immunoprecipitation Kit (Sigma) according to the suppliers' protocol with a minor modification to the buffer. Sigma lysis buffer was adjusted with Protease Inhibitor Cocktail, EDTA-free (Roche); 1 tablet/10 ml, 1 mM PMSF, 10 mM $MgCl_2$, 3 µl of SUPERase In™ RNase Inhibitor (Ambion)/500 µl of buffer) was used. Sigma 1x wash buffer prepared from 10x concentrated stock with DEPC ddH_2O was adjusted the same as lysis buffer except the volume of SUPERase In, which was lowered to 0.5 µl/ml. Cell or mitochondrial lysates (preparation: subsection 2.5.1) were incubated with anti-FLAG M2-Agarose Affinity Gel for 3 hr on the rotating wheel, at 4°C. Pull-downs from ¼ of the resin were eluted as described in subsection 2.5.10. The rest of the resin was re-suspended in 250 µl of TRIzol reagent (Ambion) and RNA extractions were performed following the supplier protocol. In case of mitoplasts pellets (~50 µl volume, obtained according to the subsection 2.5.2), 200 µl of lysis buffer was used with 3 µl of SUPERase In. Lysed mitoplasts were incubated 2 hr with Sigma resin, followed by 3 washes with buffer described above, except that first wash contained 10 mM EDTA.

2.6   CLIP Technique.
2.6.1 CLIP of endogenous protein.

The protocol for CLIP assay was followed as described in Ule et al., 2005. Below are presented only main steps of the method, followed by a detailed protocol used to investigate MRPL12 and RBFA proteins.

The steps illustrated in Fig. 2.2 are briefly described below.

I. Cells grown in 150 mm plates were UV-irradiated on ice leading to formation of a covalent bond between protein and RNA.

II. Partial digestion of RNA after cell lysis.

III. Immunoprecipitation of protein-RNA complexes.

> **a)** Dephosphorylation of RNA.
>
> **b)** 3'-RNA linker ligation.
>
> **c)** Radioactive labelling of RNA by γ ^{32}P on the 5' terminus.

IV. SDS-PAGE electrophoresis of protein-RNA complexes and transfer to nitrocellulose.

V. Thin region of the membrane corresponding to protein–RNA complexes of appropriate size was localized by expose to X-ray film and cut out.

VI. Protein was digested by proteinase K and 5' RNA linker was ligated to free RNA.

VII. CLIP tags were then amplified by RT-PCR, cloned, sequenced and analysed.
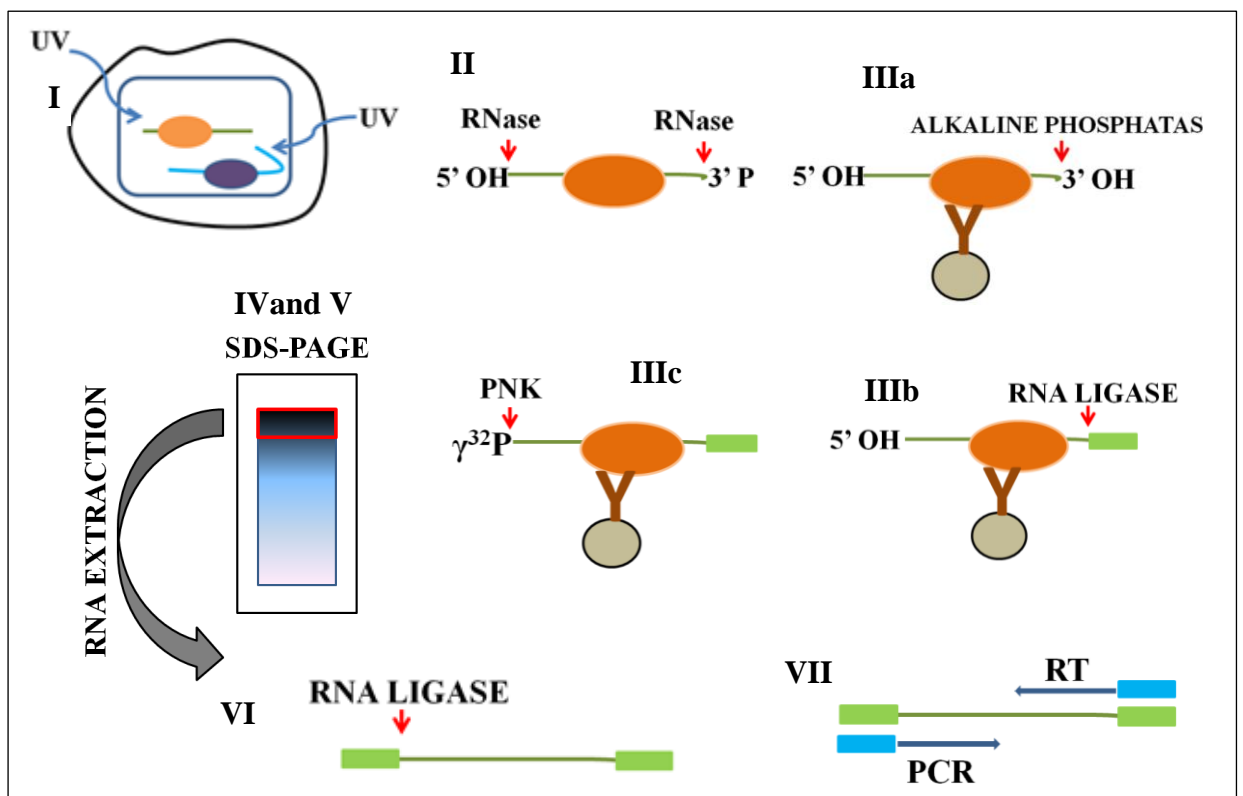
Figure 2.2. Schematic representation of main steps in CLIP method.
Detailed description is given in the text.

Solutions:

<u>Lysis Buffer</u>
From FLAG Immunoprecipitation Kit cat no. FLAGIPT1
Adjusted with:
- ✓ 0.1% SDS
- ✓ Protease Inhibitor Cocktail, EDTA-free (Roche)
- ✓ RNAsin (Promega)

<u>1xPNK buffer</u>
    50 mM Tris-HCl pH 7.4
    10 mM $MgCl_2$
    0.5% NP-40

<u>1xPNK+EDTA buffer</u>
    50 mM Tris-HCl pH 7.4
    20 mM EDTA
    0.5% NP-40

<u>1xProteinase K (PK) buffer</u>
    100 mM Tris-HCl pH 7.4
    50 mM NaCl
    10 mM EDTA

- An adequate number of cells were seeded into 150 mm dishes to achieve a culture of about 70-80% confluence on the day of UV treatment.
- The cells were fed the day before the experiment or split if needed.

UV cross-linking

- The cells were rinsed once with Dulbecco's PBS (Ca^{2+}, Mg^{2+} free). Enough of cold PBS was added to keep the cells moist (~10ml/ plate area). Next, the plate was placed on the tray with ice on the bottom of the Stratalinker 2400 (STRATAGENE) and cells were irradiated one time for $400mJ/cm^2$.
- The cells were harvested and pelleted at 4°C, the pellet was washed with ice-cold PBS, snap -frozen at -80˚C until use (each eppendorf contained ~200 µl of cells).

Bead Preparation

- 20 µl of Dynabeads protein G (Invitrogen) was used for each eppendorf of cross-linked material. Beads were washed 3x with 0.1 M Na-phosphate, pH 8.1.
- These were re-suspended in 60 µl 0.1 M Na-phosphate pH 8.1 and 20 µl of antibody.
- This was rotated at room temperature for 30-45 min.
- Next, beads were washed 3x with lysis buffer.

Cell lysis and partial RNA digestion

- Each of cell pellets was resuspended in 1ml of lysis buffer (FLAG IP kit, Sigma), containing proteinase inhibitor cocktail, EDTA-free (Roche), 0.1% SDS and supplemented with 15ul RNAsin (Promega).

- Cells were lysed for 30 min on the rotating wheel at 4°C.

- 50 µl of DNAse I (RNase free, 1U/µl, Epicentre Biotechnologies) was added to each eppendorf, followed by incubation at 37°C for 5 min, 1000 rpm in Thermomixer.

- Dilutions of RNase T1 (Ambion, 1000U/µl) at 1/100 (overdigested sample) and at 1/5000 (underdigested sample) were prepared in the lysis buffer.

- 20 µl of each RNase T1 dilution was added to one of the duplicate eppendorfs, and incubated at 37°C for 10 min.

- Next, 3 µl of SUPERase In (Ambion, 2U/µl) was added to each duplicate, in order to inhibit RNase T1.

- Lysates were centrifuged at 20800 *g* in Eppendorf centrifuge 5414R for 20 min at 4°C.

- Supernatants were transferred onto Invitrogen magnetic Dynabeads protein G coated with specific antibody.

- Beads/lysate mix was rotated for 1 hr at 4°C.

- Next, the supernatants were removed and beads washed twice with 1 ml of lysis buffer and twice with PNK buffer, the over-digested sample was resuspended in PNK buffer.

Next two steps: CIP treatment and 3' RNA linker ligation are performed only with sample treated with low RNase concentration (1:5000). The over-digested sample is left at 4°C in PNK buffer until PNK treatment step.

CIP treatment (on beads)

- **CIP mix (total volume: 80µl):**

    8 µl 10x dephosphorylation buffer (Roche)

    3 µl alkaline phosphatase (Roche, 10713023), kept at 4°C

    69 µl H_2O

- The last 1x PNK wash was removed from the beads and CIP mix was applied.

- Beads were incubated at 37°C for 10 min; 1000 rpm every 3 min for 15 s.

- Next, the beads were washed twice with 1 ml of 1x 'PNK+EDTA' buffer and twice with 1ml of 1xPNK buffer.

3' RNA Linker ligation

- **<u>Linker mix (40 µl):</u>**

  8 µl L3 3' RNA Linker at 20 pmol/µl

  32 µl DEPC H_2O

The 1x PNK buffer was carefully discarded from the beads and 40 µl of the linker mix was added to each tube of beads. Followed by 40 µl of ligase mix (with final L3 conc. at 2 pmol/µl).

- **<u>Ligase mix (40 µl):</u>**

  8 µl 10x buffer (NEB, contains ATP)

  1 µl T4 RNA ligase I (20U, NEB M0204S)

  31 µl DEPC H_2O

Beads were incubated in the Thermomixer at 16°C over-night (1000 rpm every 5 min for 15 s).

PNK treatment on beads

✓ The beads were washed 3 times with 1ml of 1x PNK buffer.

✓ **<u>PNK mix (total volume 80 µl):</u>**

  8 µl 10x buffer (NEB)

  1 µl $\gamma^{32}P$ (ATP)

  4 µl T4 PNK enzyme (NEB, M0201S)

  67 µl DEPC H_2O

- 80 µl of the mix was added to each sample and incubate in Thermomixer at 37°C for 10 min (1000 rpm every 4 min for 15s).

- Next, 1 µl of 10 mM ATP was added to each sample and the reaction mix was incubated for an additional 5 min.

- The beads were washed 3x with 1 ml 'PNK+EDTA' buffer.

Elution

- After the third wash the beads were resuspended in 25 µl of 1x 'PNK+EDTA' buffer with 1x Novex loading dye (containing reducing agent in case of RbfA), Invitrogen, incubated in Thermomixer at 70°C for 10 min (1000 rpm), and the supernatant taken for loading.

SDS- PAGE and BA-85 nitrocellulose transfer

- Samples were loaded on 10 well Novex NuPAGE 10% Bis-Tris gel, Invitrogen.

- Separated under reducing conditions in case of RBFA (for MRPL12 protein no reducing agent was used) according to the manufacturer protocol (*Novex Pre-Cast Gel Electrophoresis Guide*).

- RNA-protein complexes were transferred to BA-85 nitrocellulose (PerkinElmer) using the Novex wet transfer system according to the manufacturer protocol (*Novex Pre-Cast Gel Electrophoresis Guide*).

- After the transfer, the nitrocellulose was rinsed in 1x PBS and wrapped in SARAN film.

- This was exposed to the x-ray film for few hr or O/N at -80°C with an intensifying screen.

RNA isolation and purification

- A 4 mg/ml Proteinase K solution was made in 1x Proteinase K buffer; pre-incubated at 37°C for 20 min.

- A fresh stock of 100 mM PMSF was made up in isopropanol.

- The autoradiogram was matched with the membrane.

- The over-digested sample, was used to determine the specificity of the RNA-protein complexes according to the following requirements:

  1. *In the over-digested sample lane, the band should be localized ~7 kDa above the expected MW of the investigated protein.*

  2. *The distance from the closest contaminating band, should not be less than 10 kDa, it guarantees the specificity of purified RNA.*

  3. *The RNA-protein complexes that were treated with a low concentration RNase T1 will appear as a diffuse radioactivity around 15-20 kDa above the expected MW of investigated protein (average MW of 50 nucleotides long RNA is ~16 kDa, plus attached 20 nucleotides long linker L3).*

  4. *The band cut out from the membrane should be as thin as possible (~3 kDa wide) approximately 20 kDa above the expected MW of the protein.*

- The excised nitrocellulose piece or pieces were incubated in 200 μl of Proteinase K solution each, for 20 min at 37°C at 1000 rpm (Thermomixer).

- 200 μl of 1x Proteinase K buffer with 1 mM PMSF was added; incubated for 5 min, 37°C at 1000 rpm.

- RNA was extracted by addition of 400 µl of RNA - phenol pH 6.7 and 130 µl of chloroform 49:1 with isoamyl alcohol; incubated for 20 min at 37°C at 1000 rpm.
- Next, this was centrifuged at 17900 g for 5 min, at 4°C.
- The aqueous phase was mixed with 50 µl 3 M NaOAc, pH 5.2, 0.5 µl glycoblue (Ambion, 9510), 1 ml of 1:1 EtOH : Isopropanol.
- RNA was precipitated O/N at -20°C.
- Next, this was centrifuged for 20 min at maximum microfuge speed, at 4°C.
- Pellet or pellets were washed twice with 200 µl ice-cold 75% ethanol and air dried briefly.
- RNA was resuspended in 8 µl RNase free water.

5'RNA Linker Ligation

- **Ligation mix (total volume: 10 µl)**

    1 µl 10x T4 RNA Ligase buffer (NEB, contains ATP)

    1 µl L5 RNA linker 20 pmol/µl

    7 µl RNA

    1 µl T4 RNA ligase, diluted first 1:5 to give 4U/µl

- Reaction was incubated for 5 hr at 16°C.
- Next, volume of the ligation reaction was increased to 200 µl with DEPC ddH$_2$O.
- RNA was extracted with 200 µl phenol pH 6.7 and 65 µl chloroform; vortexed and centrifuged at 13000 rpm (microfuge), 5 min at 4°C.
- The RNA from aqueous phase was precipitated O/N with 50 µl NaOAc pH 5.2, 0.5 µl glycoblue and 1 ml 1:1 EtOH: Isopropanol at -20°C.
- RNA was centrifuged for 20 min at maximum speed, at 4°C.
- Pellet was washed twice with 200 µl ice-cold 75% ethanol and air dried briefly.
- RNA was resuspended in 9 µl RNase free water (**not** treated with DEPC).

Reverse Transcription

- The reaction was set up as follows:

    9 µl of RNA solution mixed with 1 µl P3 primer (10 pmol/µl) was incubated at 65°C for 5 min. Next the master mix was added.

    Master mix:

    1 µl 10 mM dNTPs

    4 µl 5x 1st strand buffer

2 µl 0.1 DTT

1 µl SUPERase In

1.5 µl RNase free water

Sample was incubated for 5 min at 42°C, followed by the addition of 0.5 µl Superscript
II (Invitrogen). The final reaction mix was incubated for 1 hr at 42°C, 15 min at 70°C.

PCR reaction

- **Total volume: 30 µl**

  3 µl   10x Reaction Buffer IV (Thermo Scientific)

  1.5 µl   10 mM dNTPs mix

  2.4 µl   25 mM MgSO$_4$

  1 µl   P5 primer (10 pmol/µl)

  1 µl   P3 primer (10 pmol/µl)

  17.5 µl   ddH$_2$O

  0.6 µl   *Taq* DNA Polymerase (Thermo Scientific)

  3 µl of Reverse Transcription Reaction (cDNA) was used as a template.

PCR settings:

95°C 5 min

95°C 20 s

67°C 30 s   35 cycles

72°C 30 s

72°C 5 min

Separation of the PCR product on agarose gel and product extraction.

- Entire PCR reaction was separated on 4% low melting agarose gel, against 50 bp
  molecular weight marker (NEB).

- The gel piece with DNA of 80-90 bp length of ~100 µl volume was cut out.

- DNA from the crushed gel was phenol/chloroform extracted

- First, ddH$_2$O was added up to 400 µl to the excised gel.

- Sample was incubated at 65°C for 10 min at 1000 rpm.

- DNA was purified by:

  ✓ 2x extraction with 400 µl phenol (pH)

- ✓ 1x 200 µl phenol/200 µl chloroform
- ✓ 1x 400 µl chloroform

- DNA was precipitated 3h at -80°C or O/N at -20°C with 40 µl 3 M NaOAc, 1 µl glycoblue, 1 ml 100% ice-cold ETOH.
- Next, this was centrifuged at maximum speed for 15 min at 4°C.
- Pellet was washed twice with ice cold 75% ETOH.
- Air dried DNA pellet was resuspended in 10 µl ddH$_2$O.

Re-amplification of DNA:

PCR reaction

- **Total volume: 50 µl**

    5 µl 10x Reaction Buffer IV (Thermo Scientific)

    2 µl 10 mM each dNTPs mix

    3 µl 25 mM MgSO$_4$

    5 µl P5 primer (10 pmol/µl)

    5 µl P3 primer (10 pmol/µl)

    27 µl H$_2$O

    1 µl *Taq* DNA Polymerase (Thermo Scientific)

    2 µl of first PCR reaction was used as a template

- DNA was reamplified with the same thermal program but with 20 cycles and 63°C annealing temperature.
- The PCR product was again separated on an agarose gel and extracted according to the required size of ~ 80-90 bp as previously described by phenol/chloroform extraction.
- Obtained DNA pellet was resuspended in 12 µl of ddH$_2$O.

Examination of CLIP tags

- Amplified CLIP tags were cloned with TOPO TA Cloning KIT (Invitrogen: following the manufacturer's protocol) and transformed into One Shot TOP10 Chemically Competent *E. Coli* cells (Invitrogen; procedure performed according to manufacturer protocol).
- Bacterial colonies were grown on agar plates with 100 µg/ml of ampicillin, were screened by colony PCR

✓ Single colonies were resuspended in 50 µl of 10% Triton X-100 and then frozen at -80°C, followed by thawing.

✓ Standard 25 µl PCRs were set up with M13 primers as follows:

      2.5 µl 10x Reaction Buffer (Fermentas)

      0.5 µl dNTPs mix

      0.5 µl M13 forward primer (50 µM)

      0.5 µl M13 reverse primer (50 µM)

      19.625 µl ddH$_2$O

      0.125 µl Dream *Taq* Polymerase (Fermentas)

      1.25 µl Triton X-100/colony lysate was used as a template

PCR settings:

    95°C 3 min

    95°C 45 s

    48°C 1 min   30 cycles

    72°C 30 s

    72°C 7 min

- 5 µl of PCR product was separated on 2% agarose gel, chosen clones that contained CLIP tags of expected size were sequenced.

- Steps ahead of CLIP tags sequencing procedure with Genetic Analyzer 3130*xI* (Applied Biosystems) are as follows:

    ✓ 5 µl of colony PCR performed with Dream *Taq* Polymerase was mixed with TSAP Thermosensitive Alkaline Phosphatase (Promega) and incubated:

    15 min at 37°C

    15 min at 80°C

    ✓ 2 µl of above reaction was mixed with:

    7 µl ddH$_2$O

    3 µl sequencing buffer (Applied Biosystems)

    1 µl M13 forward primer

    2 µl Big Dyes v3.1 (Applied Biosystems)

The reaction mix was amplified in the sequencing PCR.

Cycle sequencing settings:

95°C 5 min

95°C 30 s

48°C 10 s   30 cycles

72°C 4 min

4°C

Precipitation of samples was kindly performed by Charlotte Alston.

Table 2.4. Linkers and primers sequences used in CLIP method.

Name of the primer	Sequence
L5 RNA linker (Thermo Scientific)	5'-OH AGG GAG GAC GAU GCG G 3'-OH
L3 RNA linker (Thermo Scientific)	5'-P GUG UCA GUC ACU UCC AGC GG 3'-puromycin
P5 DNA primer (Operon)	5'-AGG GAG GAC GAT GCG G-3'
P3 DNA primer (Operon)	5'-CCG CTG GAA GTG ACT GAC AC-3'
M13 Forward (-20)	5'-GTAAAACGACGGCCAG-3'
M13 Reverse	5'-CAGGAAACAGCTATGAC-3'

- In order to obtain more comprehensive data, CLIP tags were sequenced with the IonTorrent. The final PCR products were prepared, following manufacturer's instructions. Reads were collected and aligned to mtDNA as a reference sequence using the Torrent Suite software on the IonTorrent server.

2.6.2 CLIP of FLAG tagged protein.

CLIP assay was performed according to the protocol described in 2.6.1 apart from few modifications in following steps:

- ✓ HEK293 cell line expressing FLAG tagged SLIRP (provided by Dr Paul Smith) was treated with UV two days after induction of the protein with tetracycline at 1 µg/ml final concentration.

- ✓ Immunoprecipitation step was performed with beads from FLAG Protein Immunoprecipitation Kit, Sigma.
- ✓ Beads were equilibrated by 5 washes in 1x wash buffer (prepared in DEPC ddH$_2$O, from 10x concentrated stock (FLAG Protein Immunoprecipitation Kit, Sigma)
- ✓ After immunoprecipitation, beads were washed 3 times with 1 ml of 1x wash buffer, 2x with 1 ml of 1x PNK buffer.

    RNA/FLAG-protein complexes were removed from beads by incubation in Thermomixer at RT for 45 min (1000 rpm) with elution mix:

    >   5 µl 3x FLAG peptide (IP kit, Sigma)

    >   45 µl 1x wash buffer

2.7 Primer extension assay.

In this study a primer extension assay was used in order to investigate the relative amounts of modified, methylated bases on 12S rRNA. The RNA-dependent DNA polymerase (M-MLV, Promega) extends a cDNA chain from the annealed radiolabelled primer. A limited nucleotide concentration and lowered amount of enzyme in the reverse transcription reaction was applied to determine the location of modified bases. The reduction in these parameters is designed so that the elongation process stops at the site of modification. To exclude confusion with pause sites caused by secondary structure of RNA enforcing the reverse transcriptase to pause, the negative control of un-methylated *in vitro* synthesized RNA was used in a parallel reverse transcription reaction, and was electrophoresed on 10% sequencing gel alongside investigated samples. The nucleotide dGTP was excluded from RT reaction mix. This limited the DNA strand from being extended beyond the position of the first 'C' nucleotide where a dGTP would need to be inserted. This restricted the full length readthough product to 23 nucleotides. This allowed a comparison of the readthrough signal with the methylation site induced stop signal.

The steps in primer extension assay are as follows:

1. Primer radiolabelling reaction: 1 hr at 37°C, stopped by 15 min incubation at 65°C.

- ✓ **Total volume: 10 µl**
    - 3.4 µl ddH$_2$O
    - 0.8 µl 100 µM primer
    - 1 µl 10x buffer (NEB)
    - 0.8 µl T4 PNK enzyme (NEB, M0201S)

4 µl γ^{32}P (ATP)

Radiolabelled primer was purified on Illustra™ MicroSpin™ G-25 column (GE Healthcare) and eluted in 50 µl of ddH$_2$O.

4 µg of total RNA or 800 ng extracted from beads after immunoprecipitation of monosome through FLAG tagged MRPS27 or FLAG-ICT1 in 3 µl of ddH$_2$O were mixed with 3 µl diluted ^{32}P-primer (1 µl of primer + 2 µl of ddH$_2$O) and incubated 2 min, at 95°C, centrifuged and left at room temperature for 10 min in order to annealing process occur. Next RNA was transcribed into cDNA.

2. Reverse Transcription Reaction: 45 min, at 37°C, stopped by addition of 2x loading buffer (80% (v/v) formamide, 1 mM EDTA, 0.1% (w/v) BFB, 0.1% (w/v) XCFF).

✓ **Total volume: 12 µl**

6 µl annealing mix

2.93 µl ddH$_2$O

2.4 µl M-MLV RT 5x Buffer (Promega)

0.24 µl M-MLV Reverse Transcriptase (Promega)

0.4 µl SUPERase In (Ambion)

0.024 µl 20 mM dNTPs mix without dGTP (final concentration: 0.04 mM)

3-5 µl of samples were separated on 10% polyacrylamide / 8 M urea sequencing gel, at 50 W in 1x TBE buffer. Afterwards the gel was removed from the glass plates and dried for 2 hr, at 80°C. Next it was placed in a SARAN wrap and exposed to a screen in Phosphor-Imager cassette. Detection of signal was performed with Typhoon FLA9000 and analysed using Image-Quant software (Molecular Dynamics, GE Healthcare).

10% polyacrylamide / 8 M urea sequencing gel (55 ml)

27 g   Urea

5.5 ml   10x TBE

18.33 ml   Acrylamide / Bis-Acrylamide (30% Ratio 29:1, NBS Biologicals)

Up to 55 ml ddH$_2$O

90 µl   TEMED

400 µl   10% APS

10x TBE (1 L)

108 g Tris Base

55 g Boric Acid

20 ml 0.5 M EDTA, pH 8.0

<u>The preparation of the un-methylated *in vitro* synthesized RNA used in reverse transcription reaction as a negative control.</u>

100 ng of total DNA extracted from HeLa cells were used in 50 µl PCR reaction with 12S rRNA primers (Table 2.5). *Taq* DNA Polymerase (ThermoScientific) was used in order to generate template with a site to initiate transcription with SP6 RNA polymerase using AmpliScribe SP6 Transcription Kit (Epicentre Technologies). The PCR product was purified by phenol-chloroform extraction, followed by ethanol precipitation. 3 µl of sample was separated on 1% (w/v) agarose gel in order to confirm the size of the product. 800 ng of DNA was used in the following transcription reaction:

✓ **<u>Total volume: 20 µl</u>**

    2.5 µl RNase-free water

    1.5 µl 100 mM ATP

    1.5 µl 100 mM CTP

    1.5 µl 100 mM GTP

    1.5 µl 100 mM UTP

    2   µl 100 mM DTT

    2   µl 10x Reaction Buffer

    5   µl SP6 DNA template (800 ng)

    0.5 µl SUPERase In (Ambion)

    2   µl AmpliScribe SP6 Enzyme Solution

The above reaction was incubated for 2 hr, at 37°C. In order to remove DNA template, the sample was treated with 1 µl of RNase-free DNase (1U/ul, Epicentre Biotechnologies) for 15 min, at 37°C. RNA was purified by phenol-chloroform extraction, followed by precipitation in 1:1 isopropanol:ethanol. RNA was air-dried and resuspended in RNase-free water. Again the size of the product was checked on 1% agarose gel.

Table 2.5. **Sequences of oligonucleotides used in primer extension assay.**

Name of the primer	Sequence
AA primer	5'GGT TCG TCC AAG TG3'
SP6 primer	5'ATT TAG GTG ACA CTA TAG A AC ACA CAA TAG CTA3'

The sequence in red indicates the SP6 promoter, in green is presented a fragment of 12S mt-rRNA. AA primer was used in the primer extension assay for investigating di-methylation of two adjusted adenines near the 3'end of 12S.

5'CCAGTTGACACAAAATAGACTACGAAAGTGGCTTTAACATATCT**GAACACACAATAGCTA**AG
ACCCAAACTGGGATTAGATACCCCACTATGCTTAGCCCTAAACCTCAACAGTTAAATCAACAAAACTGCT
CGCCAGAACACTACGAGCCACAGCTTAAAACTCAAAGGACCTGGCGGTGCTTCATATCCCTCTAGAGGAG
CCTGTTCTGTAATCGATAAACCCCGATCAACCTCACACCTCTTGCTCAGCCTATATACCGCCATCTTCAG
CAAACCCTGATGAAGGCTACAAAGTAAGCGCAAGTACCCACGTAAAGACGTTAGGTCAAGGTGTAGCCCA
TGAGGTGGCAAGAAATGGGCTACATTTTCTACCCCAGAAAACTACGATAGCCCTTATGAAACTTAAGGGT
CGAAGGTGGATTTAGCAGTAAACTAAGAGTAGAGTGCTTAGTTGAACAGGGCCCTGAAGCGCGTACACAC
CGCCCGTCACCCTCCTCAAGTATACTTCAAAGGACATTTAACTAAAACCCCTACGCATTTATATAGAGGA
GACAAGTCGTAACATGGTAAGTGTACTGG**AA**AGTG**CACTTGGACGAAC**3'

Figure 2.3. Sequence of 12S mt-rRNA.

The 2 adenosine residues that are modified by dimethylation are indicated in red. Positions of both primers (AA primer (blue); used in the primer extension assay and SP6 primer (green) used in the synthesis of unmethylated RNA control with AA primer) are also specified.

Chapter 3

Investigating the sequence specificity of the mitochondrial RNA binding protein SLIRP using <u>C</u>ross-<u>l</u>inking <u>I</u>mmuno<u>p</u>recipitation – CLIP

3. Chapter 3: Investigating the sequence specificity of the mitochondrial RNA binding protein SLIRP using Cross-linking Immunoprecipitation - CLIP.

3.1 Introduction.

SLIRP (SRA stem-loop interacting RNA binding protein) was originally reported to bind STR7, which is a functional substructure of SRA (steroid receptor RNA activator) (Hatchell et al., 2006). The latter is a complex RNA molecule anticipated to contain numerous stable stem-loop structures of which STR7, an 89 nt sequence, is the largest and one of the most stable (Lanz et al., 2002). SRA serves as a catalytic RNA transcript, regulating eukaryotic gene expression via the nuclear steroid receptors. The predicted SLIRP structure is almost exclusively built of an RRM motif as seen in figure 3.1 (Hatchell et al., 2006), which is present in nearly all cellular compartments that contain RNA of animals, plants, fungi, and bacteria.
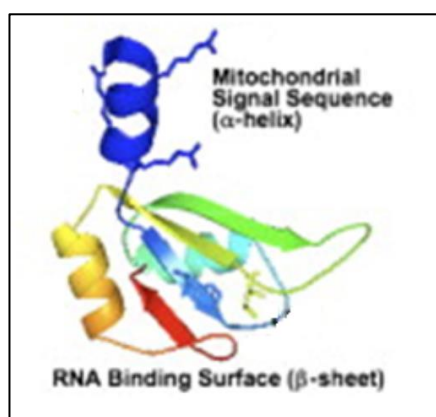
Figure 3.1. Structural model of SLIRP protein. Mitochondrial signal sequence and RNA binding domain are indicated. Image adapted from Hatchell et al., 2006.

This extensive conservation suggests its early evolution and the importance of its functions (Burd and Dreyfuss, 1994). A specific element of the RRM motif is its consensus sequence that is built of two short, canonical sequences, RNP1 and RNP2. These sub-motifs contain highly conserved amino acids crucial for RNA binding, and positioned on the two central β-strands (Nagai et al., 1990) of RRM βαββαβ secondary structure. However, the specificity of binding is determined by the most variable regions of the RRM motif. In general, the domain of the RRM responsible for interacting with the RNA structure, is composed of a conserved β-sheet, the specificity of which is modulated by more changeable residues located in the loops and the C-, N-terminal regions of RNA binding domain (Bentley and Keene, 1991,Görlach et al., 1992).

SLIRP has been proposed to repress nuclear receptors *trans*-activation in a SRA- and RRM-dependent way. The highest levels of SLIRP among human tissues were detected in heart, liver, skeletal muscle, and testis. Furthermore, over 90% of endogenous SLIRP was detected in mitochondria suggesting dual function of this protein. The location of SLIRP in mitochondria is in agreement with the presence of the N-terminal mitochondrial targeting sequence visible in the predicted structural model of this protein as an independent α-helix linked to the RRM that defines its cellular distribution (Figure3.1).

3.2 SLIRP binds mt-RNA *in vivo*.

Prior to published data, the mitochondrial location of SLIRP was confirmed and specified to the matrix by Dr. Paul Smith in my host laboratory. This preliminary data suggested its involvement in maintenance of mt-mRNAs. As a part of the project I performed CLIP assay (*cf* subsection 2.6.2), using a HEK293T cell line designed to be able to inducibly overexpress FLAG tagged SLIRP (generated by Dr. Paul Smith) in order to identify the specific binding sequences on mt-RNA. The CLIP tags obtained were initially cloned and sequenced and later the generated tags were IonTorrent sequenced by Dr. Helen Tuppen. Reads were collected and aligned to mtDNA as a reference sequence using the Torrent Suite software on the IonTorrent server. The alignment is presented in the form of a graph in Figure 3.2, where the x axis is a linear representation of the human mtDNA. The peaks indicate the locations of SLIRP binding sites and the number of 'hits' for which more than 50 CLIP tags were identified.
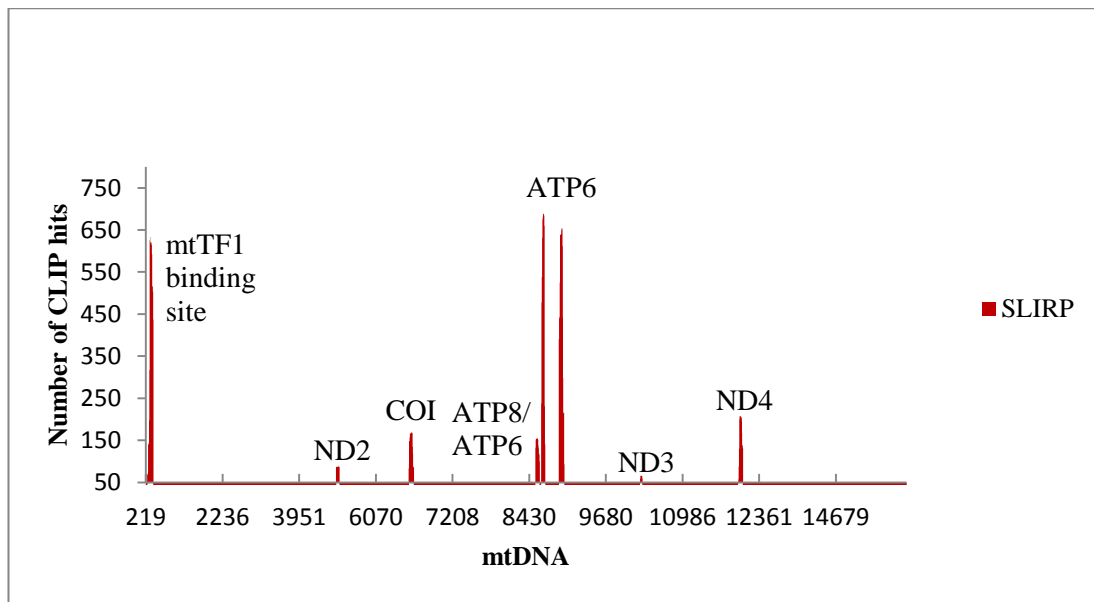
Figure 3.2. Alignment of SLIRP CLIP tags on mtDNA sequence. Human Cambridge reference sequence of mtDNA is presented as the x-axis and the number of CLIP tags in each position is given on the y-axis. Using IonTorrent derived data for CLIP on FLAG tagged SLIRP protein the threshold for the minimum number of hits at one site was set up at 50. Thus the peaks indicate only genes for which the number of CLIP hits exceeded 50. Y-axis starts from the nucleotide for which at least one hit was detected.

The positions where the number of hits exceeded this threshold were located in six mt-mRNAs: *MTND2, MTCO1, MTATP8/6, MTATP6, MTND3* and *MTND4*. The highest number of CLIP tags was identified for the mtTF1 binding site (~600 hits), *MTND2* (~87 hits), *MTCO1* (~ 160 hits), *MTATP8/ATP6* (~150 hits), *MTATP6* (position I: almost 700 hits, position II: over 600 hits), *MTND3* (over 60 hits), *MTND4* (over 200 hits). Locations of binding sites with reads lower than 50 were also identified (Appendix 1.4). These were found in *MTCOI, MTCOII, MTCOIII, MTCYB, MTND1, MTATP8, MTND4L,* and *MTND5*. The last four had only one binding site mapped with approx. 12, 29, 16, 26 hits respectively. Whereas two sites were identified in *MTCOII* (approx. 40 and 30 hit) and *MTCYB* (approx. 37 and 28 hits) and three binding sites mapped to *MTCOIII* each with 30, 26 and 20 hits. The number of binding sites in *MTCOI* was the highest among all identified mt-mRNAs with five locations mapped. The first binding site had approximately 30 hits, second 40, third 160, fourth 20 and fifth 20. The only mRNA for which no CLIP sequences were found was *MTND6*. Interestingly, mt-rRNA was also targeted, although minimally, with 20 hits located at the 3'end of 12S rRNA. Intriguingly, one of the highest number of CLIP tags are positioned at the H strand origin, where binding sites of mtTF1 are assigned. Analysis of SLIRP RNA binding sites *in vivo* did not show any discernible specificity of the sequence or structure, which would be shared by all RNA fragments. Still the sequences

with the highest number of hits are rich in A and T(U) residues (Appendix 1.4). Moreover 12 out of 25 identified binding sites contain CGC or CTG sequence. Seven of the binding sites contain both CGC and CTG sequences. Ten binding sites contain GAG sequence.

Further investigation was not pursued because of publications arising in the literature concerning SLIRP function in mitochondria and characterising aspects of this protein (described in Introduction), (Baughman et al., 2009, Sasarman et al., 2010, Ruzzenente et al., 2011, Chujo et al., 2012). All of the now available data show an important function of SLIRP in maintenance of mt-mRNA species. Moreover, the last three of the publications cited above, present an interacting partner of SLIRP, LRPPRC. This protein was initially characterised as mutations were found to cause the French Canadian variant of Leigh syndrome, as described in the introduction (Sasarman et al., 2010). SLIRP and LRPPRC are found in complexes with mature mt-mRNAs and their precursors. Furthermore, both are implicated as playing a role in the polyadenylation status of mt-mRNAs, potentially by suppressing 3'deadenylation (Chujo et al., 2012). These proteins not only play an important function in stabilizing RNA but their steady state levels appear to be dependent on it (Sasarman et al., 2010). Further, there appears to be a mutual reliance between these two proteins; depletion of one has been shown to cause a decrease of the other (Sasarman et al., 2010). Although recently published data reveal a lot of interesting information about the functional implications of the ribonucleoprotein complex in which SLIRP is a significant participant, none of them specify whether this protein binds mitochondrial RNA directly *in vivo* and what are the positions of these binding sites. This chapter specifically identifies the RNA species present physiologically in ribonucleoprotein complexes that were immunoprecipitated with SLIRP-FLAG.

3.3 Discussion.

The CLIP data presented here show that there is direct binding of SLIRP to all mt-mRNA species, apart from *MTND6*. Particular transcripts had two binding sites (*MTCOII*, *MTATP6*, *MTND4*, *MTCYB*), three (*MTCOIII*) or even five in case of *MTCOI* (Appendix 1.4). The number of hits per transcript for specific mRNAs including *MTCOII*, *MTATP8*, *MTCOIII*, *MTCYB*, *MTND1*, *MTND4L* and *MTND5* were specific but not abundant. This could have been due to the low level of SLIRP-FLAG expression in the HEK293T cell line, allowing the endogenous protein to occupy the sites on the RNA and thus, although binding the RNA, these species would not be

immunoprecipitated via the anti-FLAG antibody. The preferential amplification of some CLIP tags during sample preparation for IonTorrent analysis also cannot be ruled out. It is important to underline that SLIRP protein was reported to be in large molecular complexes with LRPPRC protein, however, the CLIP sequences reported here are exclusively bound by SLIRP protein. The specificity of the complex excised from the nitrocellulose membrane corresponded to migration of SLIRP/RNA and not to a higher molecular weight complex that could have represented LRPPRC/SLIRP/RNA. It is highly possible that the number of hits is lower than might be expected because a significant amount of mRNA species was bound in complexes that contained both proteins rather than SLIRP alone. In order to further validate the broad range of binding sites by SLIRP protein on mt-mRNA species at least one more repeat of the CLIP assay would be required. However, this data fits well with findings published during last few years showing interaction of LRPPRC/SLIRP complex with all mt-mRNA species (Chujo et al., 2012, Ruzzenente et al., 2011) but with very low abundance of interaction with *MTND5* and *MTND6*. The former, has been described as having only A5-8 as a tail (Temperley et al., 2010b), whereas, *MTND6* is not routinely found as polyadenylated (Slomovic et al., 2005). So the complex does not appear to be necessary for their elongation or protection, which is in line with CLIP data. Moreover, the very low number of hits located on *MTND1* could be due to its short half-life, estimated to be only 74 min in HeLa cells (Chujo et al., 2012). Surprisingly, there was also evidence of limited binding to the 12S rRNA in the CLIP sequences. This could be explained as a side effect of interaction between mRNA in complex with LRPPRC/SLIRP and the small subunit of the mitochondrial ribosome. In general the steady state levels of mitochondrial COX polypeptides were shown to be most affected in SLIRP depleted HeLa cells (Chujo et al., 2012). This is in agreement with the CLIP data that I obtained, which showed high binding to *MTCOI* (with four more sites of interaction below 50 hits) and multiple binding sites to *MTCOII* and *MTCOIII,* although for the last two the number of hits in a single position did not exceed 50 reads. The high number of hits recorded for *RNA14* (*MTATP8/6*) and *MTND4* is also supported by the reported outcome of SLIRP silencing, which caused a significant decrease in the steady state levels of these subunits (Chujo et al., 2012). The possibility of multiple binding sites on mt-mRNAs was also suggested in the most recent publication, postulating high abundance of LRPPRC in mitochondria, with 7 molecules of this protein per 1 molecule of mRNA (Chujo et al., 2012). As SLIRP is proposed to be in complex with LRPPRC,

again the CLIP data confirmed this assumption showing that for most of mt-mRNAs there is more than one binding site.

In summary, the CLIP assay result clearly states direct interaction of SLIRP-FLAG with all mt-mRNAs apart from *MTND6,* which correlates with published data concerning the role of LRPPRC/SLIRP complex.

Chapter 4

Characterization of the effect of the p.Ala181Val mutation in MRPL12 protein.

4. Chapter 4: Characterization of the effect of the p.Ala181Val mutation in MRPL12 protein.

4.1 Introduction.

The mt-LSU of the mammalian mitochondrial ribosome has a distinct structure called the L7/L12 stalk (Sharma et al., 2003). It is a highly conserved element of ribosomes in all three kingdoms: prokaryote, archaea and eukaryote (Wahl and Möller, 2002). The prokaryotic proteins are designated as L7/L12 and the eukaryotic, cytosolic as P1/P2. L7/L12 are identical in amino acid sequence, differentiated only by acetylation of the N-terminus converting L12 to L7. P-proteins can be phosphorylated, and this alteration regulates interaction of the polypeptides with the ribosome *in vitro* (Vidales et al., 1984). These are the only RPs bound to the large subunit through an interaction with other protein, L10 or P0 respectively, thus creating the stalk protuberance. L7/L12 and P1/P2, are acidic in character and occur on large subunits in dimers or multimers of dimers. They have a distinctive amino acid composition due to the large number of alanines, few aromatic residues and hardly any arginine, cysteine, or tryptophan. Acidic ribosomal proteins of archaea and eukaryotes are analogues of bacterial L7/L12, with a conserved functional domain organization (Rich and Steitz, 1987, Wool et al., 1991). In contrast to other RPs that are almost exclusively found complexed with translational machinery, the acidic ribosomal stalk proteins of both prokarya and eukarya have also been found in free cytosolic pools in *E. coli* (Ramagopal, 1976), *S. cerevisiae*, *A. salina*, and HeLa cells (Rich and Steitz, 1987). The studies on *Saccharomyces cerevisiae* showed that the amount of P-protein bound to a ribosome is changeable and depends on the metabolic state of the cell (Saenz-Robles et al., 1990). Approximately 40% more of it interacts with ribosomes in exponentially growing cultures than in stationary phase. Furthermore, the cytosolic pool is significant and can be comparable to the number of these molecules associated with ribosomes. It is important to mention interesting data concerning studies of four acidic proteins in yeast classified in two groups, YP1α/β and YP2α/β, corresponding to P1 and P2 mammalian cytosolic ribosomal proteins (Remacha et al., 1995). The analysis of translation rates in strains deprived of ribosome-bound acidic proteins show only 30% activity compared to WT strains and a changed pattern of protein expression, but had no effect on the translational accuracy of the ribosomes. The authors propose that the alterations in translation rate of different mRNAs can be caused by aberrant ribosomes that are less efficient at disruption of some particular complex RNA structures of the messengers. Thus the lower level of protein synthesis on particular templates would not be specific but dictated by

incompetence of ribosomes from mutant strains to resolve the unique motifs of some templates. Interestingly, bacterial ribosomes lacking L7 and L12 proteins remain active under particular *in vitro* conditions (Koteliansky et al., 1977). However, this experimental approach was dismissed as incorrect by another research group, who showed a strong dependence of the translation rate on the presence of L7/L12 in prokaryotic ribosomes *in vitro* (Pettersson and Kurland, 1980). Moreover, removal of L7/L12 from the ribosome was reported to reduce significantly the accuracy of protein synthesis (Kirsebom and Isaksson, 1985) but no *in vivo* data has yet been published to show that translation can occur in the absence of L7/L12.

E. coli L7/L12 protein is one of the most studied r-proteins. Four copies of L12 are present in the *E. coli* ribosome (Brot and Weissbach, 1981). Some of which are modified post-translationally by acetylation of the N-terminal serine, to form L7 with a molecular mass increase of 42 Da (Terhorst et al., 1973). Interestingly, this modification is very common among eukaryotic proteins but in prokaryotes there are only four known polypeptides with N-terminal acetylation (Polevoda and Sherman, 2002). Two of these are SSU proteins, S18 and S5, and the third is L7. In contrast to S18 and S5, which are always present in the bacterial cells as acetylated, the ratio of L12 to L7 is changeable and depends on growth phase as well as nutrient availability (Subramanian, 1975, Gordiyenko et al., 2008). The N-terminal domain of L12 is responsible for strong dimer interaction via methionine residues (Gudkov, 1997) and their oxidation causes disconnection of the dimers. Monomers are unable to bind L10 protein, which anchors the dimers to the ribosome. Mass spectrometry studies have shown that the N-terminal methionine promotes helical folding of NTD and thus binding to L10, which is enhanced by presence of acetyl group in L7 (Gordiyenko et al., 2008). In general this modification was proposed to increase stability of the L7/L12 stalk on the ribosome under stress conditions. Detailed structural studies of L7/L12 polypeptide are available and present this molecule as composed of two distinct organized domains linked by a flexible hinge (Dey et al., 1995, Dey et al., 1998, Wahl et al., 2000, Diaconu et al., 2005). The helical, N-terminal domain of elongated shape, the function of which was described above, is connected by a short region to a globular C-terminal domain built of three α-helices and three β-sheets. The latter can take different conformations, from a compact helix to an extended random coil (Wahl et al., 2000, Moens et al., 2005). The flexible hinge gives the C-terminal domain a high freedom of movement, which contributes significantly to its ability to span a volume with a radius of 45 A. It is

proposed that this dynamic feature of L12 facilitates the recruitment of translation factors and also regulates the different states of the ribosome during the translation process (Berk and Cate, 2007). Indeed, the conserved region of the L12 C-terminal domain has been found to interact directly with initiation factor; IF2, elongation factors; EF-Tu (which brings the aa-tRNAs to the A-site of the ribosome), EF-G (which translocates peptidyl-tRNAs from the A-site to the P-site) and release factor RF3 (recycles release factors RF1 and RF2 after removal of the nascent peptide) (Helgstrand et al., 2007). All of these factors catalyse the main steps of protein synthesis in a GTP-dependent manner. Two of these factors, elongation factors Tu and G, together with L7/L12 proteins have been shown to activate GTP hydrolysis (Mohr et al., 2002) and take part in the rapid subunit association into the 70S initiation complex (Huang et al., 2010). This process requires specific interaction between L7/L12 stalk present on the 50S and IF2-GTP on the 30S subunit, although L7/L12 is not the GTPase activator for IF2 protein in contrast to elongation factors Tu and G.

A broad range of L12 studies have also included experiments investigating the reasons for multiple L12 dimers presence on the bacterial ribosome. There are data showing that the activity of a single L12 dimer associated through a truncated L10 protein with the ribosome was almost equal to two-dimer particles in an *in vitro* polyphenylalanine synthesis assay (Griaznova and Traut, 2000). Another publication, using the same assay presented high activity of chimeric molecules composed of two monomers of L12 in which one was lacking the C-terminal domain (Oleinikov et al., 1998). Although interesting, these two articles present activity of L12 molecules in very simplified conditions, which cannot be easily compared to complex process of translation *in vivo*. In a recent publication, the *E. coli* strain JE105 with only a single dimer was reported to have a significant growth defect (Mandava et al., 2012). Moreover, ribosomes isolated from this strain showed lower efficiency of initiation and elongation steps involving IF2 and EF-G factors *in vitro*. The authors propose that the activity of bacterial ribosomes can be modulated by altering the number of L12 dimers bound to them in response to the growth conditions. This variation is seen in mesophilic archaea, *Methanococcus vannielii* and *Methanosarcina barkeri*, in which ribosomes with two L12 dimers are predominant at the early stages and during the lag phase of growth, whereas three dimers are most abundant in the exponential growth phase (Gordiyenko et al., 2010). In *E. coli* the stability of stalk is regulated by acetylation of the L12 protein (Gordiyenko et al., 2008). It has been also shown that the L7 content on

ribosomes changes according to the growth stage, with the highest abundance of the acetylated form in the stationary phase (Ramagopal and Subramanian, 1974), but the average number of L7 and L12 per ribosome remaining constant. Moreover, once integrated into the ribosome L7/L12 proteins do not undergo acetylation or deacetylation. Recently, the mechanism of L7/L12 monomer and dimer exchange between ribosomes was proposed based on kinetic analysis (Deroo et al., 2012). It has been also shown that binding of elongation factor EF-G decreases the rate of exchange via dimers by 47% and monomers by 27%. These new data fit well with previous observations and assumptions that in the bacterial cell a few populations of ribosomes can coexist with different ratios of L7 to L12 polypeptide, which can modulate the pace of translation in response to changing cellular requirements.

The gene of human mitochondrial MRPL12 protein was identified almost 10 years ago, as a delayed-early response. The protein has been shown to accumulate in the G_1 phase of growth-stimulated cells (Marty and Fort, 1996) and described as a homologue of chloroplastic and bacterial L12 protein. Expression of the truncated form of MRPL12 lacking 76 amino acids from the CTD in HeLa cells, caused cell growth inhibition and ATP production impairment. Wild type (WT) and mutant were found to localize in mitochondria and co-fractionate with ribosomes (Marty and Fort, 1996). More recently, two pools of MRPL12 have been identified in mammalian mitochondria, ribosome-bound and free (Surovtseva et al., 2011). The free pool was shown to selectively interact with the mitochondrial RNA polymerase and stimulate mitochondrial transcription *in vitro* and *in vivo* (Wang et al., 2007, Surovtseva et al., 2011). Interestingly, in human cells MRPL12 was identified as one of the interacting partners of NOA1 (C4orf14), which is postulated to be involved in 28S subunit biogenesis and mtDNA maintenance (He et al., 2012). The authors proposed that the free pool of MRPL12 interacting with POLRMT may play a role in the handover of mRNA from the transcription to the translation machinery, the assembly of which is believed to start from association of mt-SSU with mt-mRNA. Interestingly, MRPL12 has been also identified in a complex of 200 kDa with MRPL10, MRPL53, MRPL45, MRPS21, LRPPRC, SLIRP and COX7A2, in a mitochondrial fraction obtained from HEK293 cells (Wessels et al., 2013).

MRPL12 was also reported to be phosphorylated in mammalian mitochondria (Koc and Koc, 2012). A study using hybrid *E. coli* ribosomes carrying chimeric L7/L12

proteins that consist of the *E. coli* N-terminal domain and the mitochondrial C-terminal domain showed their ability to trigger the GTPase of elongation factor EF-G, interact with EF-Tu and support the translation activity (Terasaki et al., 2004). In other studies, applying core bacterial ribosomes stripped of L7/L12 stalk and replaced with mitochondrial MRPL10-MRPL12 complex in the presence of eight fold excess of recombinant MRPL12, the translation ability of these hybrid particles was restored to 80% in comparison to the bacterial system, reconstituted with recombinant bacterial L10 and L7/L12 *in vitro* (Han et al., 2011). These last two publications described give at least partial evidence for a conserved function of MRPL12 protein in the translation process, with the ability to bind elongation factors and support protein synthesis on hybrid ribosomes. Han et al., 2011, present evidence partially confirming the structural and functional organisation of the stalk in mammalian mitochondria showing that both MRPL12 and MRPL10 are necessary for reconstitution of translational activity. In bacteria L12 dimers are linked to the ribosome via L10 protein. The high-resolution crystal structure of a complex consisting of L10 and 6 L12 NTDs from *T. maritima* determined the α8-helix at the C-terminus of protein L10 as a site for L12 dimers attachment (Diaconu et al., 2005).

The available data concerning the role of mammalian mitochondrial MRPL12 are still insufficient to draw sound conclusions of its functions. The relatively superficial information suggests that this is a highly conserved protein, which apart from taking part in the translation process as a ribosomal component, may also be involved in the modulation of the transcription process. So it could be that MRPL12 is a multifunctional factor of mammalian mitochondria with a range of regulatory functions linking different steps of mtDNA expression pathway.

Immortalised fibroblasts with a mutated form of MRPL12 were made available to my host lab allowing us to study its function in human mitochondria. The cells originate from a patient with a severe clinical presentation consistent with mitochondrial disease (dysmorphy, growth retardation, lactic acidosis, hyperlactatemia, epilepsy). The measurements of the mitochondrial respiratory chain enzyme activities were performed by our collaborators and showed decreases in CI and CIV activities in the patient muscle biopsies, confirming a mitochondrial defect (Serre et al., 2013). The mutation was found to be a homozygous c.542C to T transition in exon 5, changing a highly

conserved alanine into a valine, p.Ala181Val (Figure 4.1; received from collaborators), which was identified and predicted by Polyphen2 software to be potentially damaging. Genome wide sequencing of the patient's DNA failed to detect any other pathogenic mutations. It is important to underline that this mutation was absent from over 100 sequenced controls. Both parents were heterozygous and a healthy girl sibling were wild type homozygous. Affected twin foetuses were homozygous the same mutation as the sibling from whom the fibroblasts originate.

Figure 4.1. Fragment of sequenced MRPL12 gene with point mutation in patient compared with mother and control. The arrow shows the position of the mutation. Below, alignment of the CTD fragment of L12 protein containing the conserved A (alanine) in eukaryote and prokaryote, substituted in the patient gene to encode V (valine).

The three dimensional structure of the human MRPL12 was modelled on the crystallized L12 protein from *Thermotoga maritima*. Based on this, the amino acid change in the mutant polypeptide chain was located in the highly conserved α-helical fragment of MRPL12 C-terminal domain (Serre et al., 2013).

Figure 4.2. The structural model of the human MRPL12. Polypeptide chain of human MRPL12 (residues 64 to 198) was modeled using the Swiss-Model on the L12 from *Thermotoga maritima* as a template. The model of MRPL12 contains just residues 64 to 198 as the homology between human MRPL12 and the prokaryotic L12 does not extend across the entire length of the protein sequence. The A181 residue is indicated in red. CTD, C-terminal domain; NTD, N-terminal domain. Image adapted from Serre et al., 2013.

Although substitution of alanine by valine is classified as a conservative mutation, it has been reported to cause changes in helix propensity (Gregoret and Sauer, 1998). Alanine is considered as one of the best helix-forming residues in contrast to valine, which is a poor helix former. As the C-terminal domain of MRPL12 is putatively involved in translation factor interactions with the ribosome, this substitution could affect mitochondrial polypeptides synthesis.

4.2 Point mutation in the *MRPL12* gene affects steady state level of the protein and other proteins of the mt-LSU.

In order to assess the influence of the mutation in the *MRPL12* gene on the steady state level of the protein, western blot analysis of immortalised control and patient fibroblast lysates (50 µg) was performed (Figure 4.3). Membranes were incubated with antibody against MRPL12 as well as two other mt-LSU proteins MRPL3 and ICT1. The levels of three mt-SSU proteins, DAP3, MRPS18B and MRPS25 were also assessed. Figure 4.3 is a representative western blot of a minimum of at least three independent samples for each protein.

	Patient % relative to Control
MRPL12	32.5%
ICT1	26.8%
MRPL3	63.0%
DAP3	70.7%
MRPS18B	74%
MRPS25	56.0%
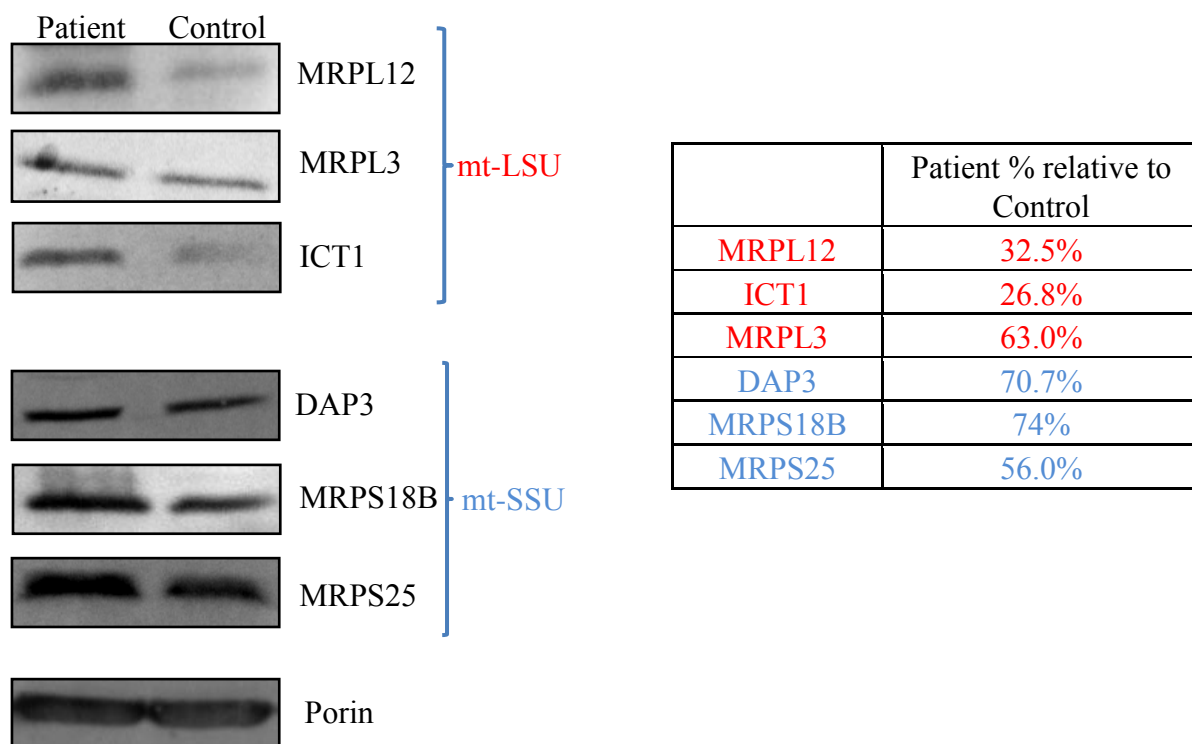
Figure 4.3. Steady state levels of selected mt-LSU and mt-SSU proteins in immortalised MRPL12 patient fibroblasts are affected compared to control. Cell lysates (50 μg) were resolved on 12% SDS-PAGE gel. Antibodies for mt-LSU proteins: MRPL12, ICT1, MRPL3; mt-SSU proteins: DAP3, MRPS18B, MRPS25; and porin used as a loading control were detected via Storm PhosphoImager. Quantification of steady state levels of presented proteins (table) was performed with Image-Quant software (Molecular Dynamics, GE Healthcare).

The steady state level of MRPL12 in patient fibroblasts was decreased by 70% versus control. Two other mt-LSU proteins were also reduced; ICT1 (by 70%) and MRPL3 (by 40%). The levels of mt-SSU proteins were only modestly decreased to 70.7% (DAP3), 74% (MRPS18B), and 56% (MRPS25) of control value. The reduction in mitochondrial large subunit proteins in the subject's fibroblasts suggested destabilization of mitoribosome or its assembly. So, next the steady state levels of chosen respiratory chain proteins were assessed in order to confirm the results of the collaborating laboratory who presented a reduction of complexes I and IV by BN-PAGE of mitochondria prepared from fibroblasts of patient and control (Appendix 1.5, Figure 1B).

4.3 Steady state levels of respiratory chain proteins are selectively affected by the decrease in MRPL12 steady state level.

Western blots were performed to analyse steady state levels of COX2, NDUFB8 and cytochrome *c* (cyt *c*) presented in Figure 4.4 as described in the previous subsection. The mitochondrially encoded subunit of complex IV, COX2 showed a significant

reduction in the steady state levels. This was also true for NDUFB8, which although not mitochondrially encoded is used as a marker for complex I as it is sensitive to degradation in the absence of assembled complex I. These data confirm the results of BN-PAGE analysis that showed a decrease of both of these complexes in patient fibroblasts versus control. The level of cytochrome *c* was also determined, as a control for the respiratory chain and porin was used as a loading control.
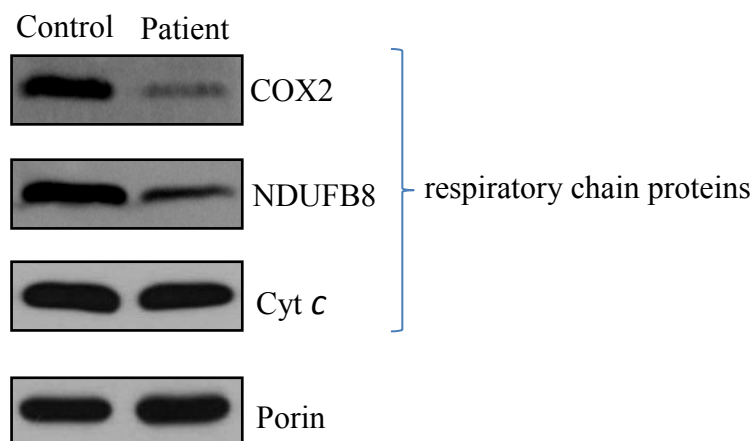
Figure 4.4. **Steady state levels of selected respiratory chain proteins in immortalised MRPL12 patient and control fibroblasts.** Patient and control fibroblasts lysates (50 µg) were separated by 12% SDS-PAGE followed by western blot analysis with antibodies against COX2 and NDUFB8. Cyt *c* level was determined as a control for the respiratory chain. Porin was used as an indicator of mitochondrial mass. Antibodies for presented proteins were detected via Storm PhosphoImager/ImageQuant.

The significant reduction in the steady state level of MRPL12 protein as well as two other proteins of the ribosomal mt-LSU, ICT1 and MRPL3 seen in Fig 4.3, suggested possible deregulation in mitoribosome assembly. In conjunction with the decreases seen in subunits of complex I and IV (Fig 4.4) this strongly supported an aberrant function of the translational machinery in patient fibroblasts. To identify whether these changes had an impact on cell viability, the growth rate of immortalised patient fibroblasts versus control was also assessed.

4.4 Patient fibroblasts have a decreased rate of growth.

In order to assess the influence of the mutated form of MRPL12 on patient derived fibroblast viability, cells (10 000) were seeded in 6-well plates. Control and patient fibroblasts were plated in triplicate on day 0. Cells were counted three times at 48 hours intervals as described in subsection 2.1.5. Each point on the graph (Figure 4.5)

presenting the growth curves for control and patient fibroblasts, is the mean number of cells from three independent wells.
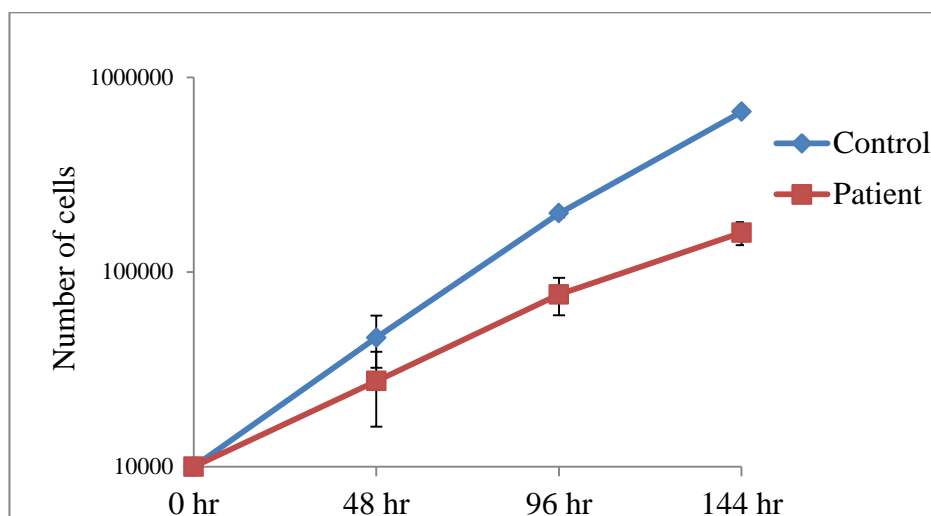
Figure 4.5. Cells growth analysis of patient and control fibroblasts. Cells were grown in 6 well plates in glucose containing media. On "day 0" 10^4 cells were seeded and counted every second day in triplicates. n = 3 control (blue) and patient (red). Error bars are +/- SD.

The growth rate of patient fibroblasts was reduced in comparison with the control cell line, which is in agreement with data showing disruption of OXPHOS complexes. All of the preliminary data described so far prompted further investigations aiming to specify the molecular basis of step or steps of mitochondrial gene expression where mutated MRPL12 failed to function correctly. In order to determine whether the mutation in MRPL12 affected integration into the ribosome, sucrose gradient fractionation of mitochondrial lysates was performed.

4.5 Analysis of mt-SSU, mt-LSU and monosome location in isokinetic sucrose gradients of mitochondrial lysates of patient fibroblasts.

Isokinetic sucrose gradient fractionation allows for the separation of particles according to their molecular mass. Thus, if the assembly of either the mt-LSU or the complete mitoribosome was altered, the distribution of individual MRPs would be expected to differ for the subject's gradient profile versus the control. Mitochondrial lysates (300 µg; prepared as in subsection 2.5.1 and 2.5.2) of control or patient fibroblasts were independently loaded onto 10-30% isokinetic sucrose gradients and separated by centrifugation (described in subsection 2.5.8). Fractions of 100 µl were collected and 10 µl aliquots were analysed by western blotting (Figure 4.6).
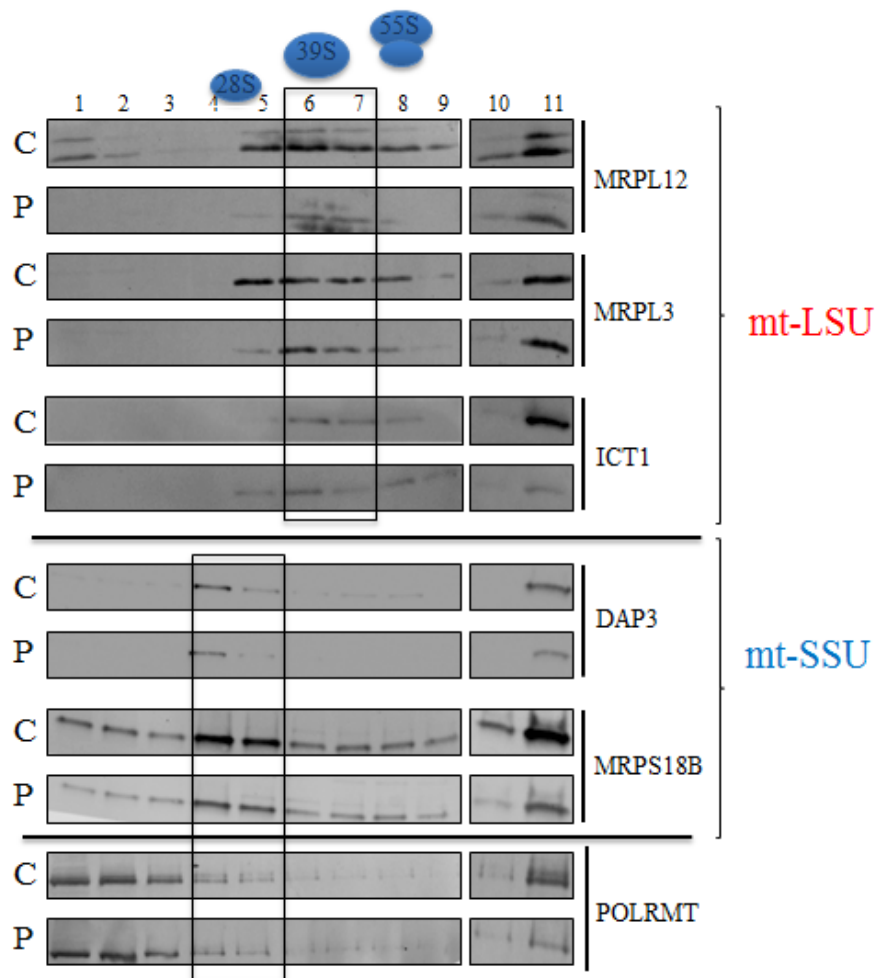
Figure 4.6. Isokinetic gradient centrifugation to analyse MRPs distribution in patient samples. Mitochondrial lysates (300 μg) from control (C) and patient (P) immortalised fibroblasts were loaded on 10-30% sucrose gradients. Fractions were collected for each sample, where sample 1 corresponds to the top and fraction 11 the bottom of the gradient. 15 μl of each fraction was separated on 12% SDS-PAGE gel and proteins of mt-LSU: MRPL12, ICT1, MRPL3, mt-SSU: DAP3, S18B and POLRMT were detected via western blot analysis using Storm PhosphoImager and ImageQuant software. Mitochondrial ribosomal subunits (28S, 39S) and monosome (55S) are depicted above the fractions in which they would be expected to migrate. 28S: boxed fractions 4 and 5, 39S: boxed fractions 6 and 7, 55S: fraction 8.

Surprisingly, analysis of the gradients did not show any significant changes in location of 28S, 39S or 55S as can be seen by the similar migration of control and patient proteins in the boxed regions, showing the position of the mt-SSU (fractions 4 and 5) and mt-LSU (fractions 6 and 7) on the gradient. The most significant difference in the patient can be observed in the overall strength of the MRPL12 signal, reflecting both the lack of detectable signal in fractions 1 and 2 (the free pool) and also substantially decreased amounts in mt-LSU fractions. Since it has been published that the free pool of MRPL12 interacts with POLRMT (Surovtseva et al., 2011), this redistribution of MRPL12 may have influenced the distribution of POLRMT. The

distribution of mitochondrial RNA polymerase in sucrose gradient fractions and its steady state level was therefore analysed (Figure 4.6 and 4.8). Although steady state level of POLRMT was decreased to 63% in patient fibroblasts versus control, the position of the signal within the gradient did not differ, suggesting that the physiological interactions had not been affected. The abundance of patient MRPL3 was slightly reduced in fractions 5, 6, 7 and 8, but there was no significant shift in the migration pattern in the patient fibroblast sample. The position and strength of the ICT1 signal was very similar in subject cells versus control, apart from fraction 11, where a clear decrease in the amount of this protein occurs. The same reduction in amount of protein present in fraction 11 is also seen for MRPL12. The small subunit proteins, DAP3 and MRPS18B, were affected to an even lesser extent. The distribution of their signals in the sucrose gradient of patient fibroblasts was comparable with control. The biggest but nevertheless modest difference is in MRPS18B, where there is a reduced abundance in patient fractions 4 and 5. Both of the mt-SSU proteins assessed were reduced in fraction 11 in subject fibroblasts in comparison with control. It was necessary to determine directly whether these relatively minor changes seen on the gradient analyses, had an impact on mitochondrial translation.

4.6 *De novo* mitochondrial proteins synthesis in patient fibroblasts versus control.

To further characterise the effect of mutated MRPL12 on mitoribosomes analysis of mitochondrial translation was performed. Metabolic labelling with ^{35}S-met/cys of *de novo* synthesised mitochondrial proteins under conditions of inhibited cytosolic translation was performed in immortalised control and patient fibroblasts together with Dr. Francesco Bruni.

Cultured immortalised control and patient fibroblasts of ~70% confluency were preincubated in methionine/cysteine free DMEM, followed by incubation with emetine to inhibit cytosolic translation (*cf* 2.5.7). Radiolabel was added for 1 hour and chased for the same period of time. Samples were prepared and separated on 15% SDS-PAGE. A generalised decrease in signal for almost all mt-encoded proteins was seen in patient fibroblasts compared to control (Figure 4.7) indicating a global decrease in mitochondrial translation. Densitometric evaluation of the signals revealed that in particular, translation of COXI, COXII and COXIII subunits of complex IV were significantly reduced, as was ATP6 of complex V. Mitochondrial polypeptides of

complex I were also decreased but to a lesser extent and cytochrome *b* was not affected. Following analysis, the gel was rehydrated and Coomassie blue stained to confirm equal loading.
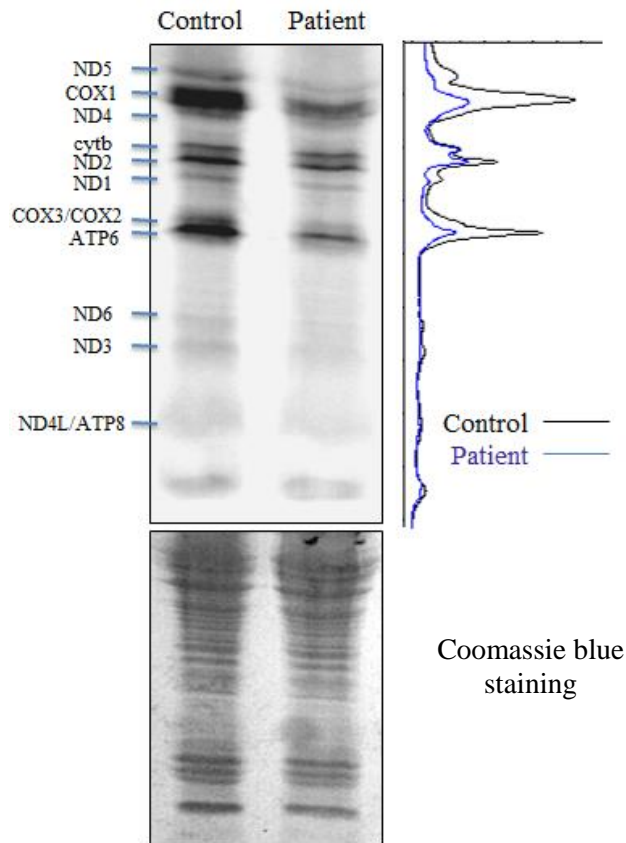
Figure 4.7. *In vivo* ^{35}S-met/cys metabolic labelling of mitochondrial proteins. Whole cell lysates (50μg) from immortalised control and MRPL12 patient fibroblast following metabolic labelling were separated by 15% SDS-PAGE. ^{35}S-methionine/cysteine incorporated into *de novo* synthesized mitochondrially encoded OXPHOS subunits were visualised after overnight exposure of the dried gel to a PhosphorImage screen, analysis with Typhoon FLA900 and Image-Quant software (Molecular Dynamics, GE Healthcare). Coomassie blue staining of the rehydrated gel is shown in the lower panel. To the right of the autoradiograph are presented densitometric profiles of control (black trace) and patient (blue trace). The figure was provided by Dr. Francesco Bruni.

The result of the *de novo* mitochondrial translation assay is in agreement with western blot analysis of COXII and NDUFB8, where both techniques demonstrate a significant reduction in the steady state levels (subsection 4.4). Moreover, our collaborators BN-PAGE analysis of OXPHOS complexes also presented a significant decrease in complex I and IV with no change in complex III level in subject fibroblasts. Despite publications suggesting a potential role for MRPL12 in translational accuracy, there were no aberrant polypeptides detected in the analysis of the patient cell line. There is, however, evidence

of malfunction of the mitoribosome. Although the pattern of protein synthesis is clearly changed in patient fibroblasts, a particular feature is the inequality of translational efficiency for different mitochondrially encoded subunits. Intriguingly, mitoribosomes in fibroblasts with the mutated form of MRPL12 are capable of producing cytochrome *b* with the same efficiency as control, but fail most profoundly in synthesis of COX subunits. In order to clarify whether the MRPL12 defect had its effect at the transcriptional rather than translational level the steady state levels of mt-rRNA; 16S, 12S and selected mt-mRNA species: *MTCO1*, *MTND1* and *MTCYB* were assessed.

4.7 The effect of mutant MRPL12 on 16S, 12S and mt-mRNAs levels.

Diversity in translational efficiency and lowered signal of POLRMT in fraction 11 of sucrose gradients (Figure 4.6), which was confirmed by western blot analysis of POLRMT steady state levels presented in figure 4.8, dictated assessment of mitochondrially encoded RNAs in patient fibroblasts.
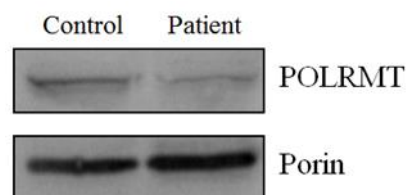
Figure 4.8. The steady state level of POLRMT in patient fibroblasts. Western blot analysis of immortalised patient and control fibroblast lysates (50µg) was performed with antibodies against POLRMT. Porin was used as a loading control. The blot is representative of 3 independent repeats.

Northern blot analysis of *MTRNR1*, *MTRNR2* and mt-mRNAs steady state levels was performed (*cf* subsection 2.4.2.). Different amounts of RNA from the same sample were loaded to improve the quantification in case signals were weak or saturating. RNA species were visualised with radiolabelled probes and indicated that *MTRNR2* level was lowered by 32.5% in subject fibroblasts and *MTRNR1* was decreased by 20% (Figure 4.9).

A

RNA amount	MTCO1 Patient/Control	MTND1 Patient/Control	MTCYB Patient/Control
2µg	95%	132%	124%
5µg	98%	153%	100%
10µg	97%	131%	97%
	96.7%	**138.7%**	**107%**

RNA amount	MTRNR2 Patient/Control	MTRNR1 Patient/Control
2µg	66.8%	79%
5µg	65.9%	78.7%
10µg	70%	80%
	67.5%	**79.2%**

B

C
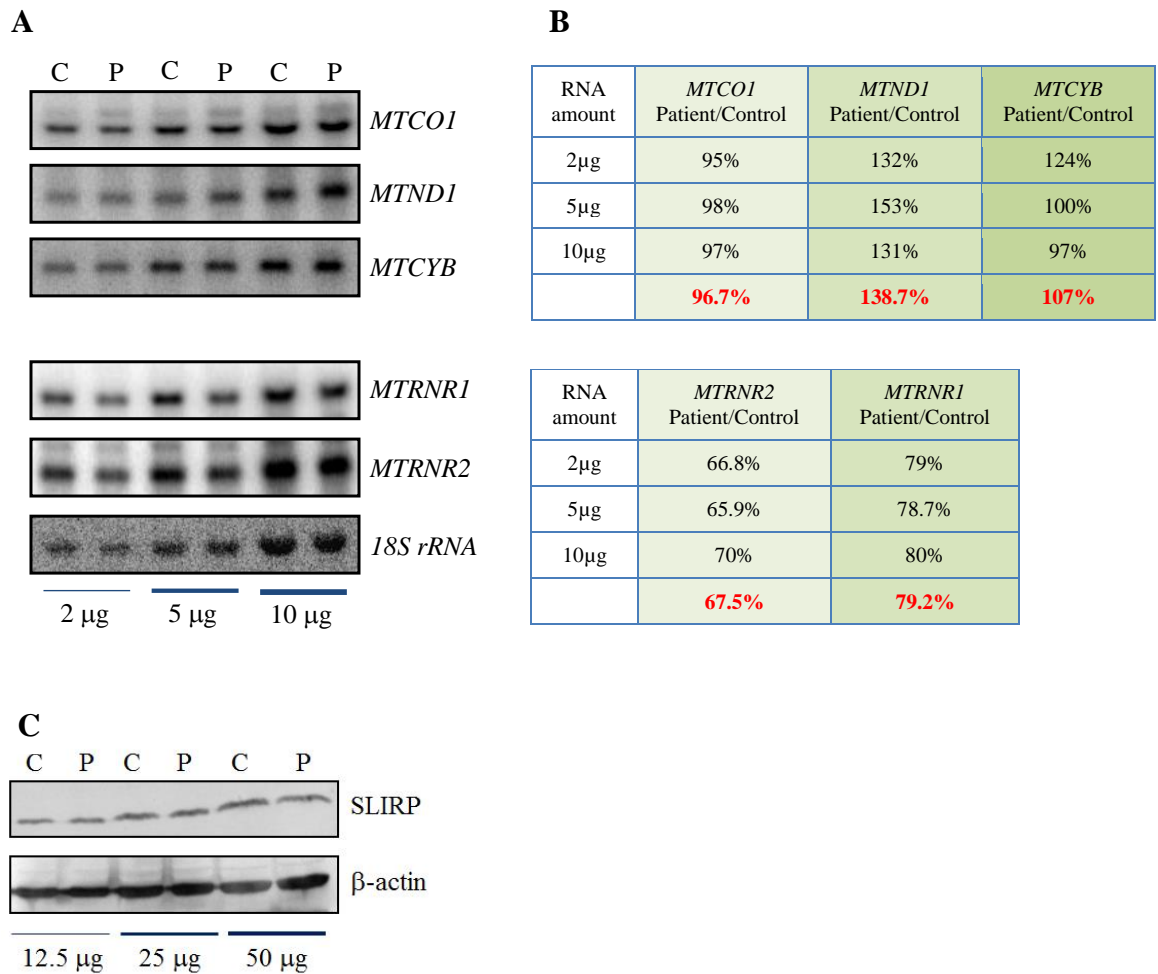
Figure 4.9. Northern blot analysis of control and patient total RNA.
A. RNA was extracted and separated on 1.2% agarose gel under denaturing conditions, transferred to the GeneScreen Plus membrane and probed for *MTRNR1*, *MTRNR2* and *MTCO1*, *MTND1, MTCYB*, and 18S cytosolic rRNA as a loading control. **B**. Tables containing the densitometric quantification of signals derived for mt-rRNAs and mt-mRNAs. **C**. Immortalised patient and control fibroblasts lysates (50 µg) were separated by 12% SDS-PAGE and the subsequent western blot was decorated with antibodies against SLIRP protein, and with β-actin as a loading control. Signals were detected via Storm PhosphoImager and analysed by Image-Quant software.

The data for the 2 ribosomal RNAs shows that the mutation in MRPL12 affects the large ribosomal subunit to a higher extent than mt-SSU. This is in agreement with the results of steady state ribosomal proteins levels and sucrose gradient fractionation of mitochondrial lysates, which also showed a greater reduction in amounts of mt-LSU proteins than in mt-SSU proteins, in the patient samples. The levels of *MTCO1* and *MTCYB* in patient fibroblasts were not affected, but *MTND1* was elevated by ~38% comparing with control. SLIRP protein is part of the ribonucleoprotein complex that is dependent on the presence of mt-mRNA (Sasarman et al., 2010). Therefore, it was appropriate to see if the change in mt-mRNA levels have an effect on the steady state

level of SLIRP in patient fibroblasts compared to control. Western blot analysis was performed and showed that there was no change in the steady state level (Figure 4.9C), which is consistent with the lack of reduction in mt-mRNAs.

The reduction of *MTRNR2* and the lower signal for MRPL12 in sucrose gradient fractions (Figure 4.6) both of which are components of the mt-LSU (fraction 6 and 7) and fully assembled mitoribosome (fraction 8) suggested a protective function of this protein on the 16S rRNA. This could be indirect by affecting 39S assembly or integrity, or directly by specific interactions with the rRNA. In order to investigate this potential ability of MRPL12 to bind rRNA *in vivo* and map the location of interaction if any, the CLIP method was used (protocol is provided in subsection 2.6.1). The assay was performed with endogenous protein for which an affinity purified antibody was generated (described in subsection 2.5.9). CLIP sequences were analysed by IonTorrent and aligned to a linear map of mtDNA. As expected the highest number of hits was identified in 16S rRNA. The specific position of binding was between nucleotide ~1750-1790, with almost 500 reads for control fibroblasts and 570 for patient fibroblasts (data presented in Appendix 1.2). There were three more positions identified that suggested direct binding to 16S but each with a lower number of reads. Overall, the number of CLIP sequences identified as 16S rRNA was considered as too low in order to unequivocally confirm a close and direct interaction with MRPL12, when compared with another ribosome interacting protein, RBFA, where over 3000 hits were mapped to one position on the 12S rRNA. The MRPL12 data also included a high number of reads for 18S rRNA, which was used as one of controls, (data presented in Appendix 1.1; Table 1). It would be interesting to repeat the CLIP for MRPL12 with HEK293 lysate in order to clarify its ability to bind rRNA directly. It has to be taken in consideration that fibroblasts have a lower mitochondrial mass comparing with HEK293 (used in CLIP for RBFA protein) so it could be the reason for the lower number of hits on 16S rRNA and 18S sequences amplified preferentially. Interestingly, some mt-tRNA species were also identified among the CLIP tags in the patient sample. Although patient and control exhibited the same pattern of possible binding to 16S rRNA, the interactions with tRNA^{Glu} (over 200 reads) and tRNA^{Met} (100 reads) are specific for mutated form of MRPL12.

Because the levels of mt-mRNA species were not decreased, even elevated in case of *MTND1,* but the steady state level of POLRMT was reduced (Figure 4.8) and

free pool of MRPL12, which interacts with POLRMT, was not detected in subject fibroblasts (sucrose gradient fractionation; Figure 4.6), the stability of a subset of mt-messenger RNAs was assessed to check if the half-lives were extended to compensate for a possible lowered transcription rate.

4.8 Stability of mt-mRNAs in patient fibroblasts versus control.

The stability of transcripts was determined by exposing patient and control fibroblasts to ethidium bromide, which selectively inhibits mt-transcription at a final concentration of 250 ng/ml, and isolating and analysing RNA taken at time points thereafter.

A
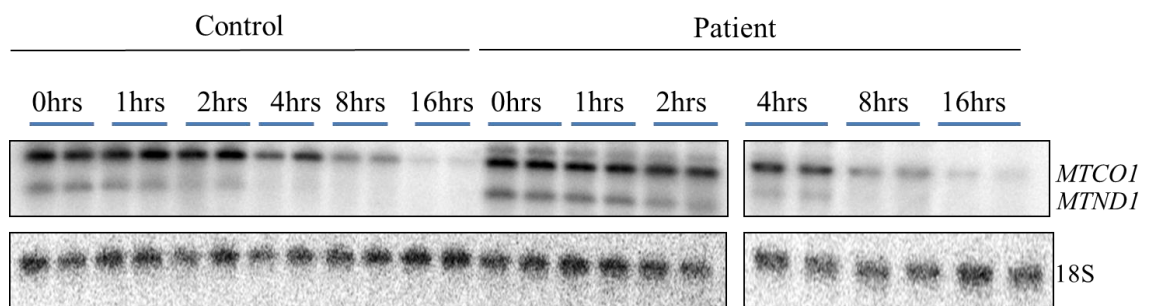
B
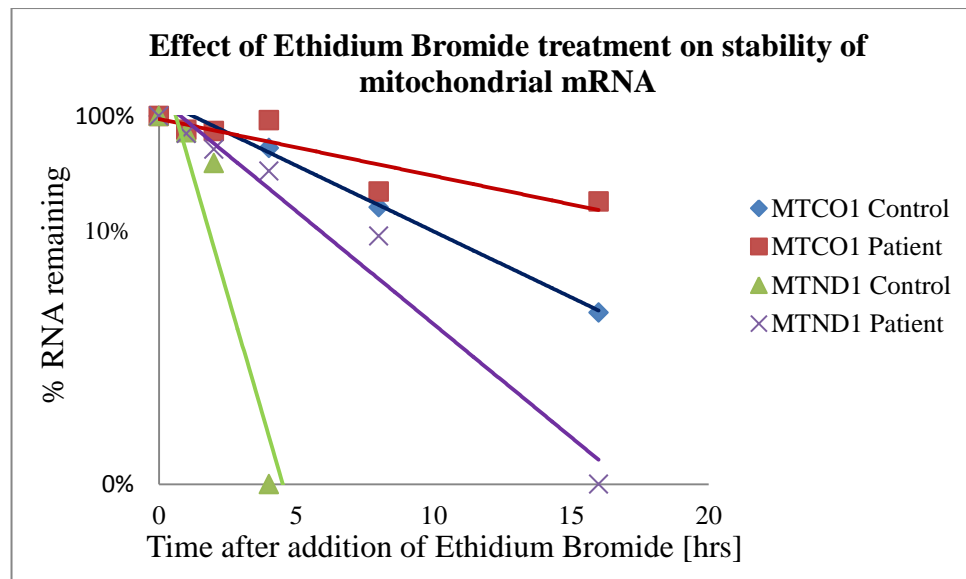
Figure 4.10. Stability of mt-mRNA species in control and patient fibroblasts.
Cells were grown in 6-well plates in presence of transcription inhibitor and harvested at 0, 1, 2, 4, 8 and 16 hr post ethidium bromide addition (n = 2). **A**. Northern analysis was performed probing for mt-mRNA species *MTCO1* and *MTND1*. **B**. The rate of decay is plotted for each transcript in each sample. Signals were detected via Storm PhosphoImager and analysed by Image-Quant software (Molecular Dynamics, GE Healthcare).

Fibroblasts were collected for each time point (n=2 for both control and patient cells). RNA was isolated and analysed by northern blot (Figure 4.10 A) and the quantification of the half-lives for *MTCO1* and *MTND1* shows elevated stability of transcripts in patient fibroblasts (Figure 4.10 B). Especially *MTND1* appears to be stabilized, this might compensate for the decrease in the level of POLRMT (Figure 4.8). Since, the steady state levels of mt-mRNAs are not reduced but the translation efficiency is decreased for most of the mitochondrial transcripts (Figure 4.7; *de novo* mitochondrial translation) further investigation of ribosome assembly was undertaken. RNA from isokinetic gradient fractions of fibroblast lysates was analysed by northern blot to assess the location of 12S and 16S mt-rRNA as well as selected mt-mRNAs. This was performed as a more sensitive technique than western blot to determine whether mt-rRNA was protected and subunits were assembled.

4.9 Location of 16S, 12S and mt-mRNA in sucrose gradient fractions.

In order to determine potential, subtle changes in mitoribosome assembly, cell lysates (700 µg; *cf* 2.5.1) of control and patient fibroblasts were loaded on the 10-30% isokinetic sucrose gradient (*cf* 2.5.8). Fractions (100 µl) were collected and 90% used for LS Trizol RNA extraction (*cf* 2.4.1).
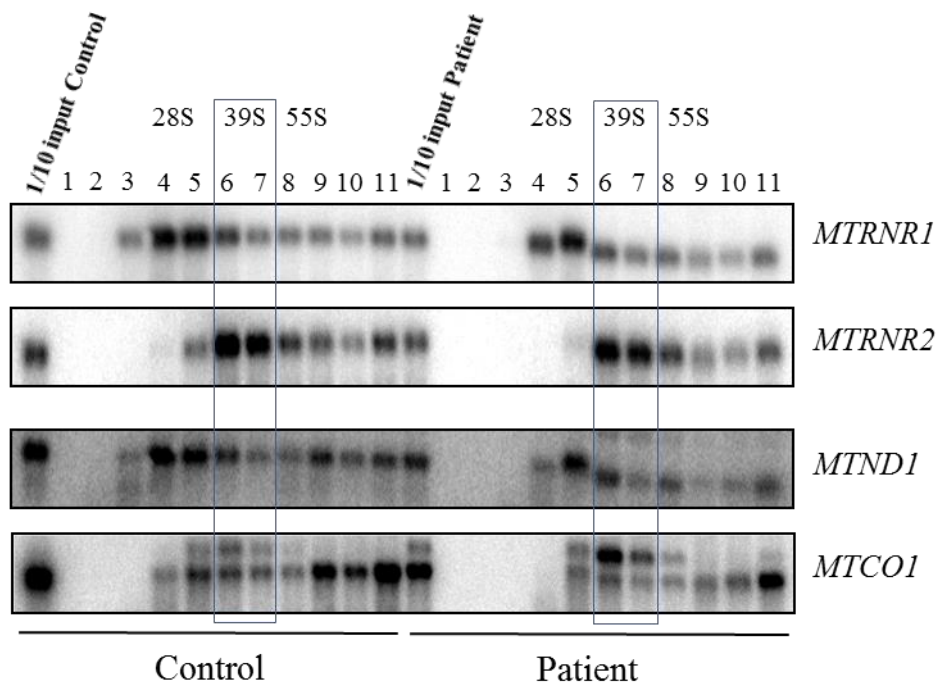
Figure 4.11. **Northern analysis of mitochondrial RNA species extracted from sucrose gradient fractions of cell lysates.** Patient and control RNA from gradient fractions analysed by northern blot with probes for mt-rRNAs; *MTRNR1, MTRNR2* and mt-mRNAs; *MTCO1, MTND1* as indicated. The positions of the 28S mt-SSU, 39S mt-LSU and 55S monosome are indicated above the fraction numbers, where 1 is top of the gradient and 11 the bottom. Signals were detected via Storm PhosphoImager/ ImageQuant software.

Northern analysis (*cf* 2.4.2, Figure 4.11) revealed the distribution of *MTRNR1*and *MTRNR2* in sucrose gradient fractions. This was consistent with the position within the gradients of the mt-SSU and mt-LSU obtained by western blot (Figure 4.6), which showed no major relocation of ribosomal subunits in patient fibroblasts. Although the location of mt-mRNAs (*MTND1* and *MTCO1*) was not changed, the *MTND1* signal is stronger in patient fraction 8 in contrast to control fraction 9, but clearly decreased in patient fraction 4. The strong signal of precursor (higher band from the doublet) of *MTCO1* is located in patient fraction 6. There is also reduced signal of *MTCO1* in patient fractions 9 and 10. The precursors were not detected for any other mt-RNA species described.

4.10 Further investigation of mitoribosome assembly in patient fibroblasts.

The western and northern blot analysis of sucrose gradient fractions did not unequivocally answer whether ribosome assembly is altered in subject fibroblasts. One question that remained unanswered was whether the MRPL12 mutation affected

dimerization or multimerisation, which in turn could affect binding to the monosome and translation efficiency.
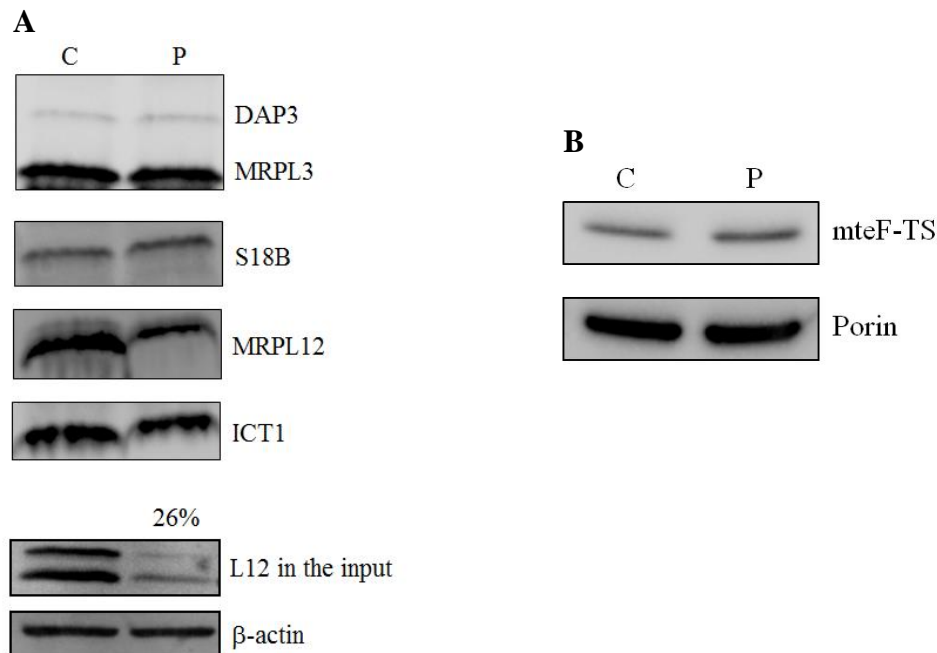
Figure 4.12. **Immunoprecipitation of mitoribosomes via MRPL12 protein. A**. Mitochondrial lysates (830 µg) from control and patient were incubated for 90 min with protein G beads (Dynal Invitrogen), coated with MRPL12 antibody. Half of the elution and mitochondrial lysate (input: 15µg) was analysed by western blot. Mt-SSU (DAP3, S18B) and mt-LSU (MRPL3, ICT1, MRPL12). In case of the mitochondrial lysate (input) β-actin was used as a loading control. **B**. Steady state level of mt eF-TS (mitochondrial elongation factor). Western blot analysis of immortalised patient and control fibroblast lysates (50µg) was performed with antibodies against mt eF-TS. Porin was used as a loading control. Proteins levels were visualised by Storm PhosphoImager.

Immunoprecipitation of monosomes from patient and control mitochondrial lysates was performed to determine if it was possible to distinguish whether less monosome was formed or whether monosome was formed but had less MRPL12 associated. Affinity purified antibodies to MRPL12 were used and relative amounts of co-immunoprecipitating MRPs were analysed.

The immunoprecipitation experiment was performed (*cf* subsection 2.5.10) with 830 µg of mitochondrial lysate. After incubation (1hr) with protein G/ MRPL12 beads, supernatant was removed from pelleted beads and the pull-down was eluted from washed beads with 25 µl of 1x sample buffer (described in 2.5.4). After 3 min incubation at 95°C eluates from control and patient were analysed by western blot. Half of the obtained samples were separated on 14% SDS-PAGE alongside 15 µg of fibroblast mitochondrial lysates (input) (Figure 4.12 A). In order to assess monosome

abundance antibodies for mt-SSU (DAP3, MRPS18B) and mt-LSU (MRPL12, ICT1, MRPL3) proteins were used. Western blot analysis of the eluates shows equal levels of mt-SSU proteins but decreased MRPL12 and ICT1 relative to approximately control levels of MRPL3 in subject eluate versus control (Figure 4.12 A). As the immunoprecipitation was performed with MRPL12 antibody, the eluates contained not only fully assembled mt-ribosomes, but also mt-LSU and free fraction of MRPL12. Similar levels of mt-SSU (DAP3, S18B) proteins in patient and control samples suggest that the mutated form of MRPL12 has no influence on the assembly of monosomes. This is in agreement with western and northern analysis of sucrose gradient fractions (Figures 4.6 and 4.11). The level of mt-LSU protein MRPL3 is unchanged in contrast to MRPL12, whereas ICT1 appears to be modestly decreased. The control eluate also consists of a free pool of this MRPL12 as well as mt-LSU and monosomes, so the signal is a sum of three pools; free, 39S and 55S. In the case of the patient sample most of the signal consists of two pools; mt-LSU and monosome bound, as the free pool of MRPL12 was below detection in sucrose gradient fractions (Figure 4.6). A substantial part of the decrease in the level of MRPL12 in patient cells may potentially be accounted by the loss of a fraction interacting with POLRMT, independent of the ribosome bound protein. It can not be excluded, however, that some portion of decrease in the signal detected for mutated form of MRPL12 is caused by partial loss of this protein bound to mt-LSU as the sucrose gradient analysis show clearly a reduction of it in fractions of mt-LSU and monosome.

Overall, the immunoprecipitation result stays in agreement with previous experiments, confirming the presence of fully assembled monosomes in subject fibroblasts, but with decreased contribution from MRPL12.

The MRPL12 was shown to interact with translational elongation factors. As its mutant form is substantially decreased, the steady state level of mteF-Ts was checked in order to assess if there is any correlation in the levels of these possible interactors (Figure 4.12B). Western blot analysis of mt eF-Ts did not show any reduction in the steady state level of this protein. Further investigation would be necessary to clarify how the mutated form of MRPL12 deregulates the process of translation in subject fibroblasts. In order to clarify whether any disruption occurs in the interaction between subject monosomes and translation factors, location of those proteins in sucrose gradient fraction could be analysed as well as their level in the eluate of immunoprecipitates obtained from immunoprecipitation of MRPL12 from patient and control mitochondrial lysates.

4.11 Discussion.

The point mutation in MRPL12 gene that changes A181 to V causes a significant decrease in the steady state level of this protein by 70% in patient fibroblasts versus control (Figure 4.3). This reduction influences other proteins of mt-LSU including ICT1 steady state level decreased to 26.8% and MRPL3 to 63% of control value. Whereas proteins of mt-SSU are affected to lesser extend with DAP3 reduced to 70,7%, MRPS18B to 74 % and MRPL25 to 56% versus control. As expected the decrease in the abundance of ribosomal proteins had an effect on the steady state level of OXPHOS subunits with COXII and NDUFB8 clearly reduced in subject fibroblasts (Figure 4.4). This observation is in agreement with Blue-Native analysis of mitochondrial complexes (performed by collaborating laboratory), which revealed a substantial decline in the amount of CI and CIV (Serre et al., 2013). In order to establish whether the mutated form of MRPL12 influences assembly of the mt-LSUs and/or monosomes, mitochondrial lysates of patient and control were separated in isokinetic sucrose gradients. Western blot analysis of the sucrose gradient fractions showed no significant changes in location of mt-LSU, mt-SSU or monosome in subject versus control (Figure 4.6), which strongly suggest that mutated form of MRPL12 does not influence mt-ribosome biogenesis. However, using antibodies to MRPL12 (Figure 4.6) clearly showed the lack of a free pool of MRPL12 in patient fibroblasts and a decreased signal in fractions assigned to mt-LSU and monosome. Interestingly, all of the MRPs detected in the sucrose gradient fractions are visibly reduced in patient fraction 11, apart from MRPL3. The final fractions harbour the heaviest particles, which may represent non-translating aggregated ribosomes. The presence of a ribosomal pool that is not participating in protein synthesis has been acknowledged in publications (Remacha et al., 1995). Whatever the role of this subset is, the source of molecules that could be reused to generate newly formed monosomes or the reserves waiting to increase the translation process as required is distinctly reduced in patient fibroblasts.

It is difficult to draw final conclusions regarding the number of MRPL12 molecules per monosome in human mitochondria. In bacteria there are two or three dimers associated with 70S, but the dimerization status and the number of dimers in human mitochondrial monosomes is unknown. Although published results concerning the use of chimeric ribosomes composed of core bacterial ribosomes stripped of L7/L12 stalk and replaced with mitochondrial MRPL10-MRPL12 complex showed the necessity of eight fold excess of recombinant MRPL12 to restore their activity to 80% of bacterial system in *in vitro* translation reactions (Han et al., 2011).

In order to elucidate if the stoichiometry of patient MRPL12 per mt-LSU was adjusted, I performed the immunoprecipitation on patient and control mitochondrial lysates using antibody against MRPL12 (Figure 4.12). Western blot analysis of the eluate clearly demonstrated reduction in the mutated MRPL12 as well as ICT1 although to a lesser extent. This reduction had no influence on MRPL3 protein assembled into the mitochondrial LSUs. Overall, the amount of mutated MRPL12/39S appears to be reduced. The level of mt-SSU proteins in fully assembled monosomes appears to be unaffected. The immunoprecipitation of subject and control monosomes via 28S protein could clarify whether the reduction in MRPL12/39S influences assembly of mt-SSUs. Unfortunately this approach had to be excluded from the experimental investigation as the antibody that would immunoprecipitate endogenous mt-SSU proteins was not available.

Summarizing, immunoprecipitation of MRPL12, which collects free MRPL12, mt-LSUs and monosomes shows no detectable difference in the amount of proteins of mt-SSU in patient fibroblasts versus control in contrast to proteins of mt-LSU, where MRPL12 and ICT1 signal is clearly decreased. This observation strongly supports both western and northern blot analysis of sucrose gradient fractions confirming presence of assembled monosomes and mt-LSUs possibly lacking at least partially MRPL12. It has to be underlined that in the control fibroblasts the free fraction of MRPL12 represents a significant subset of this protein, which is absent in patient cells and may account for the reduced signal in the immunoprecipitation.

Free MRPL12 was reported to be associated with mitochondrial RNA polymerase and thereby to have an influence on the transcription process. Although the steady state level of POLRMT is modestly reduced (Figure 4.8) in subject fibroblasts, the location in sucrose gradient fractions is not changed (Figure 4.6). This suggests that the distribution and by extrapolation the activity of POLRMT is not affected by the loss of free MRPL12. This is further supported by the northern blot analysis of mt-mRNAs steady state levels, which are not decreased. However, in order to determine if transcription was affected with a downstream consequence on transcript stability, the half-lives of two mt-mRNAs were analysed (*MTCO1* and *MTND1*). In this preliminary analysis, the stability was found to be elevated, which might be a compensatory mechanism for a decrease in the transcription rate caused by the absence of MRPL12 free pool. An alternative hypothesis that can not be excluded is that the stability of mt-mRNAs species is increased because the rate of translation is lowered and the templates stay associated with monosomes longer. This possibility is supported by northern blot

analysis of fibroblast sucrose gradient fractions where the *MTND1* signal is stronger in patient fraction 8 (assigned to the monosome) compared to control fraction 9 (Figure 4. 11). In contrast, the signal of *MTCO1* appears to be equal in patient and control fraction 8 but the accumulation of *MTCO1* precursor is clearly visible in patient fraction 6. There is also reduced signal of *MTCO1* in patient fractions 9 and 10. It is vital to underline that although in patient fibroblasts translation of all species takes place, it does not appear to do so to a uniform extent (Figure 4.7). Some transcripts are synthesized in patient fibroblasts equally to control such as *cyt b*, some are modestly decreased including subunits of CI or others are markedly decreased (CIV subunits). It is tempting to speculate that the variations present in the above mentioned northern blot analysis as well as divergence in the level of translation could be of dual source; 1) lack of the free pool of MRPL12, and/ or 2) dysfunctional monosomes (mutated MRPL12/39S appears to be reduced).

First, the free pool of MRPL12 was recently identified to be enriched at the nucleoids foci where mt-RNA processing begins. That could be justified by the interaction of MRPL12 with POLRMT and its role in transcription process (Surovtseva et al., 2011). However, taking into consideration the presence of *MTCO1* precursor in fraction 6 of patient sucrose gradient allows to hypotheses that MRPL12 could influence the processing of some mt-mRNAs. Moreover, the free pool interacting with POLRMT (Surovtseva et al., 2011), potentially takes part in the assembly of monosome which starts by association of mt-SSU with mt-mRNA (He et al., 2012). Furthermore, as the mutated MRPL12/39S appears to be reduced and the accumulation of the *MTND1* signal in patient monosome fraction of sucrose gradient is enhanced it is possible that the ribosomes with a mutated form of this protein are not capable of performing translation as efficiently as the control. The lower rate of translation could be due to disturbance of interactions between MRPL12 and translation factors. The eubacterial L12 homologue has been shown to interact with range of translation factors that affect participation in all stages of translation; initiation, elongation and termination of protein synthesis. Human MRPL12 shares 27.5% identical amino acid sequence to its *T. maritima* counterpart (Serre et al., 2013) and the substitution of alanine to valine is located in an α-helix of the C-terminal domain (Figure 4.2) where sequence and structural similarity are shared. Importantly loss of this CTD has been shown in eubacterial ribosomes to cause a decrease in GTPase activity, which is driven by the interaction with various translation factors. It can, therefore, be proposed that the

MRPL12 mutation found in this patient results in the failure of the monosome to interact efficiently with translation factors.

However, as mentioned before, *de novo* protein synthesis performed in subject and control fibroblasts clearly present variations in the level of mitochondrially translated proteins. If the source of decreased translation would be caused by deregulation of interactions between mutated MRPL12 and translation factors, one could easily assume a global, equal decrease in 13 mitochondrial subunits of OXPHOS system which is not seen in *de novo* mitochondrial proteins synthesis assay (Figure 4.7). However if the free pool of MRPL12 influences the rate of processing of some mt-mRNA species and their availability for the monosomes, then both disruption of posttranscriptional events and reduced efficacy of mitoribosomes could result in this mixed pattern of mitochondrial protein synthesis in patient fibroblasts. The pattern of distribution for other mt-mRNAs could be checked in sucrose gradient fractions to clarify if processing is affected. *MTND1* and *MTCO1* were chosen for this analysis as they co-build complex I and IV respectively, which presented highest deficiency in patient fibroblasts (Appendix 1.5; Table 1, Figure 1).

It can not be excluded that the variations in patient mitochondrial protein synthesis can at least partially be due to the specificity of the transcribed template or synthesised polypeptide. It has been shown in numerous publications concerning bacterial L12 that this protein is enormously flexible and the CTDs of dimers interacting with translation factors (Helgstrand et al., 2007) are in close proximity to many strategic sites of ribosome including the sarcin-ricin loop (SRL) of 23S rRNA, which is a factor-binding site essential for GTP-catalyzed steps in translation, the peptidyl-transferase domain, and the head of the 30 S subunit (Dey et al., 1998). It is tempting to speculate that these putative interactions in patient mitochondrial ribosomes are disrupted because of a decreased number of MRPL12 molecules per ribosome or by physical steric hindrance caused by the amino acid substitution. Again the enriched signal of *MTND1* in monosome fraction of sucrose gradient could be the result of mt-ribosomes stalling. It is, therefore, tempting to propose that human MRPL12 possibly influences correct conformation of ribosomes in order to efficiently disrupt the secondary structures of mt-mRNAs. Indeed, some proteins of eubacterial mt-SSU (S3 and S4) were postulated to take part in its mRNA helicase activity influencing ribosome processivity (Takyar et al., 2005). S3 protein was shown as one of interacting partners with L7/L12 (Dey et al., 1998), the same as L2 protein implicated in peptidyl-transferase activity (Diedrich et al., 2000). Interestingly, elongating ribosomes are able more readily to melt mRNA

secondary structures (Qu et al., 2011). It is possible that human MRPL12 also interacts with numerous parts of the mitoribosome influencing its velocity. Since the conformations of the templates differ it can not be excluded that ribosomes with mutated form of MRPL12 can stall on some specific structures of mRNAs as they are unable to promptly unwind them and therefore translate some species at a lower rate. The other source of mt-ribosomes stalling could be caused by distinct sequence motifs in the already translated polypeptides. Recently, it has been published that bacterial ribosomes stall on diprolyl motifs and are rescued by the EF-P (translation elongation factor) (Peil et al., 2013). Then, in the case of monosomes containing mutated MRPL12 the possible altered interaction with some translation factors can stall some of them depending on the polypeptide sequence and cause variations in the level of translation among mitochondrial polypeptides. In order to resolve if patient mitoribosomes fail to melt secondary structures of incoming mt-mRNAs or stall during translation on emerging polypeptides motifs the technique of ribosome profiling could be applied. This novel technique allows characterisation of the pattern of binding sites on mRNAs by ribosomes at any particular moment (Weiss and Atkins, 2011) and has been already used to investigate mitochondrial translation (Rooijers et al., 2013). As it is based on deep sequencing of ribosome-protected mRNA fragments ribosome profiling generate large amount of data that allow in depth analysis of translation process. By using inhibitors of initiation and later the progression of translation it is possible to assess the speed of the translating ribosomes (Weiss and Atkins, 2011). In one of the study using ribosome profiling technique the translation rate in the mouse embryonic stem cell line was established at the processing of 6 amino acids per second (Ingolia et al., 2011). Moreover this technique enables to identify the source of ribosomes stalling, for example in the Ingolia et al. study; 1500 major pauses were detected caused by the specific 3 codon arrangement Pro-Pro-Glu. Unfortunately, mitochondrial ribosome profiling has not yet been fully established in our laboratory, although this is underway. Once optimized it could answer whether monosomes in patient fibroblasts have a lower rate of translation, possibly stalling on some specific mRNAs sequences or already translated peptides.

Furthermore, the examination of the abundance of translation factors in the monosome immunoprecipitated with MRPL12 could clarify whether the interaction with mutated form is affected, which as already described can influence overall activity of ribosomes. Unfortunately, the limitation of material obtained from performed immunoprecipitation (Figure 4.12) did not allow further analysis.

Moreover, the CLIP results for MRPL12 performed with patient and control sample in order to investigate if this protein binds 16S rRNA directly and if so whether mutated MRPL12 interaction is altered causing decline in 16S level (Figure 4.9 B), would require further optimisation. The CLIP tags analysis for both MRPL12 control and mutated form present multiple sites of binding to 16S rRNA. Performing this assay with a higher concentration of SDS and introduction of additional washing steps of beads after incubation with cell lysate could possibly give a clearer more specific result. Although greater than 50 hits was suggested as showing specificity (by local experts), the number of CLIP sequences identified as 16S rRNA was considered as too low in order to unequivocally confirm a close and direct interaction with MRPL12, when compared with another ribosome interacting protein, RBFA, where over 3000 hits were mapped to one position on the 12S mt-rRNA. The MRPL12 data also included a high number of reads for 18S rRNA, which was used as one of controls, (data presented in Appendix 1.1; Table 1). Interestingly, although patient and control exhibited the same pattern of possible binding to 16S rRNA, the interactions with tRNA[Glu] (over 200 reads) and tRNA[Met] (100 reads) was specific for mutated form of MRPL12. This potentially abnormal interaction could have negative effect on protein synthesis. Further, if the repeated CLIP data with patient fibroblasts would confirm binding to tRNA[Glu] and tRNA[Met], then the steady state level of these tRNAs could be checked as well as their location on sucrose gradient fractions. The high resolution northern blot potentially could answer which fraction of mutated MRPL12 binds to these species if any. Additionally, performing CLIP with different cell types for example HEK293 could give more reads as the mitochondrial mass in fibroblasts is significantly lower than other cell lines, which could be the reason for high background. This experiment could resolve the question of direct binding between MRPL12 and 16S mt-rRNA.

The data presented in this chapter provides a complicated image of one of the most conserved proteins in the ribosome, which shares many features not only with eubacterial homologues but also with eukaryotic analogues (Wahl and Möller, 2002). Although the experimental analyses undertaken to investigate the role of MRPL12 in human mitochondria clearly show that its presence is required for mitochondrial translation they do not draw a final molecular mechanism or stoichiometry of its activity.

To clarify the exact, potentially numerous, steps in mitochondrial gene expression in which MRPL12 takes part, including coupling the transcription and translation events in response to changing cell requirements for energy, more experimental work is required.

This investigation of mutated MRPL12 presents new insights into the role of this conserved protein in human mitochondrial translation. Clearly the human homologue of bacterial L7/L12 has developed into a multifunctional protein potentially coupling transcription and translation process and surprisingly its dysfunction selectively affects different OXPHOS complexes. It is only one of few MRPs whose mutated forms have been reported as a source of mitochondrial translation deficiency triggering respiratory chain dysfunction. Two proteins of mt-SSU; MRPS16 (Miller et al., 2004) and MRPS22 (Saada et al., 2007) as well as one mt-LSU protein MRPL3 (Galmiche et al., 2011) have so far been identified in patients as a cause of multiple OXPHOS deficiencies.

Reported mutations were fatal in an early onset in case of MRPS16 (3 days of age) and MRPS22 protein (patients died at 2- 22 days of age) whereas in case of mutation in MRPL3 two out of four siblings were still alive at 3 years of age. Two siblings died at 17 months and 15 months of cardiac arrest. There is no doubt that it is important to pursue investigation into the basic biology of mitochondrial monosomes, which in the future may provide information that could lead to effective therapy, diminishing the devastating effects of mitochondrial dysfunction in young patients.

Chapter 5

RBFA; *Mitochondrial Ribosome Assembly Factor A.*

5. Chapter 5: RBFA; *Mitochondrial Ribosome Assembly Factor A*.

5.1 Introduction.

Human mitochondrial ribosome binding factor A (RBFA; C18orf22) was identified by my host laboratory as one of proteins that interacted with mtRRF-FLAG (Rorbach et al., 2008). Further investigation of this protein was then undertaken by Ricarda Richter as part of her PhD project. C18orf22 is the orthologue of bacterial RbfA that associates specifically with free 30S subunits, and that was first shown to inhibit a cold-sensitive mutation in 16S rRNA (C23U) of *E. coli* when overexpressed (Dammel and Noller, 1995). Bacterial cells lacking RbfA exhibited a cold-sensitive phenotype (Dammel and Noller, 1995) identical to a reported mutant strain that contained a C to U transition located at the 5' end pseudoknot helix of 16S rRNA (helix 1), predicted to cause weakening of the helix. C23U strain showed decreased polysome levels and accumulation of free 30S and 50S subunits (Dammel and Noller, 1993). Consistent with an involvement in 16S rRNA, RbfA was reported alongside another protein, RimM, as an essential factor for efficient processing of 16S rRNA. It was also observed that overexpression of RbfA in a strain deleted of RimM partially suppressed the slow growth and translational deficiency (Bylund et al., 1998). Thus, both proteins have been proposed to be associated with the 30S in the late stage of 16S rRNA maturation acting as accessory proteins assisting in the efficient assembly of the bacterial small ribosomal subunit. The biogenesis of eubacterial ribosome requires around 30 known assembly factors including those playing role in the rRNA modification and processing (Yang et al., 2014). In contrast, cytosolic ribosome assembly involves ~200 factors in *S. cerevisiae* (Strunk and Karbstein, 2009).

The precursor of *E. coli* 16S rRNA, is the 17S that contains 115 additional residues at the 5' end and 33nt at the 3' terminus. It requires two endonucleases RNases E and G to process its 5' end (Li et al., 1999) and four exonucleases at the 3'end (RNase II, RNase R, PNPase and RNase PH) (Sulthana and Deutscher, 2013). The correct folding of rRNA and assembly of 30S is facilitated by the Era and RsgA GTPases and chaperons such as already mentioned RbfA and RimM but also enzymes introducing modifications on selected bases (Clatterbuck Soper et al., 2013,Yang et al., 2014).

Overall features of prokaryotic RbfA are that it is a small (15kDa; *E. coli*, 10.9 kDa; *T. thermophilus*) cold shock protein, the expression level of which is rapidly increased in cells exposed to the low temperature (Jones and Inouye, 1996). Its deletion causes an inability of bacteria to adapt to the low temperatures. The level of mature 16S

rRNA and polysomes in mutant strains lacking RbfA is further reduced after exposing bacterial cells to 15ºC and as the 30S contains mostly immature pre-16S rRNA (Xia et al., 2003), whereas in the wild type cells the level of 30S-bound RbfA increases several fold. This is postulated to occur to promote rapid maturation of the bacterial small ribosomal subunit in order to overcome a translational block. NMR structure of *E. coli* RbfA lacking 25 residues at the C-terminal domain (CTD) revealed that it contains a type-II KH- domain fold topology, which is specific for RNA-binding proteins (Huang et al., 2003). It has been published that KH-domains mediate RNA-dependent protein-protein interactions (Chen et al., 1997). Interestingly, in bacteria the overexpression of a GTP-binding protein Era, also containing a C-terminal KH domain, can partially rescue bacterial cells deleted of RbfA (Inoue et al., 2003). In a similar fashion to RbfA, Era is crucial for cell growth in *E. coli* and also associates with free 30S subunits. Its deletion causes accumulation of the same pre-16S rRNA, which has been observed in RbfA deleted strains, and there is also an increase of free ribosomal subunits 30S and 50S. Overexpression of the wild type Era in cells lacking RbfA suppressed the cold-sensitive phenotype, enhanced 16S rRNA processing and ribosome assembly. In contrast, the reciprocal was not true, RbfA overproduction could not substitute for Era (Huang et al., 2003). However, another protein, KsgA, was able to rescue bacterial cells containing a cold sensitive mutation in Era (E200K; Lerner et al., 1995) that causes a growth defect below 30ºC (Lu and Inouye, 1998). KsgA is a methyltransferase that methylates two conserved neighbouring adenosine residues at the 3'end of SSU 16S rRNA (helix 45), which are situated in close proximity to the sequence complementary to the Shine-Dalgarno sequence (Formenoy et al., 1994). Strikingly, *E. coli* mutants deprived of methylation at A1518-A1519 are resistant to the antibiotic kasugamycin (Helser et al., 1971). These cells display only a slightly decreased rate of translation initiation (Poldermans et al., 1979) and decrease in accuracy of protein synthesis (Van Buul et al., 1984). Interestingly, in *S. cerevisiae* disruption of the KsgA homologue Dim1p that is the cytosolic SSU 18S rRNA dimethyltransferase, was reported to be lethal (Lafontaine et al., 1994) but this was due to additional 18S rRNA-processing function (Lafontaine et al., 1995) as the lack of methylation of the two adenosines of helix 45 did not influence cell growth (Lafontaine et al., 1998). Lafontaine et al.,1998 showed that the lack of methylation at the 3'terminus of 18S rRNA is required in the *in vitro* translation system but only fine-tunes ribosomal function *in vivo*. The rate of growth of the *E. coli* strain deleted of KsgA is comparable with WT at 37 ºC but lowered temperatures (25ºC, 20ºC) causes growth defects, accumulation of free SSUs and slowed pre-16S rRNA

processing (Connolly et al., 2008). Moreover, in the same publication it was presented that a catalytically inactive form of KsgA (E66A) with the capability to bind 16S rRNA strongly inhibited 70S ribosome formation and caused accumulation of SSUs associated with E66A. This result suggested that the methylation event is necessary for KsgA methylase to be released from the small subunit and that dissociation of KsgA is required for the SSU to be available for IF3 and/or large subunit. KsgA was described to methylate 30S subunits that were in a translationally inactive conformation (Desai and Rife, 2006), which then caused a change in the structure to optimize 70S function (Demirci et al., 2010). KsgA bound to SSUs, blocks the formation of the decoding site and ribosome assembly (Boehringer et al., 2012a). Interestingly, overexpression of RbfA in KsgA *E. coli* deletion mutants inhibited cell growth and caused the accumulation of aberrant 70S-like particles (Connolly and Culver, 2013). The authors suggest that these two proteins are linked *in vivo*. Indeed, structural analysis confirms that RbfA interacts with helices 44 and 45 positioned at the 3'end of 16S rRNA, perturbing their structure (Datta et al., 2007). KsgA also interacts directly with the conserved helix 45, methylates two adenosines and alters the structure of helix 44 (Boehringer et al., 2012b). Era also binds at the 3' end of 16S rRNA, to the 1531-AUCACCUCCUUA-1542 sequence, which is directly preceded by helix 45 (residues 1,507–1,528) (Tu et al., 2009). Authors propose that Era acts as a chaperone in the late stage of 16S rRNA maturation, possibly enabling correct cleavage at the 3' end of pre-16S rRNA and facilitating activity of KsgA. In the next publication the same group reports that Era also interacts directly with the helix 45 (Tu et al., 2011).

Interestingly, RbfA and Era both interact with 3' and 5' regions of the SSU rRNA, in particular with helix h28, which is known to interact with helix h1. RbfA is known to bind and stabilise h1 and since Era may bind to this common structural element this may allow it to partially rescue bacterial cells depleted of RbfA by indirect stabilisation of h1 (Datta et al., 2007). This suppression is curious as in bacteria, the known function of RbfA is to promote processing of 5' end of the 16S rRNA precursor, which involves direct binding with h1 whereas Era is involved at the other end of the molecule in the 3'end maturation (Sharma et al., 2005). Overall, the position of bacterial RbfA during the late stages of 30S maturation allows it broad interactions with numerous pre-16S rRNA structures, which is thought to implicate this protein in more than just the 5' end maturation of 17S rRNA precursor to 16S. In summary, prokaryotic RbfA alongside KsgA, RimM, Era and a few others is classified as one of the factors taking part in the final steps of structural changes of 30S subunit before interaction with

50S (Shajani et al., 2011). Clatterbuck Soper et al., 2013 suggest that accessory proteins such as RbfA and RimM postpone particular RNA folding events to ensure the quality of 30S assembly.

In human mitochondria homologues of Era and KsgA have already been described. ERAL1 (Era G-protein-like 1), the homologue of bacterial Era was investigated in my host laboratory and its direct interaction with ribosomal RNA was confirmed by crosslinking immunoprecipitation (CLIP) assays that I performed. The binding site mapped to the 3'end of SSU 12S mt-rRNA, which closely resembles the 3'end of the bacterial SSU rRNA as it contains a stem-loop region (Dennerlein et al., 2010) that encloses the two conserved adenine residues that are also dimethylated by a homologue of KsgA, human TFB1M (Cotney et al., 2009).

Interestingly, ERAL1 depletion in HEK293 cells causes apoptosis and a significant decrease in a nascent 12S mt-rRNA level with no perturbation of mt-mRNA levels or mitochondrial protein synthesis (Dennerlein et al., 2010). Whereas silencing of TFB1M in HeLa cells was reported to cause cell growth arrest, with a decrease of 12S rRNA level but unaffected mitochondrial mRNAs levels and reduced mitochondrial translation rate (Cotney et al., 2009).

The investigation of human RBFA carried by Ricarda Richter showed inhibition of cell growth in HEK293 cells depleted of this protein, which at 343 amino acids is approximately three times bigger than the bacterial counterpart. Sequence and structure alignment of bacterial RbfA and human mitochondrial RBFA showed marginal sequence similarity but a conserved structure of the type-II KH-domain in the mitochondrial orthologue. Analysis of mitoribosome assembly after three and six days depletion of RBFA in HEK293 cells, showed no significant changes (Appendix 1.3). Silencing of RBFA for six days did not cause significant reduction in the steady state levels of mitochondrial rRNA or any mt-mRNAs. Furthermore, 3 days RBFA depletion resulted in approximately 1.5 fold increase of the mitochondrial protein synthesis. In contrast, six days depletion caused subtle decrease in *de novo* synthesis of 15 - 20%. The depletion of RBFA did not significantly influence the steady state levels of mitochondrially encoded proteins or mtDNA. Moreover, mitochondrial ROS production was not affected nor was mitochondrial membrane potential. The mitochondrial mass was slightly increased after six days of RBFA silencing. Even after 6 days RBFA depletion only 6% more apoptotic cells were present in comparison to control. Interestingly, 3 days of ERAL1 depletion caused 35% cells to go into apoptosis. The initial CLIP assay performed by Ricarda Richter to identify binding RNA sequences of

RBFA-FLAG, failed to generate significant number of mitochondrial sequences nevertheless this preliminary data suggested an interaction of RBFA-FLAG with both the 3'end of 12S mt-rRNA and more surprisingly 5S rRNA. This intriguing result dictated that the first experiment that I performed in the further investigation of RBFA, aimed to assess the RNA binding ability of *endogenous* RBFA and precisely define the binding sequence or sequences using the CLIP technique.

5.2 CLIP data, the answer to the mystery?

I performed CLIP assay in order to identify specific binding sequences on mt-RNA by endogenous RBFA (as described in subsection 2.6.1) in HEK293T cells. The barcoded library generated from the obtained CLIP tags were IonTorrent sequenced by Dr. Helen Tuppen. All reads were collected and aligned to human mtDNA (revised Cambridge reference sequence) using the Torrent Suite software on the IonTorrent server. The alignment is presented in the form of a graph in Figure 5.1, where a linear representation of the human mtDNA acts as the x-axis and the number of reads located in each position occupies the y-axis. The locations of RBFA binding sites for which more than 50 CLIP reads were identified are indicated. The number of hits exceeding this threshold is primarily located in 12S mt-rRNA sequence. Figure 5.1 indicates that four significant binding positions on 12S mt-rRNA were identified; the first harbouring ~160 reads at position 904-918nt (1), second ~ 1300 reads at position 1181-1211 nt (2), third ~ 1000 reads at position 1292-1312 nt (3) and fourth ~ 3400 reads at position 1560-1582 nt (4). Other binding sites were identified in the sequence of tRNA[Met] (~450 hits) and tRNA[Glu] (~120 hits).
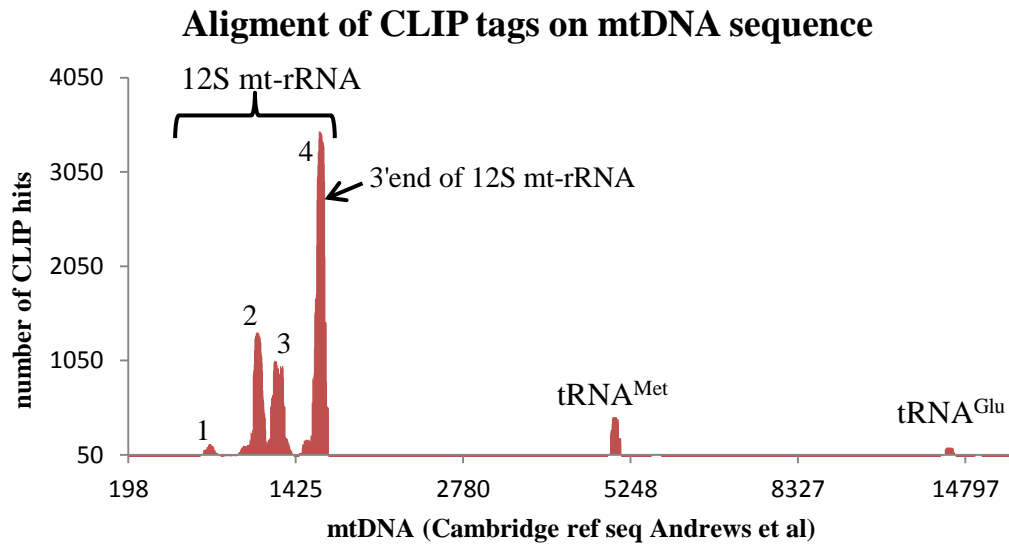
Figure 5.1. Linear display of human Cambridge reference sequence of mtDNA with depicted number of RBFA CLIP tags. Human mtDNA is displayed in a linear format with locations of the IonTorrent identified CLIP tags mapped upon it. The number of CLIP hits was deemed as significant if it exceeded 50, hence the threshold on the y-axis. Y-axis starts from the nucleotide for which at least one hit was detected. The significant hits for endogenous human RBFA protein were identified in *MTRNR1* (12S mt-rRNA) with four locations of CLIP hits. Other mapped positions were identified as tRNA^{Met} and tRNA^{Glu}.

The binding sequence harbouring the highest number of CLIP hits is situated at the 3'end of 12S mt-rRNA (helix 45), covering the stem loop that contains two dimethylated adenines. This corresponded with the exact same binding sequence that was identified for ERAL1 protein investigated by me in my host laboratory. As already mentioned, both ERAL1 and RBFA are orthologues of bacterial Era and RbfA, which are maturation factors of the prokaryotic ribosome. Consistent with the bacterial function, human mitochondrial ERAL1 was described as a 12S chaperone, as its depletion in Hek293 cells causes a significant decline in nascent 12S rRNA. The CLIP assay result prompted further investigation, aiming to establish whether RBFA has the ability to compensate for the loss of ERAL1 and/or can ERAL1 make up for the loss of RBFA in human cells.

5.3 Can RBFA and ERAL1 reciprocally compensate for each other's function following siRNA depletion in human cells?

In order to investigate any potential compensatory mechanism occurring between RBFA and ERAL1 in human mitochondria, two modified HEK293 cell lines were used. The first was engineered to be able to inducibly express RBFA-FLAG and the second ERAL1-FLAG.

5.3.1 Expression of RBFA-FLAG in the absence of ERAL1 does not compensate depletion in Hek293 cells.

The first experiment was performed to identify if over-expression of RBFA could suppress the slowed growth phenotype that was seen in ERAL1 depleted cells. To establish if this were the case control HEK293 WT cells and a derived line that could express RBFA-FLAG were used. Both cell lines, grown in 6-well plates, were transfected with either non-targetting (NT) or ERAL1 specific siRNA (described in subsection 2.1.6). In the case of the RBFA-FLAG cell line, expression of the protein was induced with doxycycline 4 hr after siRNA transfection. To ensure the desired experimental conditions had been successfully achieved western blot analysis was performed to confirm the depletion of ERAL1 and expression of RBFA-FLAG (Figure 5.2).
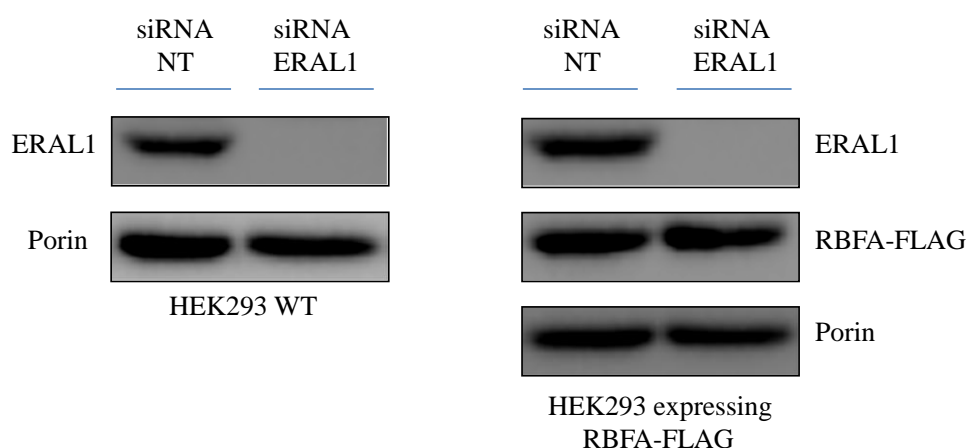
Figure 5.2. Western blot analysis of ERAL1 depletion and RBFA-FLAG induction in HEK293 cell lines. Overexpression of RBFA-FLAG and depletion of ERAL1 protein were confirmed by western blot analysis of cell lysate (50 μg, 12% SDS-PAGE). RBFA-FLAG was detected with antibody against FLAG extension. Antibodies for proteins indicated were detected with ChemiDoc MP Imaging System (BioRad).

To assess overall growth all cells were harvested and counted after 72 hr siRNA/induction treatment (see subsection 2.1.5) and the data presented as a histogram (Fig. 5.3). The graph shows that expression of RBFA-FLAG does not rescue cells depleted of ERAL1 protein. Moreover, the number of cells is even lower in case of RBFA-FLAG cell line with silenced ERAL1 compering with control.
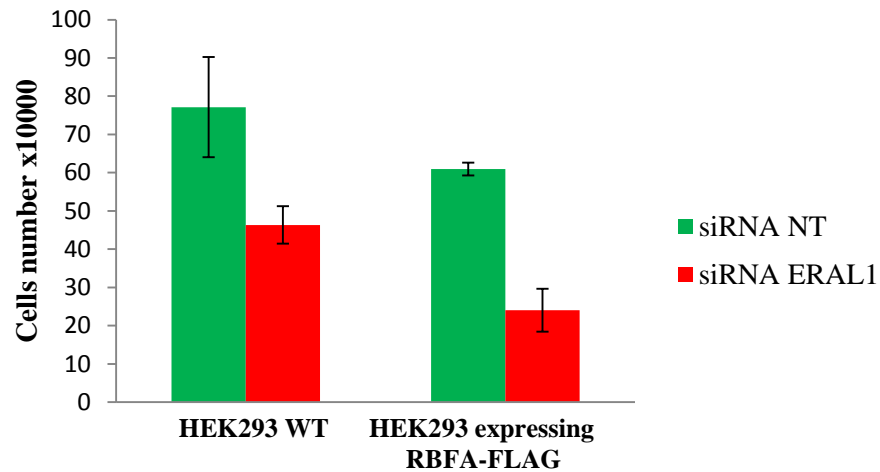
Figure 5.3. **RBFA does not compensate ERAL1 loss in cells.** Cell counts of HEK293 WT and HEK293 expressing RBFA-FLAG were taken after 72 hr siRNA treatment (NT control and siRNA targeted to the ERAL1 open reading frame were used at 33 mM final concentration). In case of RBFA-FLAG cells, the induction was triggered with doxycycline (1ng/ml final concentration) 4 hr after siRNA transfection. $15*10^4$ cells were seeded in six well plates in triplicates. Error bars are +/- SD.

5.3.2 Expression of ERAL1-FLAG does not rescue the phenotype of RBFA depleted Hek293 cells.

The second experiment aimed to assess whether ERAL1 can rescue cells depleted of RBFA. The same experimental approach was taken as described above. This time HEK293 expressing ERAL1-FLAG was used alongside control HEK293 WT. Both cell lines were transfected with RBFA or NT siRNA. Production of ERAL1-FLAG and depletion of RBFA was assessed by western blot analysis of cell lysates (CLs) (Figure 5.4).
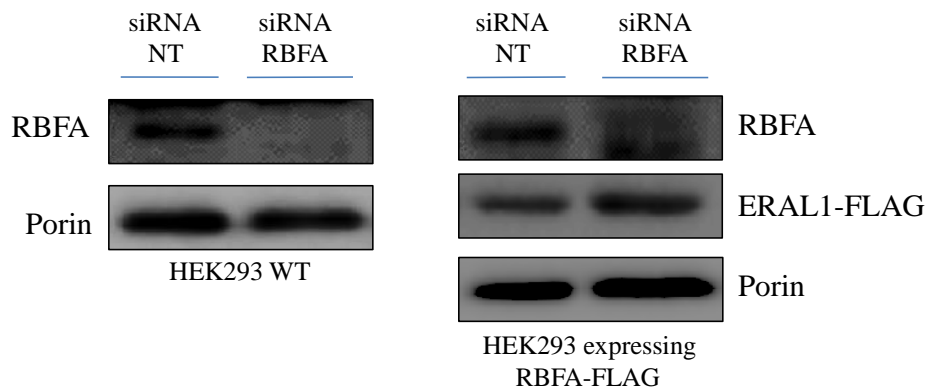
Figure 5.4. Western blot analysis of RBFA depletion and ERAL1-FLAG induction in HEK293 cell lines. Expression of ERAL1-FLAG and depletion of RBFA protein were confirmed by western blot analysis of CLs (50 µg, 12% SDS-PAGE). ERAL1-FLAG was detected with antibody against FLAG extension. Antibodies for proteins indicated were detected with ChemiDoc MP Imaging System (BioRad).

The number of cells was counted 72 hr after transfection and the data presented as a graph in Figure 5.5. Again, no compensatory mechanism was observed when ERAL1-FLAG was expressed in the absence of RBFA.
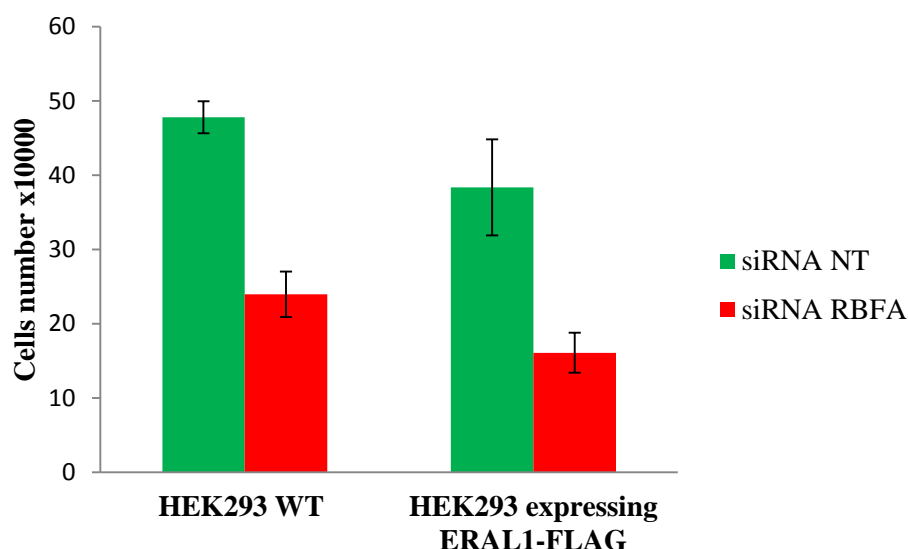
Figure 5.5. ERAL1 does not compensate for RBFA loss. Cell counts of HEK293 WT and HEK293 expressing ERAL1-FLAG were taken after 72 hr siRNA treatment (NT control and siRNA targeted to the RBFA open reading frame, used at 50 mM final concentration).
In ERAL1-FLAG cells the induction was triggered with tetracycline (1µg/ml final concentration) 4 hr after siRNA transfection. $15*10^4$ cells were seeded in six well plates in triplicates. Error bars are +/- SD.

Comparison of graphs in Figure 5.3 and 5.5 shows that there was an even lower cell number for HEK293 expressing ERAL1-FLAG in the absence of RBFA (Figure 5.5)

than in case of HEK293 expressing RBFA-FLAG in the absence of ERAL1 (Figure 5.3).

5.4 Can overexpression of RBFA protect 12S mt-rRNA from degradation in the absence of ERAL1?

In summary, no compensatory mechanism in cell growth rate was observed in the case of RBFA and ERAL1, although CLIP assay analyses showed that both proteins interact with precisely the same sequence of 12S rRNA and ERAL1 depletion causes significant decrease of 12S steady state level. In order to establish whether 12S mt-rRNA is protected by expressed RBFA-FLAG in the absence of ERAL1, two HEK293 cell lines; control and FLAG were grown under the same conditions as described in subsection 5.3.2. Western blot analysis was performed to identify whether depletion of ERAL1 and expression of RBFA-FLAG was successful. As can be seen in Figure 5.6, depletion of ERAL1 was successful in both cell lines and RBFA overexpression was also confirmed.
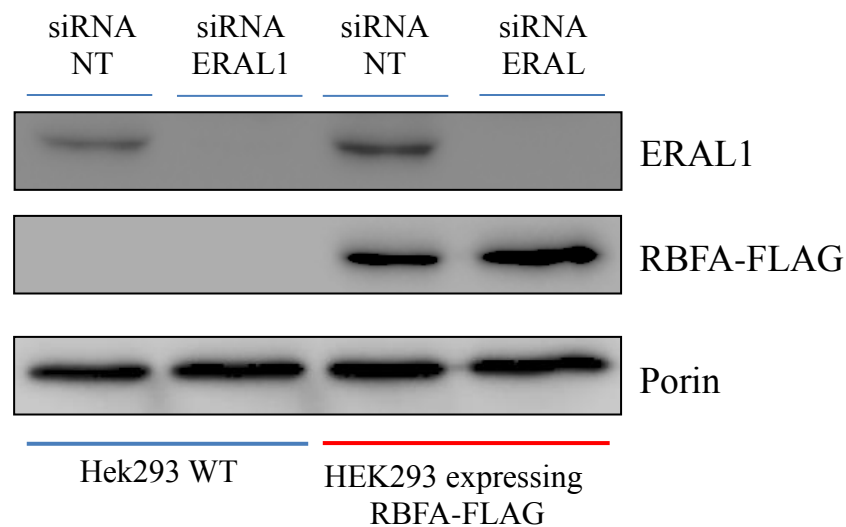
Figure 5.6. Western blot analysis of ERAL1 depletion and RBFA-FLAG induction in HEK293 cell lines. $15*10^4$ cells were seeded in six well plates in triplicates and grown for 72 hr in the presence of either si-NT or si-ERAL1 (33 mM final concentration). RBFA-FLAG was induced 4 hr after siRNA transfection. Cells from one of each triplicate were used to assess an efficiency of ERAL1 depletion and RBFA-FLAG expression. CLs (50 µg) were separated on 12% SDS-PAGE. RBFA-FLAG was targeted with antibody against FLAG extension. Antibodies for proteins indicated were detected with ChemiDoc MP Imaging System (BioRad).

RNA extracted from these cells was subjected to northern blotting. Analysis of *MTRNR1* (12S) steady state levels in the absence of ERAL1 was reduced compared to NT controls in both wild type and RBFA expressing HEK293 cells (Figure 5.7). However, loss of ERAL1 in conjuction with induction of RBFA-FLAG showed no

change in comparison with control HEK293 WT. Since 12S rRNA levels were diminished to at least the same extent with ERAL1 depletion irrespective of RBFA expression, this result allowed me to conclude that the expression of RBFA-FLAG did not protect 12S from degradation in the absence of ERAL1.
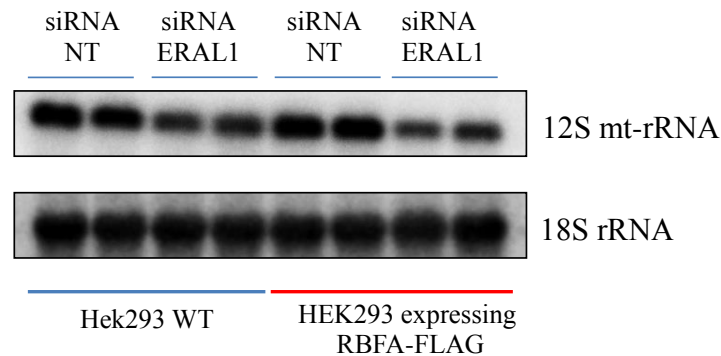
Figure 5.7. Northern blot analysis of 12S mt-rRNA (*MTRNR1*) steady state level in the absence of ERAL1 protein and expression of RBFA-FLAG. 18S rRNA was used as a loading control. Signals were detected via Storm PhosphoImager. HEK293 WT was used as a control.

The experimental data described above clearly indicate that although RBFA interacts with the same sequence of 12S mt-rRNA (helix 45) as ERAL1, their interaction time and function differs since they do not reciprocally compensate for each other if either is absent. Moreover, the inability of RBFA to protect 12S mt-rRNA in the absence of ERAL1 strongly suggests that the latter interacts first with the 3'end of 12S rRNA during late maturation events of mt-SSU. In order to clarify the role of RBFA in ribosome maturation further investigation was undertaken.

5.5 Assessment of mitoribosome assembly in RBFA depleted Hek293 cells.
The data obtained by Ricarda Richter during her PhD studies concerning RBFA showed that there were no significant changes in the steady state levels of mitochondrial ribosomal proteins in HEK293 cell line depleted of RBFA. As already mentioned, her analysis of mitoribosome assembly after three and six days depletion of RBFA in HEK293 cells, showed no significant changes (Appendix 1.3). The same outcome was seen by western blot analysis of the mitoribosomes immunoprecipitated with MRPS27-FLAG (interacting with mt-SSU). In a new experimental approach I performed immunoprecipitation of mitoribosomes with overexpressed ICT1-FLAG, which is integral to the mt-LSU. Thus, in order to investigate the influence of RBFA silencing on newly forming mitoribosomes, cells were depleted of RBFA after which ICT1-FLAG

overexpression was induced. This would allow immunoprecipitation to isolate only the mitoribosomes that were formed after depletion of RBFA had commenced. Hence, mitochondria were isolated from HEK293 cells grown in the presence of RBFA or NT siRNA for 4.5 days, where overexpression of ICT1-FLAG was induced after the first 48 hr (Figure 5.8).
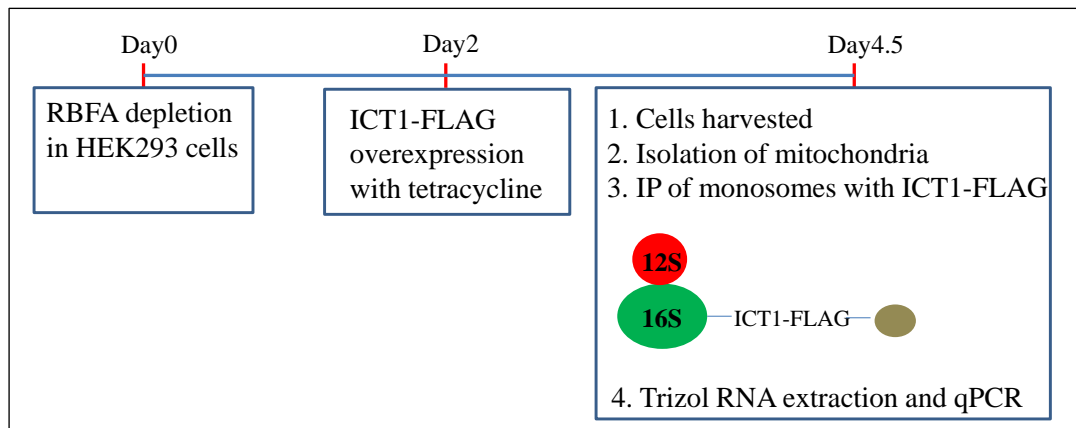
Figure 5.8. Schematic representation of experimental approach taken in order to investigate mitoribosome assembly in the absence of RBFA protein. Detailed description in the text.

Successful depletion of RBFA and overexpression of ICT1-FLAG were confirmed by western blot analysis of mitochondrial lysates (Figure 5.9A). One third of the immunoprecipitated mitoribosomes was analysed by western blot (Figure 5.9B). Proteins representing the mt-SSU (MRPS18B) and mt-LSU (MRPL3, MRPL12) of mitoribosomes were analysed and did not show any difference in their levels in the absence of RBFA compared with NT control.
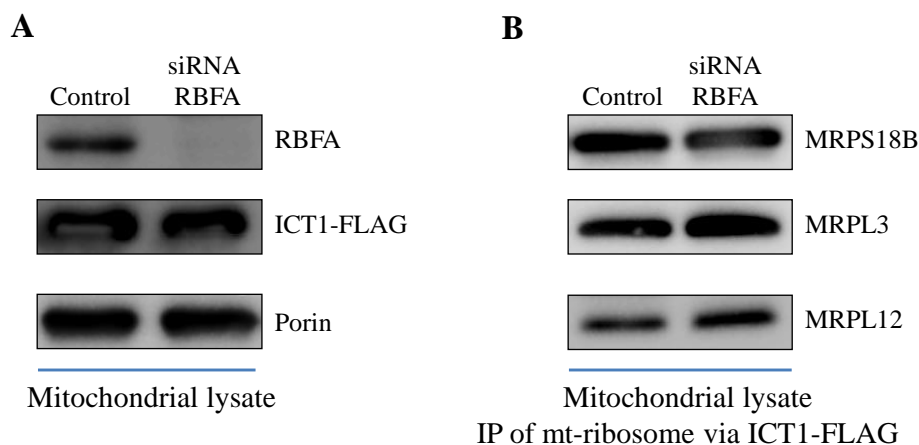
Figure 5.9. Western blot analysis of mitoribosome immunoprecipitated with ICT1-FLAG in the absence of RBFA. A. Expression of ICT1-FLAG and depletion of RBFA protein in HEK293 cell lines were confirmed by western blot analysis of mitochondrial lysates (15 µg, 12% SDS-PAGE). **B.** Western blot analysis of mitoribosome immunoprecipitated with overexpressed ICT1-FLAG in the absence of RBFA. ICT1-FLAG expression was induced for 2 days with tetracycline (1µg/ml final concentration), and RBFA depleted for 4.5 days (siRNA 50 nM final concentration). Antibodies for proteins indicated were detected with ChemiDoc MP Imaging System (BioRad). ICT1-FLAG was targeted with antibody against FLAG extension.

Total RNA, including mt-rRNAs, was extracted from two thirds of the immunoprecipitate (subsection 2.4.1), which was reverse transcribed (subsection 2.4.3) and generated cDNA was used in Real Time PCR (subsection 2.4.4). Obtained results and calculations are presented in Table 5.1. The relative mitochondrial 12S rRNA and 16S rRNA level was calculated as followed: first, the ΔC_T of control (treated with NT-siRNA) and RBFA depleted sample was calculated [$\Delta C_T = C_T$ (5S rRNA) - C_T (mt-rRNA)], then the differences between the ΔC_T of si-NT and si-RBFA were taken [$\Delta\Delta C_T = \Delta C_T$ (si-RBFA) - ΔC_T (si-NT)]. The mean $\Delta\Delta C_T$ for 12S mt-rRNA was -0.07 cycle, for 16S mt-rRNA; -0.39. Due to the exponential amplification during real time PCR, one cycle represents a difference of 50% content. The RBFA depletion did not affect 12S mt-rRNA level and 16S mt-rRNA was only decreased by 19.5%, which can be easily considered as experimental error with such a sensitive method as Real Time PCR.

Table 5.1. SYBR green Real Time PCR analysis of 12S and 16S mt-rRNA levels.

	IP of mitoribosome with ICT1-FLAG overexpressed in HEK293 cell line				
	Control (C_T)	Control ΔC_T	siRNA RBFA (C_T)	siRNA RBFA ΔC_T	$\Delta\Delta C_T$
12S	13.09 +/- 0.22	4.37	13.43 +/- 0.07	4.3	-0.07
16S	13.3 +/- 0.3	4.16	13.18 +/- 0.07	4.55	-0.39
5S rRNA	17.46 +/- 0.03		17.73 +/- 0.05		

The measurement of relative level of 12S mt-rRNA and 16S mt-rRNA were performed four times (described in subsection 2.4.4). C_T; cycle number, ΔC_T; C_T (5S rRNA) - C_T (12 or 16S mt-rRNA), $\Delta\Delta C_T$; ΔC_T (si-RBFA) - ΔC_T (si-NT).

The described experiment clearly presents that the level of 12S mt-rRNA is not affected by silencing of RBFA in HEK293 WT cells, which is in contrast to the influence of ERAL1 depletion. The data obtained by CLIP assay for RBFA described in the next subsection determined the focus of the study on 12S.

5.6 Further analysis of RBFA binding sites.

As described earlier preliminary CLIP data suggested 5S binding. Further analysis of IonTorrent data indicated clear binding to 5S rRNA. Alignment of RBFA CLIP tags to 5S rRNA sequence gave over 2000 reads. Whereas only 8 sequence reads were identified for SLIRP, 34 for MRPL12 WT and 47 for MRPL12 mutant (Table 5.2).

Table 5.2. Summary of IonTorrent sequencing results for SLIRP, RBFA and MRPL12 (in control and patient fibroblasts) CLIP reads aligned to mtDNA map and 5S rRNA.

Investigated Protein	Number of CLIP hits on mtDNA	Number of CLIP hits on **5S rRNA sequence**
SLIRP	6,010	8
RBFA	10,529	**2,407**
MRPL12 (Control)	4,487	34
MRPL12 (Patient)	4,371	47

Specificity of the interaction between RBFA and 5S rRNA is strongly supported by very low number of reads identified for two other proteins. The data show that RBFA is capable of binding two different species of rRNA. Interestingly, 5S is still widely accepted to be absent from human mitoribosomes. Preliminary evidence obtained by Ricarda Richter during her PhD studies was confirmed by CLIP data described above

indicating that RBFA associates transiently with the mt-SSU. The highest number of CLIP hits on 12S mt-rRNA was identified as binding at the 3' terminal stem loop that contains two dimethylated adenines.

The possibility of RBFA and 5S rRNA involvement in the process of dimethylation was therefore considered. The secondary structure of 5S rRNA shares similarity with known guide RNA particles taking part in introduction of post-transcriptional modifications of cytosolic rRNAs (Figure 5.10). According to the published data over 100 different analogues of the four standard ribonucleotides have been described involving modifications such as pseudouridinylation, alterations to the bases including methylation, deamination, reduction or thiolation (Chow et al., 2007). Human, cytosolic ribosomes contain over 200 modified nucleotides (Kiss, 2001) whereas *E. coli* ribosomes have only 36 identified modifications (Chow et al., 2007). Bacterial rRNA modifications are introduced by site-specific, single-protein enzymes recognising unique structures or RNA sequences. The high number of RNA modifications in eukaryotic cells is introduced by RNA-protein complexes. The noncoding RNA component of these complexes called snoRNAs is usually 60-300 nt long that guide the site specific modification of a target RNA.
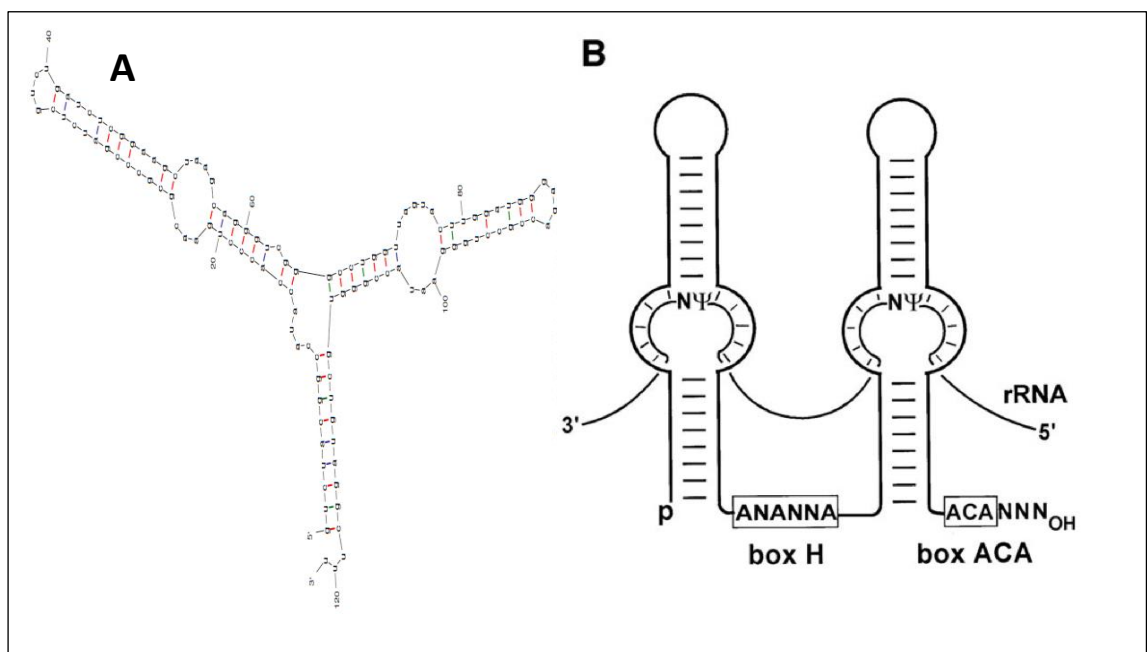
Figure 5.10. **Secondary structure of 5S rRNA resembles this of snoRNA guiding isomerization of uridine to pseudouridine (Ψ).** Secondary structure of **A.** 5S rRNA. **B.** H/ACA box snoRNA acting as a guide for pseudouridylation, taken from Kiss, 2001.

Obtaining two distinct pools of CLIP tags did not indicate if RBFA binds both RNA species at the same time. In recent years CRAC technique originating from CLIP assay

was used in studies concerning protein-snoRNA interactions in yeast. Briefly, following UV treatment, RNA-protein complexes are affinity purified under highly-denaturing conditions. Obtained RNA species are amplified after linker ligation and cDNA synthesis. PCR fragments are then sequenced on an illumina sequencing platform and identified bioinformatically. It was identified that the deep-sequencing reads can contain chimeric sequences (less than 0.5% of total) comprised of two RNA species (snoRNA and rRNA fragment, which undergoes modification) (Kudla et al., 2011). This can occur if two RNAs are aligned in very close proximity *in vivo,* which allows creation of a covalent bond between nucleotides caused by UV treatment or are ligated during the 3' linker addition step on the beads (material and methods; subsection 2.6.1, Travis et al., 2014). Therefore the CLIP data was interrogated using unix command-line text processing utilities by Dr. M. Bashton to identify if any of the 12S tags also contained 5S sequences.

Theoretical alignment of both rRNA species was postulated and this is presented in Figure 5.11. Interrogation of the 12S tags identified a chimeric 12S/5S rRNA sequence in the CLIP reads (Table 5.3), which strongly suggested simultaneous interaction of human RBFA with both ribosomal RNA species.
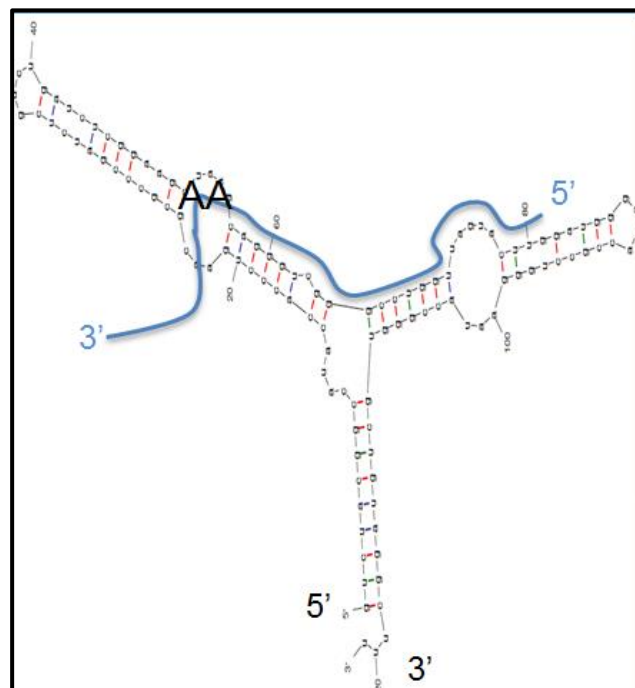
Figure 5.11. Predicted alignment of 5S rRNA with 12S mt-rRNA 3' terminal stem loop located in the helix 45 (blue). Theoretical alignment of 12S terminus with 5S was structured on the base of H/ACA box snoRNA acting as a guide for pseudouridylation (Figure 5.10 B).

The identification of any chimeric 12S/5S sequence strongly suggests that a fraction of 5S rRNA is found in human mitochondria and that it interacts at some stage with mitoribosomes even if only transiently. In order to try to obtain a higher number of chimeric sequences CLIP assay was repeated and the results are in the process of being analysed.

Table 5.3. Chimeric sequence of 5S rRNA and 12S mt-rRNA 3'end identified in Ion Torrent reads pool.

	Sequence
5S rRNA	5'-GTCTACGGCCATACCACCCTGAACGCGCCCGATCTCGTCT GATCTCGGAAGCTAAGCAGGGTC**GGGCCTGGTTAGTACTTGG ATGGGAGAC**CGCCTGGGAATACCGGGTGCTGTAGGCTTT-3'
12S mt-rRNA stem loop sequence 3'	5'-***GAGAC****AAGTCGTAACATGGTAAGTGTACTGGA**AA**GTGCACTT GGAC*GAACAAAG-3'
IonTorrent read	5'-GGG**GGGCCTGGTTAGTACTTGGATGG***GAGAC*AAGTCGTAA CATGGTAAGTGTACTGGA**AA**GTGCACTTGGAC-3'

The table contains 5S rRNA, 3'end 12S mt-rRNA and IonTorrent read sequence, where nucleotides highlighted in green are part of 5S rRNA and underlined nucleotides originate from 3'end 12S mt-rRNA. ***AA; dimethylated adenines.***

Because, the identified chimeric sequence contains 12S rRNA fragment enclosing two modified dimethylated adenines (Table 5.3), further investigation aimed to establish if RBFA influences this modification in human mitochondria. Again it is important to emphasize, that there is no experimental, published result showing activity of TFB1M *in vitro*. All of the available data describing the function of this enzyme originates from extrapolation in studies where the protein is depleted (Metodiev et al., 2009; organ specific depletion in mice) or methyltransferase-deficient form of TFB1M was overexpressed in HeLa cells (Cotney et al., 2009). It is highly probable that in order to perform the methylation *in vitro* TFB1M requires other factors.

5.7 The effect of RBFA depletion on 12S mt-rRNA post-transcriptional modifications.

In pursuance of the possible involvement of RBFA in the dimethylation process of the two adjacent adenosines in helix 45, a primer extension assay was used (protocol in subsection 2.7). Briefly, as depicted in Figure 5.12, a radiolabelled primer corresponding to the terminal nucleotides of the 12S mt-rRNA sequence was annealed to the extracted RNA. The 3' end of the primer sequence was at a distance of four

nucleotides to the first of the N6-dimethylated adenines. Elongation was allowed to proceed in a 5' to 3' direction. The first stop of the elongation process is at the point of modification, and is enforced by the use of low amounts of M-MLV reverse transcriptase and low concentration of dNTPs. The second stop (read-through) in this assay is caused by the lack of dGTP in the RT dNTPs mix, which prevents any extension past the first C in the 12S sequence (Figure 5.12; C in bold).
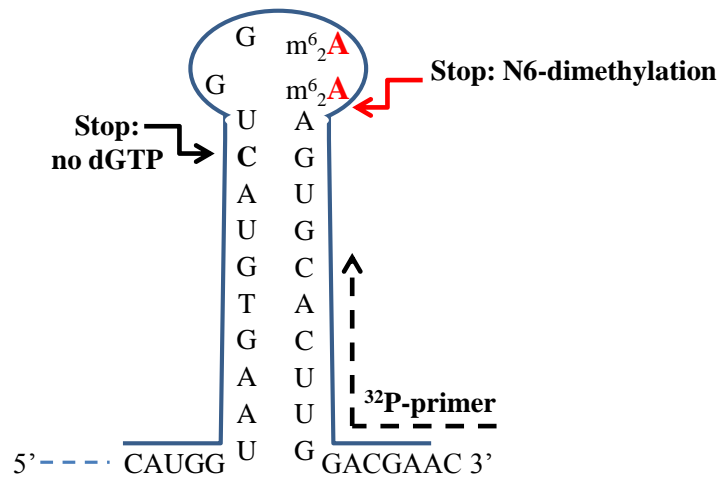
Figure 5.12. Schematic representation of primer extension assay to detect dimethylation of the AA in helix 45 of the 12S mt-rRNA 3' stem loop.

The primer extension assay used total RNA extracted from HEK293 cells, which allowed examination of the total pool of 12S mt-rRNA. Three independent RNA samples were obtained from cells grown for 7 days in specific conditions allowing investigation of nascent 12S methylation levels in the absence of RBFA. The schematic for cell treatment is presented in Figure 5.13B, where Sample 1 represents untreated control cells. Sample 2 and Sample 3 were grown in the presence of ERAL1 siRNA for the first 3 days in order to deplete the level of 12S by ~ 50%. Next, the medium containing ERAL1 siRNA was removed in order to allow cells to start to recover and
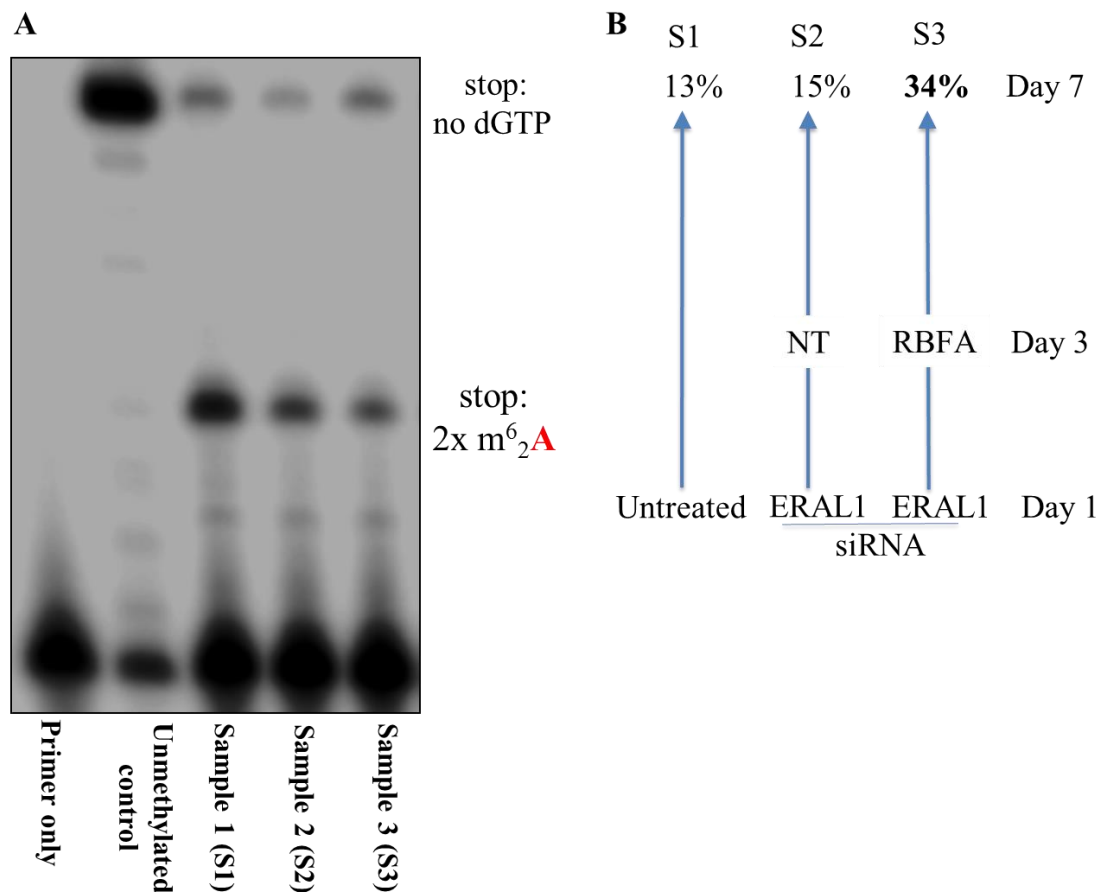
Figure 5.13. Primer extension analysis of dimethylation levels of total 12S mt-rRNA in the absence of RBFA in HEK293 cell line. **A**. Primer extension assays were performed with total RNA (4 µg) from each sample. Extension products were separated by electrophoresis in 10% urea, sequencing gel, at 50W. Extension was also performed on *in vitro* synthesised unmethylated control. Signals were detected with Typhoon FLA9000 and analysed by Image-Quant software (Molecular Dynamics, GE Healthcare). **B**. Schematic representation of the 7 day experimental approach undertaken to investigate methylation of helix 45 in the absence of RBFA. Cells were untreated (control, S1), grown for the first 3 days in the presence of ERAL1 siRNA and for further 4 days with NT siRNA (S2), or treated with ERAL1 siRNA for 3 days, but then followed by 4 days silencing of RBFA (S3). The quantitation of the data from panel A is given above each treatment protocol. The percentage represents the unmethylated population of 12S rRNA and is calculated from the read-through (stop at C) as a fraction of the total signal (stop at modification + read-through).

produce a new pool of 12S rRNA during the remaining 4 days in the presence of either NT siRNA (Sample 2: control), or RBFA targeting siRNA (Sample 3). If RBFA plays a role in the modification process then it would be expected that there would be a difference between the modification levels between NT and RBFA depleted cells. The untreated control (Sample 1) displayed 12 % unmethylated 12S rRNA, with a similar value of 15% in the control grown first in the presence of ERAL1 then NT siRNA (Sample 2), whilst the RBFA depleted sample (S3) had a 2-3 fold higher level of read-through at 34%. The latter clearly presented a stronger relative signal for the read-through, which illustrated a two to three fold increase in the unmodified pool of 12S

helix 45 in RBFA depleted cells. This interesting observation reinforced my CLIP data that showed a direct interaction of RBFA with the 3' terminal stem-loop of 12S. These data taken together implicate this protein in the methylation process of the two highly conserved neighbouring adenines in helix 45. Further investigation aimed to establish the level of 12S rRNA methylation incorporated into A) mt-SSU, and B) fully assembled mitoribosome, in the absence of RBFA (Figure 5.14).

A

IP of 12S mt-rRNA of SSU with **MRPS27-FLAG**

B

IP of 12S mt-rRNA of SSU with **ICT1-FLAG**
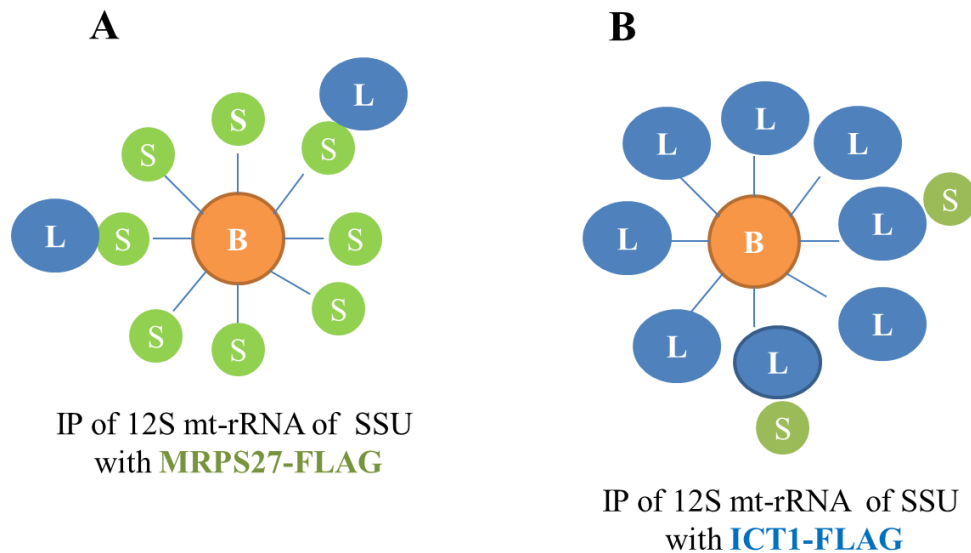
Figure 5.14. Immunoprecipitation of the 12S rRNA via MRPS27-FLAG or ICT1-FLAG. Schematic representation of 12S mt-rRNA of the mt-SSU immunoprecipitated via **A**. MRPS27-FLAG associated with mt-SSU, **B**. ICT1- FLAG incorporated into mt-LSU. B, beads; L, mt-LSU; S, mt-SSU.

The 12S mt-rRNA to be examined was extracted from the eluate of either mt-SSU immunoprecipitated by MRPS27-FLAG, or complete mitoribosomes immunoprecipitated by ICT1-FLAG from HEK293 cells. Both cell lines were grown for 5.5 days in the presence of either NT or RBFA si-RNA. The successful overexpression of FLAG tagged proteins and depletion of RBFA was confirmed by western analysis and is presented in Figure 5.15.
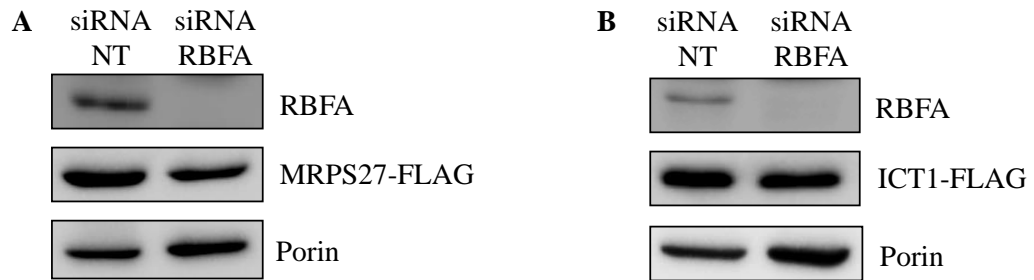
Figure 5.15. Confirmation of the mt-SSU and LSU proteins over-expression and RBFA depletion by western blot analysis. HEK293 were grown in the presence of NT or RBFA siRNA for 5.5 days (transfection was repeated after 72 hr) followed by induction to express either MRPS27-FLAG or ICT1-FLAG (induction via tetracycline; 1µg/ml). Protein samples (50 µg) were separated by 12% SDS-PAGE and western analysis performed with antibodies as indicated; MRPS27-FLAG cells (A) and ICT1-FLAG cells (B).

MRPS27-FLAG is a protein component of the mt-SSU, whilst ICT1-FLAG is an integral protein of mt-LSU. Any primer extension signal detected from the immunoprecipitation via ICT1 must represent mt-SSU associated with the mt-LSU in the form of an assembled mitoribosome. Thus the results of primer extension assay for 12S mt-rRNA represent 'free' small subunit (if immunoprecipitation is via MRPS27) or incorporated into a fully assembled 55S particle (if immunoprecipitation is via ICT1) (Figure 5.16A). Quantification of the percentage un/dimethylated helix 45 (2x m^6_2A) is presented graphically in panel B in the absence of RBFA versus control (each immunoprecipitation was performed at least twice).
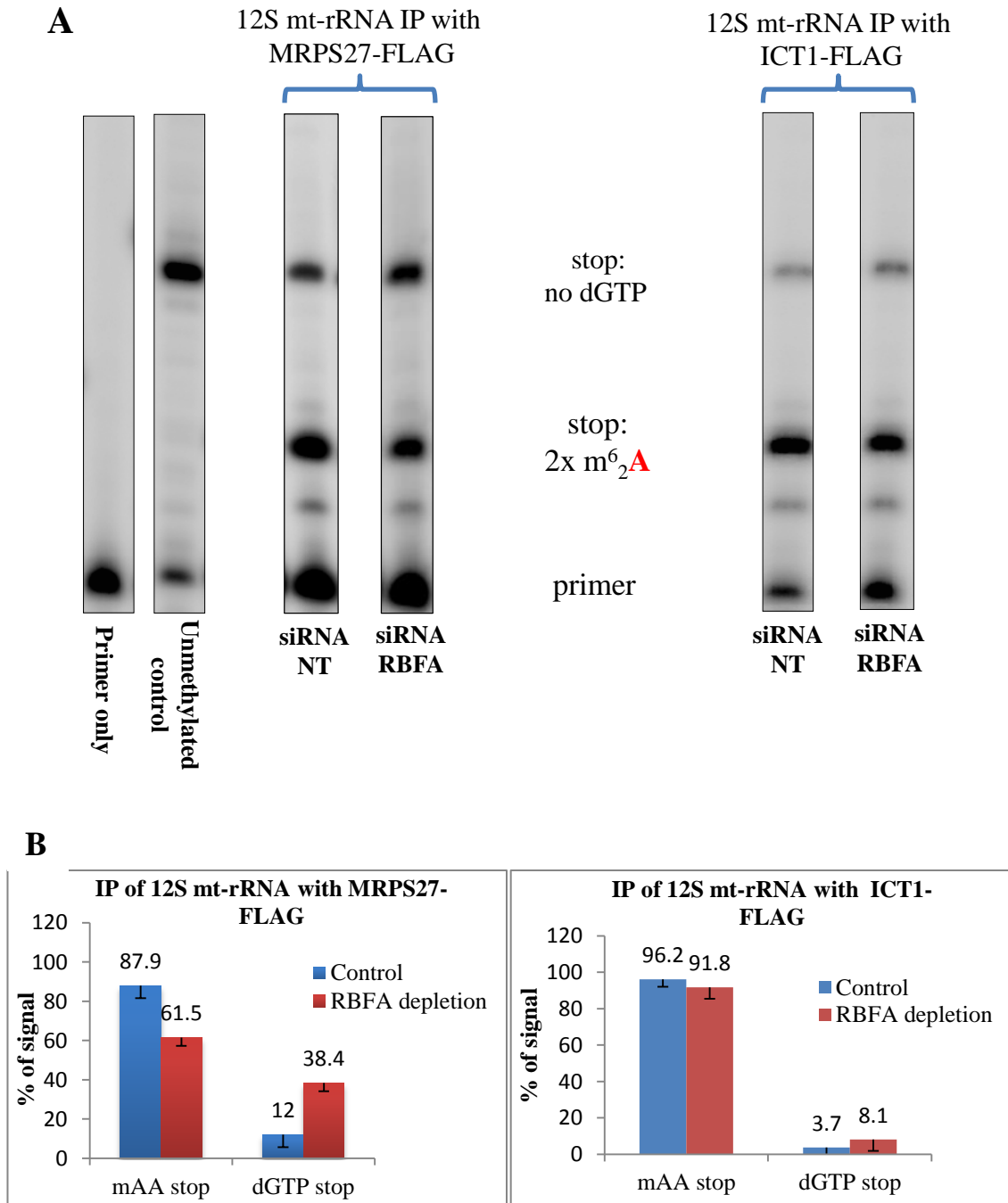
Figure 5.16. Primer extension analysis of 12S mt-rRNA to detect methylation levels in 28S and 55S particles in the absence of RBFA protein in HEK293 cell lines. **A**. HEK293 cells overexpressing MRPS27-FLAG or ICT1-FLAG were grown for 5.5 days in a presence of NT or RBFA siRNA. Harvested cells were lysed and equal amounts of proteins were independently incubated with α-FLAG–beads. After incubation 800 ng of Trizol extracted RNA from each sample was analysed by primer extension assays. Products were separated by 10% urea sequencing SDS PAGE, at 50W. In vitro synthesised unmethylated RNA was used as a control. Detection of signal was performed with Typhoon FLA9000 and analysed by Image-Quant software (Molecular Dynamics, GE Healthcare). **B**. Densitometric data from A is presented graphically with percentage of the signals quantified for the read-through (stop at C) and for the stop at a dimethylation site (A_{936}, A_{937}) for NT control and RBFA depleted cells in each cell line.

Strikingly, there was a distinct difference between the percentage of the read-through in 12S mt-rRNA immunoprecipitated from either the mt-SSU or the fully assembled mitoribosome. The read-through value obtained via MRPS27-FLAG immunoprecipitation is over three times higher in the absence of RBFA (38.4%) than in control sample (12%) obtained from cells transfected with NT si-RNA. This result suggests that silencing of RBFA decreases dimethylation level at the 3'end of 12S, where a lower percentage of adenines is modified, which allows M-MLV enzyme to proceed the extension reaction until the enforced stop caused by a lack of dGTP (read-through signal). In contrast, the signal of the read-through for 12S mt-rRNA obtained from immunoprecipitation of the complete monosome via ICT1-FLAG in the absence of RBFA presents only 8.1% of the total signal (which is the sum of the methylation stop and read-through) compared with NT control (3.7%). In summary, the majority of the 12S mt-rRNA incorporated into 55S mitoribosomes contains modified A_{936}, A_{937}, even in the absence of RBFA. Whereas, 26.4% more of 12S immunoprecipitated via MRPS27-FLAG lack this modification in cells depleted of RBFA in comparison to control. The latter immunoprecipitation performed through small subunit of ribosome harbours free 28S and mitoribosomes. The immunoprecipitation via ICT1-FLAG gathers free large subunits (39S) and mitoribosomes, which means that all 12S obtained in this experiment, originates exclusively from fully assembled 55S.

Primer extension assay clearly show that depletion of RBFA reduces the level of dimethylated adenines, but still 61.5% of analysed 12S rRNA is modified. This could partially be due to remaining matured mt-SSUs produced prior to RBFA depletion. Moreover, since RBFA binds not only 12S but also 5S rRNA as chimeric sequences of 12S/5S were identified by CLIP suggesting interaction of RBFA with both RNA species, one could assume that the methylation process requires all three factors for the highest efficiency. Since, 5S rRNA is only 120 nt it could play a function as a guide RNA in the dimethylation reaction of adjacent adenosines at 3'end of 12S mt-rRNA, with RBFA playing a role of a factor enabling optimal alignment of both RNAs for the methyltransferase. This exciting possibility will be further investigated in *in vitro* reactions containing unmethylated12S rRNA 3'end of 53 nt length, RBFA, 5S rRNA, and TFB1M.

5.8. The level of methylation at the 3' terminus of 12S mt-rRNA when bound with RBFA-FLAG or ERAL1-FLAG.

As previous experiment strongly suggest involvement of RBFA in the methylation process of 12S helix 45 and as ERAL1 also interacts with this sequence further experiments were performed to establish the level of methylation when 12S is immunoprecipitated with either RBFA or ERAL1. Summarizing, the two cell lines were grown with tetracycline for 72 hr to overexpress RBFA-FLAG or ERAL1-FLAG. The 12S mt-rRNA to be examined was Trizol extracted from the pool of either mt-SSU immunoprecipitated by RBFA-FLAG, or ERAL1-FLAG and the primer extension assay performed (Figure 5.17).
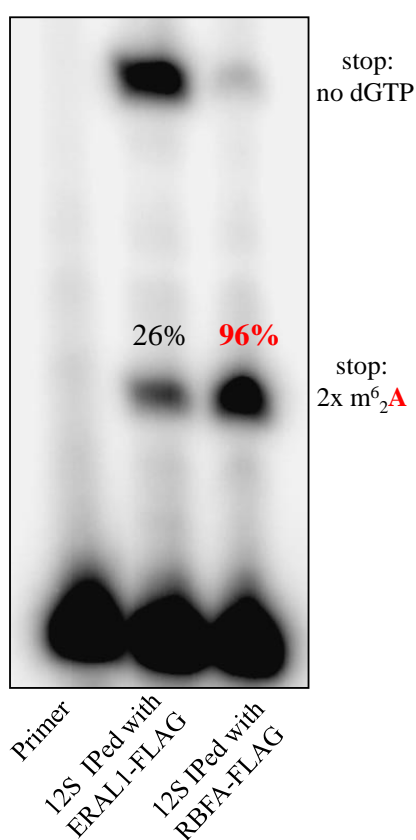
Figure 5.17. Primer extension analysis of 12S mt-rRNA to detect methylation levels in 28S immunoprecipitated with overexpressed ERAL1-FLAG or RBFA-FLAG. RBFA-FLAG or ERAL1-FLAG cell lysates were independently incubated with FLAG–beads. After incubation, 500 ng of Trizol extracted RNA from each sample was analysed by primer extension assay. Products were separated by 10% urea sequencing SDS PAGE, at 50W. Detection of signal was performed with Typhoon FLA9000 and analysed by Image-Quant software (Molecular Dynamics, GE Healthcare). The percentage of methylated 12S pool interacting with RBFA-FLAG or ERAL1-FLAG is presented above the bands.

The level of methylation immunoprecipitated with RBFA-FLAG was 96% in contrast to just 26% of modified species in the ERAL1-FLAG total pool.

This striking difference enabled to establish the order of RBFA and ERAL1 interaction with helix 45 of 12S mt-rRNA. As ERAL1-FLAG immunoprecipitated mostly unmodified 12S (74%) and previous experiment clearly demonstrated that in HEK293 cells most of the 12S is methylated at the 3' terminus (~88%) then this protein clearly interacts with helix 45 before RBFA takes over this location to facilitate methylation by direct interaction. It has to be emphasised that 26% of 12S bound by ERAL1-FLAG is modified at the 3' terminus. This result suggests that ERAL1 is also able to assist TFB1M during methylation process. As 4 days depletion of RBFA causes 2-3 fold decrease in methylated 12S, but still more than 60% remains methylated (Figure 5.13) with no decrease in the steady state level (Ricarda Richter thesis) it cannot be excluded that ERAL1 is able to present helix 45 to TFB1M although with lower efficacy so the methylation still occurs but with lower rate.

5.8 Discussion.

The inhibitory effect of RBFA depletion on the HEK293 rate growth was the only indication of an important function in human mitochondria played by this protein in the doctoral studies of Ricarda Richter. Interestingly, none of the thorough analysis performed by Ricarda Richter, aiming to establish the function of RBFA showed significant changes in the assembly of the mitoribosomes in RBFA depleted cells. Furthermore, no decline was observed in mitochondrial RNA species or mtDNA, with only marginal decrease of mitochondrial translation rate in cells grown in the presence of RBFA si-RNA for 6 days.

The experimental investigation that I have undertaken in this study was driven by the data obtained from the CLIP assay (Figure 5.1). This clearly showed that RBFA interacts directly with 12S mt-rRNA. The highest number of hits was identified for the stem loop at the 3' terminus of 12S (helix 45). The same region had been already found by my CLIP analysis to be binding site of another mt-SSU protein ERAL1, (Dennerlein et al., 2010). Although sharing the site of interaction, these two proteins do not compensate for each other when one is depleted in human cells (subsection 5.3). This was evident as overexpressed RBFA-FLAG did not protect nascent 12S mt-rRNA from degradation in the absence of ERAL1. This demonstrated separate functions for RBFA and ERAL1 and steps of the mt-SSU maturation process in which these two factors interact with 12S mt-rRNA. Clearly, human RBFA with its expanded mass in comparison to bacterial RbfA, did not lose the ability to bind directly mt-rRNA. Also its function can not be compensated by ERAL1. Although it has to be remembered that

even eubacterial EraL1 can only rescue *E. coli* cells lacking RbfA in higher temperatures (Inoue et al., 2006).The primer extension assay performed on total RNA extracted from RBFA depleted HEK293 cells indicates a 2-3 fold decrease of modified 12S at the 3' terminus (Figure 5.13). The outcome of this experiment demonstrates direct evidence of RBFA being an accessory protein in the maturation of 28S. Further investigation where 12S mt-rRNA was obtained from cells depleted of RBFA for 5.5 days and immunoprecipitated with the small subunit protein (MRPS27-FLAG) or large subunit (ICT1-FLAG) gave further insight into the biogenesis of mt-ribosome (Figure 5.14). First, analysis of 12S incorporated into mt-SSU presented as a 3-fold decrease in the level of methylation of helix45, reinforcing previous results. Interestingly, the majority of 12S incorporated into monosomes and immunoprecipitated with ICT1-FLAG despite 5.5 days depletion of RBFA, contained just 8.1% unmethylated A_{936}, A_{937} versus 3.7% in control samples. This result demonstrates that monosomes contain almost exclusively methylated 12S mt-rRNA, possibly recycling already fully matured 28S particles when cells are depleted of RBFA.

The analysis of CLIP reads for RBFA revealed an astonishing and unexpected interaction of this protein with 5S rRNA. Over 2000 hits were identified as 5S sequences, with chimeric 5S/12S sequence generating direct evidence of simultaneous interaction of RBFA with these two RNA particles, which could only occur in the mitochondrial matrix. It has to be highlighted that chimeric sequences are very rare and even in the large scale sequencing techniques generating millions of reads compared to the hundreds of thousands by IonTorrent detected only ~0.5%. Therefore, identifying the presence of only a few 5S/12S chimerae suggests that the interaction between 5S and 12S rRNA species is real. Moreover, it strongly suggests direct interaction of 5S with mt-SSU. The character of this interaction still needs to be elucidated. Since, involvement of RBFA in the process of dimethylation of two A_{936}, A_{937} in the stem loop of 12S helix 45 has been shown, it is tempting to propose that the 5S rRNA interaction with the ribosomal RNA of the mt-SSU represents a novel phenomenon in mammalian mitoribosome biogenesis, whereby the 5S molecule plays the role of a guide RNA templating helix 45 for methyltransferase activity, presumably by TFB1M. Simultaneous interaction of RBFA with both RNA species could potentially facilitate their optimal conformation for the methyltransferase to act upon. The two modified adenines in helix 45 at the 3'end of the 12S rRNA have been postulated to present a check-point in human mitoribosome biogenesis that can influence the cell homeostasis. Overexpression in HeLa cells of TFB1M, the methyltransferase that is reported as

responsible for this modification causes hypermethylation of A_{936}, A_{937}, causing faulty mitochondrial biogenesis without any effect on mtDNA level, transcription or translation. It does however, predispose cells to stress-related cell death (Cotney et al., 2009). Interestingly, hypermethylation is also characteristic for the cells with the deafness-associated A1555G mtDNA mutation, despite unaffected TFB1M level (Cotney et al., 2009). The increase in methylation was postulated to be caused by structural changes in the 12S mt-rRNA triggered by the mutation located in close proximity to A_{936}, A_{937}, which might allow enhanced accessibility for TFB1M. Therefore, it is tempting to speculate that this conserved modification requires a very specific team of factors and most of all has to be very tightly regulated since over-expression of methyltransferase-deficient form of TFB1M was reported to cause decreased steady state levels of 12S rRNA, decreased mitochondrial translation and cell growth inhibition in HeLa cells (Cotney et al., 2009) and its knock-out in mice was reported to be embryonic lethal (Metodiev et al., 2009). This modification may present the "all-clear" signal for the small ribosomal subunit to assemble into a mitoribosome and potentially represents a signal for the cell, which influences its overall activity. Therefore, the involvement of the 5S rRNA in methylation process linking cytosolic and mitochondrial ribosomes biogenesis is more than understandable. The 5S rRNA seems to be the perfect candidate for the job. It is enough small to undertake the role of a guide RNA and it is already postulated to influence p53 protein, which is the regulator of cell proliferation and guardian of cellular homeostasis (Madan et al., 2011).

In has been recently published that in cases of impaired cytosolic ribosomal biogenesis, 5S RNP (ribonucleoprotein) complex consisting of 5S rRNA, RPL5 and RPL11 interacts and inhibits MDM2 (mouse double minute 2 homologue; inhibits p53 activity through proteasome-mediated degradation) thereby activating p53 protein (Sloan et al., 2013). Moreover, p53 has been reported to positively regulate OXPHOS in mice and human cancer cell lines via transcriptional upregulation of cytochrome *c* oxidase 2 (Matoba et al., 2006). Alternatively it inhibits, glycolysis (Bensaad et al., 2006). These reported findings are of enormous importance for mitochondrial research as they show emerging pathways of bidirectional communication between mitochondria and the rest of the cell. The preliminary data obtained during this study, which suggests involvement of 5S rRNA in mitoribosomes biogenesis via conserved modification of helix 45, may be a part of a novel signalling pathway connecting mitochondrial ribosomal biogenesis with energetic requirements of the cell. Since RBFA protein has been shown to affect the level of this modification it can be easily postulated as one of

the ribosomal maturation factors with a role far beyond the double boundaries of mitochondrial membranes, possibly influencing metabolic status of the cell. Moreover, data presented in this chapter very strongly indicate that this astonishing protein has a very specific partner 5S rRNA, the presence of which in human mitochondria was controversial and its possible mitochondrial function is unknown.

The final experiment described in this chapter unveils the order of RBFA and ERAL1 interaction with 12S mt-rRNA (helix 45). A striking difference in the level of dimethylation of A_{936}, A_{937} in helix 45 was observed, when 12S was immunoprecipitated with RBFA-FLAG compared to ERAL1-FLAG (Figure 5.17). The RBFA protein binds almost exclusively modified 12S (96%) whereas ERAL1 interact with mostly unmodified helix 45 (74%). This final result is strongly supported with the outcome of the northern blot presented in the subsection 5.7 indicating that expressed RBFA-FLAG can not protect 12S mt-rRNA against degradation in the absence of ERAL1 in HEK293 cells. Taken together these data suggest that ERAL1 interacts first with the 3'end of 12S rRNA followed by RBFA binding and methylatrasnferase activity during late maturation events of mt-SSU.

In summary, the data specify that although RBFA interacts with the same sequence of 12S mt-rRNA (helix 45) as ERAL1, their interaction time and function differs since they do not compensate for each others absence. Furthermore, RBFA is unable to protect 12S mt-rRNA in the absence of ERAL1 and is bound only to methylated 12S whereas ERAL1 mostly interacts with unmodified species.

Using the data it is possible to design a model of late stage maturation of 12S mt-rRNA involving helix 45, where the methyl groups are introduced by TFB1M but the optimal conditions for this enzymatic process are delivered by the presence of RBFA protein potentially interacting with 5S rRNA and helix 45. Whereas ERAL1 guards unmethylated 12S from transcription until the process of maturation when the three factors mentioned above take over and act upon the 3' terminal stem loop, followed by assembly of mt-SSU and mt-LSU into the mitoribosome (Figure 5.18). At this point it has to be emphasised that ERAL1 does not bind exclusively to unmodified helix 45 as primer extension assay result present that ¼ of the total pool of 12S interacting with ERAL1 is modified (Figure 5.17). The MRPS27-FLAG immunoprecipitation following RBFA depletion showed a substantial pool of modified
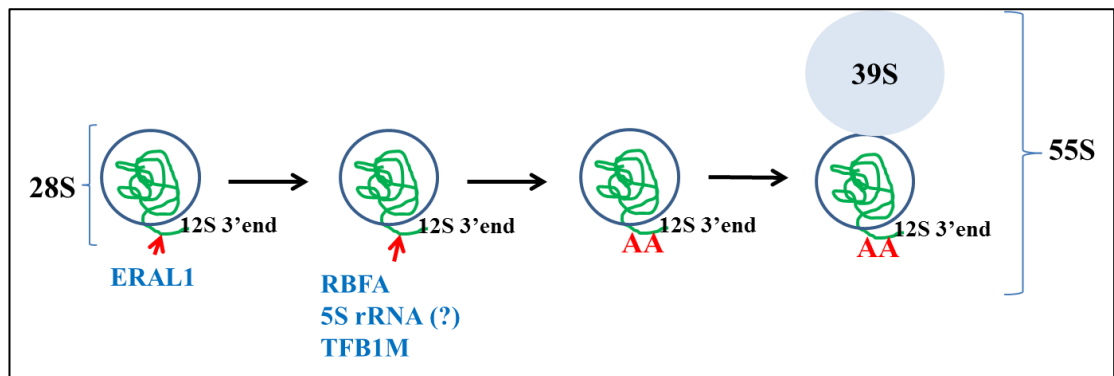
Figure 5.18. Theoretical final steps of 28S maturation involving ERAL1, RBFA, 5S rRNA and TFB1M.

12S mt-rRNA (61%) suggesting that either ERAL1 also has the ability to present helix 45 to the methyl transferase or that the enzyme can work but less efficiently before ERAL1 dissociates or on unchaperoned helix 45. Although this pathway is not optimal in 28S biogenesis, since just 26% of ERAL1-bound 12S mt-rRNA was modified, it could potentially sustain the source of newly formed and methylated at helix 45 12S. It is highly possible that the dimethylation of A_{936}, A_{937} is crucial in the biogenesis of human mt-ribosome as evolutionary changes did not erase it and there appears to be more than one pathway to introduce it. As ERAL1 cannot rescue HEK293 cells depleted of RBFA (Figure 5.5) it can be postulated that the latter, potentially with 5S rRNA, provides optimal conditions for TFB1M to dimethylate A_{936}, A_{937} in the helix 45 and/ or RBFA has other functions in the 28S assembly process. Three other binding sites mapped to 12S mt-RNA suggest this possibility (Figure 5.1). The first interaction site harbouring ~160 reads at position 904-918nt (1) corresponds to helix 18 of 12S mt-rRNA, second ~ 1300 reads at position 1181-1211 nt (2) is located in helices 28, 29 and 30, third ~ 1000 reads at position 1292-1312 nt (3) maps to helices 35 and 38 (Figure 5.1) according to the current secondary structure of 12S (Kaushal et al., 2014). The position (1) is located in the 5' domain of the mt-SSU that forms the **body**, position (2) and (3) are located in the 3' major domain (the **head** of mt-SSU). Fourth position mapped to helix 45 with the highest number of reads identified is mapped to **3' minor domain**. Datta et al., 2007, presents number of interacting sites of eubacterial RbfA on 16S rRNA including the head, the body and 3' minor domain with contacts span helices h1, h18, h28, h29, helix 44 and 45 and to a lesser extent h30.

The binding of RbfA to 30S subunit causes displacement of helix 44 which is directly involved in mRNA decoding and tRNA binding whereas helix 45 is rotated out of the 30S platform. The X-ray crystal structure of the *Thermus thermophilus* 30S ribosomal

subunit deprived of dimethylation of two adenosines in helix 45 indicates that this modification is required for the formation of the packing interaction between helix 45 and 44 (Demirci et al., 2010). Connolly and Culver, 2013 propose that eubacterial RbfA and KsgA methylase function together in the SSU maturation process. Moreover, another recent study of pre-30S complexes in *E. coli* strains lacking RbfA or RimM proteins give new insight into the late stages of assembly intermediates. The authors propose that RbfA can act upon different parts of 16S rRNA in early and late stages of 30S assembly, coordinating optimal folding of rRNA (Clatterbuck Soper et al., 2013).

Summarizing, the data described in this chapter present a new human mitochondrial protein RBFA, which interacts with 12S mt-rRNA in a very specific location containing two modified residues almost completely conserved in phylogeny. Although this broad conservation strongly suggests an important function, over two decades of studies have not fully answered what is the exact mechanism in which the m_2^6A residues take part. As already mentioned, depletion of the methyltransferase KsgA in bacteria is dispensable at 37 C, but in mice loss of TFB1M is lethal. In general the cause for the existence of modified nucleotides is still unclear but they are mapped to functionally important regions of ribosomal RNAs and their number rises with the increased complexity of the organism (Chow et al., 2007). The methylation of two adenines at the 3'end of 12S mt-rRNA was the first confirmed modification in this molecule (Rorbach and Minczuk, 2012). Very recently another methylation site was identified (cytosine 911), introduced by methyltransferase NSUN4 (Metodiev et al., 2014).

The astonishing result of the CLIP assay indicating two rRNA species as interacting partners of RBFA, followed by identification of chimeric read containing fragments of both 12S and 5S rRNA could be the first step in deciphering the role of this modification in human mitoribosome.

The data described here represent only a prelude in the description of human RBFA function, which requires further investigation. Ongoing experiments aim to establish whether addition of 5S rRNA and RBFA enable TFB1M to dimethylate A_{936}, A_{937} in the 3' stem loop of 12S rRNA in an *in vitro* reaction. Further, the CLIP assay for RBFA has been repeated and the IonTorrent reads are being analysed in order to identify more chimeric sequences. The gel shift technique will be also used to identify whether in the absence of other factors RBFA can interact simultaneously with both 5S and 12S rRNA.

6. Final Discussion

6. Chapter 6: Final Conclusions.

My PhD project was focused mainly on two mitochondrial proteins MRPL12 and RBFA.

Preliminary investigation undertaken for SLIRP protein was not followed up due to publications from competing groups that arose during the course of my studies. I present below a summary of the main achievements and advances that my work has made in each of the designated projects.

6.1 SLIRP

The CLIP assay was performed in order to assess whether or not SLIRP (SRA stem-loop interacting RNA binding protein) was able to bind mtRNA directly (Figure 3.2). The CLIP data revealed that the predicted RRM domain in SLIRP is functional and acts to bind RNA in human mitochondria. The CLIP reads were located in 12 of the 13 mt-ORFs with the exception of *MTND6.* This result remains in agreement with now published data showing dependence of mt-mRNAs stability on SLIRP presence in human and mouse cells (Sasarman et al., 2010, Ruzzenente et al., 2011, Chujo et al., 2012). SLIRP was reported to be in high-molecular weight complexes with LRPPRC. The latter also contains RNA binding domains, 22 of which are PPR motifs. The CLIP result for SLIRP shows unequivocally that this protein interacts directly, not just via interaction with LRPPRC, with messenger RNA *in vivo* in human mitochondria.

6.2 MRPL12

MRPL12 belongs to the group of conserved mitochondrial proteins having the bacterial orthologue called L7/L12. Moreover it is assigned to a unique pool of acidic ribosomal proteins, the analogues of which are present throughout phylogeny. The unique features of these proteins are due to their dynamic character and exchange of location between ribosomal LSU and the free pool, postulated to be a regulatory mechanism of translation process in response to fluctuations in cell metabolism.

Obtaining immortalised fibroblasts from the patient with mutated form of MRPL12 allowed me to study function of this protein in human mitochondria. The point mutation causing substitution of Alanine 181 by Valine in C terminal domain of MRPL12 (Figure 4.1) caused a reduction in the steady state level to only 30% of control value (Figure 4.3) with the free pool determined as absent via the sucrose gradient fractionation of mitochondrial lysate (Figure 4.6). Furthermore, a reduced number of MRPL12

molecules per mt-LSU was observed (Figure 4.12). However, the reduction in the level of MRPL12 did not affect overall mitoribosome assembly, but a visible decline in mitochondrial translation was detected in the *in vivo* ^{35}S-metabolic labelling assay (Figure 5.7). Interestingly, the decrease in the rate of translation differentiated between polypeptides with highest decrease observed in products for COX and ATP6 subunits whilst *cyt b* was unaffected. As the steady state levels of *MTCOX1*, *MTND1* and *cyt b* transcripts were not decreased (Figure 4.9) the reduced level of MRPL12/LSU can be postulated as the main reason for mitoribosome dysfunction, although the reduction in translational efficiency for different mitochondrially encoded subunits varied. Overall, my investigation revealed that although the stoichiometry of MRPL12 mutant/LSU is affected in the patient cell line, the mitoribosomes are assembled but their efficacy is lowered. The main technique, which could be applied to further investigate MRPL12 function, is ribosome profiling. It would allow to establish whether mitoribosomes with reduced numbers of MRPL12 molecules stall on specific sequences of mt-mRNAs, which slows down the translation.

6.3. RBFA.

This protein has not yet been characterised in the literature. The studies by Ricarda Richter, during her doctoral studies in my host laboratory, demonstrated an inhibitory effect of RBFA depletion on the HEK293 rate growth and clear localisation to the mt-SSU. None of the other analyses performed clarified is the function of this protein in mitoribosome assembly. The profile of mt-SSU and mt-LSU location was not changed in sucrose gradient fractions after RBFA silencing (for 3 and 6 days in HEK293 cells; Appendix 1.3). Furthermore, no decline was observed in mitochondrial RNA species or mtDNA, with only marginal decrease of mitochondrial translation rate in cells grown in the presence of RBFA si-RNA for 6 days. My project continued with characterisation and the results presented in my thesis indicate that RBFA:

- ✓ Interacts directly with 3' terminal stem loop of 12S mt-rRNA (Figure 5.1). The same sequence as already described for ERAL1 protein, by me in my host laboratory (Dennerlein et al., 2010).
- ✓ Participates in the methylation process of two neighbouring adenines located in the 3' terminal stem loop of 12S mt-rRNA (Figure 5.13).

The primer extension assay performed for 12S mt-rRNA immunoprecipitated with MRPS27-FLAG or ICT1-FLAG (Figure 5.14) from HEK293 cell lysates where RBFA was silenced for 5.5 days indicate that:

- ✓ The level of methylation at the 3' terminus of 12S incorporated into small subunit of mitoribosome (28S) was decreased by 26%.
- ✓ The mitoribosomes (55S) contained almost exclusively 28S with methylated 12S at the 3' end, even after 5.5 days of RBFA depletion. This observation clearly indicates that fully assembled mitoribosomes favour modified 12S and are able to recycle those mt-SSU, which were assembled before RBFA depletion.

The primer extension assay applied for 12S mt-rRNA immunoprecipitated with ERAL1-FLAG or RBFA-FLAG (Figure 5.17) to investigate the order in which ERAL1 and RBFA binds to the 3' terminus of the 12S presents clearly that:

- ✓ ERAL1 binds mostly unmethylated 12S (74%)
- ✓ whereas RBFA interacts almost exclusively with 12S methylated at the 3' terminus (96%).

This experiment strongly suggests that RBFA succeeds ERAL1 binding at the 3' terminus of 12S mt-rRNA (helix 45).

Overall, the results described above assign RBFA as a new member of maturation factors of the mammalian mt-SSU.

Finally, the CLIP assay revealed that RBFA binds second rRNA species 5S rRNA (Table 5.2). Identification of chimeric CLIP reads containing both 5S and 12S rRNA fragments suggest that RBFA interacts with both RNA species simultaneously in the mitochondrial matrix. Resemblance of the 5S rRNA secondary structure to the snoRNA, which guides modifications on cytosolic rRNA led to the hypothesis of a novel function for 5S rRNA to guide methylation at the 3' terminus of mt-12S rRNA.

Further investigation aims to test this hypothesis:

- ✓ Gel shift experiments will be performed to potentially show simultaneous interaction of RBFA with 5S and 12S rRNA *in vitro*.
- ✓ In order to assess influence of 5S rRNA on the level of methylation at the terminal stem loop of 12S rRNA, siRNA silencing of 5S rRNA in HEK293 cells will be attempted followed by primer extension assays.

In conclusion, obtained data strongly assign RBFA to the group of factors responsible for maturation of the mt-SSU and mitoribosome assembly.

References

Adams, K.L., Palmer, J.D., 2003. Evolution of mitochondrial gene content: gene loss and transfer to the nucleus. Mol. Phylogenet. Evol. 29, 380–395.

Agirrezabala, X., Frank, J., 2009. Elongation in translation as a dynamic interaction among the ribosome, tRNA, and elongation factors EF-G and EF-Tu. Q. Rev. Biophys. 42, 159–200.

Agrawal, R.K., Sharma, M.R., 2012. Structural aspects of mitochondrial translational apparatus. Curr. Opin. Struct. Biol. 22, 797–803.

Alam, T.I., Kanki, T., Muta, T., Ukaji, K., Abe, Y., Nakayama, H., Takio, K., Hamasaki, N., Kang, D., 2003. Human mitochondrial DNA is packaged with TFAM. Nucleic Acids Res. 31, 1640–1645.

Ames, B.N., Shigenaga, M.K., Hagen, T.M., 1993. Oxidants, antioxidants, and the degenerative diseases of aging. Proc. Natl. Acad. Sci. U.S.A. 90, 7915–7922.

Amunts, A., Brown, A., Bai, X. -c., Llacer, J.L., Hussain, T., Emsley, P., Long, F., Murshudov, G., Scheres, S.H.W., Ramakrishnan, V., 2014. Structure of the Yeast Mitochondrial Large Ribosomal Subunit. Science 343, 1485–1489.

Anderson, S., Bankier, A.T., Barrell, B.G., De Bruijn, M.H., Coulson, A.R., Drouin, J., Eperon, I.C., Nierlich, D.P., Roe, B.A., Sanger, F., Schreier, P.H., Smith, A.J., Staden, R., Young, I.G., 1981. Sequence and organization of the human mitochondrial genome. Nature 290, 457–465.

Antonicka, H., Ostergaard, E., Sasarman, F., Weraarpachai, W., Wibrand, F., Pedersen, A.M.B., Rodenburg, R.J., Van der Knaap, M.S., Smeitink, J.A.M., Chrzanowska-Lightowlers, Z.M., Shoubridge, E.A., 2010. Mutations in C12orf65 in patients with encephalomyopathy and a mitochondrial translation defect. Am. J. Hum. Genet. 87, 115–122.

Antonicka, H., Sasarman, F., Nishimura, T., Paupe, V., Shoubridge, E.A., 2013. The mitochondrial RNA-binding protein GRSF1 localizes to RNA granules and is required for posttranscriptional mitochondrial gene expression. Cell Metab. 17, 386–398.

Asin-Cayuela, J., Gustafsson, C.M., 2007. Mitochondrial transcription and its regulation in mammalian cells. Trends in Biochemical Sciences 32, 111–117.

Barciszewska, M.Z., Szymański, M., Erdmann, V.A., Barciszewski, J., 2001. Structure and functions of 5S rRNA. Acta Biochim. Pol. 48, 191–198.

Barrientos, A., Korr, D., Barwell, K.J., Sjulsen, C., Gajewski, C.D., Manfredi, G., Ackerman, S., Tzagoloff, A., 2003. MTG1 codes for a conserved protein required for mitochondrial translation. Mol. Biol. Cell 14, 2292–2302.

Bar-Yaacov, D., Blumberg, A., Mishmar, D., 2012. Mitochondrial-nuclear co-evolution and its effects on OXPHOS activity and regulation. Biochim. Biophys. Acta 1819, 1107–1111.

Baughman, J.M., Nilsson, R., Gohil, V.M., Arlow, D.H., Gauhar, Z., Mootha, V.K., 2009. A Computational Screen for Regulators of Oxidative Phosphorylation Implicates SLIRP in Mitochondrial RNA Homeostasis. PLoS Genetics 5, e1000590.

Benard, G., Karbowski, M., 2009. Mitochondrial fusion and division: Regulation and role in cell viability. Seminars in Cell & Developmental Biology 20, 365–374.

Bensaad, K., Tsuruta, A., Selak, M.A., Vidal, M.N.C., Nakano, K., Bartrons, R., Gottlieb, E., Vousden, K.H., 2006. TIGAR, a p53-inducible regulator of glycolysis and apoptosis. Cell 126, 107–120.

Bentley, R.C., Keene, J.D., 1991. Recognition of U1 and U2 small nuclear RNAs can be altered by a 5-amino-acid segment in the U2 small nuclear ribonucleoprotein particle (snRNP) B" protein and through interactions with U2 snRNP-A' protein. Mol. Cell. Biol. 11, 1829–1839.

Berk, V., Cate, J.H., 2007. Insights into protein biosynthesis from structures of bacterial ribosomes. Current Opinion in Structural Biology 17, 302–309.

Boehringer, D., O'Farrell, H.C., Rife, J.P., Ban, N., 2012a. Structural Insights into Methyltransferase KsgA Function in 30S Ribosomal Subunit Biogenesis. Journal of Biological Chemistry 287, 10453–10459.

Boehringer, D., O'Farrell, H.C., Rife, J.P., Ban, N., 2012b. Structural Insights into Methyltransferase KsgA Function in 30S Ribosomal Subunit Biogenesis. Journal of Biological Chemistry 287, 10453–10459.

Bonawitz, N.D., Clayton, D.A., Shadel, G.S., 2006. Initiation and Beyond: Multiple Functions of the Human Mitochondrial Transcription Machinery. Molecular Cell 24, 813–825.

Borowski, L.S., Dziembowski, A., Hejnowicz, M.S., Stepien, P.P., Szczesny, R.J., 2013. Human mitochondrial RNA decay mediated by PNPase-hSuv3 complex takes place in distinct foci. Nucleic Acids Res. 41, 1223–1240.

Borowski, L.S., Szczesny, R.J., Brzezniak, L.K., Stepien, P.P., 2010. RNA turnover in human mitochondria: More questions than answers? Biochimica et Biophysica Acta (BBA) - Bioenergetics 1797, 1066–1070.

Bowmaker, M., Yang, M.Y., Yasukawa, T., Reyes, A., Jacobs, H.T., Huberman, J.A., Holt, I.J., 2003. Mammalian mitochondrial DNA replicates bidirectionally from an initiation zone. J. Biol. Chem. 278, 50961–50969.

Brot, N., Weissbach, H., 1981. Chemistry and biology of E. coli ribosomal protein L12. Mol. Cell. Biochem. 36, 47–63.

Bruni, F., Gramegna, P., Oliveira, J.M.A., Lightowlers, R.N., Chrzanowska-Lightowlers, Z.M.A., 2013. REXO2 Is an Oligoribonuclease Active in Human Mitochondria. PLoS ONE 8, e64670.

Brzezniak, L.K., Bijata, M., Szczesny, R.J., Stepien, P.P., 2011. Involvement of human ELAC2 gene product in 3' end processing of mitochondrial tRNAs. RNA Biology 8, 616–626.

Bullerwell, C.E., Gray, M.W., 2004. Evolution of the mitochondrial genome: protist connections to animals, fungi and plants. Current Opinion in Microbiology 7, 528–534.

Burd, C.G., Dreyfuss, G., 1994. Conserved structures and diversity of functions of RNA-binding proteins. Science 265, 615–621.

Bylund, G.O., Wipemo, L.C., Lundberg, L.A., Wikström, P.M., 1998. RimM and RbfA are essential for efficient processing of 16S rRNA in Escherichia coli. J. Bacteriol. 180, 73–82.

Cairns, C.A., White, R.J., 1998. p53 is a general repressor of RNA polymerase III transcription. EMBO J. 17, 3112–3123.

Cámara, Y., Asin-Cayuela, J., Park, C.B., Metodiev, M.D., Shi, Y., Ruzzenente, B., Kukat, C., Habermann, B., Wibom, R., Hultenby, K., Franz, T., Erdjument-Bromage, H., Tempst, P., Hallberg, B.M., Gustafsson, C.M., Larsson, N.-G., 2011. MTERF4 regulates translation by targeting the methyltransferase NSUN4 to the mammalian mitochondrial ribosome. Cell Metab. 13, 527–539.

Chan, D.C., 2006. Mitochondria: dynamic organelles in disease, aging, and development. Cell 125, 1241–1252.

Chatre, L., Ricchetti, M., 2013. Large heterogeneity of mitochondrial DNA transcription and initiation of replication exposed by single-cell imaging. J. Cell. Sci. 126, 914–926.

Chen, H.-W., Rainey, R.N., Balatoni, C.E., Dawson, D.W., Troke, J.J., Wasiak, S., Hong, J.S., McBride, H.M., Koehler, C.M., Teitell, M.A., French, S.W., 2006. Mammalian polynucleotide phosphorylase is an intermembrane space RNase that maintains mitochondrial homeostasis. Mol. Cell. Biol. 26, 8475–8487.

Chen, T., Damaj, B.B., Herrera, C., Lasko, P., Richard, S., 1997. Self-association of the single-KH-domain family members Sam68, GRP33, GLD-1, and Qk1: role of the KH domain. Mol. Cell. Biol. 17, 5707–5718.

Cheng, N., Mao, Y., Shi, Y., Tao, S., 2012. Coevolution in RNA Molecules Driven by Selective Constraints: Evidence from 5S rRNA. PLoS ONE 7, e44376.

Cheung, E.C.C., Joza, N., Steenaart, N.A.E., McClellan, K.A., Neuspiel, M., McNamara, S., MacLaurin, J.G., Rippstein, P., Park, D.S., Shore, G.C., McBride, H.M., Penninger, J.M., Slack, R.S., 2006. Dissociating the dual roles of apoptosis-inducing factor in maintaining mitochondrial structure and apoptosis. EMBO J. 25, 4061–4073.

Chow, C.S., Lamichhane, T.N., Mahto, S.K., 2007. Expanding the nucleotide repertoire of the ribosome with post-transcriptional modifications. ACS Chem. Biol. 2, 610–619.

Christian, B., Haque, E., Spremulli, L., 2009. Ribosome shifting or splitting: it is all up to the EF-G. Mol. Cell 35, 400–402.

Christian, B.E., Spremulli, L.L., 2010. Preferential Selection of the 5'-Terminal Start Codon on Leaderless mRNAs by Mammalian Mitochondrial Ribosomes. Journal of Biological Chemistry 285, 28379–28386.

Christian, B.E., Spremulli, L.L., 2012. Mechanism of protein biosynthesis in mammalian mitochondria. Biochimica et Biophysica Acta (BBA) - Gene Regulatory Mechanisms 1819, 1035–1054.

Chujo, T., Ohira, T., Sakaguchi, Y., Goshima, N., Nomura, N., Nagao, A., Suzuki, T., 2012. LRPPRC/SLIRP suppresses PNPase-mediated mRNA decay and promotes polyadenylation in human mitochondria. Nucleic Acids Research 40, 8033–8047.

Ciganda, M., Williams, N., 2011. Eukaryotic 5S rRNA biogenesis. Wiley Interdiscip Rev RNA 2, 523–533.

Claros, M.G., Perea, J., Shu, Y., Samatey, F.A., Popot, J.L., Jacq, C., 1995. Limitations to in vivo import of hydrophobic proteins into yeast mitochondria. The case of a cytoplasmically synthesized apocytochrome b. Eur. J. Biochem. 228, 762–771.

Clatterbuck Soper, S.F., Dator, R.P., Limbach, P.A., Woodson, S.A., 2013. In Vivo X-Ray Footprinting of Pre-30S Ribosomes Reveals Chaperone-Dependent Remodeling of Late Assembly Intermediates. Molecular Cell 52, 506–516.

Cohen, B.H., Naviaux, R.K., 2010. The clinical diagnosis of POLG disease and other mitochondrial DNA depletion disorders. Methods 51, 364–373.

Connolly, K., Culver, G., 2013. Overexpression of RbfA in the absence of the KsgA checkpoint results in impaired translation initiation: Quality control of small subunit biogenesis. Molecular Microbiology 87, 968–981.

Connolly, K., Rife, J.P., Culver, G., 2008. Mechanistic insight into the ribosome biogenesis functions of the ancient protein KsgA. Molecular Microbiology 70, 1062–1075.

Cotney, J., McKay, S.E., Shadel, G.S., 2009. Elucidation of separate, but collaborative functions of the rRNA methyltransferase-related human mitochondrial transcription factors B1 and B2 in mitochondrial biogenesis reveals new insight into maternally inherited deafness. Human Molecular Genetics 18, 2670–2682.

Cotney, J., Shadel, G.S., 2006. Evidence for an Early Gene Duplication Event in the Evolution of the Mitochondrial Transcription Factor B Family and Maintenance of rRNA Methyltransferase Activity in Human mtTFB1 and mtTFB2. Journal of Molecular Evolution 63, 707–717.

Cotney, J., Wang, Z., Shadel, G.S., 2007. Relative abundance of the human mitochondrial transcription system and distinct roles for h-mtTFB1 and h-

mtTFB2 in mitochondrial biogenesis and gene expression. Nucleic Acids Res. 35, 4042–4054.

Cox, C.J., Foster, P.G., Hirt, R.P., Harris, S.R., Embley, T.M., 2008. The archaebacterial origin of eukaryotes. Proceedings of the National Academy of Sciences 105, 20356–20361.

Dairaghi, D.J., Shadel, G.S., Clayton, D.A., 1995a. Addition of a 29 residue carboxyl-terminal tail converts a simple HMG box-containing protein into a transcriptional activator. J. Mol. Biol. 249, 11–28.

Dairaghi, D.J., Shadel, G.S., Clayton, D.A., 1995b. Human mitochondrial transcription factor A and promoter spacing integrity are required for transcription initiation. Biochim. Biophys. Acta 1271, 127–134.

Dammel, C.S., Noller, H.F., 1993. A cold-sensitive mutation in 16S rRNA provides evidence for helical switching in ribosome assembly. Genes Dev. 7, 660–670.

Dammel, C.S., Noller, H.F., 1995. Suppression of a cold-sensitive mutation in 16S rRNA by overexpression of a novel ribosome-binding factor, RbfA. Genes Dev. 9, 626–637.

Datta, K., Fuentes, J.L., Maddock, J.R., 2005. The yeast GTPase Mtg2p is required for mitochondrial translation and partially suppresses an rRNA methyltransferase mutant, mrm2. Mol. Biol. Cell 16, 954–963.

Datta, P.P., Wilson, D.N., Kawazoe, M., Swami, N.K., Kaminishi, T., Sharma, M.R., Booth, T.M., Takemoto, C., Fucini, P., Yokoyama, S., Agrawal, R.K., 2007. Structural aspects of RbfA action during small ribosomal subunit assembly. Mol. Cell 28, 434–445.

Dawson, V.L., Dawson, T.M., 2004. Deadly conversations: nuclear-mitochondrial cross-talk. J. Bioenerg. Biomembr. 36, 287–294.

Demirci, H., Murphy, F., 4th, Belardinelli, R., Kelley, A.C., Ramakrishnan, V., Gregory, S.T., Dahlberg, A.E., Jogl, G., 2010. Modification of 16S ribosomal RNA by the KsgA methyltransferase restructures the 30S subunit to optimize ribosome function. RNA 16, 2319–2324.

Dennerlein, S., Rozanska, A., Wydro, M., Chrzanowska‑Lightowlers, Z.M.A., Lightowlers, R.N., 2010. Human ERAL1 is a mitochondrial RNA chaperone involved in the assembly of the 28S small mitochondrial ribosomal subunit. Biochemical Journal 430, 551–558.

Deroo, S., Hyung, S.-J., Marcoux, J., Gordiyenko, Y., Koripella, R.K., Sanyal, S., Robinson, C.V., 2012. Mechanism and rates of exchange of L7/L12 between ribosomes and the effects of binding EF-G. ACS Chem. Biol. 7, 1120–1127.

Desai, P.M., Rife, J.P., 2006. The adenosine dimethyltransferase KsgA recognizes a specific conformational state of the 30S ribosomal subunit. Arch. Biochem. Biophys. 449, 57–63.

Dey, D., Bochkariov, D.E., Jokhadze, G.G., Traut, R.R., 1998. Cross-linking of selected residues in the N- and C-terminal domains of Escherichia coli protein L7/L12 to other ribosomal proteins and the effect of elongation factor Tu. J. Biol. Chem. 273, 1670–1676.

Dey, D., Oleinikov, A.V., Traut, R.R., 1995. The hinge region of Escherichia coli ribosomal protein L7/L12 is required for factor binding and GTP hydrolysis. Biochimie 77, 925–930.

Diaconu, M., Kothe, U., Schlünzen, F., Fischer, N., Harms, J.M., Tonevitsky, A.G., Stark, H., Rodnina, M.V., Wahl, M.C., 2005. Structural Basis for the Function of the Ribosomal L7/12 Stalk in Factor Binding and GTPase Activation. Cell 121, 991–1004.

Diedrich, G., Spahn, C.M., Stelzl, U., Schäfer, M.A., Wooten, T., Bochkariov, D.E., Cooperman, B.S., Traut, R.R., Nierhaus, K.H., 2000. Ribosomal protein L2 is

involved in the association of the ribosomal subunits, tRNA binding to A and P sites and peptidyl transfer. EMBO J. 19, 5241–5250.

Donati, G., Peddigari, S., Mercer, C.A., Thomas, G., 2013. 5S Ribosomal RNA Is an Essential Component of a Nascent Ribosomal Precursor Complex that Regulates the Hdm2-p53 Checkpoint. Cell Reports 4, 87–98.

Ekstrand, M.I., Falkenberg, M., Rantanen, A., Park, C.B., Gaspari, M., Hultenby, K., Rustin, P., Gustafsson, C.M., Larsson, N.-G., 2004. Mitochondrial transcription factor A regulates mtDNA copy number in mammals. Hum. Mol. Genet. 13, 935–944.

Embley, T.M., Van der Giezen, M., Horner, D.S., Dyal, P.L., Bell, S., Foster, P.G., 2003. Hydrogenosomes, mitochondria and early eukaryotic evolution. IUBMB Life 55, 387–395.

Entelis, N.., Kolesnikova, O.., Martin, R.., Tarassov, I.., 2001. RNA delivery into mitochondria. Advanced Drug Delivery Reviews 49, 199–215.

Ernster, L., Schatz, G., 1981. Mitochondria: a historical review. J. Cell Biol. 91, 227s–255s.

Falkenberg, M., Gaspari, M., Rantanen, A., Trifunovic, A., Larsson, N.-G., Gustafsson, C.M., 2002. Mitochondrial transcription factors B1 and B2 activate transcription of human mtDNA. Nat. Genet. 31, 289–294.

Feagin, J.E., 2000. Mitochondrial genome diversity in parasites. Int. J. Parasitol. 30, 371–390.

Formenoy, L.J., Cunningham, P.R., Nurse, K., Pleij, C.W., Ofengand, J., 1994. Methylation of the conserved A1518-A1519 in Escherichia coli 16S ribosomal RNA by the ksgA methyltransferase is influenced by methylations around the similarly conserved U1512.G1523 base pair in the 3' terminal hairpin. Biochimie 76, 1123–1128.

Frey, T.G., Renken, C.W., Perkins, G.A., 2002. Insight into mitochondrial structure and function from electron tomography. Biochim. Biophys. Acta 1555, 196–203.

Frey, T.G., Sun, M.G., 2008. Correlated light and electron microscopy illuminates the role of mitochondrial inner membrane remodeling during apoptosis. Biochimica et Biophysica Acta (BBA) - Bioenergetics 1777, 847–852.

Fukuoh, A., Ohgaki, K., Hatae, H., Kuraoka, I., Aoki, Y., Uchiumi, T., Jacobs, H.T., Kang, D., 2009. DNA conformation-dependent activities of human mitochondrial RNA polymerase. Genes to Cells 14, 1029–1042.

Gagliardi, D., Stepien, P.P., Temperley, R.J., Lightowlers, R.N., Chrzanowska-Lightowlers, Z.M.., 2004. Messenger RNA stability in mitochondria: different means to an end. Trends in Genetics 20, 260–267.

Galmiche, L., Serre, V., Beinat, M., Assouline, Z., Lebre, A.-S., Chretien, D., Nietschke, P., Benes, V., Boddaert, N., Sidi, D., Brunelle, F., Rio, M., Munnich, A., Rötig, A., 2011. Exome sequencing identifies MRPL3 mutation in mitochondrial cardiomyopathy. Hum. Mutat. 32, 1225–1231.

Garrido, N., Griparic, L., Jokitalo, E., Wartiovaara, J., Van der Bliek, A.M., Spelbrink, J.N., 2003. Composition and dynamics of human mitochondrial nucleoids. Mol. Biol. Cell 14, 1583–1596.

Gaspari, M., Falkenberg, M., Larsson, N.-G., Gustafsson, C.M., 2004. The mitochondrial RNA polymerase contributes critically to promoter specificity in mammalian cells. The EMBO Journal 23, 4606–4614.

Gilkerson, R., Bravo, L., Garcia, I., Gaytan, N., Herrera, A., Maldonado, A., Quintanilla, B., 2013. The mitochondrial nucleoid: integrating mitochondrial DNA into cellular homeostasis. Cold Spring Harb Perspect Biol 5, a011080.

Glancy, B., Balaban, R.S., 2012. Role of mitochondrial Ca2+ in the regulation of cellular energetics. Biochemistry 51, 2959–2973.

Gordiyenko, Y., Deroo, S., Zhou, M., Videler, H., Robinson, C.V., 2008. Acetylation of L12 increases interactions in the Escherichia coli ribosomal stalk complex. J. Mol. Biol. 380, 404–414.

Gordiyenko, Y., Videler, H., Zhou, M., McKay, A.R., Fucini, P., Biegel, E., Müller, V., Robinson, C.V., 2010. Mass spectrometry defines the stoichiometry of ribosomal stalk complexes across the phylogenetic tree. Mol. Cell Proteomics 9, 1774–1783.

Görlach, M., Wittekind, M., Beckman, R.A., Mueller, L., Dreyfuss, G., 1992. Interaction of the RNA-binding domain of the hnRNP C proteins with RNA. EMBO J. 11, 3289–3295.

Gray, M.W., 2012. Mitochondrial evolution. Cold Spring Harb Perspect Biol 4, a011403.

Gray, M.W., Burger, G., Lang, B.F., 1999. Mitochondrial evolution. Science 283, 1476–1481.

Greber, B.J., Boehringer, D., Leitner, A., Bieri, P., Voigts-Hoffmann, F., Erzberger, J.P., Leibundgut, M., Aebersold, R., Ban, N., 2013. Architecture of the large subunit of the mammalian mitochondrial ribosome. Nature 505, 515–519.

Gregoret, L.M., Sauer, R.T., 1998. Tolerance of a protein helix to multiple alanine and valine substitutions. Fold Des 3, 119–126.

Griaznova, O., Traut, R.R., 2000. Deletion of C-terminal residues of Escherichia coli ribosomal protein L10 causes the loss of binding of one L7/L12 dimer: ribosomes with one L7/L12 dimer are active. Biochemistry 39, 4075–4081.

Gudkov, A.T., 1997. The L7/L12 ribosomal domain of the ribosome: structural and functional studies. FEBS Lett. 407, 253–256.

Han, M.-J., Cimen, H., Miller-Lee, J.L., Koc, H., Koc, E.C., 2011. Purification of human mitochondrial ribosomal L7/L12 stalk proteins and reconstitution of functional hybrid ribosomes in Escherichia coli. Protein Expression and Purification 78, 48–54.

Haque, M.E., Elmore, K.B., Tripathy, A., Koc, H., Koc, E.C., Spremulli, L.L., 2010. Properties of the C-terminal Tail of Human Mitochondrial Inner Membrane Protein Oxa1L and Its Interactions with Mammalian Mitochondrial Ribosomes. Journal of Biological Chemistry 285, 28353–28362.

Hatchell, E.C., Colley, S.M., Beveridge, D.J., Epis, M.R., Stuart, L.M., Giles, K.M., Redfern, A.D., Miles, L.E.C., Barker, A., MacDonald, L.M., Arthur, P.G., Lui, J.C.K., Golding, J.L., McCulloch, R.K., Metcalf, C.B., Wilce, J.A., Wilce, M.C.J., Lanz, R.B., O'Malley, B.W., Leedman, P.J., 2006. SLIRP, a small SRA binding protein, is a nuclear receptor corepressor. Mol. Cell 22, 657–668.

He, J., Cooper, H.M., Reyes, A., Di Re, M., Kazak, L., Wood, S.R., Mao, C.C., Fearnley, I.M., Walker, J.E., Holt, I.J., 2012. Human C4orf14 interacts with the mitochondrial nucleoid and is involved in the biogenesis of the small mitochondrial ribosomal subunit. Nucleic Acids Res. 40, 6097–6108.

Helgstrand, M., Mandava, C.S., Mulder, F.A.A., Liljas, A., Sanyal, S., Akke, M., 2007. The ribosomal stalk binds to translation factors IF2, EF-Tu, EF-G and RF3 via a conserved region of the L12 C-terminal domain. J. Mol. Biol. 365, 468–479.

Helser, T.L., Davies, J.E., Dahlberg, J.E., 1971. Change in methylation of 16S ribosomal RNA associated with mutation to kasugamycin resistance in Escherichia coli. Nature New Biol. 233, 12–14.

Holt, I.J., Lorimer, H.E., Jacobs, H.T., 2000. Coupled leading- and lagging-strand synthesis of mammalian mitochondrial DNA. Cell 100, 515–524.

Holzmann, J., Frank, P., Löffler, E., Bennett, K.L., Gerner, C., Rossmanith, W., 2008. RNase P without RNA: Identification and Functional Reconstitution of the Human Mitochondrial tRNA Processing Enzyme. Cell 135, 462–474.

Huang, C., Mandava, C.S., Sanyal, S., 2010. The ribosomal stalk plays a key role in IF2-mediated association of the ribosomal subunits. J. Mol. Biol. 399, 145–153.

Huang, Y.J., Swapna, G.V.T., Rajan, P.K., Ke, H., Xia, B., Shukla, K., Inouye, M., Montelione, G.T., 2003. Solution NMR Structure of Ribosome-binding Factor A (RbfA), A Cold-shock Adaptation Protein from Escherichia coli. Journal of Molecular Biology 327, 521–536.

Ingolia, N.T., Lareau, L.F., Weissman, J.S., 2011. Ribosome profiling of mouse embryonic stem cells reveals the complexity and dynamics of mammalian proteomes. Cell 147, 789–802.

Inoue, K., Alsina, J., Chen, J., Inouye, M., 2003. Suppression of defective ribosome assembly in a rbfA deletion mutant by overexpression of Era, an essential GTPase in Escherichia coli. Mol. Microbiol. 48, 1005–1016.

Inoue, K., Chen, J., Tan, Q., Inouye, M., 2006. Era and RbfA have overlapping function in ribosome biogenesis in Escherichia coli. J. Mol. Microbiol. Biotechnol. 11, 41–52.

Itoh, K., Nakamura, K., Iijima, M., Sesaki, H., 2013. Mitochondrial dynamics in neurodegeneration. Trends in Cell Biology 23, 64–71.

Jiang, X., Wang, X., 2004. Cytochrome C-mediated apoptosis. Annu. Rev. Biochem. 73, 87–106.

Jones, P.G., Inouye, M., 1996. RbfA, a 30S ribosomal binding factor, is a cold-shock protein whose absence triggers the cold-shock response. Mol. Microbiol. 21, 1207–1218.

Jourdain, A.A., Koppen, M., Wydro, M., Rodley, C.D., Lightowlers, R.N., Chrzanowska-Lightowlers, Z.M., Martinou, J.-C., 2013. GRSF1 regulates RNA processing in mitochondrial RNA granules. Cell Metab. 17, 399–410.

Kaushal, P.S., Sharma, M.R., Booth, T.M., Haque, E.M., Tung, C.-S., Sanbonmatsu, K.Y., Spremulli, L.L., Agrawal, R.K., 2014. Cryo-EM structure of the small subunit of the mammalian mitochondrial ribosome. Proc. Natl. Acad. Sci. U.S.A. 111, 7284–7289.

Kiparisov, S., Petrov, A., Meskauskas, A., Sergiev, P.V., Dontsova, O.A., Dinman, J.D., 2005. Structural and functional analysis of 5S rRNA in Saccharomyces cerevisiae. Mol. Genet. Genomics 274, 235–247.

Kirsebom, L.A., Isaksson, L.A., 1985. Involvement of ribosomal protein L7/L12 in control of translational accuracy. Proc. Natl. Acad. Sci. U.S.A. 82, 717–721.

Kiss, T., 2001. Small nucleolar RNA-guided post-transcriptional modification of cellular RNAs. EMBO J. 20, 3617–3622.

Kitakawa, M., Isono, K., 1991. The mitochondrial ribosomes. Biochimie 73, 813–825.

Klootwijk, J., Klein, I., Grivell, L.A., 1975. Minimal post-transcriptional modification of yeast mitochondrial ribosomal RNA. J. Mol. Biol. 97, 337–350.

Koc, E.C., Burkhart, W., Blackburn, K., Moyer, M.B., Schlatzer, D.M., Moseley, A., Spremulli, L.L., 2001. The large subunit of the mammalian mitochondrial ribosome. Analysis of the complement of ribosomal proteins present. J. Biol. Chem. 276, 43958–43969.

Koc, E.C., Haque, M.E., Spremulli, L.L., 2010. Current Views of the Structure of the Mammalian Mitochondrial Ribosome. Israel Journal of Chemistry 50, 45–59.

Koc, E.C., Koc, H., 2012. Regulation of mammalian mitochondrial translation by post-translational modifications. Biochimica et Biophysica Acta (BBA) - Gene Regulatory Mechanisms 1819, 1055–1066.

Koc, E.C., Spremulli, L.L., 2002. Identification of mammalian mitochondrial translational initiation factor 3 and examination of its role in initiation complex formation with natural mRNAs. J. Biol. Chem. 277, 35541–35549.

Koc, E.C., Spremulli, L.L., 2003. RNA-binding proteins of mammalian mitochondria. Mitochondrion 2, 277–291.

Kogure, H., Hikawa, Y., Hagihara, M., Tochio, N., Koshiba, S., Inoue, Y., Güntert, P., Kigawa, T., Yokoyama, S., Nameki, N., 2012. Solution structure and siRNA-mediated knockdown analysis of the mitochondrial disease-related protein C12orf65. Proteins 80, 2629–2642.

Koopman, W.J.H., Distelmaier, F., Smeitink, J.A., Willems, P.H., 2012. OXPHOS mutations and neurodegeneration. The EMBO Journal 32, 9–29.

Korepanov, A.P., Gongadze, G.M., Garber, M.B., Court, D.L., Bubunenko, M.G., 2007. Importance of the 5 S rRNA-binding ribosomal proteins for cell viability and translation in Escherichia coli. J. Mol. Biol. 366, 1199–1208.

Korepanov, A.P., Korobeinikova, A.V., Shestakov, S.A., Garber, M.B., Gongadze, G.M., 2012. Protein L5 is crucial for in vivo assembly of the bacterial 50S ribosomal subunit central protuberance. Nucleic Acids Research 40, 9153–9159.

Korhonen, J.A., Pham, X.H., Pellegrini, M., Falkenberg, M., 2004. Reconstitution of a minimal mtDNA replisome in vitro. The EMBO Journal 23, 2423–2429.

Kotani, T., Akabane, S., Takeyasu, K., Ueda, T., Takeuchi, N., 2013. Human G-proteins, ObgH1 and Mtg1, associate with the large mitochondrial ribosome subunit and are involved in translation and assembly of respiratory complexes. Nucleic Acids Research.

Koteliansky, V.E., Domogatsky, S.P., Gudkov, A.T., Spirin, A.S., 1977. Elongation factor-dependent reactions of ribosomes deprived of proteins L7 and L12. FEBS Lett. 73, 6–11.

Kouvela, E.C., Gerbanas, G.V., Xaplanteri, M.A., Petropoulos, A.D., Dinos, G.P., Kalpaxis, D.L., 2007. Changes in the conformation of 5S rRNA cause alterations in principal functions of the ribosomal nanomachine. Nucleic Acids Res. 35, 5108–5119.

Kudla, G., Granneman, S., Hahn, D., Beggs, J.D., Tollervey, D., 2011. Cross-linking, ligation, and sequencing of hybrids reveals RNA-RNA interactions in yeast. Proc. Natl. Acad. Sci. U.S.A. 108, 10010–10015.

Kukat, C., Wurm, C.A., Spåhr, H., Falkenberg, M., Larsson, N.-G., Jakobs, S., 2011. Super-resolution microscopy reveals that mammalian mitochondrial nucleoids have a uniform size and frequently contain a single copy of mtDNA. Proc. Natl. Acad. Sci. U.S.A. 108, 13534–13539.

Kurokawa, M., Kornbluth, S., 2009. Caspases and Kinases in a Death Grip. Cell 138, 838–854.

Lafontaine, D., Delcour, J., Glasser, A.L., Desgrès, J., Vandenhaute, J., 1994. The DIM1 gene responsible for the conserved m6(2)Am6(2)A dimethylation in the 3'-terminal loop of 18 S rRNA is essential in yeast. J. Mol. Biol. 241, 492–497.

Lafontaine, D., Vandenhaute, J., Tollervey, D., 1995. The 18S rRNA dimethylase Dim1p is required for pre-ribosomal RNA processing in yeast. Genes Dev. 9, 2470–2481.

Lafontaine, D.L., Preiss, T., Tollervey, D., 1998. Yeast 18S rRNA dimethylase Dim1p: a quality control mechanism in ribosome synthesis? Mol. Cell. Biol. 18, 2360–2370.

Lang, B.F., Gray, M.W., Burger, G., 1999. Mitochondrial genome evolution and the origin of eukaryotes. Annu. Rev. Genet. 33, 351–397.

Lanz, R.B., Razani, B., Goldberg, A.D., O'Malley, B.W., 2002. Distinct RNA motifs are important for coactivation of steroid hormone receptors by steroid receptor RNA activator (SRA). Proc. Natl. Acad. Sci. U.S.A. 99, 16081–16086.

Lapuente-Brun, E., Moreno-Loshuertos, R., Acin-Perez, R., Latorre-Pellicer, A., Colas, C., Balsa, E., Perales-Clemente, E., Quiros, P.M., Calvo, E., Rodriguez-

Hernandez, M.A., Navas, P., Cruz, R., Carracedo, A., Lopez-Otin, C., Perez-Martos, A., Fernandez-Silva, P., Fernandez-Vizarra, E., Enriquez, J.A., 2013. Supercomplex Assembly Determines Electron Flux in the Mitochondrial Electron Transport Chain. Science 340, 1567–1570.

Lee, D.Y., Clayton, D.A., 1996. Properties of a primer RNA-DNA hybrid at the mouse mitochondrial DNA leading-strand origin of replication. J. Biol. Chem. 271, 24262–24269.

Lee, H.-C., Chang, C.-M., Chi, C.-W., 2010. Somatic mutations of mitochondrial DNA in aging and cancer progression. Ageing Res. Rev. 9 Suppl 1, S47–58.

Lerner, C.G., Gulati, P.S., Inouye, M., 1995. Cold-sensitive conditional mutations in Era, an essential Escherichia coli GTPase, isolated by localized random polymerase chain reaction mutagenesis. FEMS Microbiol. Lett. 126, 291–298.

Li, N., Chen, Y., Guo, Q., Zhang, Y., Yuan, Y., Ma, C., Deng, H., Lei, J., Gao, N., 2013. Cryo-EM structures of the late-stage assembly intermediates of the bacterial 50S ribosomal subunit. Nucleic Acids Res.

Li, Z., Pandit, S., Deutscher, M.P., 1999. RNase G (CafA protein) and RNase E are both required for the 5' maturation of 16S ribosomal RNA. EMBO J. 18, 2878–2885.

Liao, H.X., Spremulli, L.L., 1989. Interaction of bovine mitochondrial ribosomes with messenger RNA. J. Biol. Chem. 264, 7518–7522.

Liao, H.X., Spremulli, L.L., 1990. Identification and initial characterization of translational initiation factor 2 from bovine mitochondria. J. Biol. Chem. 265, 13618–13622.

Lightowlers, R.N., Chrzanowska-Lightowlers, Z.M., 2013. Human pentatricopeptide proteins: Only a few and what do they do? RNA Biol 10.

Lightowlers, R.N., Chrzanowska-Lightowlers, Z.M.A., 2010. Terminating human mitochondrial protein synthesis: a shift in our thinking. RNA Biol 7, 282–286.

Lill, R., Mühlenhoff, U., 2006. Iron-Sulfur Protein Biogenesis in Eukaryotes: Components and Mechanisms. Annual Review of Cell and Developmental Biology 22, 457–486.

Litonin, D., Sologub, M., Shi, Y., Savkina, M., Anikin, M., Falkenberg, M., Gustafsson, C.M., Temiakov, D., 2010. Human mitochondrial transcription revisited: only TFAM and TFB2M are required for transcription of the mitochondrial genes in vitro. J. Biol. Chem. 285, 18129–18133.

Lu, B., Lee, J., Nie, X., Li, M., Morozov, Y.I., Venkatesh, S., Bogenhagen, D.F., Temiakov, D., Suzuki, C.K., 2012. Phosphorylation of Human TFAM in Mitochondria Impairs DNA Binding and Promotes Degradation by the AAA+ Lon Protease. Molecular Cell.

Lu, Q., Inouye, M., 1998. The gene for 16S rRNA methyltransferase (ksgA) functions as a multicopy suppressor for a cold-sensitive mutant of era, an essential RAS-like GTP-binding protein in Escherichia coli. J. Bacteriol. 180, 5243–5246.

Madan, E., Gogna, R., Bhatt, M., Pati, U., Kuppusamy, P., Mahdi, A.A., 2011. Regulation of glucose metabolism by p53: emerging new roles for the tumor suppressor. Oncotarget 2, 948–957.

Magalhães, P.J., Andreu, A.L., Schon, E.A., 1998. Evidence for the presence of 5S rRNA in mammalian mitochondria. Mol. Biol. Cell 9, 2375–2382.

Mandava, C.S., Peisker, K., Ederth, J., Kumar, R., Ge, X., Szaflarski, W., Sanyal, S., 2012. Bacterial ribosome requires multiple L12 dimers for efficient initiation and elongation of protein synthesis involving IF2 and EF-G. Nucleic Acids Res. 40, 2054–2064.

Marty, L., Fort, P., 1996. A delayed-early response nuclear gene encoding MRPL12, the mitochondrial homologue to the bacterial translational regulator L7/L12 protein. J. Biol. Chem. 271, 11468–11476.

Matoba, S., Kang, J.-G., Patino, W.D., Wragg, A., Boehm, M., Gavrilova, O., Hurley, P.J., Bunz, F., Hwang, P.M., 2006. p53 regulates mitochondrial respiration. Science 312, 1650–1653.

McCulloch, V., Seidel-Rogol, B.L., Shadel, G.S., 2002. A Human Mitochondrial Transcription Factor Is Related to RNA Adenine Methyltransferases and Binds S-Adenosylmethionine. Molecular and Cellular Biology 22, 1116–1125.

McLEAN, J.R., COHN, G.L., BRANDT, I.K., SIMPSON, M.V., 1958. Incorporation of labeled amino acids into the protein of muscle and liver mitochondria. J. Biol. Chem. 233, 657–663.

Mears, J.A., Sharma, M.R., Gutell, R.R., McCook, A.S., Richardson, P.E., Caulfield, T.R., Agrawal, R.K., Harvey, S.C., 2006. A Structural Model for the Large Subunit of the Mammalian Mitochondrial Ribosome. Journal of Molecular Biology 358, 193–212.

Mercer, T.R., Neph, S., Dinger, M.E., Crawford, J., Smith, M.A., Shearwood, A.-M.J., Haugen, E., Bracken, C.P., Rackham, O., Stamatoyannopoulos, J.A., Filipovska, A., Mattick, J.S., 2011. The Human Mitochondrial Transcriptome. Cell 146, 645–658.

Metodiev, M.D., Lesko, N., Park, C.B., Cámara, Y., Shi, Y., Wibom, R., Hultenby, K., Gustafsson, C.M., Larsson, N.-G., 2009. Methylation of 12S rRNA Is Necessary for In Vivo Stability of the Small Subunit of the Mammalian Mitochondrial Ribosome. Cell Metabolism 9, 386–397.

Metodiev, M.D., Spåhr, H., Loguercio Polosa, P., Meharg, C., Becker, C., Altmueller, J., Habermann, B., Larsson, N.-G., Ruzzenente, B., 2014. NSUN4 is a dual function mitochondrial protein required for both methylation of 12S rRNA and coordination of mitoribosomal assembly. PLoS Genet. 10, e1004110.

Miller, C., Saada, A., Shaul, N., Shabtai, N., Ben-Shalom, E., Shaag, A., Hershkovitz, E., Elpeleg, O., 2004. Defective mitochondrial translation caused by a ribosomal protein (MRPS16) mutation. Ann. Neurol. 56, 734–738.

Miller, J.L., Cimen, H., Koc, H., Koc, E.C., 2009. Phosphorylated Proteins of the Mammalian Mitochondrial Ribosome: Implications in Protein Synthesis. Journal of Proteome Research 8, 4789–4798.

Milone, M., Massie, R., 2010. Polymerase gamma 1 mutations: clinical correlations. Neurologist 16, 84–91.

Minczuk, M., He, J., Duch, A.M., Ettema, T.J., Chlebowski, A., Dzionek, K., Nijtmans, L.G.J., Huynen, M.A., Holt, I.J., 2011. TEFM (c17orf42) is necessary for transcription of human mtDNA. Nucleic Acids Research 39, 4284–4299.

Mitchell, P., 2011. Chemiosmotic coupling in oxidative and photosynthetic phosphorylation. Biochimica et Biophysica Acta (BBA) - Bioenergetics 1807, 1507–1538.

Moens, P.D.J., Wahl, M.C., Jameson, D.M., 2005. Oligomeric state and mode of self-association of Thermotoga maritima ribosomal stalk protein L12 in solution. Biochemistry 44, 3298–3305.

Mohr, D., Wintermeyer, W., Rodnina, M.V., 2002. GTPase Activation of Elongation Factors Tu and G on the Ribosome. Biochemistry 41, 12520–12528.

Montoya, J., Christianson, T., Levens, D., Rabinowitz, M., Attardi, G., 1982. Identification of initiation sites for heavy-strand and light-strand transcription in human mitochondrial DNA. Proc. Natl. Acad. Sci. U.S.A. 79, 7195–7199.

Montoya, J., Gaines, G.L., Attardi, G., 1983. The pattern of transcription of the human mitochondrial rRNA genes reveals two overlapping transcription units. Cell 34, 151–159.

Mootha, V.K., Lepage, P., Miller, K., Bunkenborg, J., Reich, M., Hjerrild, M., Delmonte, T., Villeneuve, A., Sladek, R., Xu, F., Mitchell, G.A., Morin, C.,

Mann, M., Hudson, T.J., Robinson, B., Rioux, J.D., Lander, E.S., 2003. Identification of a gene causing human cytochrome c oxidase deficiency by integrative genomics. Proc. Natl. Acad. Sci. U.S.A. 100, 605–610.

Nagai, K., Oubridge, C., Jessen, T.H., Li, J., Evans, P.R., 1990. Crystal structure of the RNA-binding domain of the U1 small nuclear ribonucleoprotein A. Nature 348, 515–520.

Nagaike, T., Suzuki, T., Katoh, T., Ueda, T., 2005. Human mitochondrial mRNAs are stabilized with polyadenylation regulated by mitochondria-specific poly(A) polymerase and polynucleotide phosphorylase. J. Biol. Chem. 280, 19721–19727.

Nakamura, T., Yagi, Y., Kobayashi, K., 2012. Mechanistic Insight into Pentatricopeptide Repeat Proteins as Sequence-Specific RNA-Binding Proteins for Organellar RNAs in Plants. Plant and Cell Physiology 53, 1171–1179.

Neupert, W., Herrmann, J.M., 2007. Translocation of Proteins into Mitochondria. Annual Review of Biochemistry 76, 723–749.

Ngo, H.B., Lovely, G.A., Phillips, R., Chan, D.C., 2014. Distinct structural features of TFAM drive mitochondrial DNA packaging versus transcriptional activation. Nat Commun 5, 3077.

Nicholls, T.J., Rorbach, J., Minczuk, M., 2013. Mitochondria: Mitochondrial RNA metabolism and human disease. The International Journal of Biochemistry & Cell Biology 45, 845–849.

Nissen, P., Hansen, J., Ban, N., Moore, P.B., Steitz, T.A., 2000. The structural basis of ribosome activity in peptide bond synthesis. Science 289, 920–930.

Nunnari, J., Suomalainen, A., 2012. Mitochondria: In Sickness and in Health. Cell 148, 1145–1159.

O'Brien, T.W., Kalf, G.F., 1967. Ribosomes from rat liver mitochondira. II. Partial characterization. J. Biol. Chem. 242, 2180–2185.

Ojala, D., Montoya, J., Attardi, G., 1981. tRNA punctuation model of RNA processing in human mitochondria. Nature 290, 470–474.

Oleinikov, A.V., Jokhadze, G.G., Traut, R.R., 1998. A single-headed dimer of Escherichia coli ribosomal protein L7/L12 supports protein synthesis. Proc. Natl. Acad. Sci. U.S.A. 95, 4215–4218.

Ott, M., Prestele, M., Bauerschmitt, H., Funes, S., Bonnefoy, N., Herrmann, J.M., 2006. Mba1, a membrane-associated ribosome receptor in mitochondria. The EMBO Journal 25, 1603–1610.

Pagliarini, D.J., Calvo, S.E., Chang, B., Sheth, S.A., Vafai, S.B., Ong, S.-E., Walford, G.A., Sugiana, C., Boneh, A., Chen, W.K., Hill, D.E., Vidal, M., Evans, J.G., Thorburn, D.R., Carr, S.A., Mootha, V.K., 2008. A Mitochondrial Protein Compendium Elucidates Complex I Disease Biology. Cell 134, 112–123.

Paul, M.-F., Alushin, G.M., Barros, M.H., Rak, M., Tzagoloff, A., 2012. The putative GTPase encoded by MTG3 functions in a novel pathway for regulating assembly of the small subunit of yeast mitochondrial ribosomes. J. Biol. Chem. 287, 24346–24355.

Peil, L., Starosta, A.L., Lassak, J., Atkinson, G.C., Virumäe, K., Spitzer, M., Tenson, T., Jung, K., Remme, J., Wilson, D.N., 2013. Distinct XPPX sequence motifs induce ribosome stalling, which is rescued by the translation elongation factor EF-P. Proc. Natl. Acad. Sci. U.S.A. 110, 15265–15270.

Pettersson, I., Kurland, C.G., 1980. Ribosomal protein L7/L12 is required for optimal translation. Proc. Natl. Acad. Sci. U.S.A. 77, 4007–4010.

Phillips, N.R., Sprouse, M.L., Roby, R.K., 2014. Simultaneous quantification of mitochondrial DNA copy number and deletion ratio: a multiplex real-time PCR assay. Sci Rep 4, 3887.

Piwowarski, J., Grzechnik, P., Dziembowski, A., Dmochowska, A., Minczuk, M., Stepien, P.P., 2003. Human polynucleotide phosphorylase, hPNPase, is localized in mitochondria. J. Mol. Biol. 329, 853–857.

Poldermans, B., Van Buul, C.P., Van Knippenberg, P.H., 1979. Studies on the function of two adjacent N6,N6-dimethyladenosines near the 3' end of 16 S ribosomal RNA of Escherichia coli. II. The effect of the absence of the methyl groups on initiation of protein biosynthesis. J. Biol. Chem. 254, 9090–9093.

Polevoda, B., Sherman, F., 2002. The diversity of acetylated proteins. Genome Biol. 3, reviews0006.

Poulton, J., Chiaratti, M.R., Meirelles, F.V., Kennedy, S., Wells, D., Holt, I.J., 2010. Transmission of mitochondrial DNA diseases and ways to prevent them. PLoS Genet. 6.

Qian, Z., Wilusz, J., 1994. GRSF-1: a poly(A)+ mRNA binding protein which interacts with a conserved G-rich element. Nucleic Acids Res. 22, 2334–2343.

Qu, X., Wen, J.-D., Lancaster, L., Noller, H.F., Bustamante, C., Tinoco, I., Jr, 2011. The ribosome uses two active mechanisms to unwind messenger RNA during translation. Nature 475, 118–121.

Raimundo, N., Song, L., Shutt, T.E., McKay, S.E., Cotney, J., Guan, M.-X., Gilliland, T.C., Hohuan, D., Santos-Sacchi, J., Shadel, G.S., 2012. Mitochondrial Stress Engages E2F1 Apoptotic Signaling to Cause Deafness. Cell 148, 716–726.

Rajala, N., Gerhold, J.M., Martinsson, P., Klymov, A., Spelbrink, J.N., 2013. Replication factors transiently associate with mtDNA at the mitochondrial inner membrane to facilitate replication. Nucleic Acids Research 42, 952–967.

Ramagopal, S., 1976. Accumulation of free ribosomal proteins S1, L7, and L12 in Escherichia coli. Eur. J. Biochem. 69, 289–297.

Ramagopal, S., Subramanian, A.R., 1974. Alteration in the acetylation level of ribosomal protein L12 during growth cycle of Escherichia coli. Proc. Natl. Acad. Sci. U.S.A. 71, 2136–2140.

Regoes, A., Zourmpanou, D., León-Avila, G., Van der Giezen, M., Tovar, J., Hehl, A.B., 2005. Protein import, replication, and inheritance of a vestigial mitochondrion. J. Biol. Chem. 280, 30557–30563.

Remacha, M., Jimenez-Diaz, A., Bermejo, B., Rodriguez-Gabriel, M.A., Guarinos, E., Ballesta, J.P., 1995. Ribosomal acidic phosphoproteins P1 and P2 are not required for cell viability but regulate the pattern of protein expression in Saccharomyces cerevisiae. Mol. Cell. Biol. 15, 4754–4762.

Rich, B.E., Steitz, J.A., 1987. Human acidic ribosomal phosphoproteins P0, P1, and P2: analysis of cDNA clones, in vitro synthesis, and assembly. Mol. Cell. Biol. 7, 4065–4074.

Richter, R., Pajak, A., Dennerlein, S., Rozanska, A., Lightowlers, R.N., Chrzanowska-Lightowlers, Z.M.A., 2010a. Translation termination in human mitochondrial ribosomes. Biochemical Society Transactions 38, 1523.

Richter, R., Rorbach, J., Pajak, A., Smith, P.M., Wessels, H.J., Huynen, M.A., Smeitink, J.A., Lightowlers, R.N., Chrzanowska-Lightowlers, Z.M., 2010b. A functional peptidyl-tRNA hydrolase, ICT1, has been recruited into the human mitochondrial ribosome. The EMBO Journal 29, 1116–1125.

Ringel, R., Sologub, M., Morozov, Y.I., Litonin, D., Cramer, P., Temiakov, D., 2011. Structure of human mitochondrial RNA polymerase. Nature 478, 269–273.

Rivera, M.C., Lake, J.A., 2004. The ring of life provides evidence for a genome fusion origin of eukaryotes. Nature 431, 152–155.

Roger, A.J., Silberman, J.D., 2002. Cell evolution: mitochondria in hiding. Nature 418, 827–829.

Rooijers, K., Loayza-Puch, F., Nijtmans, L.G., Agami, R., 2013. Ribosome profiling reveals features of normal and disease-associated mitochondrial translation. Nat Commun 4, 2886.

Rorbach, J., Gammage, P.A., Minczuk, M., 2012. C7orf30 is necessary for biogenesis of the large subunit of the mitochondrial ribosome. Nucleic Acids Res. 40, 4097–4109.

Rorbach, J., Minczuk, M., 2012. The post-transcriptional life of mammalian mitochondrial RNA. Biochemical Journal 444, 357–373.

Rorbach, J., Nicholls, T.J.J., Minczuk, M., 2011. PDE12 removes mitochondrial RNA poly(A) tails and controls translation in human mitochondria. Nucleic Acids Research 39, 7750–7763.

Rorbach, J., Richter, R., Wessels, H.J., Wydro, M., Pekalski, M., Farhoud, M., Kühl, I., Gaisne, M., Bonnefoy, N., Smeitink, J.A., Lightowlers, R.N., Chrzanowska-Lightowlers, Z.M.A., 2008. The human mitochondrial ribosome recycling factor is essential for cell viability. Nucleic Acids Res. 36, 5787–5799.

Rötig, A., 2011. Human diseases with impaired mitochondrial protein synthesis. Biochimica et Biophysica Acta (BBA) - Bioenergetics 1807, 1198–1205.

Ruzzenente, B., Metodiev, M.D., Wredenberg, A., Bratic, A., Park, C.B., Cámara, Y., Milenkovic, D., Zickermann, V., Wibom, R., Hultenby, K., Erdjument-Bromage, H., Tempst, P., Brandt, U., Stewart, J.B., Gustafsson, C.M., Larsson, N.-G., 2011. LRPPRC is necessary for polyadenylation and coordination of translation of mitochondrial mRNAs. The EMBO Journal 31, 443–456.

Saada, A., Shaag, A., Arnon, S., Dolfin, T., Miller, C., Fuchs-Telem, D., Lombes, A., Elpeleg, O., 2007. Antenatal mitochondrial disease caused by mitochondrial ribosomal protein (MRPS22) mutation. J. Med. Genet. 44, 784–786.

Saenz-Robles, M.T., Remacha, M., Vilella, M.D., Zinker, S., Ballesta, J.P., 1990. The acidic ribosomal proteins as regulators of the eukaryotic ribosomal activity. Biochim. Biophys. Acta 1050, 51–55.

Sasarman, F., Brunel-Guitton, C., Antonicka, H., Wai, T., Shoubridge, E.A., 2010. LRPPRC and SLIRP interact in a ribonucleoprotein complex that regulates posttranscriptional gene expression in mitochondria. Mol. Biol. Cell 21, 1315–1323.

Schon, E.A., DiMauro, S., Hirano, M., 2012. Human mitochondrial DNA: roles of inherited and somatic mutations. Nat. Rev. Genet. 13, 878–890.

Seidel-Rogol, B.L., McCulloch, V., Shadel, G.S., 2002. Human mitochondrial transcription factor B1 methylates ribosomal RNA at a conserved stem-loop. Nature Genetics 33, 23–24.

Serre, V., Rozanska, A., Beinat, M., Chretien, D., Boddaert, N., Munnich, A., Rötig, A., Chrzanowska-Lightowlers, Z.M., 2013. Mutations in mitochondrial ribosomal protein MRPL12 leads to growth retardation, neurological deterioration and mitochondrial translation deficiency. Biochim. Biophys. Acta 1832, 1304–1312.

Shajani, Z., Sykes, M.T., Williamson, J.R., 2011. Assembly of bacterial ribosomes. Annu. Rev. Biochem. 80, 501–526.

Sharma, M.R., Barat, C., Wilson, D.N., Booth, T.M., Kawazoe, M., Hori-Takemoto, C., Shirouzu, M., Yokoyama, S., Fucini, P., Agrawal, R.K., 2005. Interaction of Era with the 30S Ribosomal SubunitImplications for 30S Subunit Assembly. Molecular Cell 18, 319–329.

Sharma, M.R., Booth, T.M., Simpson, L., Maslov, D.A., Agrawal, R.K., 2009. Structure of a mitochondrial ribosome with minimal RNA. Proc. Natl. Acad. Sci. U.S.A. 106, 9637–9642.

Sharma, M.R., Koc, E.C., Datta, P.P., Booth, T.M., Spremulli, L.L., Agrawal, R.K., 2003. Structure of the mammalian mitochondrial ribosome reveals an expanded functional role for its component proteins. Cell 115, 97–108.

Shi, Y., Dierckx, A., Wanrooij, P.H., Wanrooij, S., Larsson, N.-G., Wilhelmsson, L.M., Falkenberg, M., Gustafsson, C.M., 2012. Mammalian transcription factor A is a core component of the mitochondrial transcription machinery. Proceedings of the National Academy of Sciences 109, 16510–16515.

Shutt, T.E., 2006. Homologs of Mitochondrial Transcription Factor B, Sparsely Distributed Within the Eukaryotic Radiation, Are Likely Derived from the Dimethyladenosine Methyltransferase of the Mitochondrial Endosymbiont. Molecular Biology and Evolution 23, 1169–1179.

Shutt, T.E., Bestwick, M., Shadel, G.S., 2011. The core human mitochondrial transcription initiation complex: It only takes two to tango. Transcription 2, 55–59.

Shutt, T.E., Lodeiro, M.F., Cotney, J., Cameron, C.E., Shadel, G.S., 2010. Core human mitochondrial transcription apparatus is a regulated two-component system in vitro. Proc. Natl. Acad. Sci. U.S.A. 107, 12133–12138.

Shutt, T.E., Shadel, G.S., 2010. A compendium of human mitochondrial gene expression machinery with links to disease. Environ. Mol. Mutagen. 51, 360–379.

Sloan, D.B., Alverson, A.J., Chuckalovcak, J.P., Wu, M., McCauley, D.E., Palmer, J.D., Taylor, D.R., 2012. Rapid evolution of enormous, multichromosomal genomes in flowering plant mitochondria with exceptionally high mutation rates. PLoS Biol. 10, e1001241.

Sloan, K.E., Bohnsack, M.T., Watkins, N.J., 2013. The 5S RNP Couples p53 Homeostasis to Ribosome Biogenesis and Nucleolar Stress. Cell Rep 5, 237–247.

Slomovic, S., Laufer, D., Geiger, D., Schuster, G., 2005. Polyadenylation and degradation of human mitochondrial RNA: the prokaryotic past leaves its mark. Mol. Cell. Biol. 25, 6427–6435.

Small, I.D., Peeters, N., 2000. The PPR motif - a TPR-related motif prevalent in plant organellar proteins. Trends Biochem. Sci. 25, 46–47.

Smeets, H.J.M., 2013. Preventing the transmission of mitochondrial DNA disorders: selecting the good guys or kicking out the bad guys. Reprod. Biomed. Online 27, 599–610.

Smeitink, J.A., Zeviani, M., Turnbull, D.M., Jacobs, H.T., 2006. Mitochondrial medicine: A metabolic perspective on the pathology of oxidative phosphorylation disorders. Cell Metabolism 3, 9–13.

Smirnov, A., Comte, C., Mager-Heckel, A.-M., Addis, V., Krasheninnikov, I.A., Martin, R.P., Entelis, N., Tarassov, I., 2010. Mitochondrial enzyme rhodanese is essential for 5 S ribosomal RNA import into human mitochondria. J. Biol. Chem. 285, 30792–30803.

Smirnov, A., Entelis, N., Martin, R.P., Tarassov, I., 2011. Biological significance of 5S rRNA import into human mitochondria: role of ribosomal protein MRP-L18. Genes & Development 25, 1289–1305.

Smirnov, A., Tarassov, I., Mager-Heckel, A.-M., Letzelter, M., Martin, R.P., Krasheninnikov, I.A., Entelis, N., 2008. Two distinct structural elements of 5S rRNA are needed for its import into human mitochondria. RNA 14, 749–759.

Smits, P., Smeitink, J., Van den Heuvel, L., 2010. Mitochondrial Translation and Beyond: Processes Implicated in Combined Oxidative Phosphorylation Deficiencies. Journal of Biomedicine and Biotechnology 2010, 1–24.

Soleimanpour-Lichaei, H.R., Kühl, I., Gaisne, M., Passos, J.F., Wydro, M., Rorbach, J., Temperley, R., Bonnefoy, N., Tate, W., Lightowlers, R., Chrzanowska-Lightowlers, Z., 2007. mtRF1a Is a Human Mitochondrial Translation Release Factor Decoding the Major Termination Codons UAA and UAG. Molecular Cell 27, 745–757.

Spelbrink, J.N., 2009. Functional organization of mammalian mitochondrial DNA in nucleoids: History, recent developments, and future challenges. IUBMB Life n/a–n/a.

Spremulli, L.L., Coursey, A., Navratil, T., Hunter, S.E., 2004. Initiation and elongation factors in mammalian mitochondrial protein biosynthesis. Prog. Nucleic Acid Res. Mol. Biol. 77, 211–261.

Sterky, F.H., Ruzzenente, B., Gustafsson, C.M., Samuelsson, T., Larsson, N.-G., 2010. LRPPRC is a mitochondrial matrix protein that is conserved in metazoans. Biochemical and Biophysical Research Communications 398, 759–764.

Stiburek, L., Fornuskova, D., Wenchich, L., Pejznochova, M., Hansikova, H., Zeman, J., 2007. Knockdown of Human Oxa1l Impairs the Biogenesis of F1Fo-ATP Synthase and NADH:Ubiquinone Oxidoreductase. Journal of Molecular Biology 374, 506–516.

Strunk, B.S., Karbstein, K., 2009. Powering through ribosome assembly. RNA 15, 2083–2104.

Stumpf, J.D., Copeland, W.C., 2011. Mitochondrial DNA replication and disease: insights from DNA polymerase γ mutations. Cell. Mol. Life Sci. 68, 219–233.

Stumpf, J.D., Saneto, R.P., Copeland, W.C., 2013. Clinical and molecular features of POLG-related mitochondrial disease. Cold Spring Harb Perspect Biol 5, a011395.

Subramanian, A.R., 1975. Copies of proteins L7 and L12 and heterogeneity of the large subunit of Escherichia coli ribosome. J. Mol. Biol. 95, 1–8.

Sugiana, C., Pagliarini, D.J., McKenzie, M., Kirby, D.M., Salemi, R., Abu-Amero, K.K., Dahl, H.-H.M., Hutchison, W.M., Vascotto, K.A., Smith, S.M., Newbold, R.F., Christodoulou, J., Calvo, S., Mootha, V.K., Ryan, M.T., Thorburn, D.R., 2008. Mutation of C20orf7 Disrupts Complex I Assembly and Causes Lethal Neonatal Mitochondrial Disease. The American Journal of Human Genetics 83, 468–478.

Sulthana, S., Deutscher, M.P., 2013. Multiple exoribonucleases catalyze maturation of the 3' terminus of 16S ribosomal RNA (rRNA). J. Biol. Chem. 288, 12574–12579.

Surovtseva, Y.V., Shadel, G.S., 2013. Transcription-independent role for human mitochondrial RNA polymerase in mitochondrial ribosome biogenesis. Nucleic Acids Research 41, 2479–2488.

Surovtseva, Y.V., Shutt, T.E., Cotney, J., Cimen, H., Chen, S.Y., Koc, E.C., Shadel, G.S., 2011. Mitochondrial ribosomal protein L12 selectively associates with human mitochondrial RNA polymerase to activate transcription. Proc. Natl. Acad. Sci. U.S.A. 108, 17921–17926.

Szczesny, R.J., Borowski, L.S., Brzezniak, L.K., Dmochowska, A., Gewartowski, K., Bartnik, E., Stepien, P.P., 2010. Human mitochondrial RNA turnover caught in flagranti: involvement of hSuv3p helicase in RNA surveillance. Nucleic Acids Res. 38, 279–298.

SzymańSki, M., Barciszewska, M.Z., Erdmann, V.A., Barciszewski, J., 2003. 5 S rRNA: structure and interactions. Biochemical Journal 371, 641.

Taanman, J.W., 1999. The mitochondrial genome: structure, transcription, translation and replication. Biochim. Biophys. Acta 1410, 103–123.

Takyar, S., Hickerson, R.P., Noller, H.F., 2005. mRNA helicase activity of the ribosome. Cell 120, 49–58.

Temperley, R., Richter, R., Dennerlein, S., Lightowlers, R.N., Chrzanowska-Lightowlers, Z.M., 2010a. Hungry codons promote frameshifting in human mitochondrial ribosomes. Science 327, 301.

Temperley, R.J., Wydro, M., Lightowlers, R.N., Chrzanowska-Lightowlers, Z.M., 2010b. Human mitochondrial mRNAs--like members of all families, similar but different. Biochim. Biophys. Acta 1797, 1081–1085.

Terasaki, M., Suzuki, T., Hanada, T., Watanabe, K., 2004. Functional compatibility of elongation factors between mammalian mitochondrial and bacterial ribosomes: characterization of GTPase activity and translation elongation by hybrid ribosomes bearing heterologous L7/12 proteins. J. Mol. Biol. 336, 331–342.

Terhorst, C., Möller, W., Laursen, R., Wittmann-Liebold, B., 1973. The primary structure of an acidic protein from 50-S ribosomes of Escherichia coli which is involved in GTP hydrolysis dependent on elongation factors G and T. Eur. J. Biochem. 34, 138–152.

Tiranti, V., 1997. Identification of the gene encoding the human mitochondrial RNA polymerase (h-mtRPOL) by cyberscreening of the Expressed Sequence Tags database. Human Molecular Genetics 6, 615–625.

Tomecki, R., Dmochowska, A., Gewartowski, K., Dziembowski, A., Stepien, P.P., 2004. Identification of a novel human nuclear-encoded mitochondrial poly(A) polymerase. Nucleic Acids Res. 32, 6001–6014.

Travis, A.J., Moody, J., Helwak, A., Tollervey, D., Kudla, G., 2014. Hyb: A bioinformatics pipeline for the analysis of CLASH (crosslinking, ligation and sequencing of hybrids) data. Methods 65, 263–273.

Trimmer, P.A., Swerdlow, R.H., Parks, J.K., Keeney, P., Bennett, J.P., Jr, Miller, S.W., Davis, R.E., Parker, W.D., Jr, 2000. Abnormal mitochondrial morphology in sporadic Parkinson's and Alzheimer's disease cybrid cell lines. Exp. Neurol. 162, 37–50.

Tsuboi, M., Morita, H., Nozaki, Y., Akama, K., Ueda, T., Ito, K., Nierhaus, K.H., Takeuchi, N., 2009. EF-G2mt Is an Exclusive Recycling Factor in Mammalian Mitochondrial Protein Synthesis. Molecular Cell 35, 502–510.

Tu, C., Zhou, X., Tarasov, S.G., Tropea, J.E., Austin, B.P., Waugh, D.S., Court, D.L., Ji, X., 2011. The Era GTPase recognizes the GAUCACCUCC sequence and binds helix 45 near the 3' end of 16S rRNA. Proc. Natl. Acad. Sci. U.S.A. 108, 10156–10161.

Tu, C., Zhou, X., Tropea, J.E., Austin, B.P., Waugh, D.S., Court, D.L., Ji, X., 2009. Structure of ERA in complex with the 3' end of 16S rRNA: implications for ribosome biogenesis. Proc. Natl. Acad. Sci. U.S.A. 106, 14843–14848.

Uchiumi, T., Ohgaki, K., Yagi, M., Aoki, Y., Sakai, A., Matsumoto, S., Kang, D., 2010. ERAL1 is associated with mitochondrial ribosome and elimination of ERAL1 leads to mitochondrial dysfunction and growth retardation. Nucleic Acids Res. 38, 5554–5568.

Ule, J., Jensen, K., Mele, A., Darnell, R.B., 2005. CLIP: a method for identifying protein-RNA interaction sites in living cells. Methods 37, 376–386.

Van Buul, C.P.J.J., Visser, W., Van Knippenberg, P.H., 1984. Increased translational fidelity caused by the antibiotic kasugamycin and ribosomal ambiguity in mutants harbouring the ksgA gene. FEBS Letters 177, 119–124.

Vanlangenakker, N., Vanden Berghe, T., Krysko, D.V., Festjens, N., Vandenabeele, P., 2008. Molecular mechanisms and pathophysiology of necrotic cell death. Curr. Mol. Med. 8, 207–220.

Vedrenne, V., Gowher, A., De Lonlay, P., Nitschke, P., Serre, V., Boddaert, N., Altuzarra, C., Mager-Heckel, A.-M., Chretien, F., Entelis, N., Munnich, A., Tarassov, I., Rötig, A., 2012. Mutation in PNPT1, which Encodes a Polyribonucleotide Nucleotidyltransferase, Impairs RNA Import into Mitochondria and Causes Respiratory-Chain Deficiency. The American Journal of Human Genetics 91, 912–918.

Vidales, F.J., Robles, M.T., Ballesta, J.P., 1984. Acidic proteins of the large ribosomal subunit in Saccharomyces cerevisiae. Effect of phosphorylation. Biochemistry 23, 390–396.

Vierna, J., Wehner, S., Höner zu Siederdissen, C., Martínez-Lage, A., Marz, M., 2013. Systematic analysis and evolution of 5S ribosomal DNA in metazoans. Heredity.

Vogel, F., Bornhovd, C., Neupert, W., Reichert, A.S., 2006. Dynamic subcompartmentalization of the mitochondrial inner membrane. The Journal of Cell Biology 175, 237–247.

Wahl, M.C., Bourenkov, G.P., Bartunik, H.D., Huber, R., 2000. Flexibility, conformational diversity and two dimerization modes in complexes of ribosomal protein L12. EMBO J. 19, 174–186.

Wahl, M.C., Möller, W., 2002. Structure and function of the acidic ribosomal stalk proteins. Curr. Protein Pept. Sci. 3, 93–106.

Wang, G., Chen, H.-W., Oktay, Y., Zhang, J., Allen, E.L., Smith, G.M., Fan, K.C., Hong, J.S., French, S.W., McCaffery, J.M., Lightowlers, R.N., Morse, H.C., Koehler, C.M., Teitell, M.A., 2010. PNPASE Regulates RNA Import into Mitochondria. Cell 142, 456–467.

Wang, Y.E., Marinov, G.K., Wold, B.J., Chan, D.C., 2013. Genome-Wide Analysis Reveals Coating of the Mitochondrial Genome by TFAM. PLoS ONE 8, e74513.

Wang, Z., Cotney, J., Shadel, G.S., 2007. Human mitochondrial ribosomal protein MRPL12 interacts directly with mitochondrial RNA polymerase to modulate mitochondrial gene expression. J. Biol. Chem. 282, 12610–12618.

Wanrooij, S., Miralles Fusté, J., Stewart, J.B., Wanrooij, P.H., Samuelsson, T., Larsson, N.-G., Gustafsson, C.M., Falkenberg, M., 2012. In vivo mutagenesis reveals that OriL is essential for mitochondrial DNA replication. EMBO Rep. 13, 1130–1137.

Wanschers, B.F.J., Szklarczyk, R., Pajak, A., Van den Brand, M.A.M., Gloerich, J., Rodenburg, R.J.T., Lightowlers, R.N., Nijtmans, L.G., Huynen, M.A., 2012. C7orf30 specifically associates with the large subunit of the mitochondrial ribosome and is involved in translation. Nucleic Acids Research 40, 4040–4051.

Weiss, R.B., Atkins, J.F., 2011. Translation Goes Global. Science 334, 1509–1510.

Wessels, H.J.C.T., Vogel, R.O., Lightowlers, R.N., Spelbrink, J.N., Rodenburg, R.J., Van den Heuvel, L.P., Van Gool, A.J., Gloerich, J., Smeitink, J.A.M., Nijtmans, L.G., 2013. Analysis of 953 Human Proteins from a Mitochondrial HEK293 Fraction by Complexome Profiling. PLoS ONE 8, e68340.

Williams, T.A., Foster, P.G., Cox, C.J., Embley, T.M., 2013. An archaeal origin of eukaryotes supports only two primary domains of life. Nature 504, 231–236.

Wool, I.G., Chan, Y.L., Glück, A., 1995. Structure and evolution of mammalian ribosomal proteins. Biochem. Cell Biol. 73, 933–947.

Wool, I.G., Chan, Y.L., Glück, A., Suzuki, K., 1991. The primary structure of rat ribosomal proteins P0, P1, and P2 and a proposal for a uniform nomenclature for mammalian and yeast ribosomal proteins. Biochimie 73, 861–870.

Woriax, V.L., Bullard, J.M., Ma, L., Yokogawa, T., Spremulli, L.L., 1997. Mechanistic studies of the translational elongation cycle in mammalian mitochondria. Biochim. Biophys. Acta 1352, 91–101.

Wydro, M., Bobrowicz, A., Temperley, R.J., Lightowlers, R.N., Chrzanowska-Lightowlers, Z.M., 2010. Targeting of the cytosolic poly(A) binding protein PABPC1 to mitochondria causes mitochondrial translation inhibition. Nucleic Acids Res. 38, 3732–3742.

Xia, B., Ke, H., Shinde, U., Inouye, M., 2003. The role of RbfA in 16S rRNA processing and cell growth at low temperature in Escherichia coli. J. Mol. Biol. 332, 575–584.

Xu, B., Clayton, D.A., 1996. RNA-DNA hybrid formation at the human mitochondrial heavy-strand origin ceases at replication start sites: an implication for RNA-DNA hybrids serving as primers. EMBO J. 15, 3135–3143.

Xu, F., Ackerley, C., Maj, M.C., Addis, J.B.L., Levandovskiy, V., Lee, J., MacKay, N., Cameron, J.M., Robinson, B.H., 2008. Disruption of a mitochondrial RNA-binding protein gene results in decreased cytochrome b expression and a marked reduction in ubiquinol–cytochrome c reductase activity in mouse heart mitochondria. Biochemical Journal 416, 15.

Yakubovskaya, E., Guja, K.E., Mejia, E., Castano, S., Hambardjieva, E., Choi, W.S., Garcia-Diaz, M., 2012. Structure of the Essential MTERF4:NSUN4 Protein Complex Reveals How an MTERF Protein Collaborates to Facilitate rRNA Modification. Structure 20, 1940–1947.

Yang, M.Y., Bowmaker, M., Reyes, A., Vergani, L., Angeli, P., Gringeri, E., Jacobs, H.T., Holt, I.J., 2002. Biased incorporation of ribonucleotides on the mitochondrial L-strand accounts for apparent strand-asymmetric DNA replication. Cell 111, 495–505.

Yang, Z., Guo, Q., Goto, S., Chen, Y., Li, N., Yan, K., Zhang, Y., Muto, A., Deng, H., Himeno, H., Lei, J., Gao, N., 2014. Structural insights into the assembly of the 30S ribosomal subunit in vivo: functional role of S5 and location of the 17S rRNA precursor sequence. Protein & Cell 5, 394–407.

Yoshionari, S., Koike, T., Yokogawa, T., Nishikawa, K., Ueda, T., Miura, K., Watanabe, K., 1994. Existence of nuclear-encoded 5S-rRNA in bovine mitochondria. FEBS Letters 338, 137–142.

Youle, R.J., Van der Bliek, A.M., 2012. Mitochondrial fission, fusion, and stress. Science 337, 1062–1065.

Yutin, N., Makarova, K.S., Mekhedov, S.L., Wolf, Y.I., Koonin, E.V., 2008. The deep archaeal roots of eukaryotes. Mol. Biol. Evol. 25, 1619–1630.

Yu-Wai-Man, P., Griffiths, P.G., Chinnery, P.F., 2011. Mitochondrial optic neuropathies – Disease mechanisms and therapeutic strategies. Progress in Retinal and Eye Research 30, 81–114.

Zick, M., Rabl, R., Reichert, A., 2009. Cristae formation—linking ultrastructure and function of mitochondria. Biochimica et Biophysica Acta (BBA) - Molecular Cell Research 1793, 5–19.

Publications arising

Publications arising from this PhD project

Lightowlers, R.N., Rozanska, A., Chrzanowska-Lightowlers, Z.M., (2014). Mitochondrial protein synthesis: Figuring the fundamentals, complexities and complications, of mammalian mitochondrial translation. FEBS Lett.

Tran Hornig-Do, H., Montanari, A., Rozanska, A., Tuppen, H.A., Almalki, A.A., Abg-Kamaludin, D.P., Frontali. L., Francisci. S., Lightowlers, R.N., Chrzanowska-Lightowlers, Z.M., (2014). Human mitochondrial leucyl tRNA synthetase can suppress non cognate pathogenic mt-tRNA mutations. EMBO Mol Med.

Joint first author
Serre, V., Rozanska, A., Beinat, M., Chretien, D., Boddaert, N., Munnich, A., Rötig, A., Chrzanowska-Lightowlers, Z.M., (2013). Mutations in mitochondrial ribosomal protein MRPL12 leads to growth retardation, neurological deterioration and mitochondrial translation deficiency. Biochim. Biophys. Acta 1832, 1304–1312.

Richter, R., Pajak, A., Dennerlein, S., Rozanska, A., Lightowlers, R.N., Chrzanowska-Lightowlers, Z.M.A., (2010). Translation termination in human mitochondrial ribosomes. Biochemical Society Transactions 38, 1523.

Appendices

Appendix 1.1

Table A1. Table of CLIP hits mapped to genes used as controls in the assay performed for SLIRP, MRPL12 protein in patient and control sample and RBFA.

Gene	SLIRP		RBFA		MRPL12 Control	
	Position in the gene	Number of hits	Position in the gene	Number of hits	Position in the gene	Number of hits
18S	1760-1805	50-66	13-81	51-52	3-114	73-141-62
			268-374	54-90-64	224-257	55-114
			393-452	50-62-50	257-378	114-**1126**-177
			492-591	53-240-53	394-491	~150
			592-691	59-345-55	493-580	901-**2145**-273 (~700 hits for patient sample)
			932-1003	52-50-52	581-590	237-119
			1084-1226	114-**1125**-63	592-683	120-300-124
			1314-1487	51-100-49	683-804	124-65
			1497-1600	49-152-52	805-997	120-**761**-77
			1754-1859	54-**545**-47	997-1239	77-**600**-132
					1245-1302-1356	158-**3005**-497
					1356-1638	300-497-400
					1755-1802-1848	77-**792**-92
28S	3034-3060	52-120-60	132-241	63-140-169-56	1-68	57-79-52
	3079-3086	353-326	1258-1263	99-132	59-371-55	102-257
			1281-1374	65-80-50	1257-1265	116-127

			1529-1625	52-80-50	1283-1418	52-80-50
			1692-1782	51-205-66	1482-1648	50-200-61
			1827-1949	50-150-83	1699-1752	55-50
			2399-2523	56-70-50	1796-1945	58-200-62
			2696-2826	55-100-50	2261-2379	54-180-94
			3642-3733	56-174-77		
			4020-4126	87-153-53	2396-2537	61~200~96
			4180-4278	52-155-50	2538-2830	98~300-82
			4314-4486	51-150-50	2880-2889	50-50
			4899-5064	62-130-68	3078-3087	332-150
					3565-3643	54-100-88
					3644-3809	91-274-51
					3872-3964	58-166-57
					4031-4099	54-60-53
					4149-4242	52-150-91
					4246-4267	140-60
					4300-4381	90-178-56
					4384-4456	121-53
					4528-4560	54-58
					4564-4717	70-**503**-54

				4728-4793	53-69-53
				4854-4887	53-61-56
				4892-5068	82-191-63

Four nuclear genes were checked for content of CLIP reads: tubulin (no significant number of reads identified), EIF4E (no significant number of CLIP sequences mapped), 18S rRNA and 28S rRNA (more than 50 sequences located in one position with approximate number of hits are presented in the table below). Considering very high abundance of all checked RNA species, can be concluded that for SLIRP and RbfA protein all controls confirm specificity of binding to mt-RNAs. In case of MRPL12 protein (mapped reads presented for control sample were comparable with patient sample unless otherwise specified in the table). The high number of hits mapped in few positions of 18S rRNA (highlighted in red) were identified for MRPL12 protein in both control and patient samples.

Appendix 1.2
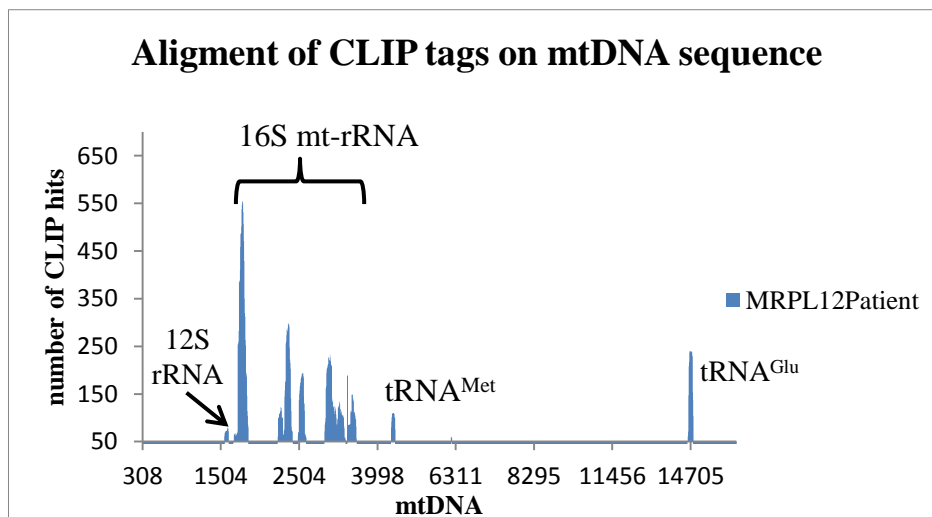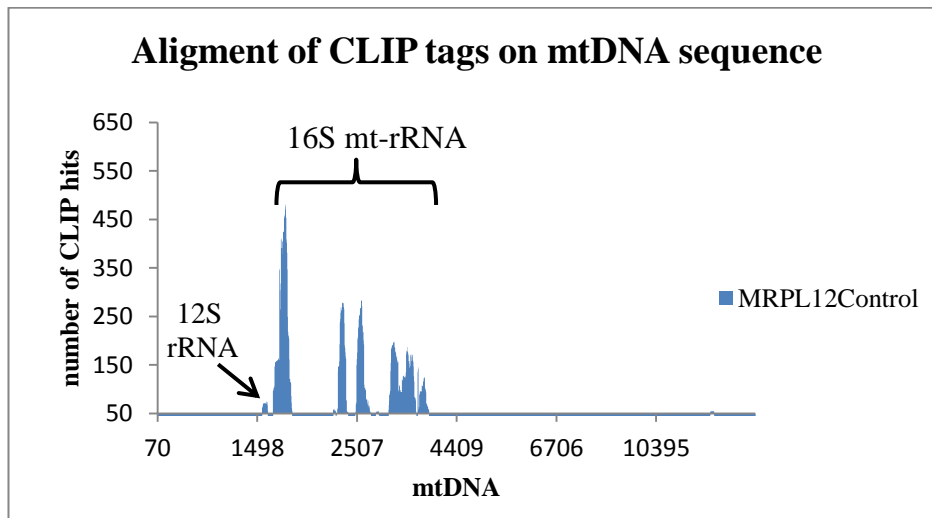
Figure A1. Alignment of MRPL12 CLIP tags from control and patient fibroblasts on mtDNA map. RNA species bound by MRPL12 *in vivo* were identified following CLIP method as described in the subsection 2.6.1 in control and patient fibroblasts. WT MRPL12 and mutated form with substitution of alanine 181 to valine had the same positions of CLIP sequences identified on 16S rRNA with the highest number of reads mapped at the 5'end (~450 reads for control and above 500 for subject sample). Three more locations on 16S were identified in the range of reads between 280-180. Two binding positions were localised in the sequences of tRNA[Met] and tRNA[Glu] in patient fibroblasts in contrast to control with no reads mapped in these two locations. In both samples ~70 reads were mapped to 3'end of 12S rRNA.

Appendix 1.3
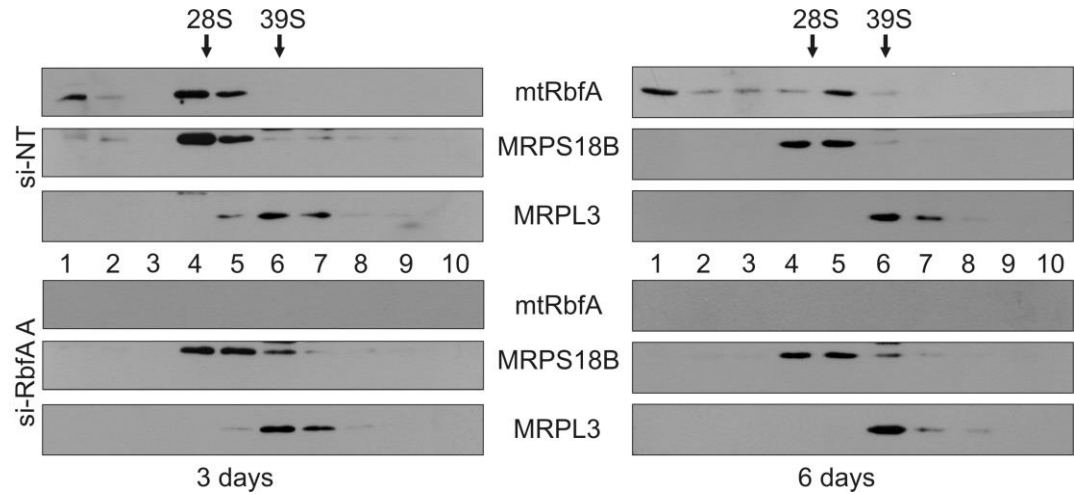
Figure A2. Western blot analysis of sucrose gradient fractions for HEK 293 cell lysates. Cells were grown for 3 and 6 days in the presence of NT or RBFA (mtRbfA) siRNA. In order to assess ribosome assembly pattern in RBFA depleted HEK 293T cells antibodies for mt-SSU protein (MRPS18B) and mt-LSU protein (MRPL3) were used. RBFA antibody was applied to check depletion efficiency in cells incubated with targeting siRNA. Analysis of ribosome assembly was performed by Ricarda Richter.

Appendix 1.4

Table A2. Table of CLIP hits mapped on mtDNA obtained for SLIRP protein.

	Gene	Position in mtDNA	No. of reads	3' to 5' CLIP read sequence
1	mtTF1 binding site	269-294	> 600	ACACAGACATCATAACAAAAAATTT
2(!)	*MTRNR1* 3'termini	1561-1594	20	CGTAACATGGTAAGTGTACTGGAAAGTGCACTTG
3	*MTND1*	4020-4048	12	CACTACAATCTTCCTAGGAACAACATATG
4	*MTND2*	5222-5262	~ 87	AGGAGGCCTGCCCCCGCTAACCGGCTTTTTGCCCAAATGG
5	*MTCOI*	5959-5988	~30	ACCTATTATTCGGCGCATGAGCTGGAGTCC
6	*MTCOI*	6122-6152	40	CATAATCGGAGGCTTTGGCAACTGACTAGTT
7	*MTCOI*	6551-6582	~ 160	CACCACCTTCTTCGACCCCGCCGGAGGAGGAG
8	*MTCOI*	6848-6871	20	CACCGGCGTCAAAGTATTTAGCTG
9	*MTCOI*	7026-7065	> 20	GCCCACTTCCACTATGTCCTATCAATAGGAGCTGTATTTG
10	*MTCOII*	7873-7900	> 40	CATCAAATCAATTGGCCACCAATGGTAC
11	*MTCOII*	8135-8177	>30	TTCACCGCTACACGACCGGGGGTATACTACGGTCAA TGCTCTG
12	*ATPase8*	8372-8394	29	CAACTAAATACTACCGTATGGCC
13	*ATP8ase8-ATPase6*	8562-8592	152	CACAATCCTAGGCCTACCCGCCGCAGTACTG
14	*ATPase6*	8657-8685	~680	CCACCCAACAATGACTAATCAAACTAACC
15	*ATPase6*	8974-9002	>600	CTCATTCAACCAATAGCCCTGGCCGTACGC
16	*MTCOXIII*	9279-9322	~30	CTCCTAATGACCTCCGGCCTAGCCATGTGATTTCACTTCCAC TC
17	*MTCOXIII*	9563-9597	~26	AGGCATCACCCCGCTAAATCCCCTAGAAGTCCCAC
18	*MTCOXIII*	9917-9948	~20	CGCCGCCTGATACTGGCATTTTGTAGATGTGG
19	*MTND3*	10161-10186	>60	ACCCCTTACGAGTGCGGCTTCGACCC
20	*MTND4L*	10644-10675	16	GTGCCTATTGCCATACTAGTCTTTGCCGCCTG
21	*MTND4*	10993-11029	~35	GGCAAGCCAACGCCACTTATCCAGTGAACCACTATCA
22	*MTND4*	11872-11896	>200	CACTATTAACCTACTGGGAGAACTC
23	*MTND5*	13682-13712	~26	CCCTACTAAACCCCATTAAACGCCTGGCAGC
24	*MTCYTB*	14814-14842	37	CCCCATCCAACATCTCCGCATGATGAAAC
25	*MTCYTB*	14956-14985	28	TCGAGACGTAAATTATGGCTGAATCATCCG
26	tRNA^Pro	15957-15991	22	CAGAGAAAAAGTCTTTAACTCCACCATTAGCACCC

The genes, specific positions and sequences of CLIP tags are presented. Short dNTPs sequences found in at least ten different tags are highlighted (12 fragments contain CGC sequence (green); 12 fragments contain CTG (yellow); 10 fragments contain GAG (purple), 7 fragments contain both CGC and CTG fragments).

Appendix 1.5

Mutations in mitochondrial ribosomal protein MRPL12 leads to growth retardation, neurological deterioration and mitochondrial translation deficiency ☆

Valérie Serre [a],[1], Agata Rozanska [c],[1], Marine Beinat [a], Dominique Chretien [a], Nathalie Boddaert [a], Arnold Munnich [a], Agnès Rötig [a],[b],**, Zofia M. Chrzanowska-Lightowlers [c],*

[a] Université Paris Descartes-Sorbonne Paris Cité, Institut Imagine and INSERM U781, Hôpital Necker-Enfants Malades, 149 rue de Sèvres, 75015 Paris, France
[b] Department of Pediatrics, Hôpital Necker-Enfants-Malades, 149 rue de Sèvres, 75015 Paris, France
[c] Wellcome Trust Centre for Mitochondrial Research, Institute for Ageing and Health, Newcastle University, Medical School, Framlington Place, Newcastle upon Tyne, NE2 4HH, United Kingdom

ARTICLE INFO

ABSTRACT

Multiple respiratory chain deficiencies represent a common cause of mitochondrial diseases and are associated with a wide range of clinical symptoms. We report a subject, born to consanguineous parents, with growth retardation and neurological deterioration. Multiple respiratory chain deficiency was found in muscle and fibroblasts of the subject as well as abnormal assembly of complexes I and IV. A microsatellite genotyping of the family members detected only one region of homozygosity on chromosome 17q24.2–q25.3 in which we focused our attention to genes involved in mitochondrial translation. We sequenced *MRPL12*, encoding the mitochondrial ribosomal protein L12 and identified a c.542C>T transition in exon 5 changing a highly conserved alanine into a valine (p.Ala181Val). This mutation resulted in a decreased steady-state level of MRPL12 protein, with altered integration into the large ribosomal subunit. Moreover, an overall mitochondrial translation defect was observed in the subject's fibroblasts with a significant reduction of synthesis of COXI, COXII and COXIII subunits. Modeling of MRPL12 shows Ala181 positioned in a helix potentially involved in an interface of interaction suggesting that the p.Ala181Val change might be predicted to alter interactions with the elongation factors. These results contrast with the eubacterial orthologues of human MRPL12, where L7/L12 proteins do not appear to have a selective effect on translation. Therefore, analysis of the mutated version found in the subject presented here suggests that the mammalian protein does not function in an entirely analogous manner to the eubacterial L7/L12 equivalent.

© 2013 The Authors. Published by Elsevier B.V. All rights reserved.

1. Introduction

The mitochondrial machinery responsible for oxidative phosphorylation (OXPHOS) comprises five enzyme complexes containing approximately 80 proteins of which only 13 are encoded by the mitochondrial genome (mtDNA) [1]. OXPHOS deficiencies affecting a single or multiple complexes can result from mutations in either mitochondrial or nuclear genes and are associated with a variety of disease mechanisms [2,3]. With the advent of Next Generation Sequencing there is an increasing number of pathogenic mutations being identified that are not solely restricted to the 80 genes encoding OXPHOS components, thus highlighting the importance of mechanisms impacting on mitochondrial gene expression [4,5]. Combined OXPHOS deficiencies can arise from alterations in mtDNA, its maintenance [6], cardiolipin levels [7,8], or where none of these are affected, from direct defects in synthesis of mitochondrially encoded proteins [9]. This last group constitutes a heterogeneous mix of patients suffering from a wide range of clinical symptoms making clinical diagnosis difficult [10]. Genetic diagnosis is yet more elusive in children with mitochondrial disease where unidentified nuclear mutations

account for the majority of cases [11]. This diagnostic problem is compounded by our relatively poor understanding of the complex molecular machinery that drives translation in mitochondria. This machinery comprises over a hundred proteins [12], all of which are putative candidate genes for translation deficiencies in human. Indeed, translation deficiencies represent a growing cause of multiple OXPHOS deficiencies with several published pathogenic mutations in genes related to the intra-organellar protein synthesis. Although many mutations associated with impaired mitochondrial translation currently map to tRNA genes [13] and a few ribosomal RNA (rRNA) [14], the list of nuclear gene mutations is steadily growing as mutations in genes encoding mitochondrial translation factors such as *GFM1* (OMIM: 606639) [15,16], *TSFM* (OMIM: 604723) [17] and *TUFM* (OMIM: 602389) [18]; mitochondrial aminoacyl-tRNA synthetases (RARS2 (OMIM: 611524) [19], DARS2 (OMIM: 610956) [20], YARS2 (OMIM: 610957) [21], SARS2 (OMIM: 612804) [22], HARS2 (OMIM: 600783) [23], AARS2 (OMIM: 612035) [24], MARS2 (OMIM: 609728) [25], EARS2 (OMIM: 612799) [26], FARS2 (OMIM: 611592) [27]; tRNA-modifying enzymes (PUS1 (OMIM: 608109) [28], TRMU (OMIM: 610230) [29], MTO1 (OMIM: 614667) [30]); other factors (C12orf65 (OMIM: 613541) [31], TACO1 (OMIM: 612958) [32], LRPPRC (OMIM: 607544) [33], C12orf62 (OMIM: 614478) [34]) and mitochondrial ribosomal proteins (MRPS16 (OMIM: 609204) [35], MRPS22 (OMIM: 605810) [36], MRPL3 (OMIM: 607118) [5]) have been successively reported (reviewed in Ref. [14]). Relatively few cases of OXPHOS deficiencies associated with mutations in mitochondrial ribosomal proteins (MRPs) have been described so far. *MRPS16* mutations have been described in only one family with agenesis of corpus callosum and dysmorphism. *MRPS22* mutations lead to cardiomyopathy, hypotonia and tubulopathy in a first family and Cornelia de Lange-like dysmorphic features, brain abnormalities and hypertrophic cardiomyopathy in another family. Finally, we recently identified *MRPL3* mutations in four siblings of the same family presenting cardiomyopathy and psychomotor retardation. Since the mammalian mitoribosome (55S) is ~2 megadalton machine consisting of approximately 80 components that make up the 28S small (SSU) and 39S large subunit (LSU), it is likely that more pathogenic mutations in the constituent polypeptides will be uncovered. One of the substantial differences between the mammalian mitoribosome and those of eubacteria (70S) or the eukaryotic cytosol (80S) is the reversal in the protein to rRNA ratio. The 70S and 80S particles contain ~70% rRNA, whilst human mitoribosomes contain ~70% protein. This change in the ratio represents both an acquisition of new MRPs as well as loss of bacterial orthologues [37,38]. MRPL12 does have a bacterial orthologue, which through its interactions with translation factors is important in protein synthesis regulating both speed and accuracy [39–41].

Here we investigate the genetic basis of disease in a subject born to consanguineous parents, who initially presented with growth retardation and then neurological distress, with evidence of compromised mitochondrial protein synthesis. We have identified the causative mutation to be in *MRPL12*, encoding a protein of the large subunit of mitochondrial ribosome. This is an important finding indicating that the function and consequence of dysfunction cannot automatically be extrapolated from an apparent orthologue. We show that proteins involved in mitochondrial translation, even close orthologues as submitted here, can defy predictions. Moreover, mutations in such genes that should affect all mitochondrially encoded gene products can exert respiratory chain complex specific defects.

2. Materials and methods

2.1. Analysis of oxidative phosphorylation activities

Spectrophotometric assays of respiratory chain and complex V enzymes were carried out as previously described [42]. Mitochondrial suspension from cultured skin fibroblasts was obtained after suspending 50 μl of frozen cells in 1 ml of mitochondria extraction medium (20 mM Tris–HCl (pH 7.2), 250 mM sucrose, 2 mM EGTA, 40 mM KCl, 1 mg/ml BSA) supplemented with 0.01% (w/v) digitonin and 10% Percoll (v/v). After 10 min at 4 °C, the sample was pelleted, washed in extraction medium and pelleted before resuspension in 30 μl of extraction medium for respiratory chain enzyme measurements.

2.2. Microsatellite genotyping and mutation screening

A genome-wide search for homozygosity was undertaken with 382 pairs of fluorescent oligonucleotides from the Genescan Linkage Mapping Set, version II (Perkin-Elmer) under conditions recommended by the manufacturer. Amplified fragments were electrophoresed and analyzed with an automatic sequencer (ABI 377). The polymorphic markers had an average spacing of 10 cM throughout the genome.

Genes encoding mitochondrial proteins were selected in Mitocarta [43]. The exons and exon–intron boundaries of the *MRPL12* gene were amplified using specific primers (sequences available on request) with initial denaturation at 96 °C — 5 min, followed by 30 cycles of 96 °C — 30 s, 55 °C — 30 s, 72 °C — 30 s, and a last extension at 72 °C for 10 min. Amplification products were purified by ExoSapIT (Amersham, Buckinghamshire, UK) and directly sequenced using the PRISM Ready Reaction Sequencing Kit (Perkin-Elmer, Oak Brook, IL) on an automatic sequencer (ABI 3130xl; PE Applied Biosystems, Foster City, CA).

2.3. Cell culture

Human skin fibroblasts were cultured in DMEM medium (Dulbecco's modified Eagle's medium, Gibco) supplemented with 10% (v/v) fetal calf serum (FCS), 2 mM L-glutamine, 50 μg/ml uridine, 110 μg/ml pyruvate, 10,000 U/ml penicillin G and 10,000 μg/ml streptomycin.

2.4. Protein analysis

For blue native-polyacrylamide gel electrophoresis (BN-PAGE), mitochondria and OXPHOS complexes were isolated as described [44]. Solubilized OXPHOS proteins (20 μg) were loaded on a 4–16% (w/v) polyacrylamide non-denaturing gradient gel (Invitrogen). SDS–PAGE analysis was performed on either solubilized mitochondrial proteins (40 μg) or cell lysate (50 μg) extracted from cultured skin fibroblasts. After electrophoresis, gels were transferred to a PVDF membrane (GE-Healthcare) and processed for immunoblotting.

2.5. Metabolic labelling of mitochondrial translation products

In vitro labeling of mitochondrial translation products was a modification from Chomyn et al. [45]. Essentially, cultured skin fibroblasts were preincubated in methionine/cysteine-free DMEM (2 × 10 min) followed by a 10 min in the presence of emetine (100 μg/ml). Radiolabel (125 μCi/ml EasyTag™ express³⁵S protein labelling mix — NEG772002MC, PerkinElmer) was then added for 1 h at 37 °C and chased for 1 h. Cells were harvested in cold 1 mM EDTA/PBS, washed 3 times in cold PBS and the pellet resuspended in 30 μl PBS containing 1× EDTA free protease inhibitors (Roche) and 1 mM PMSF. Samples were treated with 2× dissociation buffer (20% (v/v) glycerol, 4% (w/v) SDS, 250 mM Tris–HCl pH 6.8, 100 mM DTT) and 12 U Benzonase nuclease (Novagen) for 1 h and separated on a 15% (w/v) SDS–PAGE. The gel was fixed overnight (3% (v/v) glycerol, 10% (v/v) acetic acid, 30% (v/v) methanol) and vacuum dried (60 °C, 2 h). Radiolabelled proteins were visualized by PhosphorImage and analyzed with Image-Quant software (Molecular Dynamics, GE Healthcare).

2.6. Homology modeling of the human MRPL12 protein

The three dimensional structure of the human MRPL12 (residues 64 to 198) was modeled by comparative protein modeling and energy minimization, using the Swiss-Model program (http://swissmodel.expasy.org/) in the automated mode. The 2 Å coordinate set for the ribosomal protein L12 from *Thermotoga maritima* (PDB code: 1dd3) was used as a template for modeling the human MRPL12 protein. Swiss-Pdb Viewer 3.7 (http://www.expasy.org/spdbv) was used to analyze the structural insight into MRPL12 mutation and visualize the structures.

2.7. Cell lysates, Westerns and isokinetic sucrose gradients

Cell lysates were prepared from fibroblasts by addition of cold lysis buffer (50 mM Tris–HCl pH 7.5, 130 mM NaCl, 2 mM MgCl$_2$, 1 mM PMSF, 1% (v/v) NP-40) to cell pellets, which were vortexed for 30 s, centrifuged at 600 g for 2 min (4 °C) to remove nuclei and the supernatant retained. These were used for standard westerns as described [46]. Mitochondria were prepared as above and lyzed in 50 mM Tris–HCl pH 7.4, 150 mM NaCl, 1 mM EDTA, 1% Triton X-100, protease inhibitor mix (EDTA free, Roche), 1 mM PMSF, 10 mM MgCl$_2$. Mitochondrial lysates (0.3 mg) were loaded on a isokinetic sucrose gradient (1 ml 10–30% (v/v)) in 50 mM Tris–HCl (pH 7.2), 10 mM Mg(OAc)$_2$, 40 mM NH$_4$Cl, 0.1 M KCl, 1 mM PMSF, 50 µg/ml chloramphenicol), and centrifuged for 2 h 15 min at 100,000 g at 4 °C. Fractions (100 µl) were collected and 10 µl aliquots were analyzed directly by western blotting [47].

Immunodetection was performed using the following primary antibodies: anti-CI-Grim19, CII-SDHA 70 kDa, CIII-core2, CIV-COXI, CIV-COXII, CV-subunit β, cyt *c*, NDUFB8 (mouse monoclonal antibodies, MitoSciences); anti-MRPL3 goat polyclonal, MRPS18B rabbit polyclonal, MRPS25 rabbit polyclonal and ICT1 rabbit polyclonal antibodies (Protein Tech Group, Inc., Chicago); anti-DAP3 mouse monoclonal, POLRMT rabbit polyclonal (Abcam); and anti-Porin, mouse monoclonal antibodies (Invitrogen). Anti-MRPL12 rabbit polyclonal antibody was custom made (Eurogentec). Secondary antibody detection was performed using peroxidase-conjugated anti-rabbit, anti-goat or anti-mouse IgG (Abcam or Dako). The signal was generated using ECL+ (Pierce, Rockford, USA) and visualised by phosphorimaging and analyzed by ImageQuant software.

2.8. RNA and Northern blotting

RNA was isolated from fibroblasts using Trizol following manufacturer's protocol (Invitrogen). Northern blots were performed as described [48]. Briefly, aliquots of RNA (5 µg) were electrophoresed through 1.2% (w/v) agarose under denaturing conditions and transferred to GenescreenPlus membrane (NEN duPont) following the manufacturer's protocol. Radiolabelled probes were generated using random hexamers on PCR-generated templates corresponding to internal regions of the relevant genes.

3. Results and discussion

3.1. Clinical report

The subject, a boy, was born to first cousin Roma/Gypsy parents by cesarean section, at 41 weeks of pregnancy with severe general hypotrophy (birth weight 2250 g, height 48 cm, Occipitofrontal Circumference 34 cm). His clinical examination at birth was normal and initial investigations failed to identify the cause of his severe hypotrophy (normal blood caryotype, heart ultrasound, bone age, CT scan and metabolic workup). He failed to thrive thereafter and was repeatedly admitted in the first 12 months for gradual worsening of his condition (weight and height: −4SD, OFC: −2SD). Clinical examination at 10 months showed severe denutrition, muscle weakness but detectable deep tendon reflexes and no major trunk

hypotonia. He started walking with aid at 12 months. Basal growth hormone (GH) levels in plasma were normal (0.5 ng/ml) but plasma IGF1 was very low (0.07 U/ml, normal 0.2). Stimulation by ornithine triggered an adequate elevation of plasma GH with correction of plasma IGF1 (GH: 46.9 ng/ml, IGF1: 0.2 U/ml, and 0.45 U/ml following GH administration). These results ruled out a dwarfism of endocrine origin. Yet, high plasma lactate (3.5 to 4.4 mmol/l, normal below 2.2) prompted skeletal muscle, liver and skin biopsies that revealed a multiple respiratory chain enzyme deficiency in muscle and liver homogenate and cultured skin fibroblasts (Table 1) [42].

He had a first episode of generalized tonic seizure aged 2 years and his neurological condition rapidly worsened following an episode of acute fever (40 °C) caused by a respiratory infection. At that age, he had severe denutrition, flat weight curve, no weight and height gain (−5 SD) and a mildly enlarged liver. Neurological examination revealed overt psychomotor retardation, severe trunk hypotonia, inability to sit and stand unaided and no speech. Intermittent horizontal nystagmus, with cerebellar ataxia and tremor were noted. He had a mild facial dysmorphism, with round face, epicanthic folds, arched palate, short neck, low-set ears and a unique bilateral median palmar crease. Brain MRI showed T1 hyposignal and T2 hypersignal of white matter and basal ganglia. Rapid aggravation of respiratory conditions required endotracheal intubation and assisted ventilation. Plasma lactates rose to 3.3–4.2 mmol/l, he gradually developed abnormal limb movements then fell into a deep coma, and died following a cardiac arrest.

During the next pregnancy, the mother expected dizygotic twin fetuses. A prenatal diagnosis based on assessment of respiratory chain enzyme activities in cultured skin fibroblasts on amniotic fluid was offered. Hemoglobin contamination of the samples rendered the very low respiratory chain activities; despite this the activity ratios clearly showed a severe complex IV deficiency in cells from the fetus twins leading to termination of the second pregnancy. The same test was normal in the third pregnancy and a normal baby girl was born, now 14 years old (Table 1).

3.2. Blue native-PAGE analysis

Whilst skin fibroblasts were propagated for enzyme analysis it was clear that those from the subject harboring the mutation had a reduced doubling time on glucose medium compared to control lines (data available on request). Cell extracts were subsequently prepared and SDS–PAGE/western blot analysis revealed reduced steady-state level of COXII subunit, consistent with the decreased CIV activity (Fig. 1A). Moreover, we also observed a decreased amount of nuclear encoded protein NDUFB8 (Fig. 1A), which joins late in complex I assembly [44] and is consistent with the low CI activity in the biopsies. These decreases were consistent with the BN-PAGE data from fibroblast mitoplasts (Fig. 1B, method as described [49]). Both complexes I and IV, detected by anti-GRIM19 antibody or mitochondrially-encoded COXI, were severely decreased in the subject, which in contrast exhibited control levels of complex II (70 kDa SDHA subunit) and complex III (Core 2 subunit) (Fig. 1B). No partial complexes were observed.

3.3. Identifying the causative mutation by Microsatellite genotyping and mutation screening

In order to identify the causative mutation a genome-wide search for homozygosity was undertaken using 382 polymorphic microsatellite markers (Genescan Linkage Mapping Set, version II (Perkin-Elmer). We obtained evidence for homozygosity in all affected individuals at loci D17S785, D17S784, and D17S928 on chromosome 17q24.2–q25.3 (Fig. 2A). No other homozygous region was found with other markers. This 32.7 cM region was then refined by additional microsatellite markers reducing the critical region to the 25 cM interval, defined by loci D17S1352 and D17S928. This corresponds to a 8.4 Mb physical region containing more than 170 genes, 10 of which encode

Table 1
Respiratory chain activities in muscle mitochondria, liver homogenate and fibroblasts.

	Muscle mitochondria		Liver homogenate		Liver homogenate			Fibroblasts		Amniotic cells			
	P	C	P	C	Twin 1 fetus	Twin 2 fetus	C	P	C	Twin 1 fetus	Twin 2 fetus	3rd pregnancy	C
Absolute activities (nmol/min/mg prot)													
CI	–	–	–	–	–	–	–	17	27–44	–	–	–	–
CII	170	75–157	–	–	63	57	74–196	59	33–71	–	–	–	–
CIII	697	494–1004	493	128–217	106	73	70–236	505	318–820	1.44	2.1	16.5	19–21
CIV	374	540–1073	7	131–241	57	32	68–284	90	189–429	0.88	0.77	32	26–36
CV	538	209–454	–	–	–	–	–	100	53–133	–	–	–	–
CI + III	89	113–311	27	35–67	–	–	–	–	–	–	–	–	–
CII + III	443	164–357	365	50–98	37	23	38–104	167	69–146	2.22	1.38	8.7	6.5–8.4
CS	–	–	–	–	65	45	40–104	293	112–264	–	–	–	–
Activity ratios													
CIV/CI + III	4.2	3.4 ± 0.8	–	–	–	–	–	–	–	–	–	–	–
CIV/CII + III	0.8	3.1 ± 0.5	0.01	3.0 ± 0.4	1.5	1.39	2.7 ± 0.3	0.5	3.0 ± 0.2	0.61	0.55	3.6	2.1–3.3
CIV/CI	–	–	–	–	–	–	–	5.4	10.1 ± 1.0	–	–	–	–
CIV/CII	–	–	–	–	–	–	–	1.5	6.1 ± 0.7	–	–	–	–
CIV/CIII	0.5	1.5 ± 0.2	0.01	2.0 ± 0.6	0.54	0.4	1.2 ± 0.1	0.2	0.6 ± 0.04	0.39	0.37	1.9	0.7–1.2
CIV/CV	0.7	2.5 ± 0.8	–	–	–	–	–	0.9	3.5 ± 0.4	–	–	–	–

CI–CV, complexes I–V; CS, citrate synthase; P, subject; C, control. Abnormal activity values and ratios are shown in bold.
Spectrophotometric assays of respiratory chain and complex V enzymes were carried out as previously described [42]. Haemoglobin contamination of amniotic cells reduced accuracy of the absolute values of RC complex activities but not the ratios.

mitochondrial proteins or proteins predicted to be mitochondrially targeted (*FDXR* (MIM 103270), *ICT1* (MIM 603000), *ATP5H* (MIM 607196), *MRPS7* (MIM 611974), *SLC25A19* (MIM 606521), *MRPL38* (MIM 611844), *PGS1* (NM_024419), *MRPL12* (MIM 602375), *SLC25A10*

Fig. 1. Steady state levels of the oxidative phosphorylation components and complexes. A. Western blot analysis was performed on cytoplasmic extracts (40 μg) of cultured patient (P) and control (C) fibroblasts to determine steady state levels of COXII (MitoSciences). In the absence of other antibodies to mitochondrially encoded proteins, NDUFB8 (MitoSciences) was monitored as a marker for Complex I. Levels of cytochrome *c* (MitoSciences) and porin (Invitrogen) were determined as controls for the respiratory chain and mitochondrial mass respectively. B. BN-PAGE of mitochondria prepared from cultured skin fibroblasts of patient (P) and control (C) was analyzed by western using antibodies (all MitoSciences) directed against GRIM19, SDHA 70 kDa, Core 2, COXI and F₁β subunit to identify steady state levels of complexes I, II, III, IV and V respectively.

(MIM 606794), *FASN* (MIM 600212)). Considering the multiple RC deficiency observed in patient muscle, liver and fibroblasts and the abnormal BN-PAGE pattern reminiscent of translation deficiencies, we focused on genes involved in mitochondrial translation, excluding mutations in *MRPS7*, *MRPL38* and *ICT1* by direct sequencing.

Sequencing of *MRPL12* exons and exon–intron boundaries on genomic DNA (primer sequences available on request) from the affected child identified a homozygous c.542C>T transition in exon 5 (RefSeq accession number NM_002949.3, Fig. 2B). This mutation changed a highly conserved alanine into a valine (p.Ala181Val, Fig. 2C) and was predicted by Polyphen2 (http://genetics.bwh.harvard.edu/pph2/) and SIFT (http://sift.jcvi.org/) software to be "probably damaging" and "deleterious" respectively. The parents were heterozygous for the mutation, both twin fetuses were homozygous and the healthy girl was wild-type homozygous. This mutation was absent from 100 controls of the same ethnic origin and from all SNP databases. Further, no additional *MRPL12* mutation could be identified in two other unrelated subjects with similar clinical presentation and biochemical defect.

To demonstrate the deleterious nature of the p.Ala181Val MRPL12 substitution we used, overexpression of wild-type or mutant human *MRPL12* cDNA in the SV40-immortalized fibroblasts but rather recapitulating the respiratory phenotype of the patient fibroblasts, this was found to be lethal. Cells stopped growing, became polynucleated and progressively died.

3.4. In silico analysis of the putative impact of A181V substitution

Human MRPL12 is 27.5% identical in amino acid sequence to the previously crystallized *T. maritima* L12 ribosomal protein. The C-terminal domain (CTD) (107 to end in *Escherichia coli*) is conserved in evolution [50] and is required for initial binding and GTPase activation for both EF-Tu and EF-G. Indeed, both EF-Tu and EF-G have greatly diminished GTPase activity on ribosomes lacking the CTD of L12 [51,52]. Superimposition of MRPL12 with the *Thermus thermophilus* 70S ribosome (PDB code: 2WRL) lacking L7/L12 stalk proteins shows that MRPL12 Ala181 is located within this highly conserved region (Fig. 3A). Moreover, modeling of MRPL12 shows Ala181 positioned in a helix potentially involved in translation factor interactions (Fig. 3A/B). Bacterial L7/L12 CTDs also contain a number of strictly conserved residues that are involved in the initial contact with elongation factors [52,53] and crucial for translation [54]. Alanine is one of the best helix forming residues

Fig. 2. Microsatellite genotyping and mutation screening. A. Pedigree and haplotypes of the family are given (top to bottom) for loci D17S949, D17S1350, D17S1352, D17S1839, D17S785, D17S784 and D17S928. B. Sequence analysis of *MRPL12* in patient subject (left panel), mother (centre panel) and a control (right panel). The arrow indicates the position of the mutation. Amplification products were sequenced using the PRISM Ready Reaction Sequencing Kit (Perkin-Elmer, Oak Brook, IL) on an automatic sequencer (ABI 3130xl; PE Applied Biosystems, Foster City, CA). **C.** Amino acid alignment of MRPL12 (*H. sapiens* to *S. cerevisiae*) and L7/L12 (*E. coli* to *S. saprophyticus*) proteins. The arrow indicates the conserved amino acid that the *MRPL12* mutation changes from an alanine to a valine. Below * designates identity, whilst and: indicate increasing levels of similarity.

and substitutions can therefore have profound energetic effects by perturbing packing interactions or tertiary contacts [55]. Thus, the p.Ala181Val change might be predicted to alter interactions with the elongation factors, and since MRPL7/12 bound to elongation factors is predicted to have a higher affinity for the ribosome [54], the mutation may in turn affect both rate and accuracy of mitochondrial translation.

3.5. Ribosome assembly

The steady state level of MRPL12 in the subject's fibroblasts was reduced to 30% of control value (Fig. 4A and B). The mt-LSU protein ICT1 was also decreased (~30% of control values) as was MRPL3 (by 37%) suggesting that a consequence of the MRPL12 mutation is a global defect in assembly of the large ribosomal subunit (mt-LSU). In order
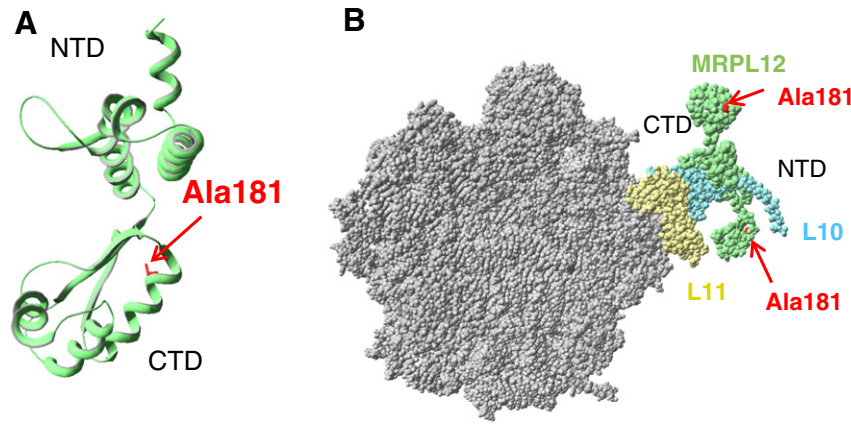
Fig. 3. MRPL12 and its position in the ribosome. A. The three dimensional structure of the human MRPL12 (residues 64 to 198) was modeled by comparative protein modeling and energy minimization, using the Swiss-Model program in the automated mode. The 2 Å coordinate set for the ribosomal protein L12 from *Thermotoga maritima* (PDB code: 1dd3) was used as a template for modeling the human MRPL12 protein. Swiss-Pdb Viewer 3.7 (http://www.expasy.org/spdbv) was used to analyze the structural insight into MRPL12 mutation and visualize the structures. The A181 residue shown (in red) is localized in a helix that is likely to be at the interface of an interaction with translation factors. B. Potential MRPL12 interactions within the ribosomal L7/L12 stalk. Swiss-Pdb Viewer 3.7 (http://www.expasy.org/spdbv) was used to superimpose MRPL12 on the *Thermus thermophilus* 70S ribosome (PDB code: 2WRL) without L7/L12 stalk proteins. MRPL12, L10 and L11 are shown in green, blue and yellow respectively. The Ala181 residue (in red) is located in the MRPL12 CTD. The p.Ala181Val change has a high probability of altering interactions of MRPL12 with elongation factors and might be predicted to affect initial binding, decreasing both rate and accuracy of mitochondrial translation. NTD: N-terminal domain; CTD: C-terminal domain.

to estimate the effect of the MRPL12 mutation on assembly of the whole ribosome, we also tested three proteins of the small ribosomal subunit (SSU), MRPS18B, MRPS25 and DAP3. These were modestly decreased with levels of ~60–80% of control (Fig. 4A and B). Correspondingly, 16S and 12S rRNA levels were decreased by 35% and 22% respectively (Fig. 7A). Since porin indicated that there was no compensatory mitochondrial biogenesis and staining of the mitochondrial network with tetramethylrhodamine methyl ester showed no significant alteration in amount or distribution of mitochondria (AR and ZCL unpublished observation) we conclude that the *MRPL12* mutation destabilizes the protein resulting in less mt-LSU and to a lesser extent of the small subunit.

In order to determine whether the MRPL12 mutation also induced changes in composition and assembly of the mitochondrial ribosomal large and small subunits, mitochondrial lysates from cultured fibroblasts (subject and control) were fractionated on isokinetic sucrose gradients (10–30%, as in Ref. [47]). If assembly of either the large subunit or the entire ribosome was affected then the distribution of

individual ribosomal proteins would change within the gradient profile. On analysis MRPL12 from the patient was substantially decreased in all fractions but detectable in the fractions consistent with mt-LSU; however it was noticeably absent from the free pool (fractions 1 and 2, Fig. 5). This was in contrast to the control that exhibited a pool of free MRPL12, which has been reported to interact with POLRMT [56]. MRPL3 was also slightly reduced in subject cells but remained in fractions consistent with the large subunit. The MRPL12 mutation impacted more modestly on the small ribosomal subunit, with DAP3 apparently unaffected and MRPS18B found in lower amounts only in fractions 4 and 5 but otherwise with similar steady state levels and distribution profile compared to control. Since POLRMT and MRPL12 have been published as interactors, we analyzed both the steady state level and gradient distribution of POLRMT to see if these were affected by the MRPL12 mutation. Overall levels in the subject sample were decreased to 63% of control value (Fig. 5B) but distribution in the gradient appeared largely unaffected with the exception of fraction 11, where levels were lower than control (Fig. 5A bottom panels).
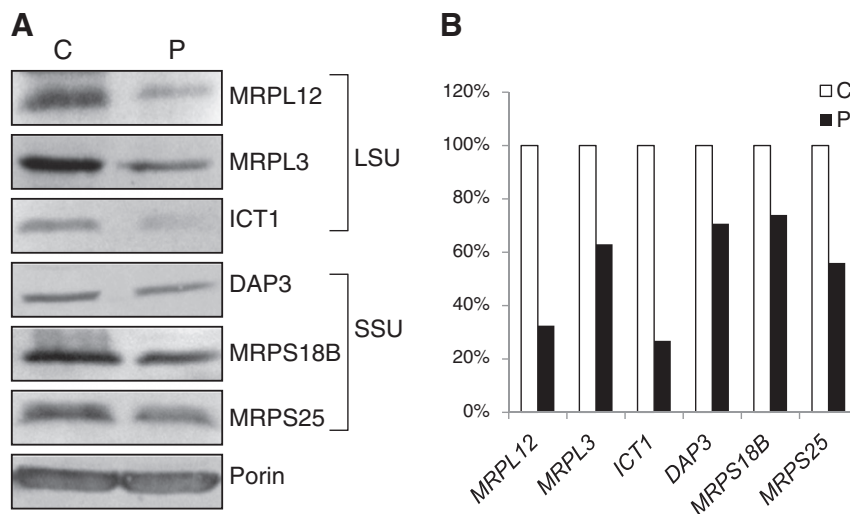
Fig. 4. Analysis of mitoribosomal components. A. Cell lysates (50 μg) from patient (P) and control (C) fibroblasts were separated by SDS–PAGE followed by western to decorate various components. Polypeptides of the large ribosomal subunit (LSU) included MRPL12 (Eurogentec), MRPL3 (PTG labs), ICT1 (PTG labs) and small ribosomal subunit (SSU) included DAP3 (Abcam), MRPS18B (PTG labs) and MRPS25 (PTG labs). Porin (Invitrogen) was used as a loading control. B. Densitometric values from 3 independent experiments as described in panel A represent the levels of MRPL12, MRPL3, ICT1, DAP3, MRPS18B and MRPS25 in subject compared to control fibroblasts.
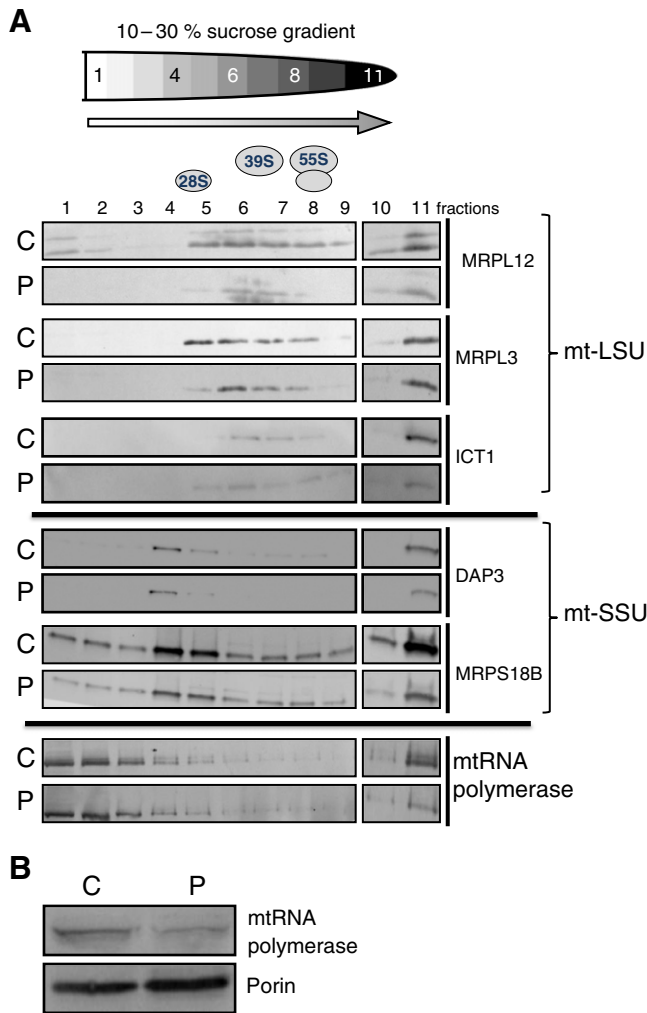
Fig. 5. Isokinetic gradient analysis of mitochondrial lysates. A. Mitochondrial lysates were prepared from patient (P) and control (C) fibroblasts and 300 μg of each was separated through 10–30% (w/v) isokinetic sucrose gradients. The levels of 28S small subunit (SSU) and 39S large subunit (LSU) proteins were determined by western blot analysis. 55S corresponds to the assembled mitoribosome. The steady state level (panel B. porin as loading control) and distribution (panel A) of POLRMT was also examined. Antibodies as in previous legends except POLRMT (Abcam).

3.6. In vitro translation

To identify any effect on global mitochondrial protein synthesis, we studied *de novo* mitochondrial translation in cultured skin fibroblasts, as described in Ref. [45]. Although there was an overall decrease in mitochondrial translation compared to control, densitometric profiles showed that certain polypeptides were more affected than others (Fig. 6). In particular, there was a significant reduction of synthesis of COXI, COXII and COXIII subunits. Consistent with the respiratory chain activities, complex I polypeptides were affected to a lesser extent and cytochrome *b* from complex III appears to be spared. Despite the potential role of MRPL12 in translational accuracy, no aberrant translation product could be detected.

3.7. Steady-state level of mitochondrial transcripts

MRPL12 has been shown to interact with the mitochondrial RNA polymerase (POLRMT) and to stimulate mitochondrial transcription [56,57]. Since the steady-state level of POLRMT in subject fibroblasts was modestly decreased, we analyzed the steady-state level of mitochondrial transcripts to see if these were similarly affected. Northern blots on control and subject fibroblast RNA did not show a decrease
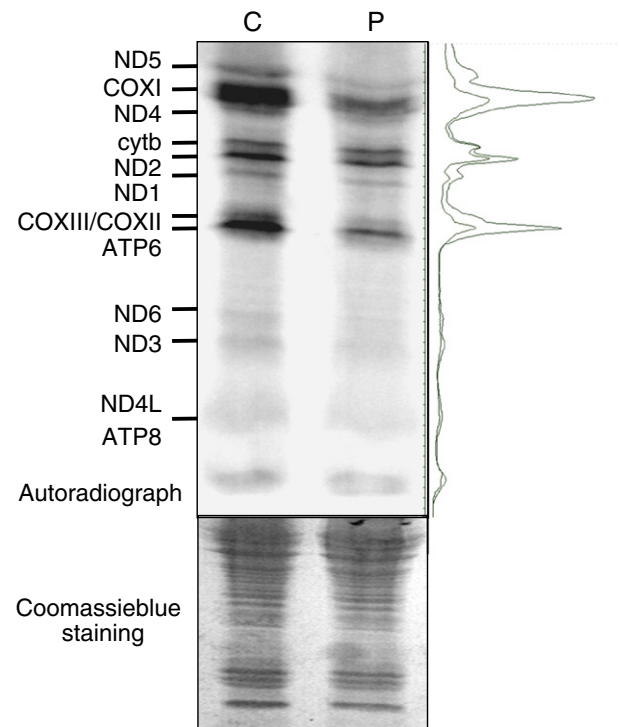
Fig. 6. Mitochondrial protein synthesis. *De novo* synthesis of mitochondrial proteins was determined in patient (P) and control (C) fibroblasts under conditions that inhibited cytosolic translation [45]. *In vivo* incorporation of ^{35}S-methionine/cysteine into mitochondrially encoded proteins was visualised by separation of cell lysate (50 μg) through SDS–PAGE, exposure of the dried gel to a PhosphorImage screen, followed by Storm and ImageQuant analysis (upper panel). To the right of the gel are the aligned densitometric profiles of the patient (lower trace) and control (upper trace). The gel was subsequently rehydrated and stained with Coomassie blue to confirm equal loading (lower panel).

that paralleled the reduced levels of POLRMT. In fact there was a slight increase of *MTND1* in subject cells compared to control, whilst *MTCOI* and *MTCYB* transcripts appeared unaffected (Fig. 7A). Conversely, as mentioned earlier, the levels of 16S and 12S rRNA were modestly decreased (Fig. 7A) in a proportion that was consistent with the loss of MRPs with which they would associate. Analysis of the distribution on 10–30% (w/v) sucrose gradients (as in Ref. [58]) of two mt-mRNAs, *MTCOI* and *MTND1*, showed a relatively similar pattern for subject and control but in each case a smaller proportion of the subject transcript sedimented to the final fraction (data available on request). This was also true for the 16S and 12S rRNA. As no major redistribution in the sucrose gradient was observed, it is unlikely that the MRPL12 mutation causes a global defect in assembly of the mitoribosome.

Since the levels of POLRMT were slightly decreased with normal or slightly elevated levels of mt-mRNA, we assessed the stability of transcripts to see if the half-lives were extended to compensate for reduced synthesis in order to maintain normal steady state levels. Mitochondrial transcription was poisoned by addition of low levels of ethidium bromide and RNA prepared at numerous time points thereafter (0–16 h). Densitometry of the subsequent Northern demonstrated that half-lives of *MTCOI* and *MTND1* were extended, the latter more so, consistent with the modest increase in steady state levels (data available on request).

3.8. MRPL12 dimerization and interaction with the mitoribosome

MRPL12 is the orthologue of eubacterial L7/L12, where L7 is identical to L12 except that it is N-terminal acetylated. L7/L12 is also phosphorylated, which can affect both conformation and binding to partner
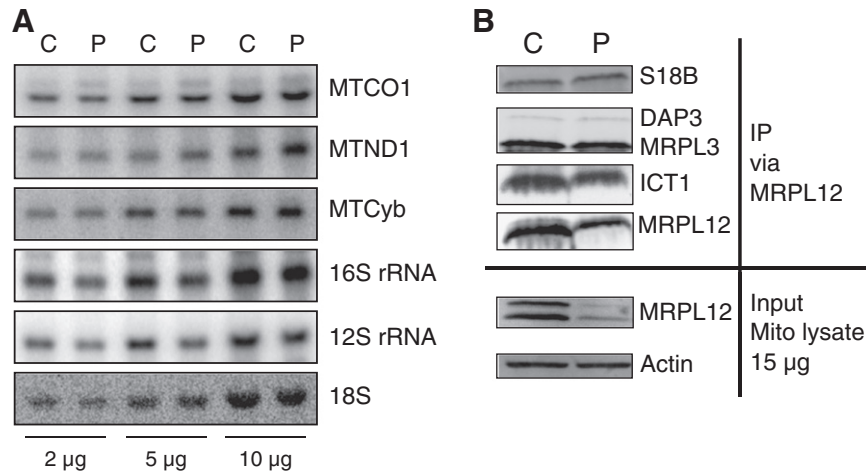
Fig. 7. Analysis of mitochondrial transcripts and of MRPs immunoprecipitating with MRPL12. A. Steady-state levels of mitochondrial transcripts from patient (P) and control (C) fibroblasts were analyzed by Northern blot. Signals were normalized against 18S cytosolic rRNA. Three different amounts (2, 5 and 10 μg) of total RNAs were loaded. B. MRPL12 was immunoprecipitated from mitochondrial lysates (835 μg) prepared from patient (P) and control (C) fibroblasts. Recovered MRPL12 and co-immunoprecipitating MRPs were analyzed by western blot (antibodies as previously described).

ribosomal proteins (reviewed in Ref. [37]). This modification has now been confirmed to be present in mammalian MRPL12 [59]. In eubacteria, association of L7/12 to the large subunit takes place via the L10 protein such that two L7/L12 heterodimers normally associate per LSU [60]. Interestingly these dimers are actively exchanged on the 70S molecule without disruption of the ribosomal particle [54,61]. The dimerization status and number of dimers attached to the human 55S has not been clarified. In order to identify if the stoichiometry of MRPL12 per mt-LSU was altered as a consequence of the mutation, we performed immunoprecipitation (IP) analysis on subject and control fibroblasts using antibodies to MRPL12. Analysis of the immunoprecipitate demonstrated similar levels small subunit polypeptides including DAP3 and MRPS18B in subject and control samples. In contrast, the total amount of MRPL12 was reduced (Fig. 7B). In the patient the IP is restricted to MRPL12 in the large subunit or the fully assembled 55S with the total amount of MRPL12 being reduced as it lacks the "free" population. The densitometric measurements indicate that the patient IP has ~49% MRPL12 compared to control, in accordance with the gradient and steady state data. ICT1 appears to be sensitive to the MRPL12 levels and so is reduced in both the IP (~58% of control) and in the steady state westerns (Fig. 4). The lower levels of MRPL12 could reflect loss of multimerization but since the region in the bacterial protein involved in multimerization is towards the N-terminus [62], this mutation is unlikely to have an impact on dimer/multimer formation. The translation factor bound dimer has been suggested to have an increased affinity for the ribosome [54,61]. Thus a possible explanation is that the mutation affects translation factor binding, thereby reducing the affinity of the mutant MRPL12 for the ribosome. If this were the case, however, then we would expect an increase in the pool of free MRPL12 whereas the subject exhibits a reduced pool of free MRPL12, which interacts with POLRMT [57]. The immunoprecipitation was performed using an MRPL12 specific antibody and so should contain all free MRPL12, MRPL12 associated with uncomplexed mt-LSU and MRPL12 as part of the fully assembled 55S. Since the levels of small and large subunit proteins appeared to be similar in subject and control, these data suggest that the mt-LSU and 55S assembly are unaffected by the mutation consistent with the gradient data for the protein and RNA components. Thus the reduced levels of mutant MRPL12 in this subject correspond to i) loss of stability, ii) a decrease in the free pool that is believed to interact with the mitochondrial RNA polymerase and iii) reduced translation potentially resulting from decreased interactions with translation factors, but with no detectable increase in aberrant translation products.

In conclusion, we report a mutation in human *MRPL12* that results in growth retardation and neurological distress. It is interesting to note that whereas the eubacterial orthologue is not essential for in vitro translation assays, this *MRPL12* mutation induces a mitochondrial translation defect in human. This lack of predictability between orthologous proteins makes it important to examine and not assume what impact mutant forms or loss of MRPs may have on mitochondrial homeostasis and the resulting clinical manifestation. The data presented here provide another example, amongst a growing list of translation factors, which despite their apparent universal contribution to the synthesis of all mitochondrially encoded proteins, has a selective effect on the different oxidative phosphorylation complexes.

References

[1] S. Anderson, et al., Sequence and organization of the human mitochondrial genome, Nature 290 (1981) 457–465.

[2] M. Zeviani, V. Carelli, Mitochondrial disorders, Curr. Opin. Neurol. 20 (5) (2007) 564–571.

[3] J.P. Kemp, et al., Nuclear factors involved in mitochondrial translation cause a subgroup of combined respiratory chain deficiency, Brain 134 (Pt 1) (2011) 183–195.

[4] S.E. Calvo, et al., Molecular diagnosis of infantile mitochondrial disease with targeted next-generation sequencing, Sci. Transl. Med. 4 (118) (2012) 118ra110.

[5] L. Galmiche, et al., Exome sequencing identifies MRPL3 mutation in mitochondrial cardiomyopathy, Hum. Mutat. 32 (11) (2011) 1225–1231.

[6] L.C. Greaves, A.K. Reeve, R.W. Taylor, D.M. Turnbull, Mitochondrial DNA and disease, J. Pathol. 226 (2) (2012) 274–286.

[7] P.G. Barth, F. Valianpour, V.M. Bowen, J. Lam, M. Duran, F.M. Vaz, R.J. Wanders, X-linked cardioskeletal myopathy and neutropenia (Barth syndrome): an update, Am. J. Med. Genet. A 126A (4) (2004) 349–354.

[8] F. Valianpour, R.J. Wanders, H. Overmars, F.M. Vaz, P.G. Barth, A.H. van Gennip, Linoleic acid supplementation of Barth syndrome fibroblasts restores cardiolipin levels: implications for treatment, J. Lipid Res. 44 (3) (2003) 560–566.

[9] E. Ylikallio, A. Suomalainen, Mechanisms of mitochondrial diseases, Ann. Med. 44 (1) (2012) 41–59.

[10] Z.M. Chrzanowska-Lightowlers, R. Horvath, R.N. Lightowlers, Mitochondrial protein synthesis in health and disease, J. Inherit. Metab. Dis. 21 (2) (2010) 142–147.

[11] R. McFarland, D.M. Turnbull, Batteries not included: diagnosis and management of mitochondrial disease, J. Intern. Med. 265 (2) (2009) 210–228.

[12] B.E. Christian, L.L. Spremulli, Mechanism of protein biosynthesis in mammalian mitochondria, Biochim. Biophys. Acta 1819 (9-10) (2011) 1035–1054.

[13] J.W. Yarham, J.L. Elson, E.L. Blakely, R. McFarland, R.W. Taylor, Mitochondrial tRNA mutations and disease. Wiley interdisciplinary reviews, RNA 1 (2) (2010) 304–324.
[14] A. Rotig, Human diseases with impaired mitochondrial protein synthesis, Biochim. Biophys. Acta 1807 (9) (2011) 1198–1205.
[15] M.J. Coenen, et al., Mutant mitochondrial elongation factor G1 and combined oxidative phosphorylation deficiency, N. Engl. J. Med. 351 (20) (2004) 2080–2086.
[16] H. Antonicka, F. Sasarman, N.G. Kennaway, E.A. Shoubridge, The molecular basis for tissue specificity of the oxidative phosphorylation deficiencies in patients with mutations in the mitochondrial translation factor EFG1, Hum. Mol. Genet. 15 (11) (2006) 1835–1846.
[17] J.A. Smeitink, et al., Distinct clinical phenotypes associated with a mutation in the mitochondrial translation elongation factor EFTs, Am. J. Hum. Genet. 79 (5) (2006) 869–877.
[18] L. Valente, et al., Infantile encephalopathy and defective mitochondrial DNA translation in patients with mutations of mitochondrial elongation factors EFG1 and EFTu, Am. J. Hum. Genet. 80 (1) (2007) 44–58.
[19] S. Edvardson, A. Shaag, O. Kolesnikova, J.M. Gomori, I. Tarassov, T. Einbinder, A. Saada, O. Elpeleg, Deleterious mutation in the mitochondrial arginyl-transfer RNA synthetase gene is associated with pontocerebellar hypoplasia, Am. J. Hum. Genet. 81 (4) (2007) 857–862.
[20] G.C. Scheper, et al., Mitochondrial aspartyl-tRNA synthetase deficiency causes leukoencephalopathy with brain stem and spinal cord involvement and lactate elevation, Nat. Genet. 39 (4) (2007) 534–539.
[21] L.G. Riley, et al., Mutation of the mitochondrial tyrosyl-tRNA synthetase gene, YARS2, causes myopathy, lactic acidosis, and sideroblastic anemia − MLASA syndrome, Am. J. Hum. Genet. 87 (1) (2010) 52–59.
[22] R. Belostotsky, et al., Mutations in the mitochondrial seryl-tRNA synthetase cause hyperuricemia, pulmonary hypertension, renal failure in infancy and alkalosis, HUPRA syndrome, Am. J. Hum. Genet. 88 (2) (2011) 193–200.
[23] S.B. Pierce, K.M. Chisholm, E.D. Lynch, M.K. Lee, T. Walsh, J.M. Opitz, W. Li, R.E. Klevit, M.C. King, Mutations in mitochondrial histidyl tRNA synthetase HARS2 cause ovarian dysgenesis and sensorineural hearing loss of Perrault syndrome, Proc. Natl. Acad. Sci. U. S. A. 108 (16) (2011) 6543–6548.
[24] A. Gotz, et al., Exome sequencing identifies mitochondrial alanyl-tRNA synthetase mutations in infantile mitochondrial cardiomyopathy, Am. J. Hum. Genet. 88 (5) (2011) 635–642.
[25] V. Bayat, et al., Mutations in the mitochondrial methionyl-tRNA synthetase cause a neurodegenerative phenotype in flies and a recessive ataxia (ARSAL) in humans, PLoS Biol. 10 (3) (2012) e1001288.
[26] M.E. Steenweg, et al., Leukoencephalopathy with thalamus and brainstem involvement and high lactate 'LTBL' caused by EARS2 mutations, Brain 135 (Pt 5) (2012) 1387–1394.
[27] J.M. Elo, et al., Mitochondrial phenylalanyl-tRNA synthetase mutations underlie fatal infantile Alpers encephalopathy, Hum. Mol. Genet. 21 (20) (2012) 4521–4529.
[28] A. Zeharia, N. Fischel-Ghodsian, K. Casas, Y. Bykhocskaya, H. Tamari, D. Lev, M. Mimouni, T. Lerman-Sagie, Mitochondrial myopathy, sideroblastic anemia, and lactic acidosis: an autosomal recessive syndrome in Persian Jews caused by a mutation in the PUS1 gene, J. Child Neurol. 20 (5) (2005) 449–452.
[29] A. Zeharia, et al., Acute infantile liver failure due to mutations in the TRMU gene, Am. J. Hum. Genet. 85 (3) (2009) 401–407.
[30] X. Li, R. Li, X. Guan, Isolation and characterization of the putative nuclear modifier gene MTO1 involved in the pathogenesis of deafness-associated mitochondrial 12 S rRNA A1555G mutation, J. Biol. Chem. 277 (30) (2002) 27256–27264.
[31] H. Antonicka, et al., Mutations in C12orf65 in patients with encephalomyopathy and a mitochondrial translation defect, Am. J. Hum. Genet. 87 (1) (2010) 115–122.
[32] W. Weraarpachai, et al., Mutation in TACO1, encoding a translational activator of COX I, results in cytochrome c oxidase deficiency and late-onset Leigh syndrome, Nat. Genet. 41 (7) (2009) 833–837.
[33] F. Xu, C. Morin, G. Mitchell, C. Ackerley, B.H. Robinson, The role of the LRPPRC (leucine-rich pentatricopeptide repeat cassette) gene in cytochrome oxidase assembly: mutation causes lowered levels of COX (cytochrome c oxidase) I and COX III mRNA, Biochem. J. 382 (Pt 1) (2004) 331–336.
[34] W. Weraarpachai, F. Sasarman, T. Nishimura, H. Antonicka, K. Aure, A. Rotig, A. Lombes, E.A. Shoubridge, Mutations in C12orf62, a factor that couples COX I synthesis with cytochrome c oxidase assembly, cause fatal neonatal lactic acidosis, Am. J. Hum. Genet. 90 (1) (2012) 142–151.
[35] C. Miller, A. Saada, N. Shaul, N. Shabtai, E. Ben-Shalom, A. Shaag, E. Hershkovitz, O. Elpeleg, Defective mitochondrial translation caused by a ribosomal protein (MRPS16) mutation, Ann. Neurol. 56 (5) (2004) 734–738.
[36] A. Saada, A. Shaag, S. Arnon, T. Dolfin, C. Miller, D. Fuchs-Telem, A. Lombes, O. Elpeleg, Antenatal mitochondrial disease caused by mitochondrial ribosomal protein (MRPS22) mutation, J. Med. Genet. 44 (12) (2007) 784–786.
[37] E.C. Koc, E. Emdadul Haque, L.L. Spremulli, Current Views of the Structure of the Mammalian Mitochondrial Ribosome, Isr. J. Chem. 50 (2010) 45–59.
[38] T.W. O'Brien, N.D. Denslow, J.C. Anders, B.C. Courtney, The translation system of mitochondrial polysomes, Biochim. Biophys. Acta 1050 (1990) 174–178.
[39] M. Helgstrand, C.S. Mandava, F.A. Mulder, A. Liljas, S. Sanyal, M. Akke, The ribosomal stalk binds to translation factors IF2, EF-Tu, EF-G and RF3 via a conserved region of the L12 C-terminal domain, J. Mol. Biol. 365 (2) (2007) 468–479.
[40] D. Dey, A.V. Oleinikov, R.R. Traut, The hinge region of Escherichia coli ribosomal protein L7/L12 is required for factor binding and GTP hydrolysis, Biochimie 77 (12) (1995) 925–930.
[41] I. Pettersson, C.G. Kurland, Ribosomal protein L7/L12 is required for optimal translation, Proc. Natl. Acad. Sci. U. S. A. 77 (7) (1980) 4007–4010.
[42] P. Rustin, D. Chretien, T. Bourgeron, B. Gerard, A. Rotig, J.M. Saudubray, A. Munnich, Biochemical and molecular investigations in respiratory chain deficiencies, Clin. Chim. Acta 228 (1) (1994) 35–51.
[43] S. Calvo, et al., Systematic identification of human mitochondrial disease genes through integrative genomics, Nat. Genet. 38 (5) (2006) 576–582.
[44] R.O. Vogel, C.E. Dieteren, L.P. van den Heuvel, P.H. Willems, J.A. Smeitink, W.J. Koopman, L.G. Nijtmans, Identification of mitochondrial complex I assembly intermediates by tracing tagged NDUFS3 demonstrates the entry point of mitochondrial subunits, J. Biol. Chem. 282 (10) (2007) 7582–7590.
[45] A. Chomyn, In vivo labeling and analysis of human mitochondrial translation products, Methods Enzymol. 264 (1996) 197–211.
[46] H.R. Soleimanpour-Lichaei, et al., mtRF1a is a human mitochondrial translation release factor decoding the major termination codons UAA and UAG, Molecular cell 27 (5) (2007) 745–757.
[47] R. Richter, J. Rorbach, A. Pajak, P.M. Smith, H.J. Wessels, M.A. Huynen, J.A. Smeitink, R.N. Lightowlers, Z.M. Chrzanowska-Lightowlers, A functional peptidyl-tRNA hydrolase, ICT1, has been recruited into the human mitochondrial ribosome, EMBO J. 29 (6) (2010) 1116–1125.
[48] Z.M. Chrzanowska-Lightowlers, T. Preiss, R.N. Lightowlers, Inhibition of mitochondrial protein synthesis promotes increased stability of nuclear-encoded respiratory gene transcripts, J. Biol. Chem. 269 (44) (1994) 27322–27328.
[49] L.G.J. Nijtmans, N. Henderson, I.J. Holt, Blue native electrophoresis to study mitochondrial and other protein complexes, Methods 26 (2002) 327–334.
[50] P. Hemmerich, A. von Mikecz, F. Neumann, O. Sozeri, G. Wolff-Vorbeck, R. Zoebelein, U. Krawinkel, Structural and functional properties of ribosomal protein L7 from humans and rodents, Nucleic Acids Res. 21 (2) (1993) 223–231.
[51] D. Mohr, W. Wintermeyer, M.V. Rodnina, GTPase activation of elongation factors Tu and G on the ribosome, Biochemistry 41 (41) (2002) 12520–12528.
[52] M. Diaconu, U. Kothe, F. Schlunzen, N. Fischer, J.M. Harms, A.G. Tonevitsky, H. Stark, M.V. Rodnina, M.C. Wahl, Structural basis for the function of the ribosomal L7/12 stalk in factor binding and GTPase activation, Cell 121 (7) (2005) 991–1004.
[53] R. Nechifor, M. Murataliev, K.S. Wilson, Functional interactions between the G' subdomain of bacterial translation factor EF-G and ribosomal protein L7/L12, J. Biol. Chem. 282 (51) (2007) 36998–37005.
[54] A.K. Kopke, P.A. Leggatt, A.T. Matheson, Structure function relationships in the ribosomal stalk proteins of archaebacteria, J. Biol. Chem. 267 (2) (1992) 1382–1390.
[55] L.M. Gregoret, R.T. Sauer, Tolerance of a protein helix to multiple alanine and valine substitutions, Fold. Des. 3 (2) (1998) 119–126.
[56] Z. Wang, J. Cotney, G.S. Shadel, Human mitochondrial ribosomal protein MRPL12 interacts directly with mitochondrial RNA polymerase to modulate mitochondrial gene expression, J. Biol. Chem. 282 (17) (2007) 12610–12618.
[57] Y.V. Surovtseva, T.E. Shutt, J. Cotney, H. Cimen, S.Y. Chen, E.C. Koc, G.S. Shadel, Mitochondrial ribosomal protein L12 selectively associates with human mitochondrial RNA polymerase to activate transcription, Proc. Natl. Acad. Sci. U. S. A. 108 (44) (2011) 17921–17926.
[58] S. Dennerlein, A. Rozanska, M. Wydro, Z.M. Chrzanowska-Lightowlers, R.N. Lightowlers, Human ERAL1 is a mitochondrial RNA chaperone involved in the assembly of the 28S small mitochondrial ribosomal subunit, The Biochem. J. 430 (3) (2010) 551–558.
[59] E.C. Koc, H. Koc, Regulation of mammalian mitochondrial translation by post-translational modifications, Biochim. Biophys. Acta 1819 (9-10) (2012) 1055–1066.
[60] E.V. Bocharov, A.T. Gudkov, E.V. Budovskaya, A.S. Arseniev, Conformational independence of N- and C-domains in ribosomal protein L7/L12 and in the complex with protein L10, FEBS Lett. 423 (3) (1998) 347–350.
[61] S. Deroo, S.J. Hyung, J. Marcoux, Y. Gordiyenko, R.K. Koripella, S. Sanyal, C.V. Robinson, Mechanism and rates of exchange of L7/L12 between ribosomes and the effects of binding EF-G, ACS Chem. Biol. 7 (6) (2012) 1120–1127.
[62] A.V. Oleinikov, B. Perroud, B. Wang, R.R. Traut, Structural and functional domains of Escherichia coli ribosomal protein L7/L12. The hinge region is required for activity, J. Biol. Chem. 268 (2) (1993) 917–922.